

ADVANCED OXIDATION TECHNOLOGIES

PHOTOCATALYTIC TREATMENT OF WASTEWATER

Jian Chen

Promotor: dr.ir. W.H. Rulkens
hoogleraar in de milieutechnologie

Co-promotor: dr.ir. H. Bruning
universitair docent bij het subdepartement milieutechnologie

PN0270', 2309

ADVANCED OXIDATION TECHNOLOGIES

PHOTOCATALYTIC TREATMENT OF WASTEWATER

Jian Chen

高级氧化技术：废水之光催化处理

陈健

Proefschrift

ter verkrijging van de graad van doctor
op gezag van de rector magnificus
van de Landbouwniversiteit Wageningen,
dr. C.M. Karssen,
in het openbaar te verdedigen
op dinsdag 9 september 1997
des namiddags te 13:30 in de Aula

un 944257

CIP-DATA KONINKLIJKE BIBLIOTHEEK, DEN HAAG

Chen, Jian

Advanced oxidation technologies: Photocatalytic treatment of wastewater

Jian Chen. - [S.l. : s.n.]

Thesis Wageningen - With ref.

With summary in Dutch

With Acknowledgement in Chinese

ISBN 90-5485-762-5

Subject headings: photocatalysis/wastewater treatment/
advanced oxidation technologies

Propositions

1. "The need to 'cite photocatalysis' in the future will have new driving forces. **Comparison** with other competitive technologies, **integration** with complementary processes such as ultrafiltration and biological treatment, **transfer** of research results into development and application activities, and **economics** and optimization of photocatalysis are the energizing themes for the 1990s and beyond."

D.F. Ollis, H. Al-Ekabi, *Photocatalytic Purification and Treatment of Water and Air*, Elsevier Science Publishers, Amsterdam, 1993.

2. The heterogeneous system obtained by integrating UV, photocatalyst and Fenton reagent will be one of the most efficient systems for commercial application in wastewater treatment.

This thesis, Chapter 4.

3. The mechanism of the photocatalytic oxidation of organic pollutants in aqueous solutions is more likely to be a reaction on the photocatalyst surface, as concluded in Chapter 2 of this thesis, than a free radical reaction, as proposed by Yasumori *et al.*

A. Yasumori, K. Yamazaki, S. Shibata and M. Yamane, "Preparation of TiO_2 fine particles supported on silica gel as photocatalyst," *J. of the Ceramic Society of Japan*, 102(8), 702 - 707, 1994.

4. The effort to develop new energy resources should be focused on water splitting by photocatalysis to produce hydrogen rather than on nuclear energy because the former is safe, convenient and environmentally friendly and will be feasible as long as the Sun exists.
5. "Although the principles of decomposing water with sunlight appeared relatively simple, the experimental difficulties encountered proved formidable, even for a such a seemingly simple chemical transformation."

N. Serpone and E. Pelizzetti, *Photocatalysis, Fundamentals and Applications*, John Wiley & Sons, NY, 1989.

6. Photocatalysis is like a baby. After being raised with great care, it may shock the world.

7. For each developed country, industrialization was a very painful process that resulted in much harm to the environment. During the developing process presently occurring in China, it would be better for the environment if the developed countries showed less blame and a more cooperative attitude.
8. It is very likely that the Dutch word "loempia" originates from China rather than from Indonesia.
9. Persistence is the father of success.
10. The later you smile, the better you do so.
11. Chinese history shows that social progress is promoted best by means of the "catalyst" that its activity and selectivity have the following sequence:
survival > education > welfare > freedom > democracy.
12. Truth cannot exist without first being tested in practice.

These propositions are included in the thesis entitled "Advanced Oxidation Technologies: Photocatalytic treatment of wastewater".

Jian Chen

Wageningen, September 9, 1997.

To: my parents, Jing and Rong
献给：我的父母，王晶与戎戎

ACKNOWLEDGEMENT

I am ever so grateful to my parents for how they have helped me. Nobody knows better than I how they have encouraged me and supported me financially from my early youth up to now. They cannot be appreciated too deeply. This dissertation is the best gift I can give to them and it is what they deserve.

I wish to express my great gratitude to my supervisor, Prof.Dr.ir. Wim H. Rulkens, not only for enabling me to study for my doctorate here, but also for so much his precious time, responsibilities and very careful works to help me with attaining results in my research, drawing conclusions, and writing a dissertation. Under his supervision, many of my works have been published and presented during many international conferences. Without his help, this dissertation would not have been written. In the name of my wife, son and parents, I also wish to thank my supervisor's wife, Riet, so much for her very warm friendship. She often invited my family to their home, and traveled together to introduce them to many things in the Netherlands. What she did made us feel at home and proved the great friendliness of the Dutch people to the Chinese people.

During my research at the Dept. of Chemical Engineering of North Carolina State University, USA, Prof. Dr. David F. Ollis, one of famous professors in chemical engineering, helped me tremendously. During my stay at his laboratory, he gave me many important instructions and much freedom of action in my research. Without his great and kind help, I would not have found most of the experimental data contained in this dissertation. His help is greatly appreciated.

This dissertation also reflects the work of Dr.ir. Harry Bruning, the co-promoter of my PhD programme. He spent a lot of time on correcting my thesis, made many constructive suggestions, and key improvements on dealing with experimental data. His excellent mathematical skills and keen scientific insight on my dissertation are highly valued and greatly appreciated.

Many great and sincere thanks are to present to my dear wife, WANG Jing. It was clear to me that her so much occupied businesses in China that she didn't join me in my studies abroad over the last seven years. She has done all her best to support me while I was abroad lonely. If she had not supported me, I would have been forced to work in another field and could not have written this dissertation. Doubtless, the dissertation is also the result of her support. I especially wish to thank my dear son, Rong. During most of the time when I was doing research in the US, we depended on each other for survival. We shared many so happy and exciting experiences in US and Canada. He always showed me his good spirits and provided me many practical help he could. These were so great comforts to me so that I could go ahead during this most difficult period of my life. Without him, I could not image how was the life I would have experienced.

I would like to express my great appreciations especially to Professor ZHUANG Qixing who died three years ago. He supported me greatly during my work at the Department of Chemistry of Xiamen University. I also wish to express many deep appreciations for the help I received from many other teachers, such as Prof. CAI Qirui, WANG Huilin, FU Jinyin, LIN Guodong, ZHANG Pangxian and CHEN Zhubin, as well as from my students.

Finally, I must show my great, cordial thanks to all my best friends and colleagues. During all these years of hard study, they gave me terrific help and support in my life and work. I will always remember for what they have done for me. Thank you again, my faithful friends.

谨以此文献给帮助，支持和理解我的人

此篇博士论文的完成，首先要感谢我的父母亲。为了我的今天，他们付出了极大的心血。留学经历使我深深地体会到，中国的父母竭其一生之代价去换取下代之幸福与希望。他们乃至今日，仍尽其所能，给予了我无数的精神与经济上的帮助。怎么感激他们都不过分。这篇论文是他们的期待，也是献给他们最好的礼物。

我要向我的导师，荷兰瓦赫林根农业大学，环境技术系主任卢肯斯教授表示深深的谢意。他不仅给了我出国读博士的机会，而且在其繁重的日常行政，教学与科研中，为我付出了大量的宝贵时间与精力。他常利用凌晨，周末，甚至旅途反复几遍地阅读修改我的论文，以超乎寻常的认真，罕见的细致与责任感对待我的实验数据，结论和论文写作，为我的论文付出了极大的心血。在他的指导下，我的许多数据得到了顺利的发表。另外，我要为我的妻子，儿子和父母，向卢肯斯太太莉特对我们非常热情的接待与照顾表示衷心的感谢。她常邀请我们去她家做客，并带我的家人去参观荷兰许多地方，使我们在荷兰就象在家一样。从卢肯斯教授一家身上，我们看到了荷兰人民的善良，友好与热情。

我还要向奥利斯教授，世界著名生物工程与光催化专家，美国北卡罗莱那州立大学杰出教授，对我在该校化工系三年半助理研究员期间所显示出的善良人品和巨大帮助表示深深的敬意与感谢。他给予你关键的指点以及充分的研究自由度，让你发挥自己的才能。没有他的帮助，这篇论文中的大部份实验就无法完成。

这篇博士论文凝聚着我的付导师，布鲁林博士的大量心血。他在此论文中表现出了超凡的数学才能与功底，以及敏锐的科学眼光。他对实验数据的处理技巧以及结论提出许多建设性的意见，给了我关键性的帮助。我在此对他表示深深的感谢。

我要特别向我的妻子王晶在精神上与经济上对我在国外六年有余所做的不懈的巨大支持表示衷心的感谢。为了各自的事业，我们相隔万里之遥，做出了巨大的牺牲。这篇博士论文的完成主要归功于她。没有她的支持，这篇博士论文就会由于我的转行半途而终。我还要好好谢谢我的儿子戎戎，与我一道，相依为命，共渡在美国那段孤独的艰难岁月。他那九岁年龄少见的独立生活能力减轻了我许多的负担。他的活泼与无忧无虑，以及面对困难所展示的乐观与进取，给了我莫大的精神安慰与鼓励。在那艰难岁月里，爷俩一道，留下了许多令人难忘的幸福愉快的回忆。

我要以此篇文献给我的庄启星老师。这篇论文里的许多数据也凝聚着他的巨大的心血。对我们在厦门大学十年的合作，他所给予我的充分信任和巨大支持，我要表示万分的感谢，并对他三年前不幸逝世表示沉痛的哀悼。我还要特别感谢厦门大学化学系其它老师对我在该系十四年里所给予我的巨大帮助与教诲。他们是蔡启瑞先生，万惠林老师，傅金印老师，林国栋老师，张潘贤老师和陈祖炳老师等。同时，也感谢我的学生们对实验数据的贡献。

最后，我要向我的好朋友以及同事对我们共渡的难忘时光，以及对我在生活与工作中所做的巨大的无私的帮助与支持表示深深的感激。独自异乡，求学七载，历程之艰辛，唯朋友知己。若无朋友之肝胆相照，鼎力相助，谈何论文！我将永远记住他们。

陈健，1997年7月20日
于 荷兰 瓦赫林根

CONTENTS

CHAPTER 1 INTRODUCTION	1
1.1 ADVANCED OXIDATION TECHNOLOGIES AND PROCESSES FOR WASTEWATER TREATMENT	2
1.1.1 AOPs (UV/ozone/hydrogen peroxide) for water remediation	2
1.1.1.1 Ozonation for organic compound oxidation	3
1.1.1.2 Applications of UV/ozone for organic compound oxidation	5
1.1.1.3 Applications of UV/hydrogen peroxide and Fenton reactions for organic compound oxidation	5
1.1.2 Non-thermal plasmas (NTP) for air and wastewater treatment	8
1.1.3 Electrohydraulic cavitation and sonolysis for wastewater treatment ..	9
1.1.4 Electron beam and gamma-ray irradiation	9
1.1.5 Catalytic oxidation for air treatment	10
1.1.6 Wet air oxidation for wastewater treatment	10
1.1.7 Supercritical water oxidation treatment	11
1.1.8 Electrochemical redox reactions for wastewater treatment	11
1.1.9 Photocatalysis for wastewater and air treatment	12
1.2 PHOTOCATALYSIS	12
1.2.1 Types of photocatalysis	12
1.2.2 Definition and discussion of photocatalysis	13
1.2.3 Fundamental theory of semiconductor	14
1.2.3.1 Energy bands, band edge and band gap of semiconductor	14
1.2.3.2 n-type and p-type semiconductors, Fermi level, doping, and hole	16
1.2.3.3 Electron equilibrium at a semiconductor-liquid interface in the dark. The formation of a space charge layer and band bending	17
1.2.3.4 Electron equilibrium at a semiconductor-liquid interface during illumination	18
1.2.3.5 Flat band potential and overpotential of semiconductor ..	21
1.2.3.6 Redox potential on a semiconductor	21
1.2.3.7 Optical property of semiconductor	23
1.2.3.8 Metal-semiconductor junctions	25
1.2.4 Brief history of photocatalysis	27
1.2.5 Typical examples of photocatalysis for pollutant treatment	28
1.2.5.1 The photodegradation of halogenated hydrocarbons	28

1.2.5.2 The photocatalytic degradation of insecticides	32
1.2.5.3 The photocatalytic degradation of s-triazine herbicides . . .	32
1.2.5.4 The photocatalytic degradation of surfactants	34
1.2.6 Advantages of and problems associated with photocatalysis compared with other methods	34
1.2.6.1 Advantages	34
1.2.6.2 Problems	35
1.3 OUTLINE OF THIS DISSERTATION	35
1.4 REFERENCES	37
 CHAPTER 2 PHOTOCATALYZED OXIDATION OF ALCOHOLS AND ORGANOCHLORIDES IN THE PRESENCE OF OXYGEN AND METALLIZED TiO₂ SUSPENSIONS	 51
2.1 INTRODUCTION	52
2.2 EXPERIMENTAL	53
2.2.1 Reagent	53
2.2.2 Photocatalyst preparation	53
2.2.3 Apparatus for photocatalytic oxidation	54
2.2.4 The procedure and conditions of the photocatalytic experiments . .	54
2.2.5 Analyses	56
2.3 RESULTS AND DISCUSSION	57
2.3.1 Photocatalytic oxidation of methanol, ethanol, chloroform and TCE in the presence of oxygen: preliminary experiments	57
2.3.2 Photocatalyzed oxidation of methanol in an aerated system	58
2.3.3 Photocatalyzed oxidation of ethanol in an aerated system	59
2.3.4 The effect of pH on the oxidation of alcohols in an aerated system	62
2.3.5 The possible mechanisms of photocatalytic reaction of alcohols . . .	68
2.3.5.1 General introduction	68
2.3.5.2 Cathodic processes in the photocatalyst cathodic area of TiO ₂ , Pt/TiO ₂ or Pd/TiO ₂	69
2.3.5.3 Methanol conversion process on the anodic area of Pt/TiO ₂ in aerated and deaerated system	71
2.3.5.4 Ethanol conversion process on the anodic area of Pt/TiO ₂ in aerated and deaerated system	74
2.3.5.5 Conclusions regarding the role of metallization of TiO ₂ in the photocatalytic oxidation	76
2.3.6 The mechanism of photocatalyzed oxidation of organochlorides in an aerated system	76
2.4 CONCLUSION	81
2.5 REFERENCES	82

CHAPTER 3	KINETIC PROCESSES OF PHOTOCATALYTIC MINERALIZATION OF ALCOHOLS ON METALLIZED AND NATIVE TITANIUM DIOXIDE	85
3.1	INTRODUCTION	86
3.2	THE KINETIC PROCESSES OF HETEROGENEOUS CATALYSIS AND PHOTOCATALYSIS	88
3.2.1	Introduction	88
3.2.2	Langmuir adsorption isotherm for gas phase reactions	90
3.2.3	The kinetic equation for gas reactions in heterogeneous catalysis	91
3.2.4	The mechanism of the photocatalytic oxidation of methanol	94
3.2.5	Powder micro-cell model of a photocatalyst in a slurry system	96
3.2.6	The photocatalytic reduction of oxygen on TiO_2 and Pt/TiO_2	96
3.3	EXPERIMENTAL	97
3.3.1	Reagents	97
3.3.2	Catalyst preparation	97
3.3.2.1	Preparation of TiO_2	97
3.3.2.2	Preparation of 1% wt. Pd/TiO_2	98
3.3.2.3	Preparation of 1% Pt/TiO_2	99
3.3.3	The apparatus used and procedure of the photocatalytic experiments	100
3.3.3.1	The apparatus of the photocatalytic experiments	100
3.3.3.2	The procedure and conditions of the photocatalytic experiments	100
3.3.3.3	X-ray powder crystal diffraction of M/TiO_2 photocatalyst	100
3.3.3.4	The Electron Beam Probe (X-ray exciting spectrum) for surface element analysis of an M/TiO_2 photocatalyst	101
3.3.4	Analytic method	101
3.3.4.1	pH	101
3.3.4.2	Methanol and ethanol concentration	102
3.3.4.3	Carbon dioxide analysis	102
3.3.4.4	Oxygen analysis	102
3.4	RESULTS AND DISCUSSION	102
3.4.1	The results of X-ray powder crystal diffraction of powder Pt/TiO_2 catalysts	102
3.4.2	The results of the X-ray exciting spectrum, and a discussion of a porous micro-cell model	104
3.4.3	Application of the heterogeneous catalysis theory on gas reactions to photocatalytic reactions in aqueous liquids: The Langmuir form of photocatalytic kinetic processes	105
3.4.4	The effect of oxygen concentration on the photocatalytic degradation	

of methanol and ethanol	109
3.5 CONCLUSION	112
3.6 REFERENCE	113
 CHAPTER 4 THE ELIMINATION OF PHENOLS AND COD FROM INDUSTRIAL WASTEWATER BY EMPLOYING PHOTOCHEMICAL METHODS	117
4.1 INTRODUCTION	118
4.2 EXPERIMENTS CARRIED OUT WITH PHOTOCATALYSTS	122
4.2.1 Introduction	122
4.2.2 Experimental procedure for a heterogeneous system of UV/ferric or aluminium compound photocatalyst	122
4.2.3 Experimental procedure for a heterogeneous system of UV/ferric or aluminium compound photocatalyst/calcium oxide or hydroxide as a promoter	124
4.2.4 Experimental procedure for a heterogeneous system of UV/ferric compound photocatalysts/promoter/ hydrogen peroxide	125
4.2.5 Results and Discussion	126
4.2.5.1 Elimination of phenols and COD from industrial wastewater by a heterogeneous system of UV/photocatalyst of Fe_3O_4 or Al_2O_3	126
4.2.5.2 Elimination of phenols and COD from industrial wastewater by a heterogeneous system of UV/photocatalyst of Fe_3O_4 or Al_2O_3 /promoter	128
4.2.5.3 Elimination of phenols and COD from industrial wastewater by a heterogeneous system of UV/photocatalyst of Fe_3O_4 /promoter/hydrogen peroxide	129
4.3 EXPERIMENTS USING PHOTOLYSIS	130
4.3.1 Introduction	130
4.3.2 Experimental procedures of a homogeneous photolytic system ..	131
4.3.3 Results and Discussion	131
4.3.3.1 UV photolytic degradation of phenol	131
4.3.3.2 UV/ H_2O_2 destruction of phenol	131
4.3.3.3 UV/ $\text{FeCl}_3/\text{Fe}^{2+}$ destruction of phenol	133
4.3.3.4 UV/ $\text{H}_2\text{O}_2/\text{FeCl}_3$ destruction of phenol	133
4.4 CONCLUSIONS	134
4.5 REFERENCE	136
 CHAPTER 5 PHOTOCATALYZED DEPOSITION AND CONCENTRATION OF SOLUBLE URANIUM(VI) FROM AQUEOUS SOLUTIONS SUSPENDING TiO_2 OR Pt/TiO_2	139
5.1 INTRODUCTION	140

5.1.1 Traditional treatment of radioactive wastewater	140
5.1.2 Application of photocatalysis on metal-ion deposition	140
5.1.3 Basic principles of photocatalysis for the removal of metal ions in aqueous solutions	141
5.2 EXPERIMENTAL	143
5.2.1 Reagents	143
5.2.2 Catalyst preparation	143
5.2.3 Apparatus and procedures of experiments	144
5.2.4 Analysis	145
5.2.4.1 Uranium(VI) (uranyl)	145
5.2.4.2 CO ₂ and pH	146
5.3 RESULTS AND DISCUSSION	146
5.3.1 Uranium adsorption on TiO ₂	146
5.3.2 Photocatalytic reduction of uranyl on TiO ₂	147
5.3.3 Photocatalytic reduction of uranyl on Pt/TiO ₂	151
5.3.3.1 Initial concentration of uranium(IV) 50 ppm	151
5.3.3.2 Initial concentration of uranium(VI) 25 ppm	153
5.3.4 The most relevant factors that affect uranyl deposition and EDTA mineralization on TiO ₂ or Pt/TiO ₂	157
5.3.5 Decarboxylation of EDTA	159
5.3.6 The possible reductive products of uranyl, and the reduction mechanism	160
5.4 CONCLUSIONS	163
5.5 REFERENCES	164

CHAPTER 6 PHOTOCATALYTIC DEHYDROGENATION OF ETHANOL ON M/CdS USING VISIBLE LIGHT, AND THE ROLES PLAYED BY PHOTOCATALYST PROMOTERS

6.1 INTRODUCTION	168
6.2 EXPERIMENTAL	169
6.2.1 Reagents	169
6.2.2 Preparation of photocatalysts	169
6.2.2.1 Preparation of the photocatalyst Pd/CdS, and its pretreatment before use	169
6.2.2.2 The preparation of a monometallic-component photocatalyst (M/CdS)	170
6.2.2.3 Preparation of bimetalized photocatalysts (M ₂ +M ₁ /CdS)	170
6.2.3 Reaction apparatus	171
6.2.4 Reaction procedure	171
6.2.5 Analysis	173

6.2.6 Surface-structure measurements	173
6.3 RESULTS AND DISCUSSION	173
6.3.1 The effect of the amount of photocatalyst Pd/CdS suspended in solution on the photocatalytic dehydrogenation of ethanol	173
6.3.2 The effect of the particle size of deposited palladium on the photocatalytic activity of CdS	175
6.3.3 The effect of reaction temperature on the photocatalytic activity of Pd/CdS	177
6.3.4 The effect of the concentration of ethanol on its photocatalytic dehydrogenation and on CdS corrosion	177
6.3.5 The effect of pretreatment at a high temperature on the photocatalysts CdS and Pd/CdS	178
6.3.6 The selectivity of the photocatalytic dehydrogenation of ethanol on Pd/CdS	179
6.3.7 The dehydrogenation activity of M/CdS photocatalysts containing a monometallic component	180
6.3.8 The optimum amount of platinum deposited on Pt/CdS	182
6.3.9 The dehydrogenation activity of $M_2 + M_1$ /CdS (<i>i.e.</i> , CdS photocatalysts containing bimetallic components)	182
6.3.10 Optimum proportion of promoter component M_2 on photocatalyst of	185
6.3.11 Possible reaction mechanisms for heterogenous photocatalysis . .	186
6.3.11.1 Surface reaction mechanism at the photocatalyst	186
6.3.11.2 Complex catalysis mechanism involving Pd^{2+} and Pd^0	187
6.3.12 The rate-determining step of ethanol dehydrogenation	187
6.4 CONCLUSIONS	188
6.5 REFERENCES	190
 CHAPTER 7 SUMMARY AND CONCLUSIONS	 191
7.1. Summary and conclusions	192
7.2. Samenvatting (Dutch)	198
 APPENDIX I REFERENCES ON PHOTOCATALYTIC DEGRADATION OF ORGANIC COMPOUNDS (IN TABLE 1.4)	 205
 INDEX	 221

CHAPTER 1 INTRODUCTION

1.1 ADVANCED OXIDATION TECHNOLOGIES AND PROCESSES FOR WASTEWATER TREATMENT

Chemical oxidation technologies for water treatment and disinfection date back to the early 1990s. At that time, the chlorination process became a widespread method for drinking water disinfection. Since that time, ozone processes have also been used for the disinfection of drinking water in Europe. Advanced Oxidation Technologies (AOTs), including Advanced Oxidation Processes (AOPs) and other physicochemical conversion methods, have been widely investigated for about twenty-five years.

Since the 1970s, when drinking water production from surface water using chlorination methods was found to produce toxic trihalomethanes¹, traditional views regarding drinking water preparation changed. Environmental regulations concerning the so-called micropollutants were greatly affected by this and other such discoveries, and this has culminated in the current establishment of regulations restricting maximum contaminant levels of many organic compounds to the $\mu\text{g/L}$ range. There has also been an increasing interest in developing alternative methods for improving the production of drinking water from water containing organic pollutants. Oxidation with ozone or hydrogen peroxide has been found to be an important alternative to chlorination, because the oxidation does not result in toxic chlorinated organic compounds.

In the 1990s, with the rapid development of AOTs for wastewater treatment, many AOTs have received wide interest and have been discussed in various reports^{2,3} and conferences^{4,5}. In addition to traditional AOPs which involve the use of ozone, hydrogen peroxide and ultraviolet light (UV), AOTs presently include several other technologies, such as non-thermal plasmas, electrohydraulic cavitation and sonolysis, electron beam and gamma irradiation, catalytic oxidation, wet air oxidation, supercritical water oxidation, electrochemical oxidation and reduction (electrolysis), photocatalysis and a combination of these technologies, or a combination with biological technologies⁶.

The theme of this dissertation is photocatalytic process for wastewater treatment. Before discussing photocatalytic technology in detail, a short introduction to all of the above-mentioned AOTs for wastewater treatment is presented below.

1.1.1 AOPs (UV/ozone/hydrogen peroxide) for water remediation

The concept of advanced oxidation processes was defined by Glaze *et al.*⁷ in 1987 as processes that "involve the generation of hydroxyl radicals in sufficient quantity to affect water purification." In this context, advanced oxidation processes generally mean the application of either advanced oxidation technologies using UV/O₃, O₃/H₂O₂, UV/H₂O₂ or the photo Fenton

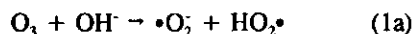
reaction (UV/H₂O₂/Fe²⁺ or Fe³⁺). Peyton⁸ gave a detailed overview and description of AOPs in 1990.

1.1.1.1 Ozonation for organic compound oxidation

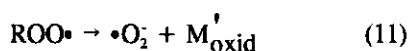
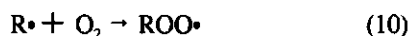
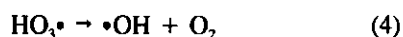
The most important contributions to understanding the chemistry of ozonation during water and wastewater treatment were published by Hoigné and coworkers^{9,10,11,12,13,14}, Glaze *et al.*^{15,16,17,18,19} and Peyton *et al.*^{20, 21, 22, 23}. Other authors^{24,25,26,27,28} have also published very important contributions to UV/ozone and ozone/hydrogen peroxide chemistry.

Mechanisms of the ozonation of organic soluble substrate (M) in aqueous solutions were diagrammed and clearly explained by Staehelin and Hoigné¹³ (see Fig.1.1). The main processes of this complicated diagram involving radical reactions are:

Initiation steps (steps 1a, and d¹), which generate radicals via reactions with OH⁻ and substrate (M) in an aqueous solution:



Propagation steps (steps 3, 4, 9, 10, 11), which maintain the radical reaction chain:



In these steps, radical groups are propagated and maintained through reactions with H⁺ and an organic substrate (M) that has alkyl groups (R). The radical propagation results in the oxidation of the alkyl groups of the substrate (step 11).

Termination step (step 8):



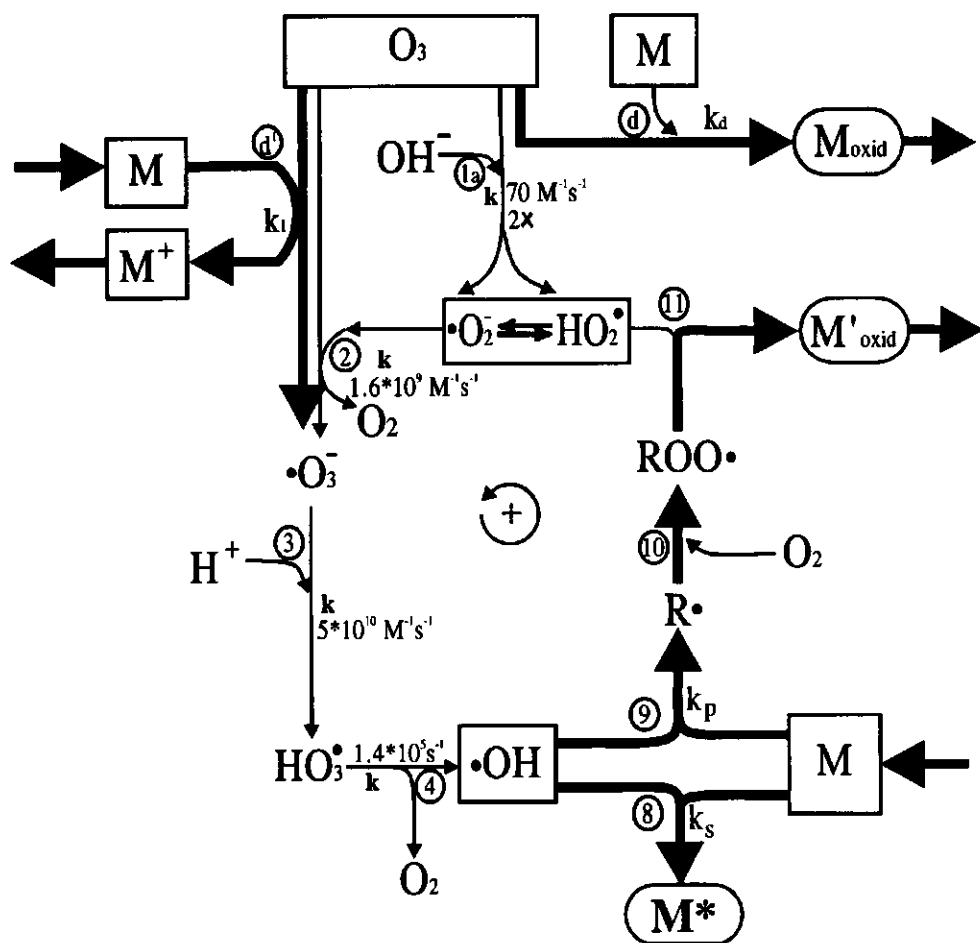


Fig. 1.1 Reactions of aqueous ozone in the presence of an organic compound M which reacts with O_3 or interacts with $\cdot OH$ by scavenging it and/or converting it into HO_2^\cdot . M is an oxidizable substrate in solution; k , k_i , k_d , k_p , k_s are reaction constants.

In step 8, M (e.g., organic substrate or bicarbonate) acts as a radical scavenger, and the radical chain reaction is ended by the formation of product M^* .

1.1.1.2 Applications of UV/ozone for organic compound oxidation

During UV/ozone processes, ozone adsorbs UV light (wavelength shorter than 310 nm) and is photolyzed to produce hydrogen peroxide and hydroxyl radicals (Fig. 1.2(a))⁷ which are able to oxidize organic compounds^{21,22,29}. For efficient ozone photolysis, UV light must have a wavelength at/or shorter than 254 nm. Fronk³⁰ reported that a concentration of 50-384 $\mu\text{g/L}$ of halogenated alkenes and aromatic hydrocarbons could be reduced by 87% and 82%, respectively, by applying an ozone dose of 6 mg/L. Glaze¹⁷ *et al.* and Peyton²³ *et al.* found that halogenated micropollutants such as chloroform, bromodichloromethane and tetrachloroethylene were destroyed four to fifty times faster by UV/ozone than by ozone alone. During these experiments, ozone dose rates of 0.1 - 1.3 mg/L.min and UV intensities of 0.09-0.38 watt/L were used. Since the effect of UV on ozone in an aqueous solution is the production of hydrogen peroxide (Fig. 1.2(a)), an alternative method is to add hydrogen peroxide to the ozone solution (ozone/hydrogen peroxide system) instead of producing it in situ by ozone photolysis (as shown in Fig. 1.2(a)). It is clear from the literature that the oxidative activity and selectivity of ozone depend on the organic compound used as a substrate. A survey of ozonation rate constants for various organic compounds was given by Neta *et al.*^{31,32}

1.1.1.3 Applications of UV/hydrogen peroxide and Fenton reactions for organic compound oxidation

The processes involved in the destruction of organic compounds with UV/hydrogen peroxide are shown in Fig. 1.2(b). Hydrogen peroxide can be photolyzed to produce two hydroxyl radicals if the wavelength of the photons is shorter than 370 nm; these radicals can oxidize organic compounds containing an alkyl group R. Compared with the photolysis of ozone, the photodecomposition efficiency of hydrogen peroxide is very low if the UV light wavelength is longer than 254 nm, which is produced by normal mercury lamps. This is only 0.7% of the adsorption efficiency of ozone at 254 nm^{33,34}. In this respect, a very promising development of the UV/hydrogen peroxide process is the development of lamps that emit efficiently at shorter wavelengths (185 nm), such as the antimony halide lamp^{35,36}.

Since the AOPs using hydrogen peroxide are based on hydroxyl radicals attacking organic compounds in wastewaters, the key to enhancing the oxidation efficiency of hydrogen peroxide is to accelerate its decomposition, producing as many hydroxyl radicals as possible. In addition to employing UV to decompose hydrogen peroxide, a catalyst can be used. An appropriate ferrous ion catalyst was discovered by Fenton in 1894³⁷. The Fenton reagent, a mixture of

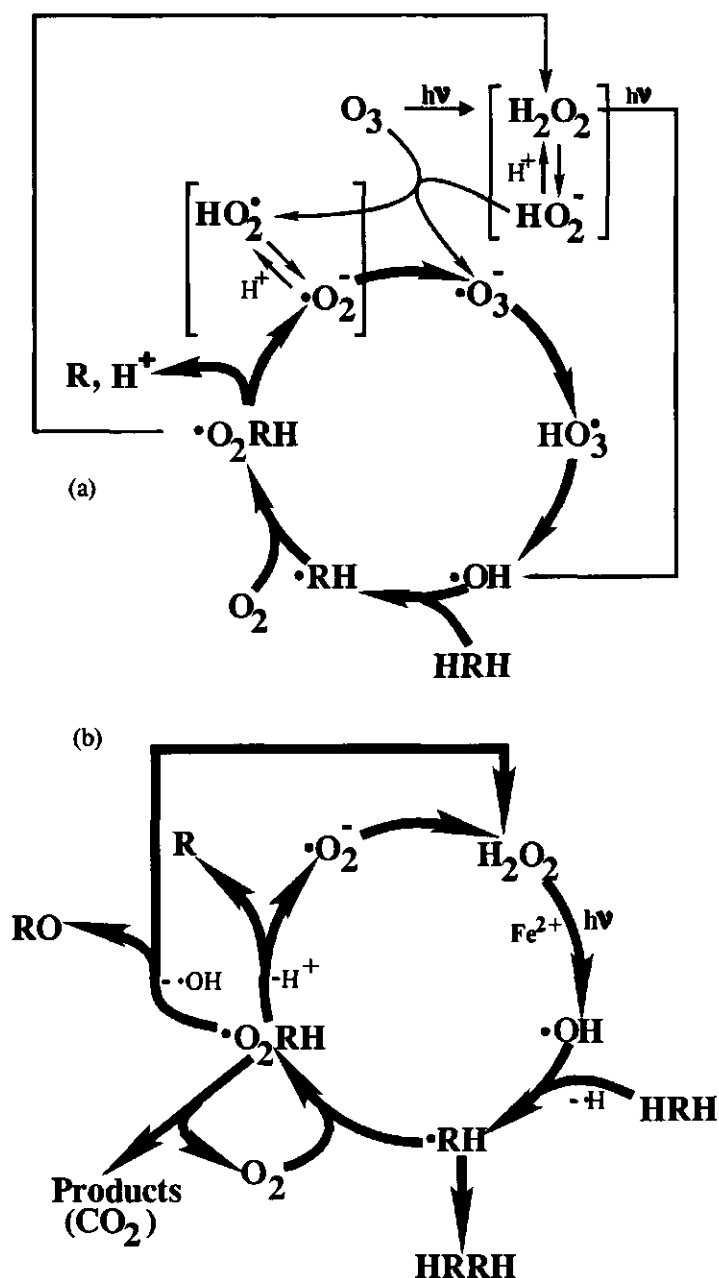
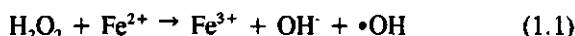
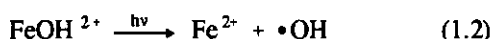


Fig. 1.2 (a). Reaction pathways in ozone/UV and ozone/hydrogen peroxide systems. HRH: organic compounds with alkyl group R. $\cdot RH$: organic alkyl compound with a carbon radical. $\cdot O_2RH$: organic peroxide. (b). Reaction processes in hydrogen peroxide/UV systems and photo Fenton/UV systems⁷.

hydrogen peroxide and ferrous ions has recently been demonstrated to be a very valid oxidant for organic compound degradations. These types of oxidations are called Fenton reactions^{38,39}. In the presence of ferrous ions, hydrogen peroxide can be rapidly decomposed producing hydroxyl radical as below:⁴⁰



Another recent application for wastewater treatment is the use of irradiation with UV or visible light during both Fenton ($\text{H}_2\text{O}_2/\text{Fe}^{2+}$) and Fenton-like ($\text{H}_2\text{O}_2/\text{Fe}^{3+}$) reactions^{41,42}. This application is called the photo Fenton reaction ($\text{UV}/\text{H}_2\text{O}_2/\text{Fe}^{2+}$ or $\text{UV}/\text{H}_2\text{O}_2/\text{Fe}^{3+}$). This reaction shows a higher efficiency during organic compound oxidation than reactions using only Fenton reagent, because Fe^{3+} -photosensitized reactions occur, which involve mainly the photolysis of hydroxide complexes of Fe^{3+} (Eq.1.2), produce hydroxyl radicals and regenerate Fe^{2+} ^{43,44,45}.



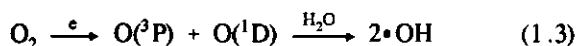
The processes in $\text{H}_2\text{O}_2/\text{UV}$ systems are shown in Fig.1.2b. An interesting application of this reaction was reported by Hager⁴⁶ *et al.*, who studied treatment on a pilot scale of groundwater contaminated with a TCE (trichloroethylene) concentration of 2000-10,000 $\mu\text{g/L}$. This groundwater had a relatively low iron concentration (< 0.05 mg/L) and manganese concentration (< 0.1 mg/L), and contained 160 mg/L bicarbonate. They found the optimum treatment conditions for a 60 gal/min stream to be 50 mg/L hydrogen peroxide and UV lamps with a power of 30 KW. Under these conditions, reduction of TCE from 3700-4000 $\mu\text{g/L}$ to 0.7-0.8 $\mu\text{g/L}$ occurred in 50 seconds at a cost of approximately \$1.00/kgal ($\sim \$ 0.26/\text{m}^3$). Other applications of the photo Fenton reaction are the elimination of herbicides^{47,48}, PCB⁴⁹, phenol⁵⁰, chlorophenol⁵¹, nitrobenzene and nitrophenols⁵² from wastewater. Rate constants of hydroxyl radical reactions with organic compounds have been given in the literature³².

There are some chemical limitations to the use of hydroxyl radical as an oxidant for the degradation of organic compounds, because it is not very suitable for the degradation of such organic compounds such as poly- or per-fluorinated or -chlorinated alkanes. The reason for this is given in § 4.2.5.3.

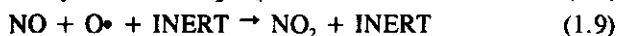
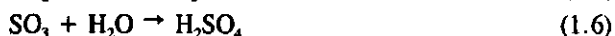
1.1.2 Non-thermal plasmas (NTP) for air and wastewater treatment

Non-thermal plasma technology (NTP)⁵³ is a new advanced oxidation technology which is applied to treat air pollutants⁵⁴ and may also be applied to treat wastewater⁵⁵. The plasma⁵⁶ produced by an electron beam, a pulsed corona discharge or a dielectric-barrier discharge is employed to create large quantities of highly reactive free radicals (mainly atomic oxygen in the ground energy state (O^3P) and oxygen in the first excited energy state (O^1D)⁵⁷, and hydroxyl radicals) in a gaseous medium at a near-ambient temperature. These radicals subsequently react with entrained hazardous organic chemicals, converting them to either nonhazardous substances (CO_2 , H_2O and acids, *i.e.*, mineralized compounds) or other easily manageable compounds. The key to success in the non-thermal plasma approach is that plasma is produced in which most of the electrical energy is converted into highly energetic (reactive) electrons in molecules, rather than a high temperature. Because NTP processes can simultaneously remove or convert different types of pollutant, *e.g.*, volatile organic compounds and oxides of sulphur and nitrogen frequently found in flue gases, it is particularly attractive for many present and future environmental applications⁵⁸.

As an example, we give the mechanism of oxidation of SO_2 and NO by NTP^{59,60,61} in a gas phase also containing H_2O . First we have:



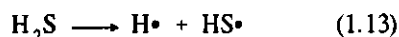
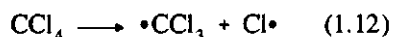
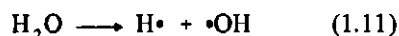
The oxygen atoms ($O \bullet$) produced in different energy states (shown in Eq.1.3) and hydroxyl radicals can react with SO_2 to form H_2SO_4 , and can react with nitrogen oxides to form HNO_3 :



where INERT is any available third compound (usually N_2 or O_2), which is a chemically inert molecule in the reaction meant to stabilize the reaction product⁶². The final product H_2SO_4 (Eq.1.6 and 1.8) forms liquid droplets, while the gaseous reaction product HNO_3 (Eq.1.10) can be removed by the injection of NH_3 or $Ca(OH)_2$ resulting in NH_4NO_3 and $Ca(NO_3)_2$, respectively. H_2SO_4 droplets and particles of NH_4NO_3 or $Ca(NO_3)_2$ can then be removed from the gas stream by using a wet scrubber or an electrostatic precipitator.

1.1.3 Electrohydraulic cavitation and sonolysis for wastewater treatment

Electrohydraulic cavitation involves the formation and behaviour of bubbles in liquids^{63,64}. It is induced by applying electrical energy directly in a water phase^{65,66}. The electrical power is provided by a pulse-powered plasma discharge producing pulsed and/or continuous ultrasonic irradiation (*i.e.*, sonolysis) in water. Kinetic and sonoluminescence measurements indicate that an extremely high temperature (> 5000 °K) and pressure (> 100 atm) are generated during the nearly adiabatic and short-time (< 1 μ s) implosions occurring at the cavitation sites. When a bubble fills with gas and vapour pulses and collapses, molecules inside the bubble or close to the bubble surface are fragmented, escape into the bulk of the solution and react in various ways outside (or inside) the bubble^{67,68}. In this situation, water or pollutants split into radicals as shown in Eq. 1.11 - 1.13.



After the production of these radicals, pollutants such as tetrachloromethane and hydrogen sulphide in the water can be oxidized to final products such as CO_2 , Cl^- and SO_4^{2-} ^{69,70,71}.

1.1.4 Electron beam and gamma-ray irradiation

High-energy electron beams and gamma-rays (*i.e.*, ionizing radiation) are very effective tools for water pollutant degradation. The development of new powerful electron accelerators (*e.g.*, an energy level of 1.0 MeV and a power level of 50 KW, or an energy level of 4.5 MeV and a power level of 400 KW) enables very effective radiation processing of wastewater streams⁷². When a high-energy electron beam or gamma-ray irradiates water, the water (as well as organic compounds contained in it) split into a number of primary species of e_{aq}^- (electrons in aqueous solutions), $\text{H}\cdot$, $\cdot\text{OH}$, H_2 , H_2O_2 , H^+ and OH^- . Some of these primary species then collide with other substrates in water to form more radical species that are oxidants and therefore able to oxidize organic pollutants^{73,74}. As has been observed when using this technology, many organic compounds can be promptly oxidized such as polychlorinated biphenyls (PCBs)^{75,76,77,78}, tetrachloromethane⁷⁹, trichloroethylene (TCE)⁸⁰, tetrachloroethylene (PCE)⁸¹ and benzene⁸².

1.1.5 Catalytic oxidation for air treatment

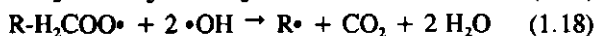
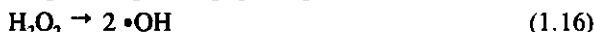
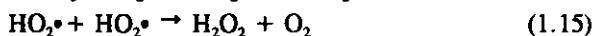
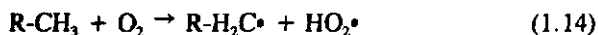
Catalytic oxidation for the treatment of air pollution is an important environmental technology, which has been employed for environmental protection for twenty years^{83,84,85,86}. Catalytic oxidation, also known as catalytic incineration, is the complete chemical conversion of a gaseous organic compound with oxygen at a certain temperature (below or above 100°C) and pressure (one or more than one atm) while both substances are in contact with a solid material (catalyst) that increases the rate of the oxidation reaction. This technology is used for the treatment of organic pollutants in a gas phase, such as automotive emission control^{87,88,89,90}, military life-support systems⁹¹ and control of industrial gas emissions^{92,93}.

Gas phase catalytic oxidation technology has a lot of advantages over other gas phase treatment techniques. At concentrations over 20 to 60 ppm, it is sometimes cheaper than granular activated carbon adsorption and it requires less fuel and less expensive construction materials than high-temperature treatment processes such as incineration. Recent developments of this technology concentrate on the removal of volatile organic compounds^{94,95,96}, including halo-organic compounds^{97,98,99}, from air, as well as on the removal of other organic compounds from other industrial gaseous emissions^{100,101,102,103,104,105}.

1.1.6 Wet air oxidation for wastewater treatment

Wet air oxidation (WAO) is a well-established technology for wastewater treatment, particularly for the treatment of toxic and highly concentrated organic wastewaters^{106,107,108}. It is a chemical oxidation process involving organics or oxidizable inorganic components in an aqueous liquid phase at high temperatures (125 - 320 °C) and pressures (0.5 - 20 MPa), using a gaseous source of oxygen (normally air). WAO has been demonstrated to mineralize various organic compounds to carbon dioxide, water and other inorganic end products such as ammonia, nitrate, nitrogen, chloride, sulphates and phosphate. The oxidation capability of WAO is greatly enhanced if catalysts^{109,110} and oxidants^{111,112,113} such as ozone and hydrogen peroxide are present¹⁰⁸.

Normally, the mechanisms of WAO reactions are radical ones^{114,115}. When WAO is applied at elevated temperatures and pressures without a catalyst, the following reactions may occur in the presence of an organic pollutant R-CH₃:



Eq. 1.18 shows that a long alkyl (R) carboxylic acid molecule will be degraded to a molecule with fewer carbon atoms. Except for carboxylic acids of low molecular weight (especially acetic and propionic acid) and polychlorinated biphenyls (PCBs), most compounds are easily degradable by WAO. At a feed COD higher than 20,000 mg/L, WAO becomes energetically self-sustaining (*i.e.*, no additional fuel is required) and may in fact produce energy in the form of high-pressure steam. One of the most important applications of WAO is the treatment of sewage sludge from municipal wastewater treatment plants¹¹⁶. Most WAO plants built are used for this purpose^{117,118}.

1.1.7 Supercritical water oxidation treatment

Supercritical water oxidation (SCWO) is an intensive version of the WAO process. In recent years, SCWO has become a rapidly developing innovative waste treatment technology for the oxidation of organic wastes and hazardous materials in water^{119,120}. The SCWO process involves the mixing of wastes with an oxidant (oxygen, air, or hydrogen peroxide). The reaction with organic pollutants is carried out at pressures and temperatures above the water critical point (374 °C and 22.13 MPa). The general SCWO reaction temperature range is between 400 and 650 °C¹²¹. Under these conditions, oxidation occurs rapidly (within a few seconds or minutes) and simple products (such as CO₂ and H₂O, and N₂ in the case of nitro-organics) are produced¹²².

SCWO has great advantages as regards the treatment of some refractory organic compounds, including a rapid chemical reaction and no production of nitrogen oxides. The pressure and temperature required can be attained using readily available high-pressure and high-temperature equipment. SCWO has proven to be successful for the disposal of phenol¹²³, halogenated organics¹²⁴, biopharmaceutical wastes¹²⁵, chemical warfare agents, hydrolysed solid rocket propellant, and biological sludges¹²⁶.

1.1.8 Electrochemical redox reactions for wastewater treatment

Electrochemical methods oxidize and reduce pollutants in wastewater by means of electrode reactions (electrolysis). The electrodes needed are available in various shapes (bar, plate, porous and fibre) and are made from various materials. In wastewater, such oxidizable pollutants as organic compounds are oxidized at the anode surface, and such reducible pollutants as most inorganic metal cations are reduced and deposited (in most cases) at cathode surfaces. To bring about the required reaction, a certain electropotential is applied to the anode and cathode. Electrochemical methods are employed mainly for metal ion elimination such as the recovery of copper and lead^{127,128}, mercury(II) and zinc(II)¹²⁹, cobalt(II)¹³⁰, and cadmium, *etc.* Removal of metal ions from the 1-20 ppm level to the ppb level has been reported¹³¹.

Another interesting application of electrochemical methods is cyanide oxidation in wastewater. In most metal-finishing and hydrometallurgical industrial wastewaters containing metal ions (such as gold, silver, chromium) and cyanides, the electrochemical method has an advantage in that simultaneously cyanide is decomposed (oxidized) at the anode and heavy metals are deposited (reduced) at the cathode without causing a sludge problem¹³².

1.1.9 Photocatalysis for wastewater and air treatment

Photocatalysis is the combination of using a photocatalyst and UV or visible light for the treatment of wastewaters and gaseous pollutants. When illuminating a photocatalyst using UV or visible light, various organic compounds (*e.g.*, aromatic, organochloride and organophosphorus compounds) can be oxidized and mineralized at the photocatalyst surface or oxidized in solution under ambient and atmospheric conditions. This is because strong oxidation and reduction sites are produced at the photocatalyst surface when this surface is illuminated with light of the appropriate wavelength. Radicals formed at the surface dissolve in solution and then react with pollutants. It has often been demonstrated that various organic pollutants can be oxidized photocatalytically under the influence of large amounts of free solar energy.

Photocatalysis is one of the most important advanced oxidation technologies. It can be used not only for oxidative treatment of wastewater containing various organic and inorganic compounds, but also for reductive treatment such as reductive deposition of metals from wastewater. Because photocatalysis is the main subject of this dissertation, it is discussed in detail in the paragraphs below.

1.2 PHOTOCATALYSIS

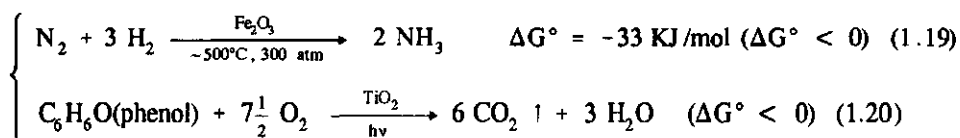
1.2.1 Types of photocatalysis

Most of the research reports about AOTs published over the last twenty years concern photocatalysis. There are two types of photocatalysis: homogeneous photocatalysis, in which a photocatalytic reaction takes place in a homogeneous phase, and heterogeneous photocatalysis, in which the photocatalyst and reactant are present in different phases and the photocatalytic reaction occurs at their interface. Examples of homogeneous photocatalysis in a water phase are the photocatalytic degradation of chlorophenols by the soluble polyoxometalates¹³³ $W_{10}O_{32}^{4-}$, $PW_{12}O_{40}^{3-}$ and $SiW_{12}O_{40}^{4-}$, and the photocatalyzed valence isomerization of norbornadiene to quadricyclane by copper(I) chloride¹³⁴. Photosensitizers, which consist of certain soluble organic dyes, can also be considered homogeneous photocatalysts^{135,136}. Heterogeneous photocatalysis involves a reaction at the surface of a

heterogeneous solid photocatalyst. Photocatalysts are usually semiconductors (TiO_2 , ZnO , Fe_2O_3 , etc.), but they can also be homogeneous photocatalysts (such as water-soluble organic dyes) fixed on a solid carrier¹³⁷. Semiconductor photocatalysts can be applied either as a catalyst fixed on a carrier for wastewater or polluted air treatment^{138,139,140,141}, or as a catalyst-suspension system for wastewater treatment^{142,143,144}. Such a suspension of a powdery semiconductor photocatalyst in water is studied in this thesis.

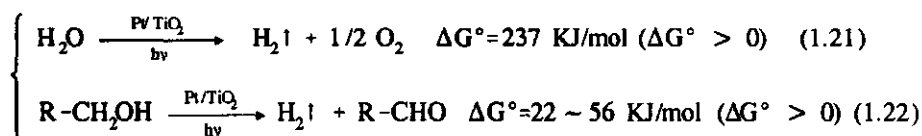
1.2.2 Definition and discussion of photocatalysis

The word "photocatalysis" is composed of the words "photo" and "catalysis" and therefore means catalysis in the presence of light. It implies that the process of a photocatalytic reaction must involve light and a catalyst. "Catalysis" is defined as "an action process of a catalyst on a chemical reaction". "Catalyst" is defined as "a substance which increases the rate at which a chemical reaction approaches equilibrium, without being consumed in the process"¹⁴⁵. The definition of "catalyst" has two important implications: Firstly, it implies that the position of equilibrium attained in the presence of a catalyst is the same as that ultimately attained when no catalyst is present, *i.e.*, a catalyst cannot change the equilibrium of a reaction, it can only reduce the time it takes to reach equilibrium. Secondly, it implies that a catalyst can only increase the rate of reactions with a reaction free energy $\Delta G^\circ < 0$. Examples of such reactions are:



A normal catalyst cannot initiate a reaction with a reaction free energy $\Delta G^\circ > 0$ (for example, the reactions given in Eq. 1.21 and 1.22). In this thesis, "photocatalysis" is defined as "an action process of a photocatalyst on a chemical reaction." "Photocatalyst" is defined here as "a substance associated with photons to activate a chemical reaction and/or to accelerate the rate at which a chemical reaction approaches equilibrium, without being consumed in the process." In contrast to a normal catalyst, a photocatalyst can not only increase the rate of a reaction with a free energy $\Delta G^\circ < 0$, such as ammonia synthesis (Eq. 1.19)^{146,147} and phenol mineralization (Eq. 1.20)^{148,149,150}, but can also initiate a reaction with a free energy $\Delta G^\circ > 0$. Other definitions of photocatalysis are given in the literature^{151,152,153}. Two examples of reactions in which $\Delta G^\circ > 0$ are: the photocatalytic splitting of water to hydrogen and oxygen at the surface of a semiconductor photocatalyst^{154,155,156,157,158}, and the photocatalytic oxidation of alcohol in deaerated systems at the surface of a metallized semiconductor photocatalyst to

produce hydrogen and aldehyde^{159,160,161,162}. Without a photocatalyst or the use of light, the reactions given in Eq.1.21 and 1.22 cannot happen under the standard states of thermodynamic law.



1.2.3 Fundamental theory of semiconductors

In this section, definitions of the most important concepts and terms of semiconductor photocatalysis are briefly presented and explained. For detailed, fundamental, mathematical descriptions and deduction of the semiconductor principles and the photocatalytic process, references are made to the literature^{163,164,165}.

1.2.3.1 Energy bands, band edge and band gap of semiconductors

The electronic state of a single atom or a single molecule can be described by means of electron orbitals with a definite energy. According to the band theory of solid state physics on the formation of a crystal from a large number of atoms or molecules, electron orbitals of similar energy level combine to form a so-called **energy band**. It may be assumed that the energy levels of the electron orbitals in a band are continuous, and that electrons can move easily within a band if it is not fully occupied. Atomic or molecular orbitals with different energy levels form different energy bands. The orbitals of the valence electrons (the highest filled orbits) form the **valence band (VB)**, and the lowest unoccupied orbitals of atoms form the **conduction band (CB)**. The highest energy level in the valence band is called the **valence band edge (E_v)**, which is presented as the energy of the valence band. The lowest energy level in the conduction band is called the **conduction band edge (E_{cb})**, which is presented as the energy of the conduction band.

The energy difference between the valence band edge and the conduction band edge is called **band gap** (or energy gap (E_g)). Materials can be simply classified as conductors (*e.g.*, metal), semiconductors (*e.g.*, certain metal oxides) and insulators based on their band gap. This is shown in Fig. 1.3. There is no band gap for conductors, because in conductors the valence band and conductor band overlap. Therefore, in conductor, electrons can be excited by a tiny external force from fully filled orbitals (VB) to empty orbitals (CB), and moving freely among empty orbits of atoms. Semiconductors have a band gap of around 0.2-4 eV, and as a result of excitation by some types of external force (such as visible light) electrons can move to the

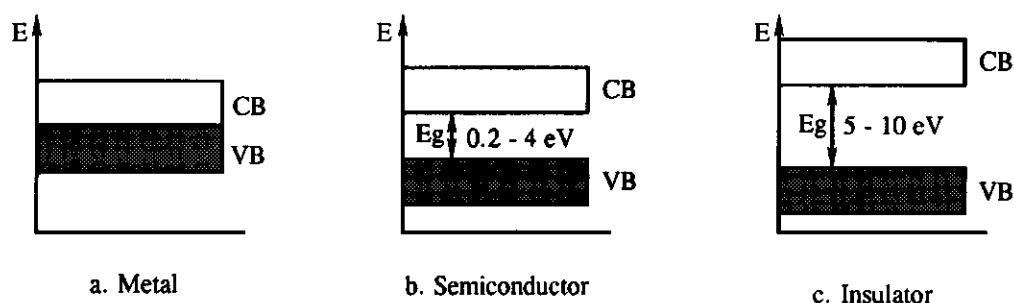


Fig.1.3. Simple diagram of the band and band gap of a metal, semiconductor and insulator. CB: conductor band; VB: valence band; there is a band gap (E_g) between CB and VB. E: energy level.

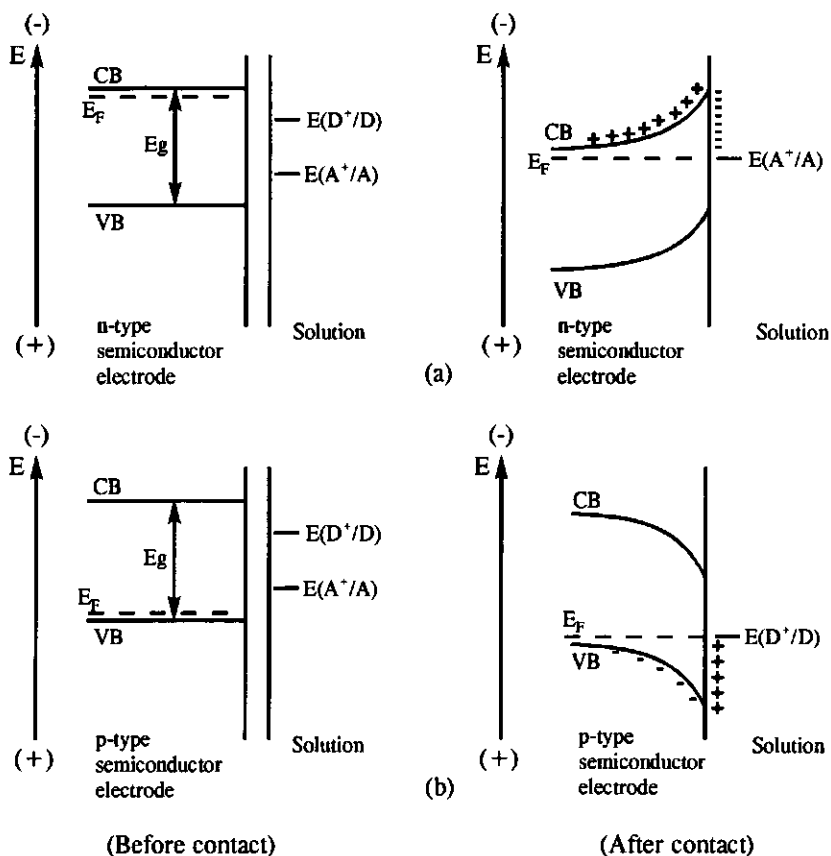


Fig.1.4 The formation of a junction in the dark between a semiconductor and a solution¹⁶⁷ (a) for an n-type semiconductor, (b) for a p-type semiconductor. A^+/A : redox couple accepting electrons. D^+/D : redox couple donating electrons.

empty band of electron energy levels and move among atoms. Some data on band gaps of semiconductors are shown in Table 1.1. Insulators have a band gap of 5 eV or more.

Table 1.1 Energy band gap E_g between the valence and conductor bands as a function of absolute temperature¹⁶⁶

Crystal	E_g (eV)		Crystal	E_g (eV)	
	0 K	300 K		0 K	300 K
Diamond	5.4	-	PbS	0.286	0.34-0.37
Si	1.17	1.14	PbSe	0.165	0.27
Ge	0.744	0.67	PbTe	0.190	0.30
α -Sn	0.00	0.00	CdS	2.582	2.42
InSb	0.24	0.18	CdSe	1.840	1.74
InAs	0.43	0.35	CdTe	1.607	1.45
InP	1.42	1.35	ZnO	3.436	3.2
GaP	2.32	2.26	ZnS	3.91	3.6
GaAs	1.52	1.43	SnTe	0.3	0.18
GaSb	0.81	0.78	AgCl	-	3.2
AlSb	1.65	1.52	AgI	-	2.8
SiC (hex)	3.0	-	Cu ₂ O	2.172	-
Te	0.33	-	TiO ₂	3.03	-
ZnSb	0.56	0.56			

1.2.3.2 n-type and p-type semiconductors, Fermi level, doping, and hole

Normally, a pure (or eigen-) semiconductor is useless for practical application because of its low electrical conductivity. The presence of a trace amount of an impurity in a semiconductor will greatly enhance its electrical conductivity. For example, the addition of boron to silicon at a ratio of 1 to 10^5 can increase the conductivity of pure silicon at room temperature by a factor of 10^3 . A stoichiometric deficiency of one constituent in a semiconductor will act as an impurity. Such semiconductors are referred to as deficit semiconductors. The deliberate addition of impurities to a semiconductor is called **doping**.

If an impurity atom of valence five (*e.g.*, phosphorus, arsenic, antimony) is present in the lattice place of a normal silicon atom, one valence electron of the impurity atom will be left after four covalent bonds with the nearest neighbour have been established. The extra electron is a major charge carrier. An impurity atom that can give up an electron as a free electron in a semiconductor is a donor. This type of impure semiconductor, in which the major charge carrier is an electron, is called an **n-type semiconductor**.

If an impurity atom of valence three (*e.g.*, boron, aluminum, gallium, indium) is present in the lattice place of silicon, it will accept one electron from the valence band to form four valence bonds with the nearest neighbour. In the valence band, a **hole** remains, which seems to move freely within the valence band due to the fact that an electron in a neighbouring atom moves to this hole and produces a new hole at the neighbour. Thus, this type of semiconductor has holes as major charge carriers. An impurity atom that can accept an electron is an acceptor. This type of impure semiconductor is called a **p-type semiconductor**.

The **Fermi level** (E_F) of a semiconductor can be thought of as the average energy of mobile electrons^{163d}. Normally, it is related only to the composition of the semiconductor and to temperature. The Fermi level of n-type semiconductors, in which the major mobile carriers are electrons, is close to the edge of CB because of the distribution of impurity electrons. The Fermi level of p-type semiconductors, in which the major mobile carriers are holes, is close to the VB because of the distribution of holes produced by the impurity. These Fermi levels are diagrammed in Fig. 1.4(a) and (b) where the junction between semiconductors and solution is shown¹⁶⁷.

The Fermi level of electrons in solution refers to a redox couple in solution (*i.e.*, $E_f(\text{redox})$). In photoelectrochemistry, $E_f(\text{redox})$ is frequently considered that it is equal to the redox potential expressed in the vacuum scale (E_{vac}). However, it is not the case in accuracy according to some researches. Detailed discussion and review are given by M. Grätzel and related references^{164, 173a}.

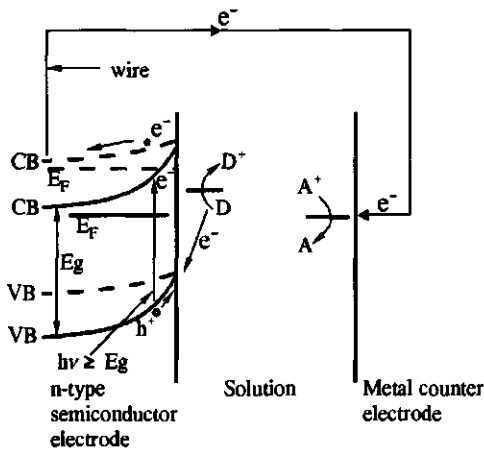
1.2.3.3 Electron equilibrium at a semiconductor-liquid interface in the dark. The formation of a space charge layer and band bending

When a piece of n-type semiconductor is immersed in an aqueous solution, a semiconductor-liquid junction is formed. Fig. 1.4 also shows the equilibrium and the transfer of charges in the dark at the semiconductor electrodes. The electrochemical potential of a solution (*i.e.*, its Fermi level) is determined by one of the redox couples in the solution. In Fig. 1.4a, $E(A^+/A)$ represents a redox couple accepting electrons, and in Fig. 1.4b, $E(D^+/D)$ represents a redox couple donating electrons. For an n-type semiconductor (Fig. 1.4a), the electrochemical

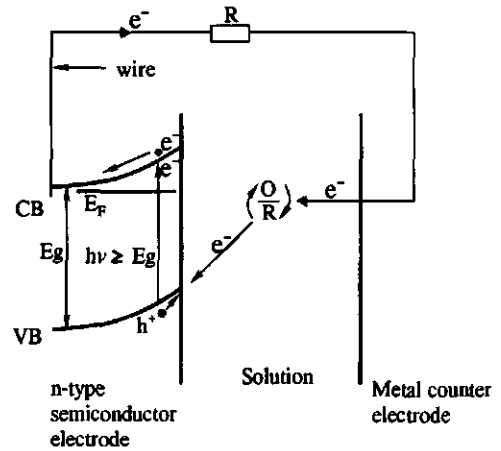
potential of the electrons in the semiconductor (Fermi level E_F) is more negative than that of the redox couple in the solution ($E(A^+/A)$), and electrons will flow from the high-energy n-type material to the low-energy redox species in the solution. This non-Faradaic current will flow until equilibrium is reached, and the electrochemical potentials of these two phases are identical. As a result, in the semiconductor a barrier layer will be formed in which hardly any charge carriers are left. This layer is called **space depletion region** or **space charge layer**; in this layer, the charge carriers moving from the bulk of the semiconductor to the solution are slowed down or stopped. The excess space charge within this layer is distributed by immobile positively ionized donor states, and influences the energy states of the semiconductor. Within the space charge layer, the valence and conduction bands are bent (**band bending**). For a p-type semiconductor, the space charge layer and band bending are diagrammed in Fig. 1.4b.

1.2.3.4 Electron equilibrium at a semiconductor-liquid interface during illumination

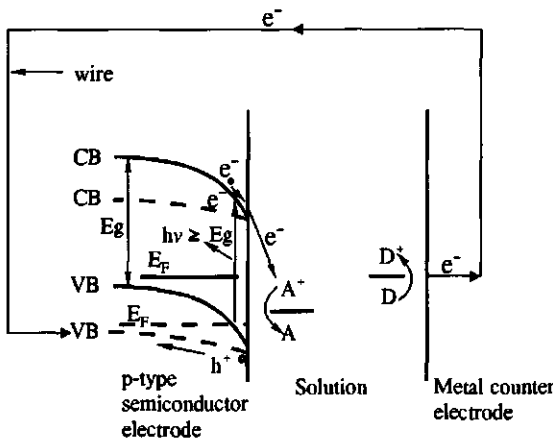
The electron equilibrium states at a semiconductor-liquid interface and the photocatalytic oxidation and reduction processes occurring at this interface are shown in Fig. 1.5¹⁶⁸. In Fig. 1.5a, which shows an n-type semiconductor illuminated using light with an energy ($h\nu$) content larger than or equal to the band gap of the semiconductor ($h\nu \geq E_g$), electron-hole pairs (e^-h^+) are generated. As a result of excitation, electrons in the valence band move to the conduction band, leaving holes in the valence band. As a result of the increase in highly negative energy electrons in the conduction band, the bending of energy bands will decrease (*i.e.*, the energy band will move in a negative direction), because the positively ionized donors in the space charge layer are neutralized by the excited electrons. The holes with the conduction band potential accumulate at the semiconductor surface and either oxidize substrates in the solution (D^+/D) or recombine with electrons in the conduction band. Under the influence of the space charge layer, the excited electrons move to the bulk of the semiconductor and then move to the surface of the metal counter electrode via an external wire, where they can reduce substrates in the solution (A^+/A). Figures 1.5a and 1.5c show photocatalytic cells storing chemical energy. Figures 1.5b and 1.5d show photochemical cells producing electric power which is applied for external load R (*e.g.*, a lamp). In Figures 1.5c and 1.5d, p-type semiconductors are used, and the flow of charge carriers is opposite to that occurring in the case of n-type semiconductors. Under the influence of the space charge layer, electrons accumulate at the semiconductor surface, and holes move to the surface of the metal counter electrode. For a powdery semiconductor photocatalyst suspended in an aqueous solution, the electron equilibrium at the semiconductor-liquid^{164, 173(a)} interface and the photocatalytic oxidation and reduction processes are shown in Fig. 1.6, which are in fact similar to those shown in Fig. 1.5.



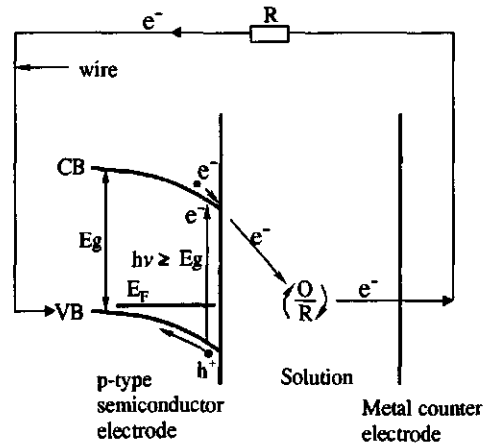
(a). Photocatalytic cell with an n-type semiconductor



(b). Photochemical voltaic cell with an n-type semiconductor



(c). Photocatalytic cell with a p-type semiconductor



(d). Photochemical voltaic cell with a p-type semiconductor

Fig.1.5. Photochemical cells¹⁰⁸. (a) and (c): photocatalytic cells which convert photo energy into chemical energy via oxidizing (D^+/D) and reducing (A^+/A) redox couples in solution such as splitting water to hydrogen and oxygen, or eliminating pollutants in water. The dashed lines express band bending decrease and Fermi level E_F increase after illumination. (b) and (d): photochemical voltaic cells of converting photo energy into electric energy which is used by the external load (R) connected to the cells, where O/R is a redox couple.

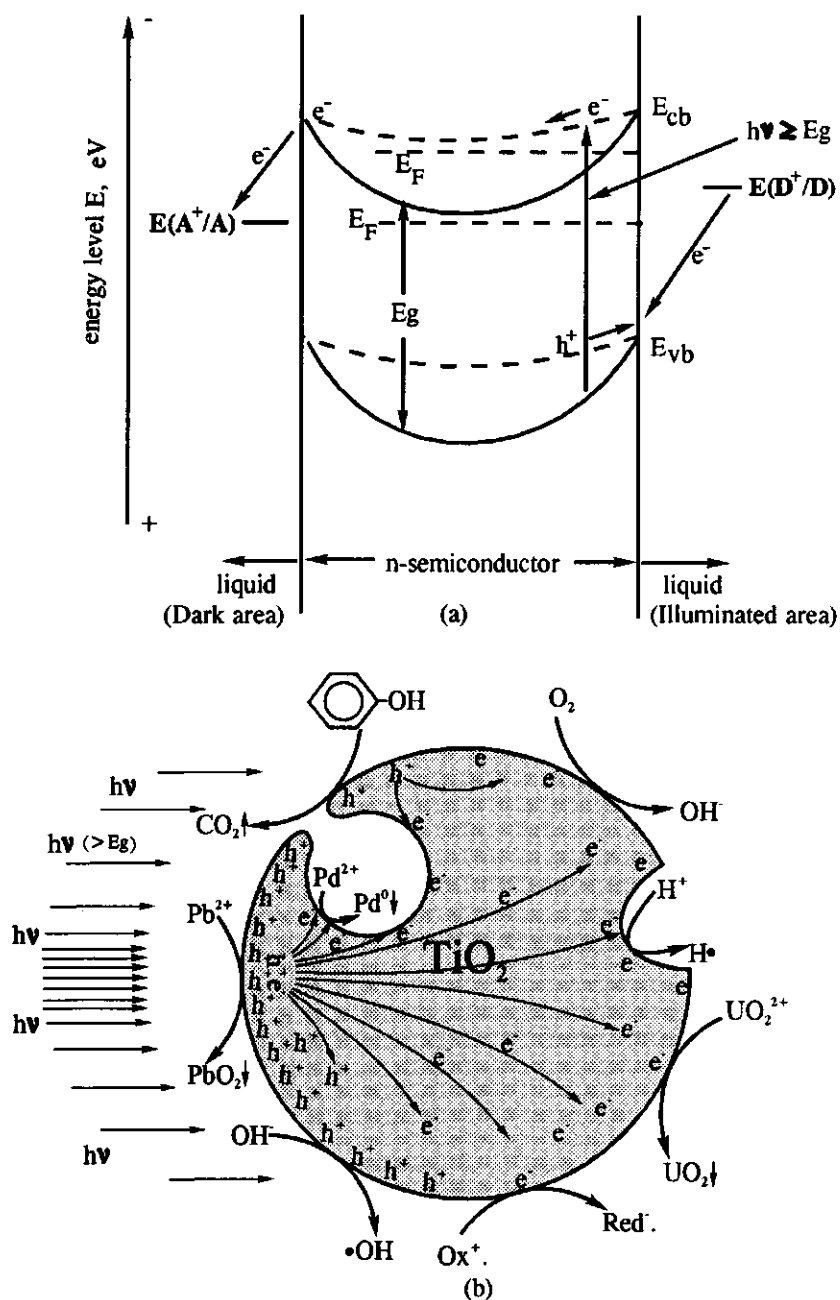


Fig. 1.6 (a) The process of charge transfer and equilibrium at the interface of a solid and a liquid for an n-type semiconductor in an aqueous solution. The solid line indicates the situation in the dark, and the dashed line indicates the situation in the case of illumination. E_{cb} is the conduction band edge. E_{vb} is the valence band edge^{164(a)}. (b) A model of a porous micro-cell for a powdery semiconductor photocatalyst suspended in a liquid.

1.2.3.5 Flat band potential and overpotential of semiconductors

When a semiconductor is immersed in a solution, the energy bands bend because of the electron transfer from the semiconductor to the redox couples in the solution. During illumination, the bending of bands decreases and the Fermi level of the semiconductor gradually moves to its original position. If the light density is strong enough and the electrons can accumulate in the CB without moving out of it (*i.e.*, into solution or by recombination) too fast, the space charge region or depletion field will disappear and the bands will become flat. The potential of the Fermi level at this flat band position is called the **flat band potential**. For n-type semiconductors the flat band potential is close to CB, and for p-type semiconductors it is close to VB¹⁶⁷. The flat band position is the maximum potential that semiconductors can reach and that can be measured during experiments. It is an important parameter for assessing whether a semiconductor photocatalyst has suitable potential to oxidize or reduce pollutants.

The **overpotential** (η) is defined as¹⁶⁹:

$$\eta = E - E_e \quad (1.23)$$

where E is the electrode potential of a considered electrode reaction under given conditions, and E_e the equilibrium electrode potential of the electrode reaction. For example, the E_e of the H^+/H_2 couple under standard conditions is $E_e = 0$ Volt, but under the same conditions, hydrogen production at a nickel surface requires an E_e of -0.21 Volt, at a zinc surface one of -0.70 Volt, and at a platinum surface one of -0.005 Volt. Thus, in this example platinum has the lowest overpotential ($\eta = -0.005$ V)^{170, 171}. In practice, an overpotential requires much more energy to carry out a reaction than in theory. This is generally due to electrode polarization and the diffusion of reactants. Semiconductor oxides normally have a high overpotential. As a result, some reactions which are normally thermodynamically possible become impossible. Fig.1.7 shows the band edge positions (energy levels) and band gaps for a number of semiconductors^{164, 173(a), 172}. The flat band potential at the TiO_2 surface is around -0.05 Volt; theoretically, the H_2/H^+ reaction (resulting in H_2) can be carried out at this potential. However, due to the high overpotential of TiO_2 for this reaction, in practice this is not possible. TiO_2 surfaces are therefore modified with a noble metal of low overpotential, such as platinum.

1.2.3.6 Redox potential on a semiconductor

In a semiconductor, the band edges of the filled VB and empty CB are the only energy levels that an electron can occupy to be involved in reactions with substrates in a liquid. The redox potentials of a semiconductor are determined based on the band edge positions of VB and CB (as shown in Fig.1.7) and its Fermi level. During illumination, it is thermodynamically

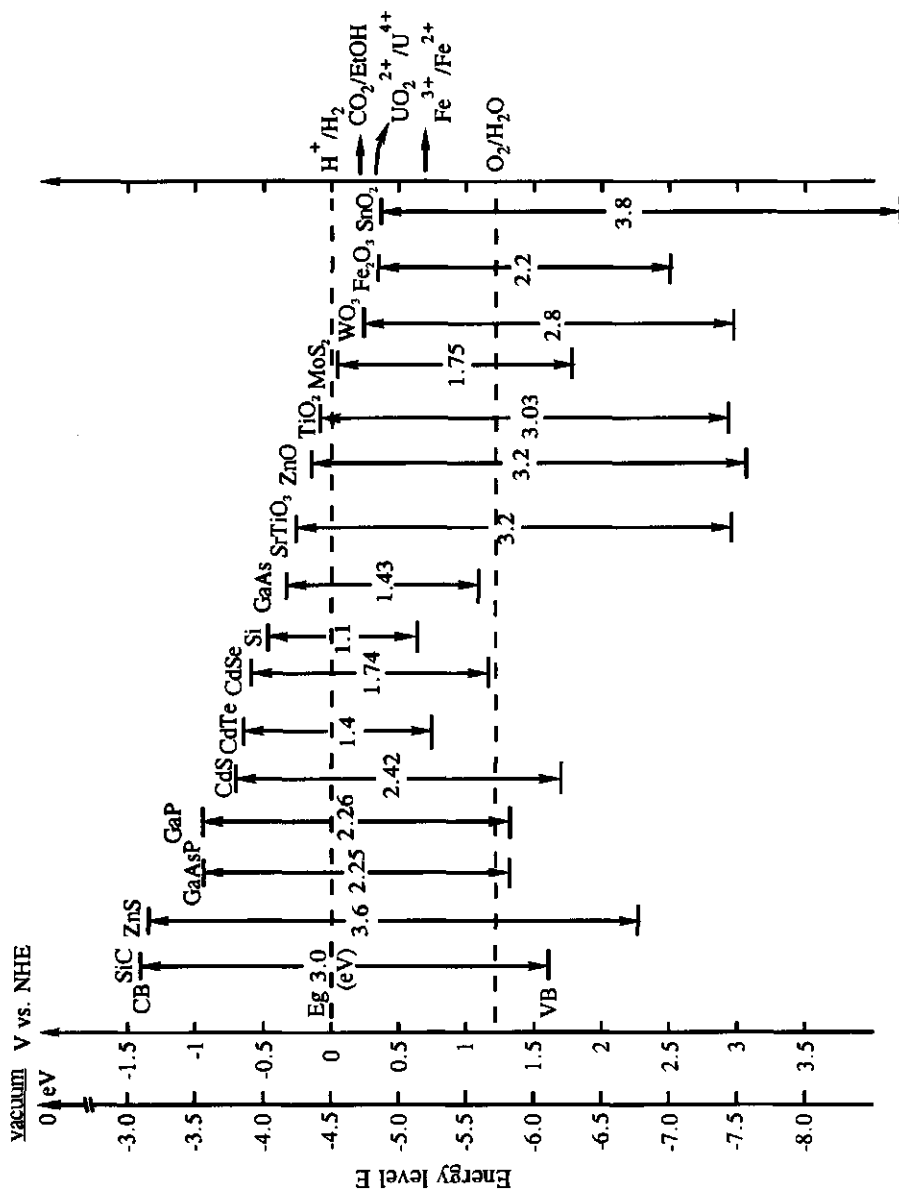


Fig. 1.7. The band edge positions (energy values) of the conduction band (CB) and the valence band (VB) (vs. standard hydrogen electropotential NHE), and the band gap energies (Eg) of various semiconductors at pH = 0^{164(0.172)}. The dashed lines indicate standard electrochemical potentials of the redox couple H₂/H⁺ and H₂O/O₂. Vacuum indicates the zero energy level.

possible for an electron at the edge of the CB to reduce a reactant whose redox potential position is lower than the CB edge, and for a hole at the edge of the VB to oxidize a reactant whose redox potential position is higher than the VB. To be a good photocatalyst, a semiconductor therefore must have a suitable flat band potential for the required redox reactions in solutions. For example, according to Fig.1.7 the excited electron in the semiconductor CdS can reduce oxygen to water, because its flat band potential is more negative than the potential of the O_2/H_2O couple, and the hole in the valence band can oxidize ethanol (EtOH) to carbon dioxide because its potential is more positive than that of the $CO_2/EtOH$ couple. GaAs can oxidize ethanol to CO_2 but cannot oxidize water to oxygen, because its valence band edge is more negative than the potential of the O_2/H_2O couple. MoS_2 can reduce oxygen to water but cannot reduce protons to hydrogen (H^+/H_2).

1.2.3.7 Optical property of semiconductors

One of the important properties of a semiconductor is its optical property. Since a semiconductor has a band gap of around 0.2 to 4 eV, which is moderate, the photo energy of ultraviolet and visible light can be converted to electric or chemical energy through the excitation of electrons from the valence band to the conductor band. Fig.1.8 shows the spectrum range of electro-magnetic radiation^{164, 173, 173}. The range of radiation in which we are interested is ultraviolet and visible light with a wavelength of between 100 nm and 1,000 nm. The wavelength of light must be equal to or lower than a certain threshold value, *i.e.*, the energy of photons must be equal to or larger than the band gap of semiconductors. Threshold wavelength λ_{photo} can be expressed as:

$$\lambda_{photo} \text{ (nm)} = 1,240/E_g(\text{eV}) \quad (1.24)$$

For example, the band gap of TiO_2 is 3.03 eV. Therefore, the threshold wavelength is $\lambda_{photo} = 1,240/3.03 = 409$ nm, which is near-UV light. It means that only a light wavelength lower than 409 nm can excite electrons in the TiO_2 valence band to the conductor band.

The absorption of photons in a semiconductor can be expressed using the exponential law:

$$I/I_0 = \exp(-\alpha(E)l) \quad (1.25)$$

where $\alpha(E)$ is the absorption coefficient for a photon with energy E , l the distance over which light penetrates into the solid, I the intensity of the transmitted light, and I_0 the intensity of the incident light. For TiO_2 , $\alpha = 2.6 \times 10^4 \text{ cm}^{-1}$ at 320 nm, which means that light of 320 nm wavelength is extinguished by 90% after being transmitted over a distance of 3,900 Å in the bulk of TiO_2 .

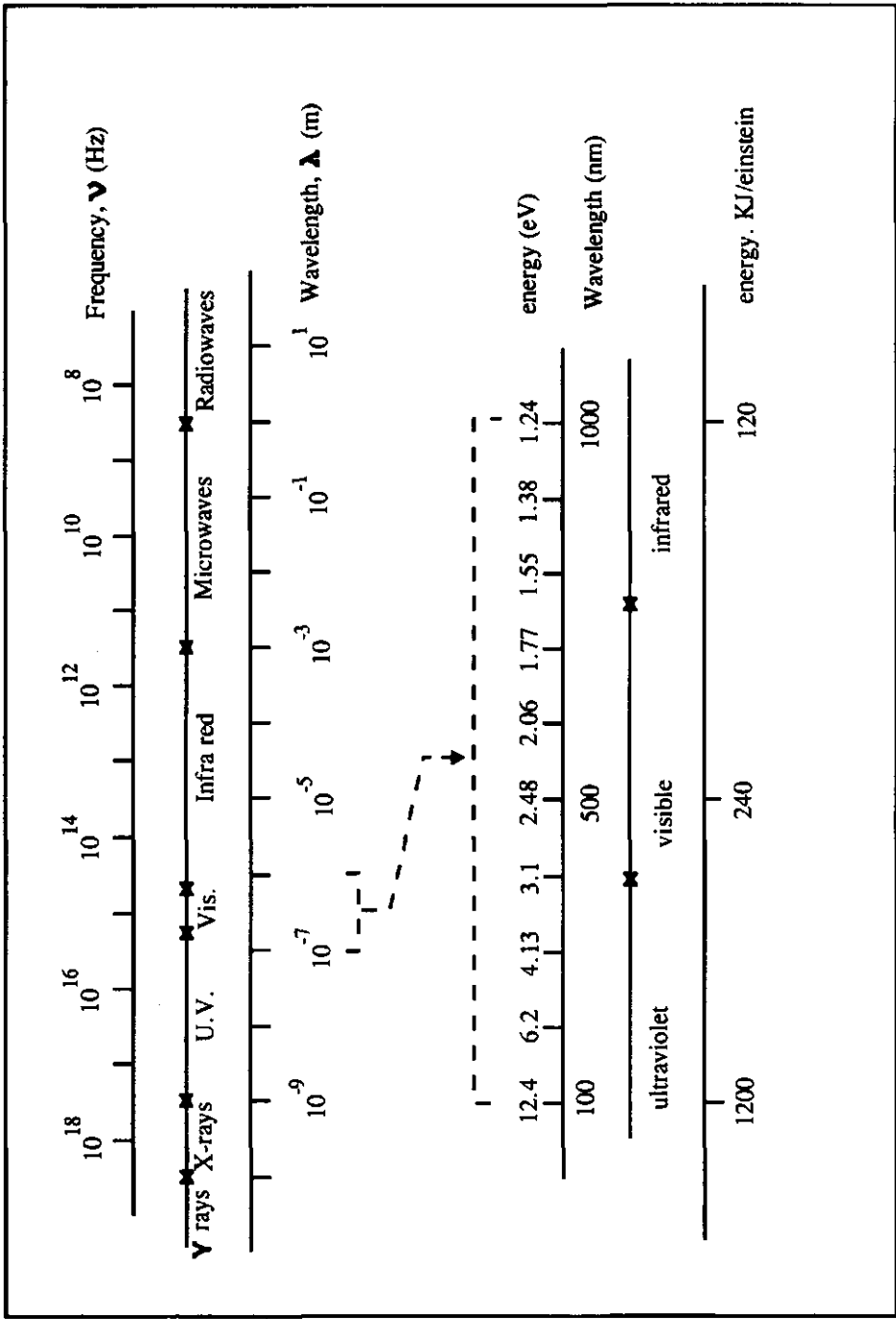


Fig.1.8. The spectrum ranges of various electromagnetic radiations^{[64a],173}

1.2.3.8 Metal-semiconductor junctions

The metal-semiconductor junction is an important concept for a photocatalyst consisting of a metallized semiconductor (e.g., Pt/TiO₂, Pd/TiO₂, Pt/CdS). When a metal is in contact with a semiconductor, an electrostatic potential barrier is formed between the metal and semiconductor whose value depends on their work functions ϕ . **Work function ϕ** is the energy needed to excite an electron from Fermi level to vacuum level (defined as 0 eV). Schottky developed a simple theory called the Schottky contact or Schottky barrier theory, which describes the contact between a metal and a semiconductor. Fig. 1.9 diagrams how Schottky barriers occurring are formed when a metal and a semiconductor physically come into contact with each other^{163(b)}.

To understand the property of a Schottky barrier, consider an ideal contact between a metal with work function ϕ_m and an n-type semiconductor with **electron affinity χ** (defined as the energy required to transfer an electron from the bottom of the conduction band to the vacuum level). Diagrams of the energy bands existing just after contact between a metal and an n-type semiconductor are represented in Figures 1.9a and c. Work function ϕ_s of the semiconductor is the difference in energy between the semiconductor's Fermi level and vacuum level. For an n-type semiconductor, the difference between χ and ϕ_m is very small, because its Fermi level is very close to the bottom of the conduction band. However, for a p-type semiconductor, the difference between χ and ϕ_m is almost the entire width of the band gap.

There are two types of situations that can arise when a metal and a semiconductor are brought into contact with each other. If $\phi_m > \phi_s$, electrons will flow from the semiconductor to the metal. As a result (see Fig. 1.9b), the metal will get a negative surface charge, but its Fermi level will not change. Because of the loss of electrons, the Fermi level of the semiconductor will decrease. Because the donors are of relatively low density, they will become ionized over a region extending into the bulk of the semiconductor, *i.e.*, a space charge region is created. In this case, at the junction an electrostatic potential barrier is formed, which is called a **Schottky barrier** or a **Schottky contact**.

An important electrical property of a Schottky barrier is its rectifying ability, meaning that electrons can flow in only one direction, namely from the semiconductor to the metal (see Fig. 1.9b). If an external electrical field is added of which the charge sign is the same as that of the Schottky barrier, this field intensifies the Schottky barrier and thus slows down the flow of electrons. However, if an external electrical field is applied of which the charge sign is opposite to that of the Schottky barrier, this barrier will be weakened and electrons can flow in the one direction from semiconductor to metal.

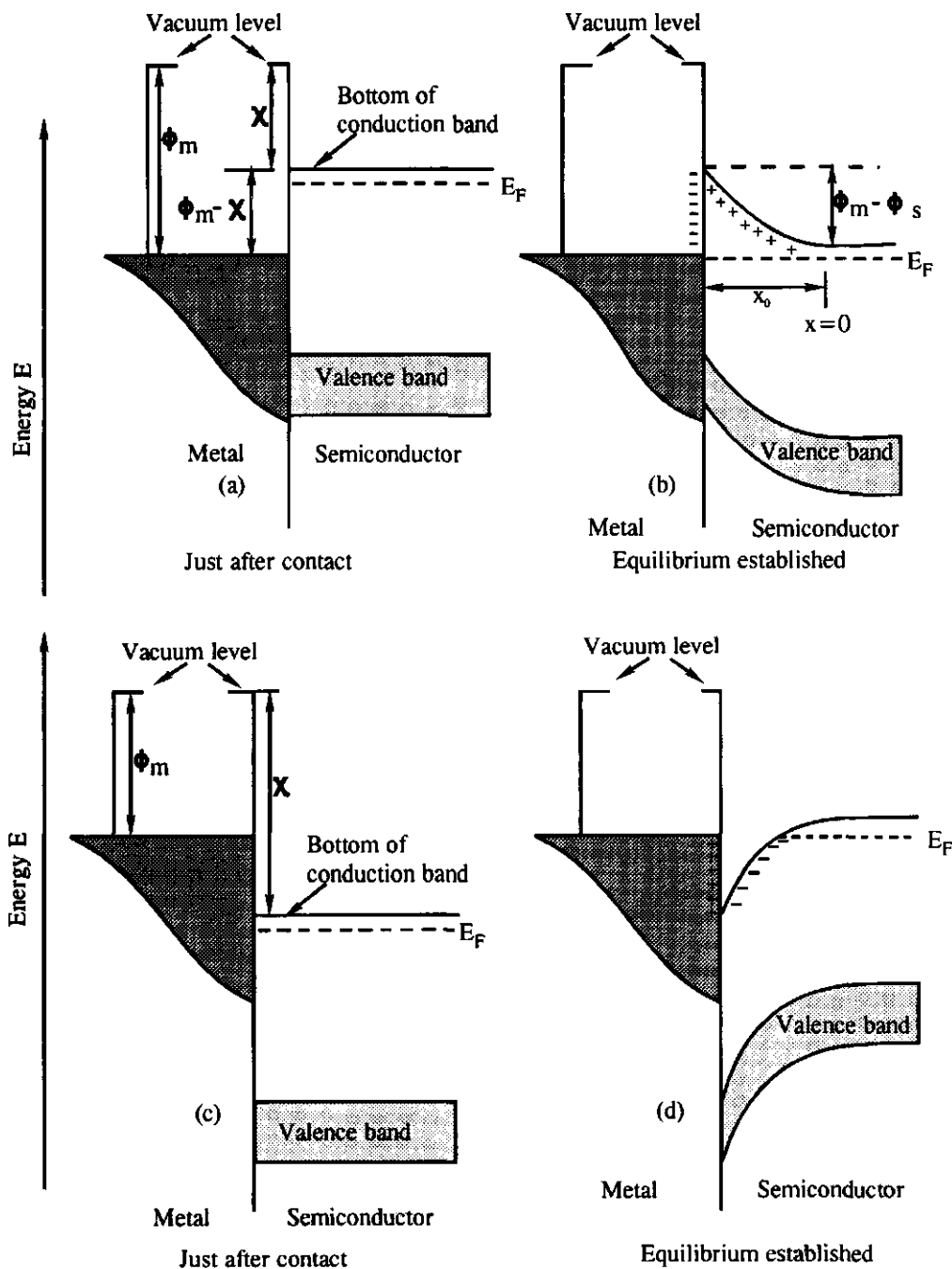


Fig.1.9. The formation of Schottky barriers of metal-semiconductor junction (n-type semiconductor)^{163(b)}. $\phi_m - \phi_s$ is the amount of band bending. X_0 is the width of the space charge layer. (b) is a Schottky barrier, which has a rectifying property. (d) is a Schottky

Another important property of the Schottky barrier is shown in Figures 1.9c and 1.9d. If $\phi_m < \phi_s$, electrons will flow from the metal to the semiconductor, because in a metal electrons have a higher energy level than in a semiconductor. Next, (see Fig. 1.9d) the metal gets a positive surface charge because of losing electrons, and the Fermi level of the semiconductor increases because the semiconductor receives electrons. The transmission of charge and formation of a space charge region will approach a state of equilibrium in which the Fermi level of the semiconductor is equal to that of the metal. The values for $\phi_m - \phi_s$ in Figures 1.9d and 1.9b differ, because in Figure 1.9d the space charge region created is not a potential barrier but a potential trap, which can be called a Schottky trap. The difference between a Schottky trap and a Schottky barrier is that in the case of Schottky trap electrons can flow in two directions at the metal-semiconductor junction depending on the direction of an added external electrical field. Such a metal-semiconductor junction forming a Schottky trap is normally called an **Ohmic contact** because it satisfies Ohm's law. Some data on the work function of metals (ϕ_m) are listed in Table 1.2, and the work function of a semiconductor (ϕ_s) can be estimated based on Fig. 1.7.

The distinction between a Schottky contact and an Ohmic contact has important consequences for the catalytic properties of metals at a semiconductor surface. In the case of a Schottky contact, the metal acts as a reduction position. From Table 1.2 and Fig. 1.7, it can be derived that this is the case for Pt/TiO₂ and Pd/TiO₂.

Table 1.2 Values of work function ϕ_m (eV) for some common metals¹⁶⁵.

Metal	Pt	Ni	Pd	Au	Co	Cu	Mo	W	Fe	Cr
ϕ_m	5.65	5.15	5.12	5.1	5.0	4.65	4.6	4.55	4.5	4.5
Metal	Sn	Ti	Al	Ag	Ta	Ga	In	Mg	Ca	Ba
ϕ_m	4.42	4.33	4.28	4.26	4.25	4.2	4.12	3.66	2.87	2.7

1.2.4 Brief history of photocatalysis

Research into photocatalysis dates back to the 1930s when Plotnikov defined photocatalysis in his book "Allgemeine Photochemie"¹⁷⁴. In the early 1950s, Markham and Laidler reported a kinetic study of photo-oxidation at the surface of zinc oxide in aqueous suspensions¹⁷⁵. In 1971, reports appeared about the surface properties of such metal oxides as TiO₂ and ZnO and the chemical reactions occurring at their surface^{176,177,178,179,180}. Internationally, photocatalysis

received much more attention since the beginning of the 1970s, when the war in the Middle East caused the first energy crisis and researchers discovered that water can be decomposed photocatalytically into hydrogen and oxygen at ambient temperature and atmospheric pressure in a photoelectrochemical cell using a TiO_2 single-crystal anode¹⁸¹. This principle was considered very important for the final solution of the energy problem of man. Water cannot be split under ambient and moderate chemical conditions (*e.g.*, at ambient temperature and pressure) because the free energy (ΔG°) of this reaction is larger than zero, unless extra power is used, *e.g.*, by irradiation with photons.

At the end of the 1970s and at the beginning of the 1980s, with the start of an increasing awareness of the urgent need to protect our environment, people involved in environmental protection began to pay attention to this new technology of photocatalysis. Photocatalysis is not only an advanced oxidation technology for the elimination of organic compounds from wastewater and air, but can also be applied for the reductive elimination of many inorganic compounds from wastewaters.

A large number of reports on the photocatalytic treatment of organic and inorganic compounds have appeared since 1980. During investigations into the general applicability of the technology, a wide variety of toxic chemicals were degraded in the presence of various semiconductor photocatalysts. Several books have been published on the topic of photocatalysis^{182,183,184,185, 186,187,188} and a lot of review papers have appeared since the 1970s^{167,168,189,190,191,192,193,194,195,196,197}. Most studies on photocatalytic treatment are the studies of kinetic processes, of the elimination and mineralization of pollutants from wastewater and polluted gases, of the effect of various parameters on photocatalytic processes, and of the properties of various intermediates. The topics of all these studies are represented in Tables 1.3 and 1.4, which summarise the photocatalytic elimination of various inorganic compounds and organic compounds.

1.2.5 Typical examples of photocatalysis for pollutant treatment

Many reports on the photo-elimination of organic and inorganic pollutants have been published, including reports on various photocatalytic theories, designs, methods and technologies. Some typical examples are given below.

1.2.5.1 The photodegradation of halogenated hydrocarbons

Between 1983 and 1985, Ollis *et al.*¹⁹⁵ first carried out a series of thorough experiments regarding the heterogeneous photocatalytic degradation of halogenated hydrocarbons and suggested the possible applicability of photocatalysis as an innovative environmental technology. During these experiments, photocatalytic dechlorination, debromination and

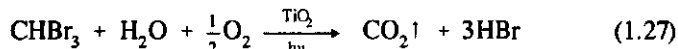
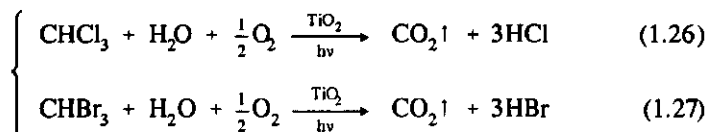
mineralization of halogenated hydrocarbons in water were studied. Examples of reactions are given in Eq. 1.26 and 1.27.

Table 1.3 Inorganic compounds that can be degraded or recovered by photocatalytic processes.

Compounds	References
Ammonia	198, 199, 200
Cobalt (Co^{2+})	201201
Cadmium (Cd^{2+})	202202, 203203, 204204
Carbon oxide	205205, 206206, 207207
Chromate (Cr^{6+})	202, 208208, 209209
Copper (Cu^{2+})	202, 203, 204
Cyanide (CN^-)	210210, 211211
Gold (Au^{3+})	211, 212212
Hydrogen sulphide (H_2S)	213213, 214214
Lead (Pb^{2+})	201, 215215
Manganese (Mn^{2+})	201
Mercury (Hg^{2+})	203, 216216
Nickel (Ni^{2+})	203
Nitric oxide	198, 206
Palladium (Pd^{2+})	212
Persulphate ($\text{S}_2\text{O}_8^{2-}$)	211
Platinum (Pt^{4+})	203, 212
Rhodium (Rh^{3+})	212
Silver (Ag^+)	203, 217217
Sulphite (SO_3^{2-})	214
Thallium (Tl^+)	201
Uranium (U^{6+})	218, 219

Table 1.4 Organic compounds and classes of compounds that can be oxidized using photocatalytic processes. (The references for Table 1.4 are given in Appendix I).

Acetic acid	Dichlorobiphenyl	Organic carbon
Acetylene	Dichloroethane	Organic solutes
Alcohols	Dichloromethane	Organics
Aldehydes	Dimedthoxybenzenes	Organo-nitrates
Aliphatic alcohols	Dimethyl-2-butene	Organochlorine
Alkanes	Dodecane	Organophosphate
Alkylbenzaldehydes	Dye compounds	Organophosphorous
Anthraquinone-2-sulphonic	Ethanoic acid	Polychlorinated biphenyls (PCBs)
Aromatics	Ethoxyethanol	Pentachlorophenol
Atrazine	Ethylene glycol	Perchloroethylene
Bentazon	Formic acid	Pesticides
Benzene	Furandimethanol	Ph ₃ CCOOH
Benzoic acid	Halobenzenes	Phenol(s)
Butanol	Haloorganics	Polychlorinated dioxins
Chlorinated dioxins	Halothane	Polynuclear aromatic compounds
Chlorinated phenols	Hydrocarbons	Propan-2-ol
Chloro-3-(pddm)-diazirine	Hydroxybenzoic acid	Propene
Chloro-4-hydroxybenzoic	Isobutane	Propionic acid
Chlorofluorocarbons	Isopropanol	Pyridine
Chlorofluoromethanes	Methanol	Salicylic acid
Chloroform	Methyl orange	Sulphonated aromatics
Chloromethane	Methyl viologen	Surfactants
Chloronitrobenzenes	Methylbutane	Tetrachloroethene
Chloroorganics	Methylbutanols	Tetrachloromethane
Chlorophenol	Methylene blue	Thioethers
Chlorosalicylic acid	Naphthalene	Toluene
Cyclic ethers	Nitrogen-organics	Trichloroethane
Cyclohexane	Nitroguanidene	Trichloroethylene
DDT	Nitrophenol	Tetrachloroethylene
Dibromo 3-chloro propane	Odour compounds	Trichlorophenols
Dibromoethane	Oligocarboxylic acids	Trichlorophenoxy-acetic acid
Dichlorobenzene	Organic acids	Triethylamine



The degradation rate constant (k) and the apparent adsorption constant (K) of the reactant at the catalyst surface were first calculated by Ollis *et al.* according to the Langmuir-Hinshelwood kinetic model, which is given by the equation:

$$\gamma = k KC / (1 + KC) \quad (1.28)$$

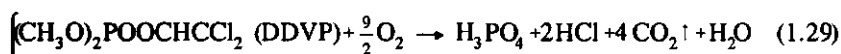
where γ is the reaction rate of the reactant and C the reactant concentration in solution. The results are shown in Table 1.5. In Chapter 3, the Langmuir-Hinshelwood kinetic model will be discussed in more detail.

Table 1.5. Rate and equilibrium constants for the mineralization of halogenated hydrocarbons on native TiO_2 ¹⁹⁵. k = the rate constant of the degradation reaction (ppm/min.g.cat.). K = the apparent adsorption constant of the reactant at the illuminated catalyst surface (ppm⁻¹).

Compound	k	K	Compound	k	K
CH_2Cl_2	1.6	0.02	$\text{H}_2\text{ClC-CClH}_2$	1.1	0.01
CHCl_3	4.4	0.003	CHBr_2CH_3	3.9	0.02
CCl_4	0.18	0.005	$\text{CH}_2\text{BrCH}_2\text{Br}$	2.2	0.02
CH_2Br_2	4.1	0.02	CH_2ClCOOH	5.5	0.002
CHBr_3	6.2	0.01	CHCl_2COOH	8.5	0.003
$\text{Cl}_2\text{C=CHCl}$	830	0.01	Cl_3CCOOH	0.0	--
$\text{Cl}_2\text{C=CCl}_2$	6.8	0.02			

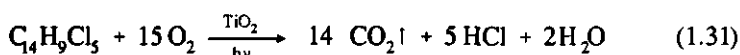
1.2.5.2 The photocatalytic degradation of insecticides

The treatment of wastewater containing insecticides and herbicides (normally organic phosphorus and/or organic chloride compounds at low concentrations in surface and ground water) is one of the hardest environmental problems. Photocatalytic methods show great advantages regarding the degradation of these compounds. Pelizzetti and Serpone *et al.*²²⁰, Grätzel *et al.*²²¹, Tanaka *et al.*²²² and Huang *et al.*²²³ reported some valuable work on these complicated compounds. DDVP (Dimethyl-2,2-dichlorovinyl phosphate) and DEP (Dimethyl-2,2,2-trichloro-1-hydroxyethyl phosphorate) can be degraded (Tanaka *et al.*)²²² in the presence of suspended TiO_2 during illumination with a super high pressure mercury lamp or with sunlight. The use of TiO_2 loaded with platinum or the addition of H_2O_2 can greatly enhance the reaction rates. The degradation reactions are:



The final degradation products of DDVP and DEP are Cl^- , PO_4^{3-} , H^+ and CO_2 . The results of the degradation of DDVP and DEP are listed in Table 1.6.

DDT (1,1,1-trichloro-2,2-bis(p-chlorophenyl) ethane) can also be eliminated by photocatalysis (Borello, Pelizzetti, Serpone, *et al.*)²²⁰ at the surface of the photocatalysts TiO_2 , ZnO , CdS , WO_3 and Fe_2O_3 (see also Table 1.6). The reaction of DDT elimination is given by the equation:



1.2.5.3 The photocatalytic degradation of s-triazine herbicides

The photocatalytic degradation of a series of s-triazine herbicides in water was thoroughly investigated by Pelizzetti²²⁴ under simulated solar light using particulate TiO_2 as a photocatalyst. The herbicides were rapidly decomposed, as shown in Table 1.6, but complete mineralization of the herbicides was not observed.

Table 1.6. Examples of a photocatalytic method for treating recalcitrant compounds' ^{220, 222, 224}. where B.I. = before illumination, A.I. = after illumination, Illum. = illumination, Sim. = simulated, AM1 = Air Mass 1 solar radiation reflecting the solar spectrum of light after it has passed through the earth' atmosphere along a line perpendicular to the earth' surface.

Compound	Concentration (B.I.)	Reaction Conditions	Illum. Hour	Concentration (A.I.)
DDVP	$1 \times 10^{-3} \text{M}$	TiO_2 , UV	5	$0.12 \times 10^{-3} \text{M}$
	$1 \times 10^{-3} \text{M}$	Pt/ TiO_2 , UV	3	~0
	$1 \times 10^{-3} \text{M}$	TiO_2 , H_2O_2 , UV	0.33	~0
	$1 \times 10^{-4} \text{M}$	TiO_2 , H_2O_2 , sunlight	1.5	~0
DEP	$1 \times 10^{-4} \text{M}$	TiO_2 , UV	2	~0
	$1 \times 10^{-4} \text{M}$	Pt/ TiO_2 , UV	0.5	~0
	$1 \times 10^{-4} \text{M}$	TiO_2 , H_2O_2 , UV	0.5	~0
	$1 \times 10^{-4} \text{M}$	TiO_2 , H_2O_2 , Sunlight	4	~0
DDT	1 ppm	Fe_2O_3 , AM1, Sim. Sunlight	5	~0.75
	1 ppm	CdS, AM1, Sim. Sunlight	5	~0.4
	1 ppm	ZnO, AM1, Sim. Sunlight	5	~0.25
	1 ppm	WO_3 , AM1, Sim. Sunlight	5	~0.15
	1 ppm	TiO_2 , AM1, Sim. Sunlight	5	~0.06
	1 ppm	Pt/ TiO_2 , AM1, Sim. Sunlight	5	~0
Atrazine	25 ppm	TiO_2 , AM1, Sim. Sunlight	0.33	~0
Simazine	3 ppm	TiO_2 , AM1, Sim. Sunlight	0.33	~0
Trietazine	15 ppm	TiO_2 , AM1, Sim. Sunlight	0.33	~0
Prometon	25 ppm	TiO_2 , AM1, Sim. Sunlight	0.33	~0
Prometryn	25 ppm	TiO_2 , AM1, Sim. Sunlight	0.33	~0

where Atrazine = 6-chloro-N-ethyl-N'-(1-methylethyl)-1,3,5,-triazine-2,4-diamine.

Simazine = 6-chloro-N,N'-diethyl-1,3,5-triazine-2,4-diamine.

Trietazine = 6-chloro-N,N,N'-triethyl-1,3,5-triazine-2,4-diamine.

Prometon = 6-methoxy-N,N'-bis(1-methylethyl)-1,3,5-triazine-2,4-diamine.

Prometryn = 6-(methylthio)-N,N'-bis(1-methylethyl)-1,3,5-triazine-2,4-diamine.

1.2.5.4 The photocatalytic degradation of surfactants

Surfactants are also sometimes problematic pollutants in domestic and industrial wastewaters. In recent years, Hidaka, Serpone, Pelizzetti *et al.*^{225,226} examined various anionic, cationic and nonionic surfactants in detail under UV illumination using dispersions of TiO_2 particles. Examples of some investigated surfactants are:

Anionic surfactants:

C_{12} -DBS: Sodium dodecylbenzene sulphonate

C_{12} -DS: Sodium dodecyl sulphate

C_{12} -LES-3: Sodium dodecyl tri(oxyethylene) sulphate

C_{14} -AOS: Sodium C_{14} - α -olefin sulphonate

C_{12} -DG: Sodium N-dodecanoyl-L-glutamate

Cationic surfactants:

C_{16} -HTAB: Hexadecyltrimethyl ammonium bromide

C_{12} -BDDAC: Benzyldimethyldodecylammonium chloride

Nonionic surfactants:

NPE_n : p-nonyl-phenyl-poly(oxyethylene) ether, where $n=7, 9, 11$, or 50 ethoxy groups in the NPE ethoxy chain.

C_{18} -PEA-15: N,N-bis[poly(coxyethylene)] octadecyl amine

C_{12-14} -BHA: N,N-bis(2-hydroxyethyl) alkanamide

C_{12-14} -PAE-10: poly(oxyethylene) ester of fatty acid

C_{12-14} -NOE: alkyl nonakis(oxyethylene) ether

C_{14-16} -NOE

For initial concentrations of about 10^{-4} M, it was observed that most of the above surfactants were completely eliminated in the presence of the photocatalyst TiO_2 after illumination for 0.5 to 3 hours. The final products of this photocatalytic elimination were CO_2 and H_2O .

1.2.6 Advantages of and problems associated with photocatalysis compared with other methods

1.2.6.1 Advantages

1. *Higher resistance to toxic compounds.* For semiconductor photocatalysts, such as inorganic oxides of TiO_2 , ZnO and Fe_2O_3 , components which are toxic to many other methods (especially to biological ones) are often very suitable substrates to be oxidized on these photocatalyst surfaces.

2. *Wide area of application.* The results of twenty years research show that photocatalytic methods can be used to eliminate many highly toxic contaminants from wastewater by chemical oxidation or reduction, to simultaneously treat various organic compounds and inorganic compounds in wastewater, and to treat polluted air.
3. *The treatment of low concentrations of pollutants.* According to research results obtained in recent years, photocatalytic methods can be used to treat ppm- and even ppb levels of organic and inorganic pollutants in ground- and surface water.
4. *Simple, light apparatus.* A photocatalytic reactor consists only of a cell with simple appendices. It can be easily built at low costs and can even be installed in a truck for rapid emergency treatment of waste in the field.

1.2.6.2 Problems

1. *Limited choice of effective photocatalysts.* Up to now only the semiconductor TiO_2 has shown high photocatalytic activity regarding various organic and inorganic compounds because of its suitable E_g (3.03 eV) and photo-stability. Compared with TiO_2 on the photocatalytic efficiency for the removal of most pollutants from wastewaters, other semiconductors show the disadvantages of a poor photocatalytic activity, a photo-instability (photo-corrosion), too large or too small an E_g value, or an unsuitable flat band potential.
2. *Low photon quantum yield.* According to most reports on the use of photocatalysis for wastewater treatment, only around 0.5% of the photons illuminating the solution can be converted into the energy needed for pollutant treatment. This is due to the lack of efficient photocatalysts and light sources. If methods were found to increase the proportion of valuable UV light ($\lambda \leq 400$ nm) in light resources and to decrease the recombination of e^-h^+ pairs, the photocatalytic efficiency of TiO_2 would greatly increase.
3. *Separation of catalysts.* During most photocatalytic treatments, semiconductor powders or colloids suspended in wastewater are used. In practice, it is hard to separate the catalyst from aqueous wastewater. Fixing catalysts on supports, such as glass fibre, ceramic and sand, may be a solution, but such catalysts have so far shown to be less efficient than suspension systems.

1.3 OUTLINE OF THIS DISSERTATION

The aim of the research was to increase the insight in photocatalytic oxidation and reduction processes and into the practical application of these process. This dissertation investigates the possibility of photocatalytic oxidation of organic pollutants and photocatalytic reduction of inorganic pollutants in wastewater under various reaction conditions. This dissertation elaborates on, among other things, the preparation and pretreatment of catalysts, the metallization of catalysts, solution pH, reactant concentrations, illumination time and the use

of promoters. Detailed experimental data, plausible kinetic equations, mechanisms, and a new porous micro-cell model for powdery photocatalysts are presented.

Chapter 2 describes the photocatalytic oxidation of methanol, ethanol and chloroform, trichloroethylene (TCE) and dichloropropionic acid (DCP) in aqueous slurries of TiO_2 , Pt/TiO_2 and Pd/TiO_2 in the presence of oxygen. The intermediates of methanol and ethanol produced during the process are discussed in detail, as are the effects of reaction pH on the mineralization of alcohol and the effect of catalyst metallization. A possible, plausible reaction mechanism was confirmed by experimental data.

Chapter 3 deals with a method for metallizing the photocatalysts 1% Pt/TiO_2 and 1% Pd/TiO_2 , X-ray powder crystal diffraction of Pt/TiO_2 , and surface element analysis of an electron beam probe (X-ray exciting spectrum) of M/TiO_2 . A new powder micro-cell porous model is proposed. Experimental data are explained based on a Langmuir adsorption isotherm, and possible kinetic equations and reaction mechanisms are discussed.

Chapter 4 describes patents for a photocatalyst and a solidified Fenton reagent, and proposes a valuable method for the photocatalytic and photochemical treatment of industrial wastewater containing phenol and other toxic organic compounds.

Chapter 5 details the photocatalysed deposition and concentration of uranium(VI) from an aqueous solution containing suspended particles of the photocatalyst titanium dioxide or metallized titanium dioxide. The photoactivities of TiO_2 regarding reductive deposition of uranium(IV) and the effect of the organic complex EDTA are described, and a possible reaction mechanism is proposed.

Chapter 6 describes the effect on the dehydrogenation activities of various photocatalysts of CdS created by modifications, such as preparation method, pretreatment method, various photocatalyst metallization percentages of Pt and Pd, and the promoting role of transition metals Cu, Ag *etc.* X-ray photoelectron spectroscopy and transmission electron microscopy were applied to investigate the surface structure of photocatalysts. A possible heterogeneous complex catalysis mechanism is proposed in detail.

Chapter 7 contains the summary and conclusions of this dissertation.

Appendix I lists extended references on the photocatalytic oxidation of various organic compounds.

1.4 REFERENCES

1. J.J. Rook, "Formation of Haloforms During Chlorination of Natural Waters," *Water Treatment Exam.*, 23, 234, 1974.
2. D. Grasso, R. Walters, G. Ellis, Y.-P. Chin, K. Morico, N. Koch, K. Flood, and R. Armstrong, "Physicochemical treatment processes," *Research Journal WPCF*, 62(4), 387-398, 1990.
3. M. R. Matsumoto, J. N. Jensen, P. McGinley, B. E. Reed, "Physicochemical treatment processes," *Water Environ. Research*, 66(4), 309-324, 1994.
4. D. F. Ollis, "Comparative Aspects of Advanced Oxidation Processes," presented at: October 1991 ACS Symposium, "Emerging Technologies for Hazardous Wastes," Atlanta, Georgia, USA.
5. W. H. Glaze, "An Overview of Advanced Oxidation Processes for Water and Wastewater Treatment," *The First International Conference on Advanced Oxidation Technologies for Water and Air Remediation*, London Convention Centre and the Radisson Hotel, London, Ontario, Canada, June 25-30, 1994.
6. J.P. Scott, and D.F. Ollis, "Integration of chemical and biological oxidation processes for water treatment: review and recommendations," *Environ. Prog.*, 14, 88-103, 1995.
7. W.H. Glaze, J-W Kang, and D.H. Chapin, "The Chemistry of Water Treatment Processes Involving Ozone, Hydrogen Peroxide and Ultraviolet Radiation," *Ozone Sci. Eng.*, 9, 335-352, 1987.
8. G. R. Peyton, *Significance and Treatment of Volatile Organic Compounds in Water Supplies*, (Eds.) N. M. Ram, R. F. Chrisman, K. P. Cantor, 1990, Lewis Publishers. Chapter 14, *Oxidative Treatment Methods for Removal of Organic Compounds from Drinking Water Supplies*, p. 313-362.
9. J. Hoigné, "The Chemistry of Ozone in Water," in *Process Technologies for Water Treatment*, S. Stucki, (Ed.), New York, Plenum Publishing Corp., 1988.
10. J. Hoigné, and H. Bader, "Beeinflussung der Oxidationwirkung von Ozon und OH-Radikalen durch Carbonat," *Vom Wasser*, 48, 283-304, 1977.
11. J. Hoigné, and H. Bader, "Ozone-Initiated Oxidations of Solutes in Wastewater: A Reaction Kinetic Approach," presented at the International Association on Water Pollution Research, 9th International Conference, Stockholm, June 1978.
12. J. Hoigné, and H. Bader, "Ozone Requirement and Oxidation Competition Values of Various Types of Water for the Oxidation of Trace Impurities," in *Oxidation Techniques in Drinking Water Treatment*, W Kuhn and H. Sontheimer, Eds., EPA-570/9-79-020, Washington DC: Office of Drinking Water, U.S. Environmental Protection Agency, 271-290.
13. J. Staehelin, and J. Hoigné, "Decomposition of Ozone in Water in the Presence of Organic Solutes Acting as Promoters and Inhibitors of Radical Chain Reactions," *Environ. Sci. Technol.*, 19, 1206-1213, 1985.
14. J. Hoigné, and H. Bader, "The formation of Trichloronitromethane (Chloropicrin) and Chloroform in a Combined Ozonation/Chlorination Treatment of Drinking Water," *Water Res.*, 22, 313-319, 1988.

15. W.H. Glaze, F.J. Beltrán, T. Tuhkanen and J.W. Kang, "Chemical Models of Advanced Oxidation Processes," *Wat. Pollut. Res. J. Can.*, 27, 23-42, 1992.
16. W.H. Glaze, M. Koga, E.C. Ruth, and D. Cancilla, "Application of Closed Loop Stripping and XAD Resin Adsorption for the Determination of Ozone By-Products from Natural Water," in *Biohazards of Drinking Water Treatment*, R.A. Larson, (Ed.), Chelsea, MI, Lewis Publishers. Inc., 201-210, 1988.
17. W.H. Glaze, G.R. Peyton, S. Lin, F. Y. Huang, and J. L. Burleson, "Destruction of Pollutants in Water with Ozone in Combination with Ultraviolet Radiation. 2. Natural Trihalomethane Precursors," *Environ. Sci. Technol.*, 16, 454-458, 1982.
18. W.H. Glaze, "Reaction Products of Ozone: A Review," *Environ. Health Pers.*, 69, 151-157, 1986.
19. W.H. Glaze, "Drinking Water Treatment with Ozone," *Environ. Sci. Technol.*, 21, 224-230, 1987.
20. G.R. Peyton, C.-S. Gee, J. Bandy, and S.W. Maloney, "Catalytic/Competition Effects of Humic Substances on Photolytic Ozonation of Organic Compounds," in *Aquatic Humic Substances: influence on Fate and Treatment of Pollutants*, I.H. Suffet and P. MacCarthy, Eds., ACS Advances in Chemistry Series. No. 219, Washington DC, American Chemical Society, 639-661, 1989.
21. G.R. Peyton, and W.H. Glaze, "Mechanism of Photolytic Ozonation," in *Photochemistry of Environmental Aquatic Systems*, R.G. Zika and W.J. Cooper, Eds., ACS Symposium Series, No. 327, Washington DC, American Chemical Society, 76-88, 1987.
22. G.R. Peyton, and W.H. Glaze, "Destruction of Pollutants in Water with Ozone in Combination with Ultraviolet Radiation. 3. Photolysis of Aqueous Ozone," *Environ. Sci. Technol.*, 22, 761-767, 1988.
23. G.R. Peyton, F.Y. Huang, J.L. Burleson and W.H. Glaze, "Destruction of Pollutants in Water with Ozone in Combination with Ultraviolet Radiation. 1. General Principles and Oxidation of Tetrachloroethylene," *Environ. Sci. Technol.*, 16, 448-453, 1982.
24. F. J. Beltrán, Juan F. Garcia-Araya, and Benito Acedo, "Advanced Oxidation of Atrazine in Water-I. Ozonation," *Wat. Res.* 28(10), 2153-2164, 1994.
25. F. J. Beltrán, Juan F. Garcia-Araya, and Benito Acedo, "Advanced Oxidation of Atrazine in Water-II. Ozonation," *Wat. Res.* 28(10), 2165-2174, 1994.
26. S. Guittonneau, J. De Laat, J. P. Duguet, C. Bonnel, and M. Doré, "Oxidation of Parachloronitrobenzene in Dilute Aqueous Solution By Ozone + UV and Hydrogen peroxide + UV: A Comparative Study," *Ozone science & Engineering*, 12, 73-94, 1990.
27. D. Freeman, E., K. Yoshino, W. H. Parkinson, and Tom G. Slanger, G. E. Gadd, "Formation of Ozone by Irradiation of Oxygen at 248 Nanometers," *Science*, 250, 1432-1434, Oct. 7, 1990.
28. S. Guittonneau, J. de Laat, M. Doré, "Kinetic Study of the Photodecomposition Rate of Aqueous Ozone by U.V. Irradiation at 253.7 nm," *Environ. Technol.*, 11, 477-490, 1990.
29. W.H. Glaze, G.R. Peyton, B. Sohm, and D.A. Meldrum, "Pilot-scale Evaluation of Photolytic Ozonation for Trihalomethane Precursor Removal," Final Report to USEPA, EPA-600/S2-84-136, 1984.
30. C.A. Fronk, "Destruction of Volatile Organic Contaminants in Drinking Water by Ozone Treatment," *Ozone Sci. Eng.* 9, 265-288, 1987.

31. P. Neta, R.E. Huie, and A.B. Ross, "Rate constants for reactions of inorganic radicals in aqueous solution," *J. Phys. Chem. Ref. Data*, **17**, 1027-1284, 1988.
32. (a). P. Neta, R.E. Huie, and A.B. Ross, "Rate constants for reactions of peroxy radicals in fluid solutions," *J. Phys. Chem. Ref. Data*, **19**, 413-513, 1990. (b). B.H.J. Bielski, D.E. Cabelli, R. Arudi, and A.B. Ross, "Reactivity of HO_2/O_2^- radicals in aqueous solution," *J. Phys. Chem. Ref. Data*, **14**, 1014-1100, 1985. (c). G.V. Buxton, C.L. Greenstock, W.P. Helman, and A.B. Ross, "Critical review of rate constants for reactions of hydrated electrons, hydrogen atoms and hydroxyl radicals ($\bullet\text{OH}/\bullet\text{O}$) in aqueous solution," *J. Phys. Chem. Ref. Data*, **17**, 513-886, 1988.
33. J. Hoigné, and H. Bader, "The Role of Hydroxyl Radical Reactions in Ozonation Processes in Aqueous Solutions," *Water Res.*, **10**, 377-386, 1976.
34. L. Nowell and J. Hoigné, "Interaction of Iron(II) and Other Transition Metals with Aqueous Ozone." in *Proceedings, 8th Ozone World Conference*, Zurich (Ashton, MD, International Ozone Association), E80-E95, 1987.
35. P.D. Francis, "Application of Oxidation by a Combined Ozone/Ultraviolet Radiation System to the Treatment of Natural Water," *Ozone Sci. Eng.*, **2**, 391-418, 1987.
36. Product Brochure No. A2. 3903.1 from Capital Controls, Colmar, PA.
37. H.J.H. Fenton, "Oxidation of tartaric acid in the presence of iron," *J. Chem. Soc.*, **65**, 899-910, 1894.
38. D.L. Sedlak, and A.W. Andren, "Oxidation of chlorobenzene with Fenton's reagent," *Environ. Sci. Technol.*, **25**, 777-782, 1991.
39. M. Barbeni, C. Minero, E. Pelizzetti, E. Borgarello, and N. Serpone, "Chemical degradation of chlorophenols with Fenton's reagent ($\text{Fe}^{2+} + \text{H}_2\text{O}_2$)," *Chemosphere*, **16**(10-12), 2225-2237, 1987.
40. R.A. Sheldon, and J.K. Kochi, "Metal-catalyzed oxidation of organic compounds," Academic Press, New York, 1981.
41. O. Legrini, E. Oliveros, and A.M. Braun, "Photochemical Processes for Water Treatment" *Chem. Rev.* **93**(2), 671-698, 1993.
42. K. W. Yost, "Ultraviolet Peroxidation: An Alternative Treatment Method for Organic contamination Destruction in Aqueous Waste Streams," *43rd. Purdue Industrial Waste Conference. Proceedings*, Lewis Publishers, Inc., Chelsea, Michigan, 1989.
43. E. Oliveros, O. Legrini, M. Hohl, T. Müller, A.M. Braun, "Large scale development of a light-enhanced Fenton reaction by optimal experimental design," International Conference on Oxidation Technologies for Water and Wastewater Treatment, May 12-15, 1996, Goslar, Germany.
44. R. G. Zepp, B. C. Faust, and J. Hoigné, "Hydroxyl Radical Formation in Aqueous Reactions (pH 3-8) of Iron(II) with Hydrogen Peroxide: The Photo-Fenton Reaction," *Environ. Sci. Technol.* **26**(2), 313-319, 1992.
45. Y. Zuo, and J. Hoigné, "Formation of hydrogen peroxide and depletion of oxalic acid in atmospheric water by photolysis of iron(III)-oxalate complexes," *Environ. Sci. Technol.*, **26**, 1014-1022, 1992.
46. D.G. Hager, C.G. Loven, and C.L. Giggy, "On-site chemical Oxidation of Organic Contaminants in Groundwater Using UV Catalyzed Hydrogen Peroxide," presented at AWWA Annual Conference and Exposition, Orlando, FL, Sales literature from Peroxidation Systems.

Inc., Tucson, AZ, 1988.

47. J.J. Pignatello, "Dark and photoassisted Fe^{3+} -catalyzed degradation of chlorophenoxy herbicides by hydrogen peroxide," *Environ. Sci. Technol.*, **26**, 944-951, 1992.
48. Y. Sun, and J.J. Pignatello, "Organic intermediates in the degradation of 2,4-dichlorophenoxyacetic acid by $\text{Fe}^{3+}/\text{H}_2\text{O}_2$ and $\text{Fe}^{3+}/\text{H}_2\text{O}_2/\text{UV}$," *Agricul. Food Chem.*, **41**, 1139-1142, 1993.
49. J.J. Pignatello, and G. Chapa, "Degradation of PCBs by ferric ion, hydrogen peroxide and UV light," *Environ. Toxicol. Chem.*, **13**, 423-427, 1994.
50. H. M. Castrantas, and R. D. Gibilisco, "UV destruction of Phenolic Compounds under Alkaline Conditions," *Emerging Technologies in Hazardous waste Management*, ACS Symp. Ser. 1991, pp. 77-99.
51. G. Ruppert, and R. Bauer, "The photo-Fenton reaction - an effective photochemical wastewater treatment process," *J. Photochem. Photobiol., A: chem.*, **73**, 75-78, 1993.
52. E. Lipczynska-Kochany, "Degradation of Nitrobenzene and Nitrophenols in Homogeneous Aqueous Solution. Direct Photolysis versus Photolysis in the Presence of Hydrogen Peroxide and the Fenton Reagent," *Water Poll. Res. J. Canada*, **27**(1), 97-122, 1992.
53. "Non-Thermal Plasma Techniques for Pollution Control," ed. B. Penetrante and S. Shultheis, NATO ASI Series G, vol. 34A and B, Springer, Berlin, 1993.
54. D. Evans, L.A. Rosocha, G.K. Anderson, J.J. Coogan and M.J. Kushner, *J. Appl. Phys.*, **74**, 5378, 1993.
55. A.K. Sharma, B.r. Locke, P. Arce, and W.C. Finney, "A Preliminary Study of Pulsed Streamer Corona Discharge for the Degradation of Phenol in Aqueous Solutions," *Hazardous Waste/Hazardous Materials*, **10**, 209-219, 1993.
56. J.S. Chang, P.A. Lawless and T. Yamamoto, "Corona Discharge Processes," *IEEE Plasma Sci.*, **19**, 1151-1166, 1991.
57. "Spectroscopy of the Excited State," Volume 12 of NATO Advanced Study Institutes Series, edited by B. D. Bartolo, Plenum Press, New York, 1976.
58. T. Yamamoto, K. Ramanathan, P.A. Lawless, D.S. Ensor, J.R. Newsome, N. Parks and G.H. Ramsey, "Control of Organic Pollutants by an AC Energized Ferroelectric Pellet Reactor and a Pulsed Corona Reactor," *Trans. IEEE Industry Applications*, **28**, 528-533, 1992.
59. S.K. Dhali and I. Sardja, "Dielectric-barrier discharge for processing of SO_2 ," *J. Appl. Physics*, **69**, 9391, 1991.
60. D. Evans, L.A. Rosocha, G.K. Anderson, J.J. Coogan and M.J. Kushner, *J. Appl. Phys.*, **74**, 5378, 1993.
61. "Chemistry of the Atmosphere," M. J. McEwan and L. F. Phillips, Ddware Arnold Ltd., London, 1975.
62. "Chemistry of the Natural Atmosphere," Peter Warneck, ACADEMIC PRESS, INC., LONDON, 1988.
63. M.R. Hoffmann, "Electrohydraulic discharge treatment of water and wastewater," International conference on oxidation technologies for water and wastewater treatment, May 12-15, 1996, Goslar, Germany.
64. A.A. Atchley, L.A. Crum, "Ultrasound, its chemical physical and biological effects," K.S. Suslick, Ed., VCH New York, 1988, Chapter one.

65. A. Kotronarou, G. Mills, M.R. Hoffmann "Ultrasonic Irradiation of p-nitrophenol in Aqueous Solution," *J. Phys. Chem.*, **95**, 3630, 1991.
66. C. Pétrier, A. Jeunet, J. Luche and G. Reverdy, "Unexpected Frequency Effects on the Rate of Oxidative Processes Induced by Ultrasound," *J. Am. Chem. Soc.*, 3148-3150, 1992.
67. A. Henglein, *Ultrasonics*, **25**, 6, 1987.
68. P. Riesz, T. Kondo, *Free Radical in Biology and Medicine*, **13**, 247, 1992.
69. A. Kotronarou, G. Mills, M.R. Hoffmann, "Ultrasonic Irradiation of Hydrogen Sulfide in Aqueous Solution," *Environ. Sci. Technol.*, **25**, 2940, 1992.
70. A. Kotronarou, G. Mills, M.R. Hoffmann, "Decomposition of parathion in Aqueous Solution by Ultrasonic Irradiation," *Environ. Sci. Technol.*, **26**, 1469, 1992.
71. C. Pétrier, M. Micolle, G. Merlin, J. Luche and G. Reverdy, "Characteristics of Pentachlorophenolate Degradation in Aqueous Solution by Means of Ultrasound," *Environ. Sci. Technol.*, **26**, 1639-1642, 1992.
72. N. Getoff, "Electron Beam Remediation of Water: A Short Review," *The First International Conference on Advanced Oxidation Technologies for Water and Air Remediation*, London Convention Centre, London, Ontario, Canada, June 25-30, 1994.
73. M. Koch, C.R. Cohn, R.M. Patrick, M.P. Schuetze, L. Bromberg, D. Reilly, and P. Thomas, *Phys. Lett.*, A **184**, 109-113, 1993.
74. L. Bromberg, D.R. Cohn, M. Koch, R.M. Patrick, and P. Thomas, *Phys. Lett.*, A **173**, 293-299, 1993.
75. L. Kokoszka and J. Flood, "A guide to the EPA-approved PCB disposal method," *Chem. Eng.*, **92**(14), 41, 1985.
76. W.V. Sherman, "Radical-initiated chain dehalogenation of alkyl halides in alkaline alcoholic solution," *J. Phys. Chem.* **72**, 2287, 1986.
77. A. Singh, W. Kremers and G.S. Bennett, "Radiolytic dechlorination of polychlorinated biphenyls," In Proceedings: International Conference on New Frontiers on Hazardous Waste Management, Report No. EPA/600/9-85/025.
78. A. Singh, W. Kremers, P. Smalley, and G.S. Bennett, "Radiolytic dechlorination of polychlorinated biphenyls," *Radiat. Phys. Chem.*, **25**, 11, 1985.
79. L.G. Christophorou, *Electron-molecule interactions and their application*, Vol. 1, Academic Press., NY, 1984.
80. E. Sanhueza, I.C. Hisatsune, and J. Heiklen, *Chem. Rev.*, **76**, 801-826, 1976.
81. W.J. Cooper, D.E. Meacham, M.G. Nickelsen, K. Lin, D.B. Ford, C.N. Kurucz and T.D. Waite, "the Removal of Tri-(TCE) and Tetrachloroethylene (PCE) from Aqueous solution Using High Energy Electrons," *J. Air Waste Manage. Assoc.*, **43**, 1358-1366, 1993.
82. M.G. Nickelsen, W.J. Cooper, T.D. Waite, and C.N. Kurucz, "Removal of Benzene and Selected Alkyl Substituted Benzenes from Aqueous Solution Utilizing Continuous High-Energy Electron Irradiation," *Environ. Sci. Technol.*, **26**, 144-152, 1992.
83. A. Balough, J. Herendi and J. Bathory, "Catalytic Purification of Gaseous Factory Effluents to Protect the Environment," *Report*, AD-A 017807, National Technical Information Service, Springfield, VA, p.15, 1975.
84. P.B. Blakey, "Process Odour Control by Catalytic Oxidation," in *Industrial Pollution Control*, K. Tearle, ed., London: Business Books, Ltd., 143-157, 1973.

85. Met-Pro, Inc., Harleysville, PA., "Air Pollution Control Systems," Bulletin 1010, 1985.
86. E. Robinson, "Low Temperature Catalytic Oxidation for Air Pollution Control and Energy Conservation," *DECHEMA-Monogr.*, **86**, 103-105, 1980.
87. M. Shelef, K. Otto and N.C. Otto, *Advances in Catalysis*, V. 27, Academic Press, New York, 311-365, 1978.
88. J.C. Summers, J.J. White and W.B. Williamson, *S.A.E.*, paper No. 89074, 1989.
89. C. Hoang-Van, B. Pommier, R. Harivololona and P. Pichat, *J. Non-Cryst. Solids*, **145**, 250, 1992.
90. Z.R. Ismagilov and M.A. Kerzhentsev, *Catal. Rev.- Sci. Eng.*, **32**, 51, 1990.
91. G.R. Lester, G.C. Joy and C.C. Hsu, Report CRDEC-CR-003, U.S. Army CRDEC (Aberdeen, MD), October, 1988.
92. G.J.K. Acres, "Platinum Catalysts for the Control of Air Pollution," *Plat. Metal Rev.*, **14**, 3-10, 1970.
93. M.A. Palazzolo, R.M. Parks and K.K. Fidler, "Control of Industrial Emissions by Catalytic Incineration," EPA-600/2-84-1186, July 1984.
94. J.J. Spivey, Complete Catalytic Oxidation of Volatile Organics," *I&EC Research*, **26**, 2165-2180, 1987.
95. M.A. Palazzolo, J.I. Steinmetz, D.L. Lewis and J.F. Beltz, "Parametric Evaluation of VOC/HAP Destruction via Catalytic Incineration," EPA-600/2-85-041, April, 1985.
96. J.J. Spivey, "Recovery of Volatile Organics from Small Industrial Sources," *Env. Progr.*, **7**(1), 31-40, 1988.
97. H. Shaw, Y. Wang, T.C. Yu, and A.E. Cerkawicz, "Catalytic Oxidation of Trichloroethylene and Methylene Chloride with Noble Metals," *Emerging Technologies for Hazardous Waste Management III*, ACS Advances in Chemistry Series No. 518, Edited by D. William Tedder and Frederick G. Pohland, Chapter 17, 358-379, 1993.
98. T.C. Yu, H. Shaw, and R.J. Farrauto, "Catalytic Oxidation of Trichloroethylene over PdO Catalyst on $\tau\text{-Al}_2\text{O}_3$," *Catalytic Control of Air Pollution: Mobil and Stationary Sources*, ACS Symposium Series No. 495, Edited by Ronald G. Silver, John E. Sawyer, and Jerry C. Summers, Chapter 11, 141-152, 1992.
99. M.A. Palazzolo, C.L. Jamgochian, J.I. Steinmetz and D.L. Lewis, "Destruction of Chlorinated Hydrocarbons by Catalytic Incineration," EPA-600/2-86-079, September, 1986.
100. M. Mirghanberi, D.J. Muno and J.A. Bacchetti, "Phthalic Anhydride Emissions Incinerated Catalytically," *Chemical Processing*, **45**(14), December, 1982.
101. P.C., Siebert, K.R. Meardon and J.C. Serne, "Emission Controls in Polymer Production," *Chem. Eng. Prog.*, 86-76, September, 1984.
102. T.H. Snape, "Catalytic Oxidation of Pollutants from Ink Drying Ovens," *Plat. Metal Rev.*, **21**(3), 90-91, 1977.
103. A. Wood, *Chem. Week*, **147**, 8, 1990.
104. A.M. Sakharov, I.P. Skibida, *Oxidation Commun.*, **1**, 113, 1979.
105. J. Schwartz and Y.M. Liu, "Catalytic Dechlorination of PCBs: A New Technology for Soil Remediation," *The First International Conference on Advanced Oxidation Technologies for Water and Air Remediation*, London Convention Centre and the Radisson Hotel, London, Ontario, Canada, June 25-30, Book of Abstracts, p. 166, 1994.

106. H. Perkov, R. Steiner, and H. Vollmuller, "WAO - a Review," *Ger. Chem. Eng.* **4**, 193-201, 1981.
107. C.R. Baillod, R.A. Lamparter, B.A. Barna, "Wet oxidation for industrial waste treatment," *Chem. Eng. Prog.*, 52-56, March 1985.
108. V.S. Mishra, V.V. Mahajani, and J.B. Joshi, "Wet Air Oxidation," *Ind. Eng. Chem. Res.* **34**(1), 2-48, 1995.
109. J. Levec, and A. Pintar, "Catalytic oxidation of aqueous solutions of organics. An effective method for removal of toxic pollutants from waste waters," *Catal. Today*, **24**, 51-58, 1995.
110. S. Imanura, I. Fukuda, S. Ishida, "Wet oxidation catalyzed by ruthenium supported on cerium(IV) oxides," *Ind. Eng. Chem. Res.*, **27**, 718-721, 1988.
111. R.S. Willms, D.D. Reible, D.M. Wetzel, D.P. Harrison, "Aqueous phase oxidation: Rate enhancement studies," *Ind. Eng. Chem. Res.* **26**, 606-612, 1987.
112. J.F. Welch, J.D. Siegwarth, "Method for Processing of organic compounds," U.S. Patent 4,861,497, 1989.
113. J. Kalman, Z. Izsaki, L. Kovacs, A. Grofcsik, I. Szebenyi, "Wet air oxidation of toxic industrial effluents," *Water Sci. Technol.*, **21**, 289-295, 1989.
114. L. Li, P. Chen, E.F. Gloyna, "Kinetic Model for wet oxidation of organic compounds in subcritical and supercritical water," *ACS Symp. Ser. (Supercrit. Fluid Sci.)*, **514**, 305-315, 1993.
115. D. Mantzavinos, R. Hellenbrand, A.G. Livingston, I.S. Metcalfe, "Reaction mechanisms and kinetics of chemical pretreatment of bioresistant organic molecules by wet air oxidation," paper in The International Conference on Oxidation Technologies for Water and Wastewater Treatment, May 12-15, 1996, Goslar, Germany.
116. J. Kalman, Gy. Palami, I. Szebenyi, "WAO of toxic sludges," in *Management of Hazardous and Toxic Wastes in the Process Industries*, S.T. Kolczkowski, B.D. Crittenden, Eds., Elsevier Applied Science, 1987.
117. T.L. Randall, M.J. Dietrich, P.J. Canney, "Wet air oxidation of hazardous organics in wastewater," *Environ. Prog.*, **4**, 171, 1985.
118. P.J. Canney, P.T. Schaeffer, (a). "Detoxification of hazardous industrial wastewaters by WAO," Paper presented at Spring National AIChE Meeting, Houston, TX, 1983. (b). "A new application of existing technology," *Toxic Hazard. Waste, Proc. 15th Mid Atl. Ind. Waste Conf.*, M.d. LaGrega, L.K. Hendrian, Eds., 227-284, 1983.
119. R.K. Helling and J.W. Tester, *Environ. Sci. Technol.*, **22**, 1319, 1988.
120. L. Li, E.F. Gloyna, J.E. Sawicki, "Treatability of DNT process wastewater by supercritical water oxidation," *Water Environ. Res.*, **65**(3), 250-257, 1993.
121. S. F. Rice and R. R. Steeper, "Oxidation kinetics of simple organic compounds in supercritical water," *The First International Conference on Advanced Oxidation Technologies for Water and Air Remediation*, London Convention Centre and the Radisson Hotel, London, Ontario, Canada, June 25-30, Book of Abstracts, p. 175, 1994.
122. A.G. Fassbender, *Proc. AWWA/WPCF Resid. Manag. Conf.*, Research Triangle Park, NC, 11-14, August, 1991.

123. R. Li, T.D. Thornton, P.E. Savage, "Kinetics of CO₂ formation from the oxidation of phenols in supercritical water," *Environ. Sci. Technol.*, **26**, 3288-3295, 1992.
124. R. Li, P.E. Savage, D. Szmukler, "2-Chlorophenol oxidation in supercritical water: Global kinetics and reaction products," *Am. Inst. Chem. Eng. J.*, **39**, 178, 1993.
125. F. Luck, C. Bonnin, G. Niel, and G. Naud, "Subcritical and supercritical water oxidation of biosolids," *The First International Conference on Advanced Oxidation Technologies for Water and Air Remediation*, London, Ontario, Canada, June 25-30, Book of Abstracts, 358-360, 1994.
126. A. Shanableh and E.F. Gloyna, *Water Sci. Tech.*, **23**, 389, 1991.
127. D.M. Boyd, and R.F. Fulk, "Treatment of plating sludge without sludge," *Proc. 43rd Ind. Waste Conf.*, Purdue Univ., West Lafayette, Ind., **42**, 499, 1988.
128. S.H. Reiber, "Copper plumbing surfaces: An electrochemical study," *J. Am. Water Works Assoc.*, **81**, 6, 114, 1989.
129. K. Loomba, G.S. Pandey, "Selective removal of some toxic metal ions (HgII, CuII, PbII and ZnII) by reduction using steel plant granulated slag," *J. Environ. Sci. Health A28*, 1689, 1993.
130. C. Gómez-Lahoz, *et.al.*, "Cobalt(II) removal from water by chemical reduction with sodium borohydride," *Water Res.(G. B.)*, **27**, 985, 1993.
131. M. Abda, and Y. Oren, "Removal of cadmium and associated contaminants from aqueous wastes by fibrous carbon electrodes," *Water Res.(G. B.)*, **27**, 1535, 1993.
132. S.P. Ho, Y.Y. Wang and C.C.Wan, "electrolytic decomposition of cyanide effluent with an electrochemical reactor packed with stainless steel fiber," *Water Res.*, **24**(11), 1317-1321, 1990.
133. A. Mylonas, E. Papaconstantinou, "Photocatalytic degradation of chlorophenols to CO₂ and Hcl with polyoxotungstates in aqueous solution," *J. of Molecular Catalysis*, **92**, 261-267, 1994.
134. D.P. Schwendiman and C. Kural, *J. Am. Chem. Soc.*, **99**, 5677, 1977.
135. X. Li, P. Fitzgerald and L. Bowen, "Sensitized photo-degradation of chlorophenols in a continuous flow reactor system," *Wat. Sci. Tech.* **26**(1-2), 367-376.
136. T. Yokota, Y. Takahata, J. Hosoya, K. Suzuki, and K. Takahashi, "Heterogeneous photosensitized oxygenation of 2,3-dimethyl-2-butene," *J. Of Chemical Engineering of Japan*, **22**(5), 543-548, 1989.
137. T. Yokota, Y. Takahata, J. Hosoya, K. Suzuki, and K. Takahashi, "Heterogeneous photosensitized oxygenation of 2,3-dimethyl-2-butene," *J. Of Chemical Engineering of Japan*, **22**(5), 543-548, 1989.
138. S. Sampath, H. Uchida, and H. Yoneyama, "Photocatalytic degradation of gaseous pyridine over zeolite-supported titanium dioxide," *J. of Catalysis*, **149**, 189-194, 1994.
139. N. N. Lichtin, J.C. Dong, and K. M. Vijayakumar, "Photopromoted TiO₂-catalyzed oxidative decomposition of organic pollutants in water and in the vapor phase," *Water Poll. Res. J. Canada*, **27**(1), 203-210, 1992.
140. L. A. Dibble, and G. B. Raupp, "Kinetics of the gas-solid heterogeneous photocatalytic oxidation of trichloroethylene by near UV illuminated titanium dioxide," *Catalysis Letters*, **4**, 345-354, 1990.

141. L. Palmisano, V. Augugliaro, M. Schiavello, and A. Sclafani, "Environmental audits of hazardous waste disposal and treatment facilities," *J. Molecular Catalysis*, **56**, 284-295, 1989.
142. J.-M. Herrmann, C. Guillard, and P. Pichat, "Heterogeneous photocatalysis," *Catalysis Today*, **17**, 7-20, 1993.
143. D. F. Ollis, E. Pelizzetti, N. Serpone, "Destruction of water contaminants," *Environ. Sci. Technol.* **25**(9), 1523-1529, 1991.
144. D. F. Ollis, in "Photochemical Conversion and Storage of Solar Energy" E. Pelizzetti and M. Schiavello (eds.), pp. 593-622, 1991.
145. G.C. Bond, "Heterogeneous catalysis: principles and applications," p. 6, Oxford Chemistry Series, Clarendon Press, Oxford, 1974.
146. L. Palmisano, V. Augugliaro, A. Sclafani, and M. Schiavello, "Activity of chromium-ion-doped titania for the dinitrogen photoreduction to ammonia and for the phenol photodegradation," *J. Phys. Chem.* **92**(23), 6710-6713, 1988.
147. M. Schiavello, L. Rizzuti, R.I. Bickley, J.A. Navio, P.L. Yue, *Proc. Int. Congr. Catal.*, 8th, 3, 383, 1984.
148. (a) K.-I. Okamoto, Y. Yamamoto, H. Tanaka, M. Tanaka, and A. Itaya, Heterogeneous photocatalytic decomposition of phenol over TiO_2 powder. *Bull. Chem. Soc. Jpn.*, **58**(7), 2015-2022, 1985. (b). K.-I. Okamoto, Y. Yamamoto, H. Tanaka, and A. Itaya, Kinetics of heterogeneous photocatalytic decomposition of phenol over anatase TiO_2 powder. *Bull. Chem. Soc. Jpn.*, **58**(7), 2023-2028, 1985.
149. J.-C. D'Oliveira, C. Minero, E. Pelizzetti, and P. Pichat, Photodegradation of dichlorophenols and trichlorophenols in TiO_2 aqueous suspensions. *J. Photochem. Photobiol. A: Chem.* **72**, 261-267, 1993.
150. E. Pelizzetti, C. Minero, E. Borgarello, L. Tinucci, N. Serpone, Photocatalytic activity and selectivity of titania colloids and particles prepared by the sol-gel technique: Photooxidation of phenol and atrazine. *Langmuir*, **9**, 2995-3001, 1993.
151. Horst Kisch, "What is photocatalysis" p.1-8, in Photocatalysis Fundamentals and Applications, edited by Nick Serpone, Ezio Pelizzetti, John Wiley & Son, Inc., New York, 1989.
152. H. Hennig, D. Rehorek and R.D. Archer, *Coord. Chem. Rev.*, **61**, 1, 1985.
153. Gene G. Wubbels, "Catalysis of photochemical reaction" *Acc. Chem. Res.* **16**, 285-292, 1983.
154. H. Dürr, S. Boßmann, and A. Beuerlein, "Biomimetic approaches to the construction of supramolecular catalysts: titanium dioxide-platinum antenna catalysts to reduce water using visible light," *J. Photochem. Photobiol. A: chem.*, **73**, 233-245, 1993.
155. K. Sayama, and H. Arakawa, "Photocatalytic decomposition of water and photocatalytic reduction of carbon dioxide over ZrO_2 catalyst," *J. Phys. Chem.* **97**(3), 531-533, 1993.
156. A. Kudo, M. Steinberg, A. J. Bard, A. Campion, M. A. Fox, T. E. Mallouk, S. E. Webber, and J. M. White, "Photoelectrochemical properties of titanium dioxide electrodes prepared from a titanium-aluminum alloy," *J. Electrochem. Soc.*, **137**(12), 1990.
157. J. C. Escudero, S. Cervera-March, J. Giménez, and R. Simarro, "Preparation and characterization of $\text{Pt}(\text{RuO}_2)/\text{TiO}_2$ catalysts: test in a continuous water photolysis system," *J. Catalysis*, **123**, 319-332, 1990.

158. B. Ryo, S. Nakabayashi, A. Fujishima, "Investigation of mechanism of hydrogen evolution during photocatalytic water decomposition on metal-loaded semiconductor powders," *J. Phys. Chem.*, **89**(10), 1902-1904, 1985.
159. A. Yasumori, K. Yamazaki, S. Shibata, and M. Yamane, "Preparation of TiO_2 fine particles supported on silica gel as photocatalyst," *J. of the Ceramic Soc. of Japan*, **102**(8), 702-707, 1994.
160. B. Ohtani, M. Kakimoto, S. Nishimoto, and T. Kagiya, "Photocatalytic reaction of neat alcohols by metal-loaded titanium(IV) oxide particles," *J. Photochem. Photobiol. A: Chem.*, **70**, 265-272, 1993.
161. P. Pichat, Marie-Noelle Mozzanega and H. Courbon, "Investigation of the mechanism of photocatalytic alcohol dehydrogenation over Pt/TiO_2 using poisons and labelled ethanol," *J. Chem. Soc., Faraday Trans. 1*, **83**, 697-704, 1987.
162. E. Borgarello, E. Pelizzetti, "UV/VIS light photocatalytic dihydrogen production from aliphatic alcohols over semiconductor particles," *La Chimica E L'Industria*, **65**(7-8), 474-478, 1983.
163. (a). R.A. Smith, "Semiconductors," Cambridge University Press, Cambridge, 1968; (b). C. Kittel, "Introduction to Solid State Physics," Fifth edition, John Wiley & Sons, Inc. N.Y. 1976; (c). Adrianus J. Dekker, "Solid State Physics," London Macmillan & Co. Ltd, 1965; (d). Nathan S. Lewis, "Theory of Semiconductor Materials," in *Photocatalysis Fundamentals and Applications*, Nick Serpone, Ezio Pelizzetti, editors, New York, John Wiley & Sons, 1989; (e). David L. Greenaway, and Günther Harbeke, "Optical Properties and Band Structure of Semiconductors," Vol 1, *International series of monographs in The Science of the Solid State*, Ed. B.R. Pamplin, Pergamon Press, Oxford, London, 1968.
164. (a). M. Grätzel, "Heterogeneous Photochemical Electron Transfer," CRC Press, Inc., Boca Raton, Florida, 1989; (b). N. Serpone, E. Pelizzetti, "Photocatalysis Fundamentals and Applications," New York, John Wiley & Sons, 1989; (c). G. A. Shreve, and N.S. Lewis, "An analytical description of the consequences of abandoning the principles of detailed balance and microscopic reversibility in semiconductor photoelectrochemistry," *J. Electrochem. Soc.*, Vol. **142**(1), 112-119, 1995; (d). H. Gerischer, and A. Heller, "Photocatalytic Oxidation of Organic Molecules at TiO_2 Particles by Sunlight in Aerated Water," *J. Electrochem. Soc.* **139**(1), 113-118, 1992.; (e). H. Gerischer, "The Impact of Semiconductors on the Concepts of Electrochemistry" *Electrochimica Acta*, **35**(11/12), 1677-1699, 1990; (f). H. Gerischer, *J. Electroanal. Chem.* **150**, 553, 1983.
165. E.H. Rhoderick and R.H. Williams, "Metal-Semiconductor Contacts," 2nd ed., Oxford University Press, New York, 1988; S.J. Fonash, "Solar Cell Device Physics," Academic Press, NY, 1981; S.M. Sze, "Physics of semiconductor devices," 2nd ed., Wiley, NY, 1981.
166. D. Long, "Energy bands in semiconductors, Interscience," *The A.I.P. Handbook*, 3rd ed., Section 9 1968.
167. M. S. Wrighton, "Photoelectrochemical conversion of optical energy to electricity and fuels," *Accounts of Chemical Research*, **12**(9), 303-309, 1979.
168. A. J. Bard, "Photoelectrochemistry and heterogeneous photocatalysis at semiconductors," *Journal of Photochemistry*, **10**, 59-75, 1979.
169. J. Koryta and J. Dvořák, "Principles of Electrochemistry," JOHN WILEY & SONS LTD., Chichester, 1987.

170. H.V. Tartar and H.E. Keyes, *J. Am. Chem. Soc.*, **44**, 557, 1922.
171. D.A. MacInnes, "The Principles of Electrochemistry," DOVER PUBLICATIONS, INC. New York, 1961.
172. T. Sakata, "Heterogeneous photocatalysis at liquid-solid interfaces," in *Photocatalysis-Fundamentals and Applications*, p. 311-338, N. Serpone, E. Pelizzetti, (eds.) New York, John Wiley & Sons, 1989.
173. P. Suppan, "Principles of photochemistry," London: The Chemical Society, printed by Adlard & Son Ltd., Bartholomew Press, Dorking, 1973.
174. J. Plotnikov, "Allgemeine Photocheie," p. 362-375, 2nd ed., Walter de Gruyter, West Berlin, 1936.
175. M. C. Markham, and K. J. Laidler, "A kinetic study of photo-oxidations on the surface of zinc oxide in aqueous suspensions" *J. Phys. Chem.*, **57**, 363-369, 1953.
176. P. C. Gravelle, F. Juillet, P. Meriaudeau, and S. J. Teichner, "Surface Reactivity of Reduced Titanium Dioxide," *Faraday Discuss. Chem. Soc.*, **52**, 140-148, 1971.
177. M. Primet, P. Pichat, and M.-V. Mathieu, "Infrared Study of the surface of titanium dioxides," *J. Phys. Chem.*, **76**(9), 1216-1220, 1971.
178. M. Primet I, P. Pichat, and M.-V. Mathieu, "Infrared study of the surface of titanium dioxides," *J. Phys. Chem.*, **76**(9), 1221-1226, 1971.
179. G. Munuera, and F. S. Stone, "Adsorption of water and organic vapors on hydroxylated rutile," *Faraday Discuss. Chem. Soc.*, **52**, , 1971.
180. J. Cunningham, J. J. Kelly, and A. L. Penny, "Reactions involving electron transfer at semiconductor surfaces. II. Photoassisted dissociation of nitrous oxide over illuminated ferric oxide and zinc oxides," *J. Phys. Chem.*, **75**(5), 617-625, 1971.
181. A. Fujishima, and K. Honda, *Nature*, **238**, 37, 1972.
182. *Photocatalysis and Environment*, M. Schiavello (ed.), by Kluwer Academic Publishers, 1988.
183. *Photocatalysis- Fundamentals and Applications*, N. Serpone, E. Pelizzetti, (eds.), New York, John Wiley & Sons, 1989.
184. *Structure and Reactivity of Surfaces*, C. Morterra, A. Zecchina, and G. Costa, (eds.), Amsterdam, Elsevier Science Publishers B.V., 1989.
185. *Heterogeneous photochemical electron transfer*, M. Grätzel, CRC Press, Inc. Boca Raton, Florida, 1989.
186. *Photochemical Conversion and Storage of Solar Energy*, E. Pelizzetti and M. Schiavello (eds.), 1991.
187. *Photocatalytic Purification and Treatment of Water and Air*, D.F. Ollis, H. Al-Ekabi (eds.), Elsevier Science Publishers, Amsterdam, ISBN: 0-444-89855-7, 1993.
188. *Photoelectrochemistry, Photocatalysis and Photoreactors*, M. Schiavello, (ed.), D. Reidel Publishing Company, 1985.
189. J.-M. Herrmann, C. Guillard, and P. Pichat, "Heterogeneous photocatalysis," *Catalysis Today*, **17**, 7-20, 1993.
190. A. Wold, "Photocatalytic Properties of TiO₂," *Chem. Mater.*, **5**, 280-283, 1993.

191. D. F. Ollis, "Solar-assisted photocatalysis for water purification: issues, data, questions," in *Photochemical Conversion and Storage of Solar Energy*, E. Pelizzetti and M. Schiavello (eds.), pp. 593-622, 1991.
192. D. F. Ollis, E. Pelizzetti, N. Serpone, "Heterogeneous photocatalysis in the environment: application to water purification," in *Photocatalysis- Fundamentals and Applications*, p. 603-637, N. Serpone, E. Pelizzetti, (eds.) New York, John Wiley & Sons, 1989.
193. L. A. Dibble, and G. B. Raupp, "Heterogeneous photocatalysis: A novel approach for the degradation of volatile organic water pollutants," pp. 221-229, in *Proceedings of the Arizona Hydrological Society 1st Annual Symposium, Survival in the Desert: Water Quality and Quantity Issues into the 21st Century*, Phoenix, Arizona, September 1988.
194. M. A. Fox, "Photocatalysis on modified semiconductor surfaces and on bipolar photoelectrodes," *Nouveau Journal de Chimie/New Journal of Chemistry*, 11(2), 129-133, 1987.
195. D. F. Ollis, "Contaminant degradation in water," *Environ. Sci. Technol.*, 19(6), 480-484, 1985.
196. S. J. Teichner, and M. Pormenti, "Heterogeneous Photocatalysis," in *Photoelectrochemistry, Photocatalysis and Photoreactors*, (ed.) M. Schiavello, pp. 457-489, by D. Reidel Publishing Company, 1985.
197. M. A. Fox, "Organic heterogeneous photocatalysis: chemical conversions sensitized by irradiated semiconductors," *Anne, Acc. Chem. Res.* 16, 314-321, 1983.
198. N. W. Cant, and J. R. Cole, "Photocatalysis of the Reaction between ammonia and nitric oxide on TiO_2 surfaces," *J. Catalysis*, 134, 317-330, 1992.
199. H. Mozzanega, J.-M. Herrmann, and P. Pichat, " NH_3 oxidation over UV-irradiated TiO_2 at room temperature," *The Journal of Physical Chemistry*, 83(17), 2251-2255, 1979.
200. P. Pichat, J. M. Herrmann, H. Courbon, J. Disdier, and M. N. Mozzanega, "Photocatalytic oxidation of various compounds over TiO_2 and other semiconductor oxides; mechanistic considerations," *The Canadian Journal of Chemical Engineering*, 60, 27-32, 1982.
201. K. Tanaka, K. Harada, and S. Murata, "Photocatalytic deposition of metal ions onto TiO_2 powder," *Solar Energy*, 36(2), 159-161, 1986.
202. M. R. Prairie, B. M. Stange, and L. R. Evans, " TiO_2 photocatalysis for the destruction of organics and the reduction of heavy metals," in *Photocatalytic Purification and Treatment of Water and Air*, D.F. Ollis, H. Al-Ekabi, (Eds.) 1993, P.353-363, ISBN: 0-444-89855-7.
203. M.R. Prairie, L. R. Evans, and S. L. Martinez, "destruction of organics and removal of heavy metals in water via TiO_2 photocatalysis," Paper in the Symposium on Chemical Oxidation: Technology for the Nineties, Nashville TN, 1992.
204. M.R. Prairie, L. R. Evans, B.M. Stange and S. L. Martinez, "An investigation of TiO_2 photocatalysis for the treatment of water contaminated with metals and organic chemicals," *Environ. Sci. Technol.*, 1992
205. H.H. Patterson, J. Cheng, S. Despres, M. Sunamoto, and M. Anpo, "Relationship between the geometry of the excited state of vanadium oxides anchored onto SiO_2 and their photoreactivity toward CO molecules," *J. Phys. Chem.*, 95(22), 8813-8818, 1991.
206. K. Ravindranathan Thampi, P. Ruterana, and M. Grätzel, "Low-temperature thermal and photoactivation of TiO_2 -supported Ru, Rh, and Cu catalysts for CO-NO reaction," *J. Catalysis*, 126, 572-590, 1990.

207. K. Ogura, A. Seno, and M. Kawano, "Photo-assisted catalytic reduction of CO₂ with pre-adsorbed ammonia on silica-supported iron," *J. of Molecular Catalysis*, **73**, 225-235, 1992.
208. J. Sabate, M. A. Anderson, M. A. Aguado, J. Giménez, S. Cervera-March, C. G. Hill, Jr. "Comparison of TiO₂ powder suspensions and TiO₂ ceramic membranes supported on glass as photocatalytic systems in the reduction of chromium(IV)," *J. Molecular Catalysis* **71**, 57-68, 1992.
209. X. Domènech, and J. Muñoz, "Photochemical elimination of Cr(VI) from neutral-alkaline solutions," *J. Chem. Tech. Biotechnol.*, **47**, 101-107, 1990.
210. J. Domènech, and J. Peral, "Removal of toxic cyanide from water by heterogeneous photocatalytic oxidation over ZnO," *Solar Energy*, **41**(1), 55-59, 1988.
211. N. Serpone, E. Borgarello, M. Barbeni, E. Pelizzetti, P. Pichat, J.-M. Hermann, and M.A. Fox, "Photochemical reduction of gold(III) on semiconductor dispersions of TiO₂ in the presence of CN⁻ ions: disposal of CN by treatment with hydrogen peroxide," *Journal of Photochemistry*, **36**, 373-388, 1987.
212. E. Borgarello, N. Serpone, G. Emo, R. Harris, E. Pelizzetti and C. Minero, "Light-induced reduction of rhodium(III) and palladium(II) on titanium dioxide dispersions and the selective photochemical separation and recovery of gold(III), platinum(IV), and rhodium(III) in chloride media," *Inorg. Chem.* **25**(25), 4499-4503, 1986.
213. E. Borgarello, N. Serpone, P. Liska, W. Erbs, M. Grätzel, and E. Pelizzetti, "Photocleavage of hydrogen sulphide in alkaline aqueous media with a RuO₂-loaded CdS catalyst supported on a polycarbonate matrix," *Gazzetta Chimica Italiana*, **115**, 599-602, 1985.
214. J. S. Sabaté Cervera-March, R. Simarro, and, J. Giménez, "Photocatalytic production of hydrogen from sulfide and sulfite waste streams: A kinetic model for reactions occurring in illuminated suspensions of CdS," *Chemical Engineering Science*, **45**(10), 3089-3096, 1990.
215. L. Darren, A. Res, R. Harris, N. Serpone, C. Minero, E. Pelizzetti, H. Hidaka, "Removal of toxic metal from solutions by photocatalysis using irradiated platinized titanium dioxide: removal of lead," *La Chimica & L'industria*, **72**, 139-146, 1990.
216. N. Serpone, Y. K. Ah-you, T. P. Tran, R. Harris, E. Pelizzetti and H. Hidaka, "AM1 simulated sunlight photoreduction and elimination of inorganic Hg(II) and organic CH₃Hg(II) chloride salts from aqueous suspensions of TiO₂," *Solar Energy*, **39**(6), 491-498, 1987.
217. K. Kobayakawa, Y. Nakazawa, M. Ikeda, Y. Sato, and A. Tujishima, *Ber. Bunsenges. Phys. Chem.*, **94**, 1439-1443, 1990.
218. R. Amadelli, A. Maldotti, S. Sostero and V. Carassiti, "Photodeposition of uranium oxides onto TiO₂ from aqueous uranyl solutions," *J. Chem. Soc. Faraday Trans.* **87**(19), 3267-3273, 1991.
219. J. Chen, D.F. Ollis, "Photocatalyzed deposition and concentration of uranium(VI) from aqueous solution suspending TiO₂ or Pt/TiO₂," preparing for publish, 1996.
220. B. Roberta, C. Menero, E. Pramauro, E. Pelizzetti, N. Serpone, H. Hidaka, "Photocatalytic oxidation of organic insecticide of DDT on catalyst surfaces of Pt/TiO₂, TiO₂, ZnO, CdS, WO₃, α -Fe₂O₃, and under the illumination of simulated sunlight," *Environmental Toxicology and Chemistry*, **8**, 997-1002, 1989.
221. (a). C. K. Grätzel, M. Jirousek and M. Grätzel, "Accelerated Decomposition of Active Phosphates on TiO₂ Surfaces," *J. Mol. Cat.* **39** 347-353, 1987. (b). C. K. Grätzel, M. Jirousek, and M. Grätzel, "Decomposition of Organophosphorus Compounds on

Photoactivated TiO₂ surfaces," *J. of Molecular Catalysis*, **60**, 375-387, 1990.

222. (a). K. Harada, T. Hisanaga, and K. Tanaka, "Photocatalytic Degradation of Organophosphorous Insecticides in Aqueous Semiconductor suspensions," *Wat. Res.* **24**(11), 1415-1417, 1990. (b). K. Harada, T. Hisanaga, and K. Tanaka, "Photocatalytic Degradation of Organophosphorus Compounds in Semiconductor Suspension," *New Journal of Chemistry*, **11**(8-9), 597-600, 1987.
223. M.-C. Lu, G.-D. Roam, J.-N. Chen, and C. P. Huang, "Factors Affecting the Photocatalytic Degradation of Dichlorvos over titanium Dioxide Supported on Glass," *J. Photochem. Photobiol. A: Chem.*, **76**, 103-110, 1993.
224. (a). E. Pelizzetti, C. Minero, E. Borgarello, L. Tinucci, N. Serpone, "Photocatalytic Activity and Selectivity of Titania Colloids and Particles Prepared by the sol-Gel Technique: Photooxidation of Phenol and Atrazine," *Langmuir* **9**, 2995-3001, 1993. (b). E. Pelizzetti, V. Maurino, C. Minero, V. Carlin, E. Pramauro, and O. Zerbini, M. L. Tosato, "Photocatalytic Degradation of Atrazine and Other S-Triazine Herbicides," *Environ. Sci. Technol.*, **24**(10), 1559-1565, 1990.
225. (a). H. Hidaka, S. Yamada, S. Suenaga, J.-C. Zhao, "Photodegradation of surfactants Part VI. Complete photocatalytic Degradation of Anionic, Cationic and Nonionic Surfactants in Aqueous Semiconductor Dispersions," *J. of Molecular Catalysis*, **59**, 279-290, 1990. (b). H. Hidaka, J.C. Zhao, S. Suenaga, N. Serpone, and E. Pelizzetti, "Photodegradation of Surfactants. VII. Peroxide and Aldehyde Pormation in the Photocatalyzed Oxidation of Nonionic Surfactants," *J. Jpn. Oil Chem. Soc. (Yukagaku)*, **39**(11), 45-48, 1990.
226. (a). E. Pelizzetti, C. Minero, V. Maurino, A. Sciafani, H. Hidaka, and N. Serpone, "Photocatalytic Degradation of Nonylphenol Ethoxylated Surfactants," *Environ. Sci. Technol.* **23**(11), 1380-1385, 1989. (b). E. Pelizzetti, E. Pramauro, C. Minero, and N. Serpone, "Sunlight Degradation of Organic Pollutants in Aquatic Systems," *Waste Management*, **10**, 65-71, 1990.

CHAPTER 2 PHOTOCATALYZED OXIDATION OF ALCOHOLS AND ORGANOCHLORIDES IN THE PRESENCE OF OXYGEN AND METALLIZED TiO₂ SUSPENSIONS

This Chapter is based on:

1. Jian Chen, David F. Ollis, Wim H. Rulkens and Harry Bruning, "Kinetics of the Photocatalytic Oxidation of Alcohols," presenting on The Third International Conference on TiO₂ Photocatalytic Purification and Treatment of Water and Air, Orlando, Sep. 1997.
2. Jian Chen, Qixing Zhuang, Jiniang He, Cheng Yu, "Photocatalytic Oxidation of Dilute Ethanol Solution on Suspending M/TiO₂," *Acta Energiae Solaris Sinica*, **7**(4), 378-383, 1986.
3. Jian Chen, Qixing Zhuang, "Research on Semiconductor Powder Photocatalytic System in Aqueous Solution of Ethanol Suspended Modified TiO₂," presented on The International Workshop on Electrocatalysis, Photoelectrocatalysis and Biomimetic Catalysis, sponsored by ESCO of United Nations, Xiamen, China, 1985.

PHOTOCATALYZED OXIDATION OF ALCOHOLS AND ORGANOCHLORIDES IN THE PRESENCE OF OXYGEN AND METALLIZED TiO_2 SUSPENSIONS

2.1 INTRODUCTION

Precious metals, such as Pt and Pd, show a high activity in thermal catalysis, presumably because they have a suitable quantity of holes in the d-band and a very low overpotential. They are therefore used for hydrogenation, dehydrogenation and oxidation in both heterogeneous catalysis and electrochemistry.

Non-metallized TiO_2 can be used as a photocatalyst to mineralize various organochlorides (typical hazardous organic pollutants) in an aqueous solution^{1,2,3,4,5}. Metallizing TiO_2 with Pt or Pd (0.1 - 5% by weight (wt.)) can enhance its photocatalytic reductive activity. In the absence of oxygen, it accelerates the dehydrogenation of organics such as methanol and ethanol and increases water photo-splitting rates^{6,7,8}. Bahnemann, Mönig and Chapman studied the photocatalytic reduction of halogenated alkanes using Pt/ TiO_2 ⁹. Several papers deal with photocatalytic reactions in aerated systems using Pt/ TiO_2 : Izumi and Bard *et al.* reported the photocatalytic oxidation of hydrocarbons using Pt/ TiO_2 ^{10,11}. Serpone, Pelizzetti and other authors reported the photocatalytic precipitation of metal ions (such as the oxidative precipitation $\text{Pb}^{2+} \rightarrow \text{PbO}_2$ ↓ and the reductive precipitation $\text{UO}_2^{2+} \rightarrow \text{UO}_2$ ↓) on photocatalyst surfaces^{12,13,14}, and the oxidation of organic compounds (*e.g.*, 3,3'-dichlorobiphenyl) with oxygen using various types of TiO_2 photocatalysts in an aqueous solution^{15,16,17}. Loaded on TiO_2 , Pt and Pd can accelerate the oxygen reduction process occurring at the cathodic area, thereby diminishing the electron accumulation on the surface of TiO_2 particles. This will accelerate the oxidation rate of alcohols, which in fact is controlled by the cathodic reduction of oxygen. According to literature, this process has been observed very often, not only for alcohols but also for other organic compounds^{18,19,20}.

This chapter elaborates upon the photocatalytic activities of metallized TiO_2 for the oxidation of methanol (MeOH), ethanol (EtOH), chloroform, trichloroethylene (TCE) and dichloropropionic acid (DCP) in the presence of dissolved oxygen and at different pH values in an aqueous solution. The possible reaction pathways are also discussed.

2.2 EXPERIMENTAL

2.2.1 Reagents

The TiO_2 used during the experiments was commercial Degussa P25. This native TiO_2 has a BET surface area of approximately $50 \text{ m}^2 \text{ g}^{-1}$ and an average particle size of 30 nm. The chloroform used was Fisher Certified Grade, Lot No. 851771, supplied with a preservative of approximately 0.75% ethanol; its solubility in water amounts to $8.2 \times 10^3 \text{ mg/L}$ at $20\text{--}25^\circ\text{C}$ ²¹. The trichloroethylene (TCE) used was Fisher Certified Grade, Lot No. 911726. The dichloropropionic acid (sodium salt) (DCP) used was 94% pure product from ALDRICH, Lot No. 03108PX. The methanol (MeOH) used was ALDRICH A.C.S. reagent, Lot No. 01707KX. The ethanol (EtOH) used was AAPER Alcohol and Chem. Co. U.S.P. ethyl alcohol (Absolute - 200 Proof, DSP-KY-417). The palladium black used was a product from ALDRICH, Lot No. 06115BY. The palladium dichloride used was Fisher purified product, LOT 915085. The chloroplatinic acid ($\text{H}_2\text{PtCl}_6 \cdot 6\text{H}_2\text{O}$) used was Fisher A.C.S. reagent, Lot No. 915412. These reagents were used without further purification.

2.2.2 Photocatalyst preparation

The 1% wt. Pt/TiO_2 photocatalyst was prepared in two different ways: by photodeposition in a way similar to the method used by Bard²², and by chemical deposition in a way similar to the method used by Pichat²³. Photodeposited Pt/TiO_2 was synthesized in a deaerated system by near-UV illumination of 467 ml of slurry containing 34.6 g of TiO_2 , 0.923 g of $\text{H}_2\text{PtCl}_6 \cdot 6\text{H}_2\text{O}$ and 25 ml of glacial acetic acid for 38 hours. After illumination, the dark grey slurry was centrifuged in a lab centrifuge (Model RC5C, Sorvall instruments, Du Pont) at 3,000 rpm for 30 minutes and then washed eight times. The dark grey solid was dried at 120°C for about three hours. It was not further pretreated before being used. Chemically deposited Pt/TiO_2 was prepared by dissolving 1 g of $\text{H}_2\text{PtCl}_6 \cdot 6\text{H}_2\text{O}$ in 500 ml of water containing 37.7 g of TiO_2 . The slurry was stirred in a rotary vacuum evaporator at 75°C for three hours. The resultant solid mass was dried in an air oven at 110°C , heated to 200°C in a nitrogen flow, and then reduced in a hydrogen flow at 480°C for two hours.

The 1% wt. Pd/TiO_2 photocatalyst was prepared in two different ways: as a physical mixture, and as a photodeposition¹⁸. A physical mixture of Pd and TiO_2 was obtained by mixing 1% wt. black Pd with TiO_2 in a mortar and thoroughly grinding the mixture. The resultant matter was pretreated consecutively at 240°C in a nitrogen flow for about one hour, and at 430°C in a hydrogen flow for six or fourteen hours. Photodeposited 1% wt. Pd/TiO_2 was prepared by dissolving 0.333 g of PdCl_2 in 13.33 ml of glacial acetic acid, diluting the solution to 270 ml in a photoreactor, adding 20.0 g of TiO_2 , closing the reactor, and illuminating the slurry for 17 hours using a 100-W medium pressure mercury lamp (Sylvania, Par 38) with a near-UV

filter. After being illuminated, the dark grey slurry was centrifuged in a lab centrifuge (Model RC5C, Sorvall instruments, Du Pont) at 3,000 rpm for 30 minutes, and then washed eight times. The dark grey solid was dried at 120°C for about three hours. It was not further pretreated before being used.

2.2.3 Apparatus for photocatalytic oxidation

All experiments were performed in a liquid-phase recycle photoreactor similar to the one used by Pruden and Ollis²⁴ (Fig.2.1a and 2.1b). The total reactor volume of this apparatus was 930 ml, including a 280-ml quartz annular photoreactor and a reactor reservoir (made from a 500-ml, 3-neck flask). The total liquid volume in the reactor was fixed at 600 ml, with 330 ml of reservoir headspace during each run.

In the case of photocatalytic oxidation of organochlorides (Fig.2.1a), three electrodes and a thermometer were mounted at the top of the reservoir. One of these electrodes was a pH electrode meant for monitoring the reaction pH. The other two were a chloride ion electrode and a reference electrode meant for the determination of Cl^- in solution. The thermometer was used to control the reaction temperature. The reaction solution was recycled through a quartz annular photoreactor using a polypropylene/ceramic pump. Illumination of 3.08×10^{-4} Einstein/min was provided by a black-light fluorescent tube (GE BLB - 15 W) mounted in the centre of the photoreactor. The predominant emission wavelength (λ) of this lamp ($320 \leq \lambda \leq 400$ nm) is suitable for the photo-excitation of TiO_2 ($\lambda \leq 360$ nm) and causes no homogeneous photoreaction (e.g., dechlorination at $\lambda \leq 300$ nm) of organochlorides such as chloroform, TCE and DCP.

In the case of photocatalytic oxidation of alcohols in an aerated system in which oxygen was consumed at a high rate, a somewhat different apparatus was used (Fig.2.1b). Instead of two electrodes for the determination of chloride ions, a pressure gauge scaled from 0 to 60 (inch of H_2O column) was mounted at the top of the reservoir in order to monitor and measure the changes in pressure occurring in the reactor.

2.2.4 The procedure and conditions of the photocatalytic experiments conducted

Before illumination, 550 cm^3 of a photocatalyst (1 wt. % Pt/TiO_2 or Pd/TiO_2) in the form of a liquid slurry (1.0 gram catalyst per liter) was added into the reservoir. The slurry was sparged with pure oxygen for 30 minutes, then the reactor was sealed, liquid reactants were added, and the total slurry was diluted to 600 cm^3 with water. Before starting the illumination, another 40 cm^3 of pure oxygen was syringed in order to maintain a positive pressure (20 inch of H_2O column) in the reactor. The control experiments were carried out by the same procedure above, but during these experiments no photocatalyst was added to the system. The

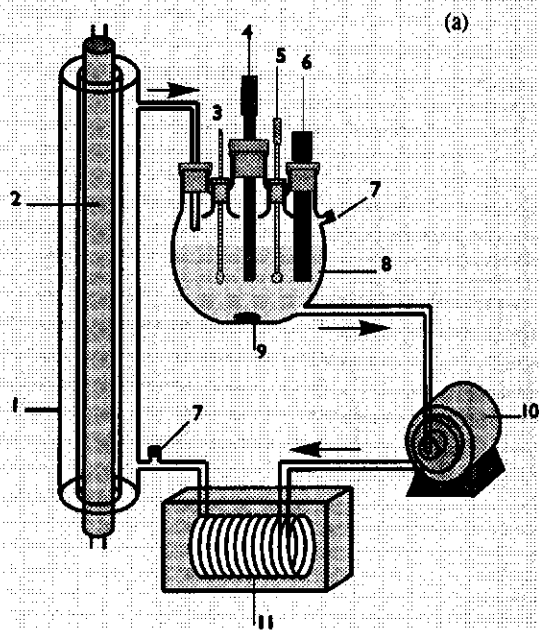
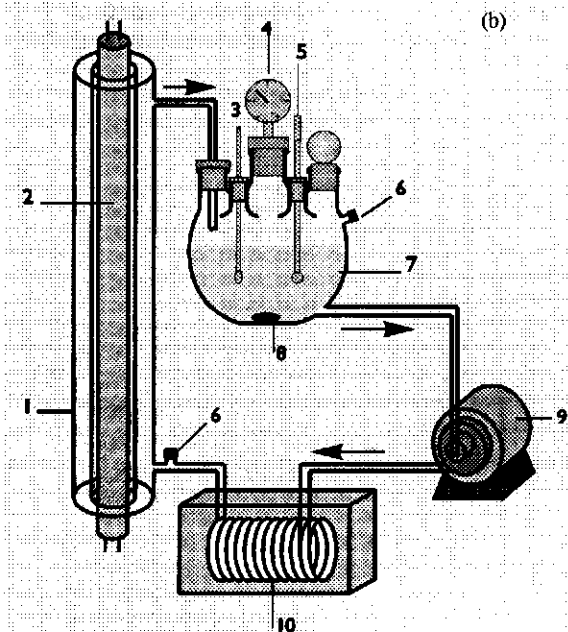


Fig.2.1a. Recycle Photocatalytic Reactor for organochloride oxidation.

1. Quartz annular photoreactor;
2. Black light tube;
3. Thermometer;
4. Chloride ion electrode;
5. pH electrode;
6. KCl reference electrode;
7. Sample port;
8. Pyrex vessel;
9. Stir bar;
10. Recirculation pump;
11. Cooling coil.

Fig.2.1b Recycle photocatalytic reactor for alcohol oxidation.

- (1). Quartz annular photoreactor;
- (2) Black light;
- (3). Thermometer;
- (4). Pressure gauge (0 - 60 in. water);
- (5). pH electrode;
- (6). Sample port;
- (7). Pyrex sample vessel;
- (8). Stir bar;
- (9). Recirculation pump;
- (10). Cooling coil.



oxygen concentration in the solution was around the oxygen saturated concentration of 41.36 ppm at 25°C²⁵. The quantity of pure oxygen dissolved in 600 cm³ of water was low compared with the total quantity of pure oxygen in the reservoir headspace (330 cm³). The total quantity of oxygen in the system was around 23.8 mmol. Because of the relatively low reaction rate and the smooth variation of reactor pressure during illumination, it was possible to keep the oxygen concentration in the liquid at a constant level by constant injection of oxygen. During the process of photoreaction, periodically a gas sample of 1 ml and a liquid sample of 0.5 or 1 ml were taken from the sample ports. In the photoreactor, the flow of slurry was recycled at the rate of around 1,500 ml/min.

2.2.5 Analyses

The chloride ion concentration was measured using an in-situ chloride selective electrode (HNU, ISE-30-17-00) and a reference electrode. The H⁺ concentration was measured using an in-situ pH electrode (Fisher, 13-620-93). An ORION 701A digital pH/mv meter was employed to monitor these electrodes.

Chloroform, TCE, methanol or ethanol was sampled periodically and determined by Flame Ionization Detection (FID) in an HP 5890A Gas Chromatograph (GC) with a capillary column (J & W Scientific Cat. No. 125-1334). The liquid samples containing volatile chloroform and TCE were placed in vials, sealed with Teflon-faced septa, and allowed to equilibrate at 37°C. About 0.2 ml of vapour samples from the vial headspace were then injected into the GC. The methanol- or ethanol-containing liquid samples from the reactor were centrifuged to remove photocatalyst, and then analyzed for methanol or ethanol by injecting 1 µl of liquid supernatant directly into the GC. The intermediary products of methanol and ethanol, such as formaldehyde, formic acid, acetaldehyde, acetic acid, methane and ethane, were detected simultaneously with methanol and ethanol by GC.

The total carbon dioxide production in the reactor, including the carbon dioxide in the gas and liquid phases (in the form of carbonate, bicarbonate and carbonic acid) was measured by injecting liquid or gas samples directly into the absorber (containing 1 N H₂SO₄) of an infrared carbon dioxide analyzer (Horiba, PIR-2000). All instruments were calibrated during operation. It should be noted that, unless indicated otherwise in figures, the CO₂ production reported in this chapter is the total quantity of CO₂ in the reactor including the CO₂ present in the liquid phase (all chemical states) and gas phase. The total quantity of CO₂ was calculated and expressed as the concentration in the liquid phase in the units of milligram per litre (ppm) or millimole per litre (mM).

2.3 RESULTS AND DISCUSSION

2.3.1 Photocatalytic oxidation of methanol, ethanol, chloroform and TCE in the presence of oxygen: preliminary experiments

The photo activity of various photocatalysts and their selectivity of oxidation were compared based on the production of carbon dioxide and chloride. The photo activities of Pt/TiO₂, Pd/TiO₂ and TiO₂ for various compounds are shown in Tables 2.1 and 2.2. Compared with TiO₂, platinized TiO₂ shows a much higher mineralization activity in the case of photo-oxidation of methanol and ethanol but a lower mineralization and dechlorination activity in the case of photo-oxidation of chloroform and TCE. Compared with TiO₂, Pd/TiO₂ shows a slightly higher activity for methanol, ethanol and TCE but a lower activity for chloroform.

Table .2.1. Photocatalytic oxidation of methanol, ethanol, chloroform and TCE using aerated native TiO₂ and Pt/TiO₂

Reactant	Initial Concentration (mM)	Catalyst	Illumination Time (minute)	Initial pH of Solution	Concentration of CO ₂ (mM)	Concentration of Cl ⁻ (mM)
Methanol	20.6	Pt/TiO ₂	180	10.9	4.3	
	20.6	TiO ₂	180	10.9	1.8	
	4.2	Pt/TiO ₂	120	5.1	1.4	
	4.2	TiO ₂	120	5.1	0.18	
Ethanol	14.5	Pt/TiO ₂ *	240	10.9	2.9	
	14.5	TiO ₂	240	10.9	1.2	
	7.4	Pt/TiO ₂	180	5.1	1.8	
	7.4	TiO ₂	180	5.2	0.43	
Chloroform	1.0	Pt/TiO ₂	180	5.4	0.37	0.43
	1.0	TiO ₂	180	5.5	0.62	0.76
TCE	0.31	Pt/TiO ₂	100	5.2	0.03	0.08
	0.29	TiO ₂	100	5.4	0.36	0.64

*: This type of Pt/TiO₂ was prepared by chemical deposition. The other platinized photocatalysts were prepared by photodeposition.

Table 2. 2. Photocatalytic oxidation of methanol, ethanol, chloroform and TCE using aerated native TiO_2 and Pd/TiO_2

Reactant	Initial Concentration (mM)	Catalyst	Illumination Time (minute)	Initial pH of Solution	Concentration of CO_2 (mM)	Concentration of Cl^- (mM)
Methanol	27.6	Pd/TiO_2	180	5.6	2.6	
	29.1	TiO_2	180	5.1	1.9	
Ethanol	14.5	Pd/TiO_2^*	140	5.1	0.23	
	14.5	Pd/TiO_2	140	5.5	0.79	
	14.5	TiO_2	140	5.2	0.66	
Chloroform	1.0	Pd/TiO_2	180	5.6	0.20	0.36
	1.0	TiO_2	180	5.3	0.74	0.88
TCE	0.29	Pd/TiO_2^{**}	100	5.4	0.41	0.66
	0.29	TiO_2	100	5.4	0.36	0.64

*: This type of Pd/TiO_2 was prepared by photodeposition.

** : This type of Pd/TiO_2 was prepared by physical mixing followed by a pretreatment at 430°C for 14 hours in a flow of hydrogen.

The other types of Pd/TiO_2 were prepared by physical mixing followed by a pretreatment at 430°C for six hours in a flow of hydrogen.

All native TiO_2 mentioned in the table (except in the case of TCE) was pretreated concurrently with the corresponding Pd/TiO_2 .

The blank experiments (*i.e.*, without suspended photocatalyst in solution) demonstrated that methanol and ethanol cannot be oxidized (photolyzed) by near-UV light illumination. Therefore it can be concluded that all oxidation products of the alcohols mentioned in Tables 2.1 and 2.2 as well as in the other figures of this chapter resulted from the simultaneous presence of a photocatalyst and illumination. Thus, they may be considered as the reaction products of photocatalytic oxidations.

2.3.2 Photocatalyzed oxidation of methanol in an aerated system

To compare in more detail the photocatalytic activity of photocatalysts in relation to methanol oxidation, the effect (or activity) of platinized TiO_2 and native TiO_2 on the production of CO_2 during photo-oxidation of methanol was measured. Fig. 2.2 shows the experimental results of CO_2 release vs. illumination time. This figure shows that the photo mineralization activity

regarding methanol as a result of using 1% Pt/TiO₂ is three times higher than that resulting from the use of native TiO₂.

To understand and apply a chemical reaction, it is very important to know its intermediates. Fig.2.3 shows the results of a gas-chromatographic examination of the possible intermediates of photocatalytic oxidation of methanol in a liquid phase such as formaldehyde and formic acid. During the analytical process carried out, the GC retention time for methanol was found to be ~1'56", for formaldehyde ~2'4", and for formic acid ~2'10", and their peaks were clearly separated. The GC analysis results show that during the photodegradation of methanol using Pt/TiO₂ no intermediates could be detected in solution. In the presence of sufficient oxygen, methanol can be easily oxidized using Pt/TiO₂, Pd/TiO₂ and even native TiO₂ via intermediates such as formaldehyde and/or formic acid to the final product of CO₂. Neither during the other experiments of photocatalytic oxidation of methanol carried out were any intermediates detected using Pd/TiO₂ or native TiO₂ as a photocatalyst. It is therefore likely that photocatalytic oxidation of methanol occurs on the photocatalyst surface and that most of the intermediates of methanol oxidation are adsorbed onto the photocatalyst surface, where further oxidation to CO₂ takes place.

2.3.3 Photocatalyzed oxidation of ethanol in an aerated system

In the previous paragraph, it was demonstrated that in relation to methanol 1%Pt/TiO₂ shows a higher oxidation activity than native TiO₂. In the case of photocatalytic oxidation of ethanol in an aerated system, 1%Pt/TiO₂ also showed a higher photo mineralization activity than native TiO₂. Fig.2.4 shows the amount of CO₂ released versus illumination time. From Fig.2.4 it can be concluded that, in relation to ethanol, the activity shown by 1%Pt/TiO₂ is approximately twice as high as that shown by native TiO₂. During the photocatalytic oxidation of ethanol, various intermediates appeared. Most of the products and intermediates resulting from the photocatalytic oxidation of ethanol can be identified based on their GC retention time and relevant information in literature^{26,27,28,29}. Under the GC conditions used, the 1'52" peak is methane, the 2' peak is acetaldehyde and the 2'18" peak is acetic acid (Fig.2.5 and 2.6). The 2'26" peak is an unknown compound which was not detected in the gas phase. In view of its longer retention time, it may be a nonvolatile compound larger than acetic acid. The fact that the different content values of the photocatalytic products and intermediates produced in the presence of Pt/TiO₂ and native TiO₂ (Fig.2.6) reveals that platinization can change the rate-controlling step of photocatalytic oxidation of organics on TiO₂ surfaces.

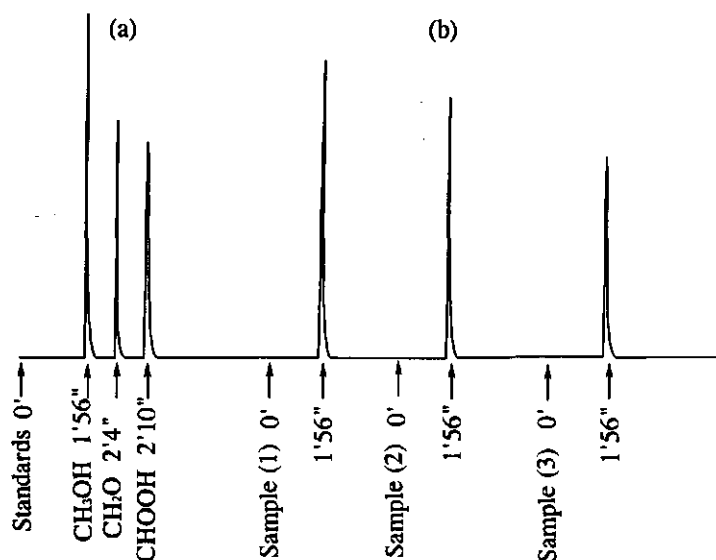


Fig.2.3. A typical GC detection graph of the possible intermediates of the photocatalytic aerated oxidation of methanol on suspended TiO_2 powder. Area (a) shows the analytical results of 0.01-ml standard gas sample of CH_3OH , CH_2O and CHOOH . Area (b) shows the results of reaction samples of the photocatalytic oxidation of methanol (initial concentration 900 ppm). Sample (1) was illuminated for 40 minutes, sample (2) for 140 minutes, and sample (3) for 420 minutes.

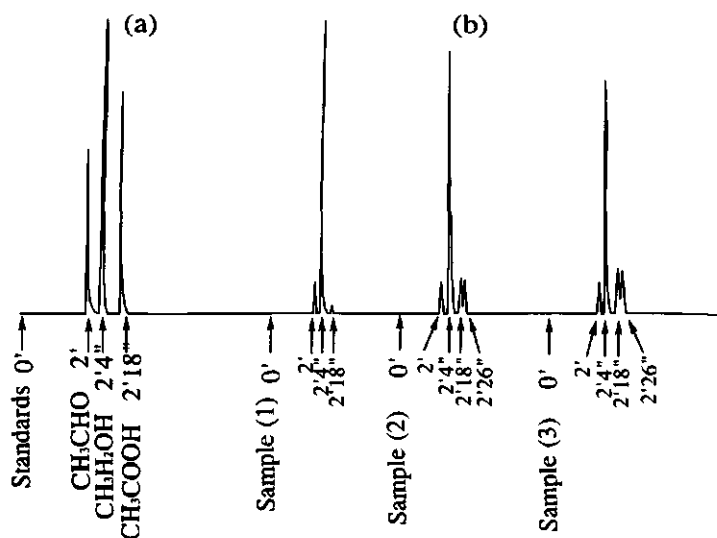


Fig.2.5. A typical GC detection graph of the possible intermediates of the photocatalytic aerated oxidation of ethanol on suspended TiO_2 powder. Area (a) shows the analytical results of 0.01-ml standard gas samples of ethanol, acetaldehyde and acetic acid. Area (b) shows the results of reaction samples of the photocatalytic oxidation of ethanol (initial concentration 620 ppm). Sample (1) was illuminated for 40 minutes, sample (2) for 140 minutes, and sample (3) for 220 minutes.

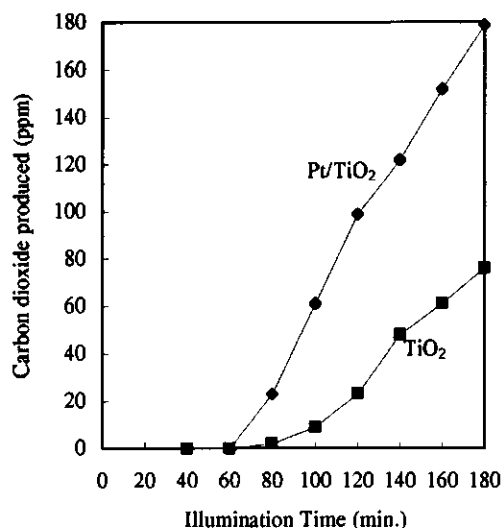


Fig.2.2. Photocatalytic mineralization of methanol on Pt/TiO₂ and native TiO₂ in the presence of O₂. Initial concentration of methanol: 660 ppm; Pt/TiO₂ was prepared by chemical deposition, followed by pretreating in an H₂ flow for 2 hours at 480°C. Type of UV light: 15-W black light lamp, 600 ml of solution, initial pH = 10.9, 1.0 g cat./L, ~25 °C.

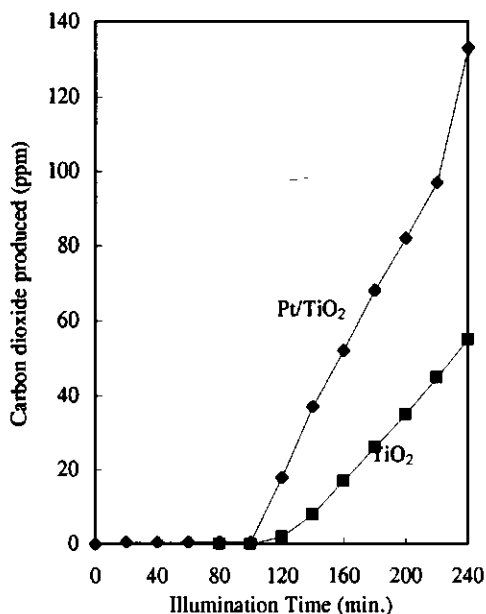


Fig.2.4 Photocatalytic mineralization of ethanol on Pt/TiO₂ and native TiO₂ in the presence of O₂. Initial concentration of ethanol: 670 ppm. The conditions are similar to those given in Fig.2.2.

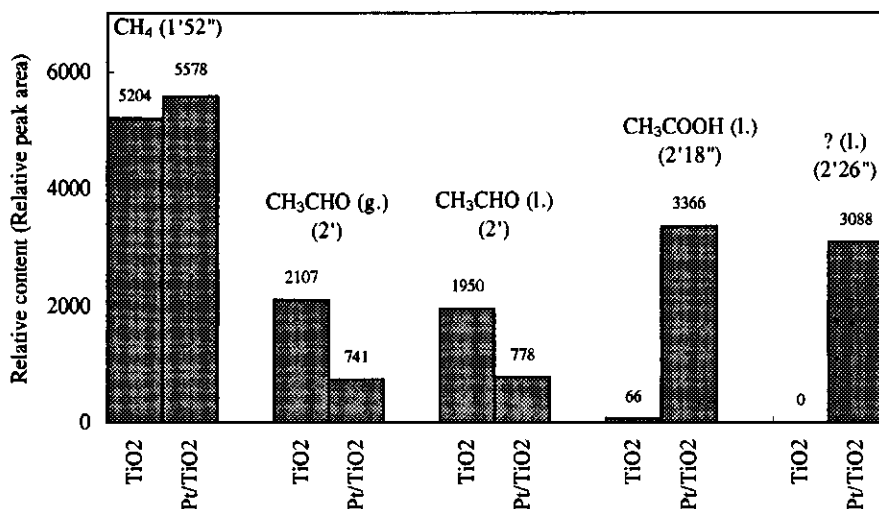


Fig.2.6. A typical example of a gas chromatogram for the intermediate distribution during the photocatalytic oxidation of ethanol in an aerated system. TiO₂ and 1%Pt/TiO₂ : 1 g/L, initial pH=5.1, 600 ml of solution, illumination with a 15-W black light lamp, 25°C, total illumination time 240 min. (g.): the compound in the gas phase, (l.): the compound in the liquid phase. The peak at 2'26" was not identified

2.3.4 The effect of pH on the oxidation of alcohols in an aerated system

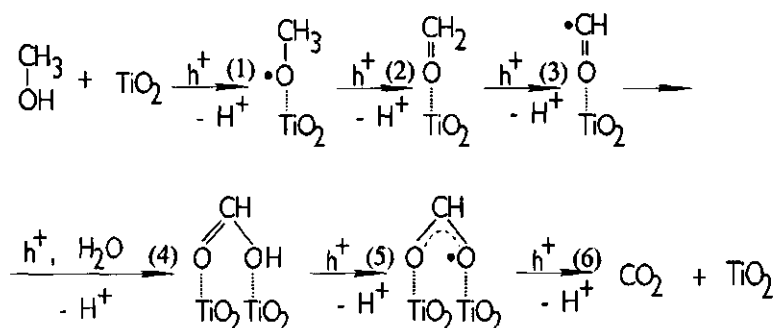
The photocatalytic conversion of alcohols of low molecular weight to carbon dioxide and water is thought to occur via progressively more oxygenated intermediates, for example for methanol:



While methanol and its first intermediate (CH_2O) are hardly ionizable, its second intermediate dissociates easily into $\text{H}^+ + \text{HCOO}^-$. The rate of methanol converted to acetaldehyde is not expected to be strongly pH-dependent, but based on experiments the production of carbon dioxide is expected to be slow at a high pH where the TiO_2 surface is negatively charged by an acetate group and a hydroxyl group. This process is also shown in Fig.2.7, which presents a more detailed scheme of the possible reaction mechanisms for both methanol and ethanol.

Fig.2.8 and 2.9 show the photocatalytic oxidation of methanol and ethanol using native TiO_2 , and Fig.2.10 and 2.11 show the photocatalytic oxidation of methanol and ethanol using 1%Pt/ TiO_2 . As shown in these figures, when the pH is initially alkaline, certain amounts of alcohols adsorb onto photocatalyst surfaces before illumination. It was observed that the mineralization of methanol and ethanol is strongly pH-dependent. During the oxidation process (starting at $\text{pH} \approx 11$), the solution pH shifts from alkaline to acidic, and (gaseous and dissolved) carbon dioxide is produced only at a low pH. At pH values > 9 , no or only very little mineralization (CO_2 production) of methanol and ethanol was observed, although methanol and ethanol can be oxidized at this pH. When the solution pH dropped below 9, CO_2 began to form rapidly. When the pH was initially acidic, CO_2 was produced immediately. This is shown in Fig.2.12 and 2.13: CO_2 was produced simultaneously with the degradation of methanol or ethanol, and no alcohols adsorbed onto photocatalyst surfaces before illumination. The fact that methanol was oxidized at pH values > 9 , while neither the final product (CO_2) nor any intermediate were detected in the liquid, suggests that photocatalytic oxidation of methanol occurred on the photocatalyst surface and that the intermediates (formaldehyde and formic acid) adsorbed onto the photocatalyst surface and were further oxidized at a low pH to the final product, carbon dioxide. Platinization of TiO_2 to 1%Pt/ TiO_2 resulted in alcohol conversion and carbon dioxide production at increasing rates. The data on pH vs. time given in Fig.2.14 for both native and metallized photocatalysts indicate, however, that mineralization is negligible at alkaline pH values, even when Pt/ TiO_2 is used as a photocatalyst. Metallization accelerates the ethanol oxidation rate (pH decreases faster than in the case of native TiO_2) and yields more oxygenated intermediates. However, no CO_2 release was observed. Only at acidic pH values, carbon dioxide was produced (as carbonate, bicarbonate, or carbonic acid) at noticeable rates.

For methanol oxidation:



For ethanol oxidation:

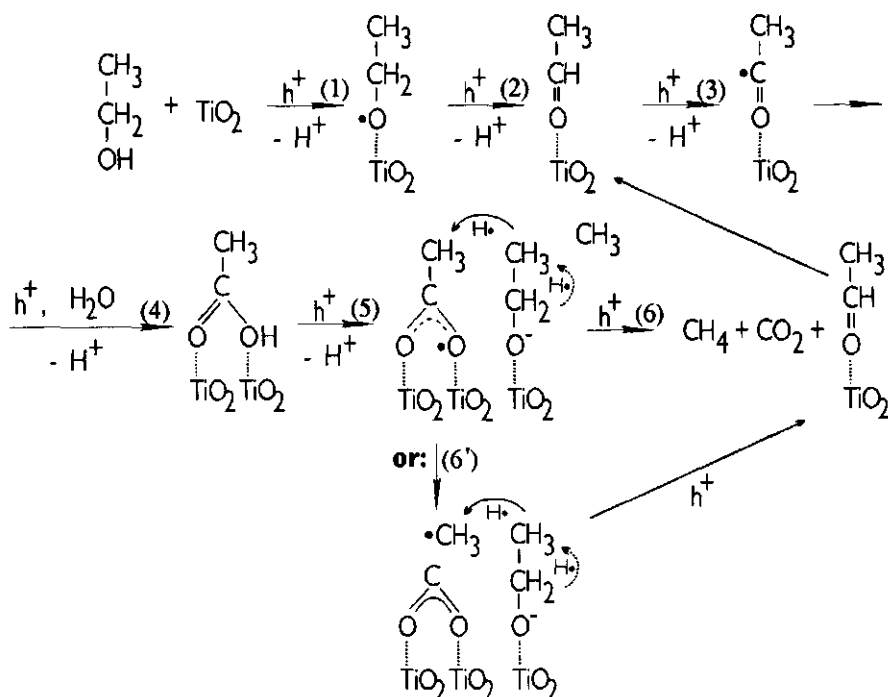


Fig.2.7. The possible surface adsorption and reaction mechanisms of photocatalytic oxidation of methanol and ethanol in aerated and deaerated systems.

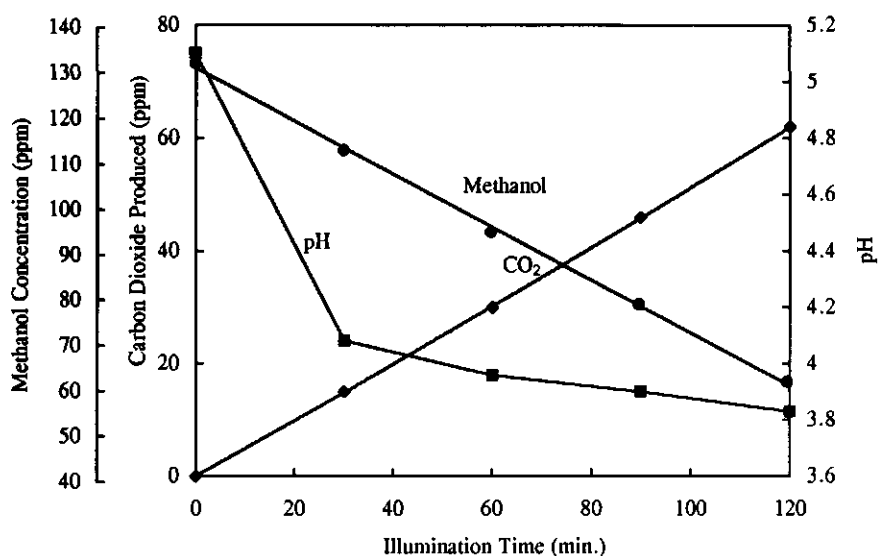


Fig.2.12. Photocatalytic oxidation of methanol as a function of illumination time. Initial concentration of methanol: 132 ppm, initial pH = 5.1, 1%Pt/TiO₂, O₂, 15-W black light lamp, 600 ml of solution, 1.0 g.cat./L, 26°C.

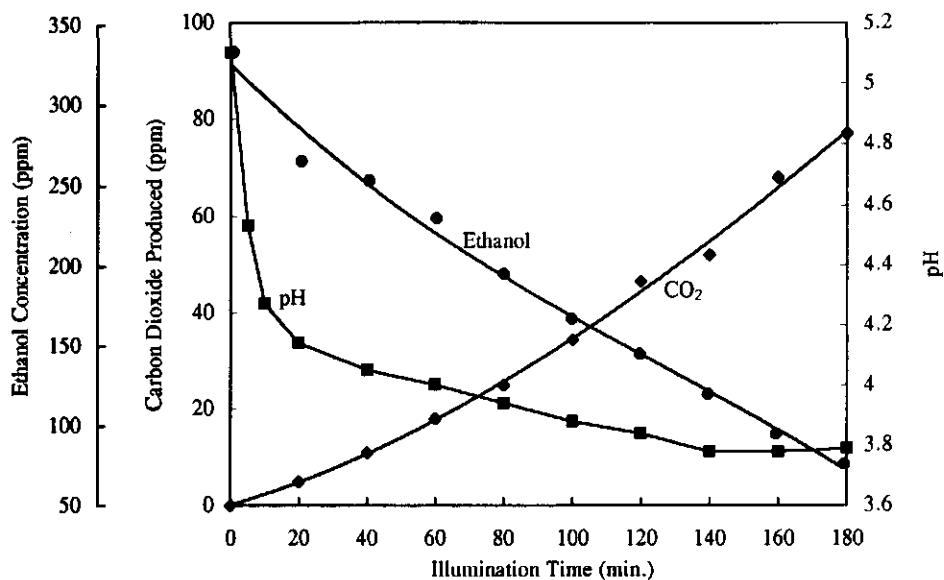


Fig.2.13. Photocatalytic oxidation of ethanol as a function of illumination time. Initial concentration of ethanol: 333 ppm, initial pH = 5.1, 1%Pt/TiO₂, O₂, 15-W black light lamp, 600 ml of solution, 1.0 g.cat./L, 26°C.

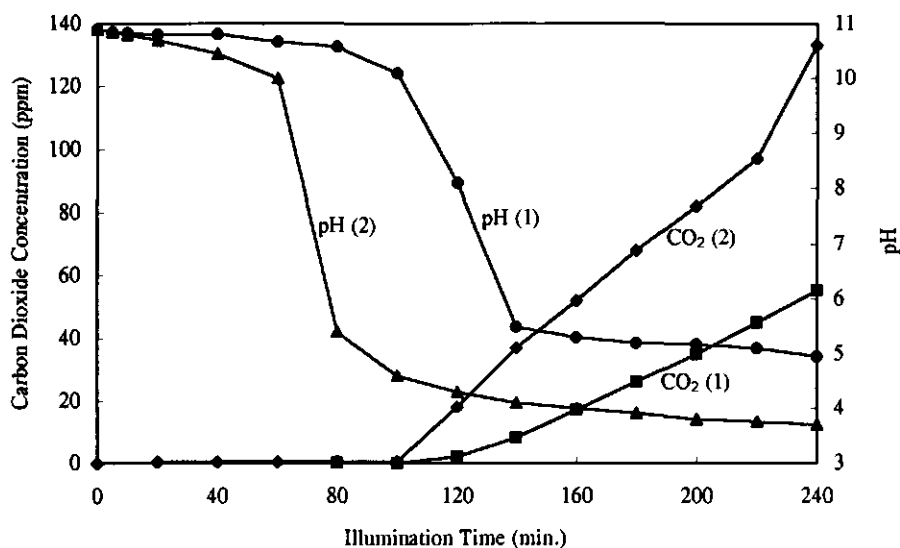


Fig.2.14 The pH change and CO₂ production on native TiO₂ and Pt/TiO₂. Initial concentration of ethanol: 670 ppm. (1). native TiO₂, no pretreatment. (2). 1%Pt/TiO₂, chemically deposited, pretreatment at 480 °C, H₂ flow for two hours. 15 W black light lamp, 600 ml of solution, initial pH = 10.9, 1.0 g.cat./L, ~ 25 °C.

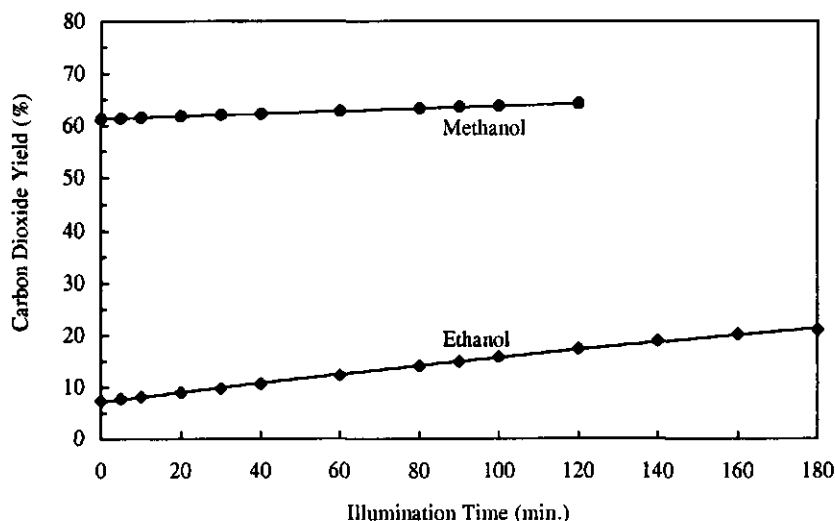


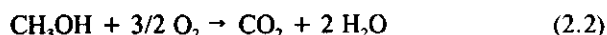
Fig.2.15. The mole yields of CO₂ during the oxidation of alcohols, calculated from Fig.2.12 and 2.13. Initial pH = 5.1, 1%Pt/TiO₂, O₂, 15-W black light lamp, 600 ml of solution, 1.0 g.cat./L, 26°C.

In the case of methanol oxidation using TiO_2 or Pt/TiO_2 , CO_2 production occurred only when the solution pH dropped below 9 (Fig. 2.8 and 2.10). In the case of ethanol oxidation using TiO_2 or Pt/TiO_2 , CO_2 appeared when the solution pH was below 7.5 and 4.5, respectively (Fig. 2.9 and 2.11). This means that during the oxidation of ethanol more oxygenated intermediates accumulated in solution than in the case of methanol. This data can be explained from the mole conversion ratio (mole yield) of the final product (CO_2) in total oxidized alcohol (Fig. 2.15). After illumination, more than 60% of the total amount of oxidized methanol was promptly converted to the final product (CO_2). This high conversion ratio (yield) is kept during the entire 120 minutes of illumination time. However, after illumination the yield of CO_2 observed during the oxidation of ethanol was only 7%, increased slowly over time, and reached only 25% after 180 minutes of illumination. This yield is low compared with that obtained in the case of methanol. This clearly indicates that the photocatalytic oxidation of methanol proceeds more rapidly through the steps of oxygenated intermediates to CO_2 than that of ethanol.

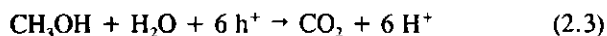
2.3.5 The possible mechanisms of photocatalytic reaction of alcohols

2.3.5.1 General introduction

Redox reactions always include two half-reactions: that of oxidation and that of reduction. For example, the total reaction of photocatalyzed degradation of methanol in an aerated system can be written as:



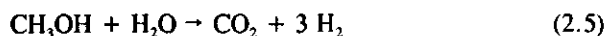
which simultaneously involves the half-reaction of methanol oxidation:



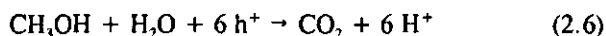
and that of oxygen reduction:



Taking the same example but now in a deaerated system results in:



This reaction, during which H_2 gas is produced, involves the half-reaction of oxidation:



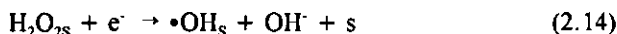
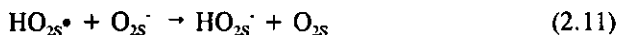
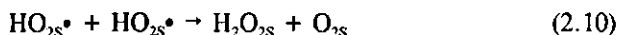
and that of reduction:



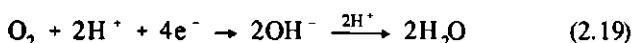
In a photocatalytic system using suspended powder photocatalyst, these two half-reactions take place separately in two different areas on photocatalyst surfaces (*i.e.*, the anodic and cathodic areas) via many chemical steps. The photocatalytic mechanisms of the degradation of an organic compound involve multiple processes in both anodic and cathodic areas on photocatalysts. Many researchers^{30,31,32,33} have assumed many possible mechanisms of photocatalytic reactions (involving alcohols such as methanol and ethanol) in the presence of TiO_2 , Pt/TiO_2 and Pd/TiO_2 , as summarised in the following pathways. Some experimental data are reported to substantiate which mechanism is favourable. Based on our experimental data on photocatalytic degradation of methanol and ethanol, the next paragraph discusses in great detail a mechanism for the photocatalytic oxidation of methanol and ethanol.

2.3.5.2 Cathodic processes in the photocatalyst cathodic area of TiO_2 , Pt/TiO_2 or Pd/TiO_2

During the oxidation of an organic compound in the anodic area in an aerated system, oxygen is reactive in the cathodic area because of its much higher positive oxidative potential ($E^\circ (\text{O}_2/\text{OH}^-) = 1.23 \text{ V}$) compared with H^+ ($E^\circ (\text{H}^+/\text{H}_2) = 0 \text{ V}$). Therefore, oxygen is the easiest reducible substrate in the solution. It must adsorb on cathode surfaces (indicated by s) first to form an adsorption state ($\text{O}_{2\text{s}}$). Subsequently, a sequence of cathodic processes of getting electrons may occur. The following reactions can occur in an aerated system:



Eq.2.8 - 2.17 give possible cathodic processes in an aerated system. Depending on the state of the photocatalyst surface (whether or not TiO_2 is metallized), the net reaction (or main process) of Eq.2.8 - 2.17 is represented by Eq.2.18 in the case of native TiO_2^{34} , the oxygen of which is not completely reduced (its valence is -1), or by Eq.2.19 in the case of platinized TiO_2 , the oxygen of which is completely reduced to a valence of -2:



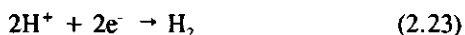
Eq.2.18 is obtained by combining Eq.2.8 - 2.13 and 2.16. In the presence of platinized TiO_2 , oxygen is reduced to hydroxide ions and then to water. During this process, four electrons are needed to reduce the oxygen completely to a valence of -2^{19,20}.

The reaction given in Eq.2.19 can occur through H_2O_2 via Eq.2.8 - 2.15. On native TiO_2 , it is obvious that the reduction of oxygen adsorbed stops on the mid-steps of only producing H_2O_2 (Eq.2.8 - 2.13) and then desorbs, splits to $\bullet\text{OH}$ (Eq.2.16, 2.17), whereas on Pt/TiO_2 oxygen is reduced completely and reaches the OH^- stage (Eq.2.14, 2.15). Thus, the rapid reduction of oxygen on Pt/TiO_2 does not increase the H_2O_2 concentration in solution, and the Eq.2.16 and 2.17 may not occur easily, although Pt enhances the total rate of methanol or ethanol oxidation. The less likely reducing reactions occurring in the cathodic area are shown in Eq.2.10 and 2.11 because two adsorption sites are involved in the reactions. On TiO_2 , Pd plays the same cathodic role as Pt, but its effect is less strong.

In a deaerated system (without oxygen), the proton in solution is the prior reductive substrate in the cathodic area; it must adsorb onto the cathodic surface, forming an adsorption state (H_s^+), after which the following cathodic processes occur:



The net reaction of Eq.2.20 - 2.22 is:



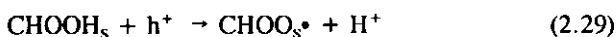
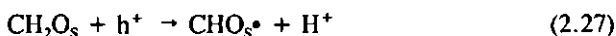
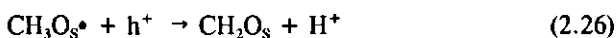
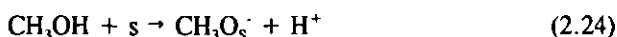
Eq.2.20 - 2.23 cannot easily occur in an aerated system, because few hydrogen atoms can be formed (Eq.2.20) in the presence of oxygen. Many data in literature ^{35,36} show that Pt can accelerate the photocatalytic oxidation of some organic compounds (*e.g.*, methanol, ethanol) on TiO₂ in both deaerated and aerated systems. This is because methanol and ethanol are proper hole scavengers, and the total rate of oxidation of alcohols depends upon the rate of reduction in the cathodic area. In a deaerated system, the primary role of Pt on TiO₂ is to expedite electron transfer from TiO₂ to protons, as shown in Eq.2.20 - 2.22. It strongly accelerates the net reaction shown in Eq.2.23. In the cathodic area in an aerated system, oxygen will be more competitive in getting (or absorbing) electrons compared to protons, since thermodynamically it can more easily be reduced than protons, and a different cathodic process occurs on TiO₂ as shown in Eq.2.8 - 2.15.

2.3.5.3 Methanol conversion process on the anodic area of Pt/TiO₂ in aerated and deaerated systems

As discussed in section 2.3.5.1, the photocatalytic oxidation of alcohols with oxygen can be separated into two half-reactions, an anodic and a cathodic one. These two half-reactions in the anodic and cathodic areas are independent of each other. The rate of the half-reaction in the anodic area is only a function of its substrates and the surface area, and is not influenced by the substrates in the cathodic area. The rate of the net reaction of alcohol and oxygen is governed by the slowest half-reaction.

In the anodic area of the photocatalyst, the mechanism of methanol oxidation has two possible pathways which are independent of the presence of oxygen in the cathodic area, since the half-reaction of the anodic process is independent of the half-reaction of the cathodic process^{37,38}. The following anodic pathways can combine with the cathodic process given in Eq.2.8 - 2.17 to form the net reaction in an aerated system, or combine with Eq.2.20 - 2.22 to form the net reaction in a deaerated system.

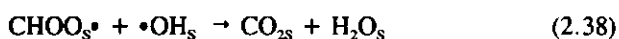
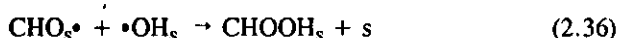
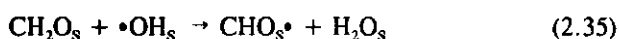
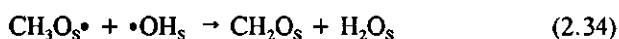
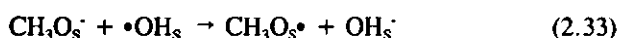
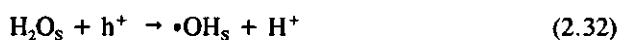
Pathway 1. Direct oxidation. Methanol adsorbed onto the anodic surface of the photocatalyst may be oxidized directly by holes and mineralized finally to CO₂:



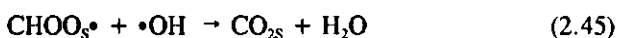
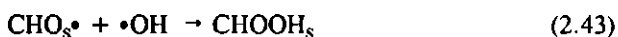
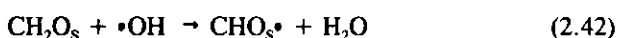
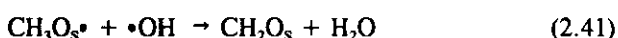
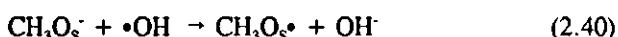


The desorption of CO_{2s} from the photocatalyst surface to the solution and gas phase is given in Eq.2.49.

Pathway 2. Indirect oxidation. In the first case, methanol adsorbed onto the catalytic surface may be oxidized indirectly by adsorbed $\bullet\text{OH}$:



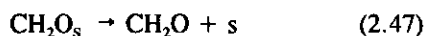
The second possible indirect pathway is that the adsorbed methanol is oxidized by the free $\bullet\text{OH}$ in solution:



The complete oxidation of methanol requires the transfer of six electrons in order to form CO_2 . The favourable pathway is probably pathway 1, because only one adsorption site and a single-molecule reaction are involved in this process. In pathway 1, only one step (Eq.2.28) involves a two-molecule reaction, which may be the rate-controlling step of this pathway. To enable pathway 2, in all steps two adsorption sites are required for methanol and $\bullet\text{OH}$ reaction. A longer reaction time is needed for the two reactants to be in contact with each other, but

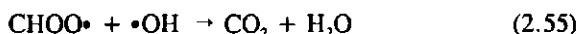
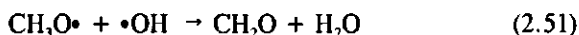
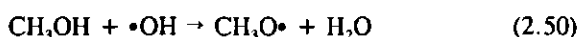
pathway 2 is in agreement with evidence obtained by electron spin resonance (ESR) spectroscopy³⁹ and with other data found in literature⁴⁰ showing the presence of $\bullet\text{OH}$ on the photocatalyst surface.

The above processes include the following desorption steps:



From Eq.2.25 - 2.30 and from Eq.2.32 - 2.38, both pathways of methanol oxidation to CO_2 are six-electron processes. Finishing such a six-electron transfer will not be easy, if on photocatalyst surfaces many stages exist such as adsorption, desorption of substrates, electron transfer, and effective reaction collision. Pathways 1 and 2 or a mixture thereof are more likely to occur than other pathways with adsorption and desorption processes during the six-electron transfer. Because intermediates were not detected during aerated photo-oxidation of methanol, Eq.2.47 and 2.48 appear to be negligible.

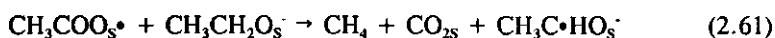
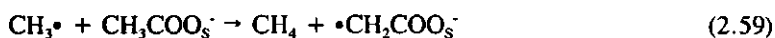
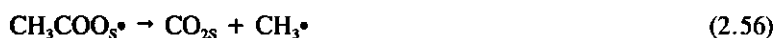
In addition, methanol may be oxidized via a third indirect pathway without adsorbing onto the photocatalyst surfaces. For example, it may be through hydroxyl radical oxidation in solution:



If this non-surface reaction mechanism were possible, the intermediates of formaldehyde and formic acid would have to exist in solution and it should be possible to detect them, which does not correspond with the results of our experiments (Fig.2.3). Micic *et al.* reported results of electron paramagnetic resonance (EPR) spectroscopy regarding photocatalytic oxidation of methanol on TiO_2 in a deaerated system and suggested that methanol be chemisorbed on TiO_2 ⁴¹. This is again experimental evidence showing that the photocatalized oxidation of methanol occurs on the surface of photocatalysts.

2.3.5.4 Ethanol conversion process on the anodic area of Pt/TiO₂ in aerated and deaerated systems

The cathodic processes of photo-oxidation of ethanol are similar to those given in Eq.2.8 - 2.22, and there are also two possible pathways for the anodic mechanisms in both aerated and deaerated systems. Because ethanol has a methyl group, its oxidation process is more complicated than the one involving methanol. There are more opportunities for the formation of intermediates. A possible pathway in the anodic area may include:

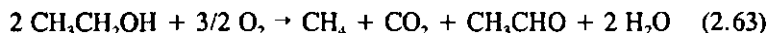


During our experiments, ethane (Eq.2.57) could not be detected. According to the results obtained by Yoneyama and Bard *et al.*²⁷ and Kraeutler and Bard^{42,43}, ethane is formed mainly at a high concentration of acetic acid or at a high current density in photoelectrochemical (PEC) cells; it is formed according to Eq.2.57. When the photocatalyst is suspended and the reactant concentration of acetic acid is low, methane is the main product in deaerated and aerated solutions; the process is given in Eq.2.59. The existence of the carboxymethyl radical ($\bullet\text{CH}_2\text{COOH}$) was established earlier by M. Kaise's during ESR experiments³⁰. During such experiments as those carried out by us, it is not likely that the reaction given in Eq.2.58 will occur, because this radical does not easily form hydrogen atoms in the presence of oxygen.

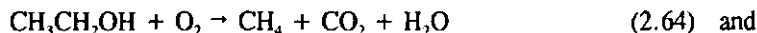
During our experiments, aerated oxidation of dilute ethanol (0.02 M) resulted in methane. We assume that little methane was formed during the reaction given in Eq.2.59 because of the very low concentration of the acetic acid intermediate. However, it was produced together with negative ions of acetaldehyde during either the reaction of free methyl radicals with ethanol (Eq.2.60), or that of acetic radicals with ethanol (Eq. 6.61), because the reactant of ethanol is the highest concentration in the solution. The negative ion of acetaldehyde can be further oxidized to acetaldehyde (Eq.2.62). The results of ESR and IR (infrared spectroscopy) show that end group adsorption (molecular stand-up adsorption on the surface, see Fig.2.7) of

alcohols on photocatalyst surfaces may occur⁴⁴. This is explained by our surface coverage calculation, which shows that ethanol has twice the surface coverage of methanol*.

The possible surface adsorption and reaction mechanisms are shown in Fig.2.7. in detail. It can be clearly concluded from Fig.2.7 that (a). Methanol and ethanol are adsorbed onto the photocatalyst surface in an upright position (end group adsorption). (b). Both of them first lose two electrons during steps (1) and (2) resulting in aldehyde, and then again lose two electrons during steps (3) and (4) and simultaneously react with H₂O to form carboxylic acid; next, they again lose two electrons during steps (5) and (6) and thus mineralize to the final product (CO₂). (c). The mineralization of methanol and that of ethanol are both processes during which multi-electron transfer occurs on the photocatalyst surface resulting in a CO₂ molecule. Such redox reactions with multi-electron transfer will obviously be slow and very complex and will lead to far more by-products than the redox reaction involving the transfer of only one or two electrons. (d). One molecule of methanol mineralizes to CO₂ by losing six electrons and simultaneously releasing six protons. This explains why the reaction pH rapidly decreases with illumination time. (e). Between steps (5) and (6) during which ethanol is oxidized, a hydrogen atom in an adsorbing ethanol transferred to the methyl group of acetic acid to form methane. This transfer mechanism is different from that suggested by Bard²⁷, in which hydrogen is transferred from acetic acid. According to the mechanism shown in Fig.2.7, the net reaction of ethanol oxidation in the presence of aerated Pt/TiO₂ is:



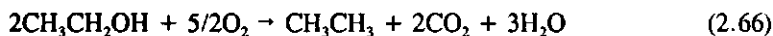
Eq.2.63 can be subdivided into the following two reactions:



This means that theoretically one ethanol molecule needs only four electrons to be mineralized to one CO₂ molecule (Eq.2.64). However, on photocatalyst surfaces it needs in reality six electrons to finish this mineralization process, because this process must include the reaction given in Eq.2.65.

If ethanol oxidation results in ethane, the following reaction occurs:

* Details can be find in Chapter 3.



The distribution of oxidation intermediates of ethanol on the surface of TiO_2 differs from that on the surface of Pt/TiO_2 . The data shown in Fig.2.6 can be easily explained based on the mechanism occurring at the surface. According to Fig.2.6, Pt/TiO_2 produces a lower quantity of the intermediate acetaldehyde and larger quantities of strongly oxidized intermediates such as acetic acid compared to native TiO_2 . If no Pt is present to accelerate the reduction of oxygen on the TiO_2 cathodic area, the anodic process (alcohol oxidation) is retarded. The reaction occurring between two adsorption sites (step 4 in Fig.2.7b) is assumed to be rate-controlling for pathway 1. This results in a much larger quantity of the intermediate acetaldehyde desorbing into solution and accumulating. With platinized TiO_2 , the rate is not controlled during a photo-cathodic process. The rate-controlling step is assumed to be either the transfer of $\cdot\text{H}$ (between steps 5 and 6 in Fig.2.7b) or the splitting of the C-C bond resulting in the release of $\cdot\text{CH}_3$ (step 6' in Fig.2.7b); it causes the accumulation of the intermediate acetic acid in solution.

2.3.5.5 Conclusions regarding the role of metallization of TiO_2 in the photocatalytic oxidation of alcohols

Metallization of TiO_2 can accelerate the oxidation of alcohols in both aerated and deaerated systems. In a deaerated system, Pt/TiO_2 exhibits a higher photocatalytic activity than TiO_2 regarding the production of hydrogen and the oxidation of alcohol^{6,28} as well as hydrocarbons⁴⁵ and carboxylic acid^{27,46}, etc. This is apparently because of the role played by Pt on TiO_2 in a deaerated system: it can accelerate the transfer of electrons from TiO_2 to an adsorbed proton and promote the desorption of hydrogen (Eq.2.20 - 2.22). Because of the presence of oxygen in an aerated system, for thermodynamical reasons oxygen is reduced before protons are reduced. Pt accelerates the reduction of oxygen in the cathodic area (Eq.2.8 - 2.15). Consequently, the reaction-controlling step of the photocatalyzed oxidation of alcohols depends on the cathodic reduction of oxygen or protons on TiO_2 surfaces. Pt accelerates only the cathodic processes.

2.3.6 The mechanism of photocatalyzed oxidation of organochlorides in an aerated system

All processes of photocatalyzed oxidation of organochlorides discussed here were performed in aerated systems. Tables 2.1 and 2.2, in which the results of the photocatalytic oxidation of chloroform and TCE are presented, and Fig.2.16 and 2.17, in which the photocatalytic conversion of chloroform and TCE is given as a function of illumination time, show that the use of native TiO_2 as a photocatalyst results in even better photocatalytic oxidation than 1% Pt/TiO_2 or 1% Pd/TiO_2 . Metallization of TiO_2 can accelerate the oxidation of alcohols in both aerated or deaerated systems. The fact that Pt and Pd do not do this during the oxidation

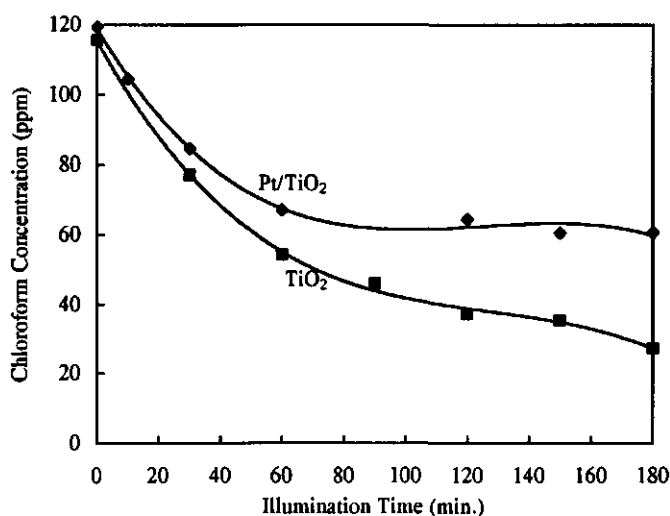


Fig.2.16. Photocatalytic oxidation of chloroform as a function of illumination time on 1%Pt/TiO₂ and TiO₂ catalysts in the presence of oxygen. 1%Pt/TiO₂, prepared from physical mixture followed by treating at 430°C during 14 hours in H₂ flow. TiO₂, 430°C, H₂ 14 hours pretreatment. 15-W black light lamp, 600 ml of solution, initial pH = 5.4, 1.0 g cat./L, ~25°C.

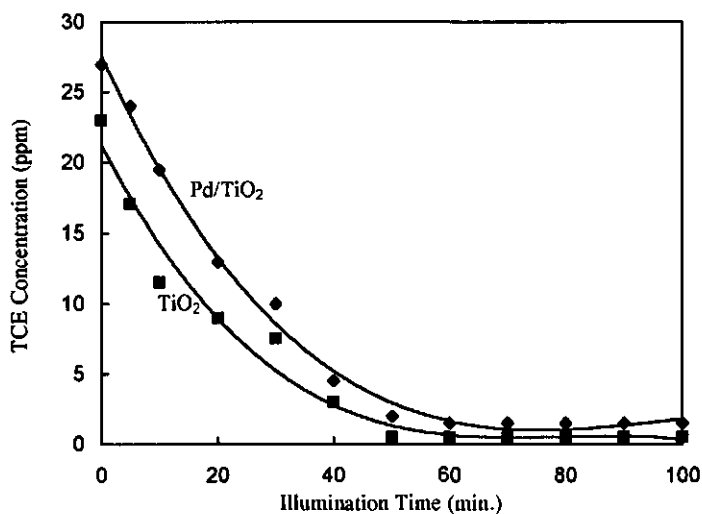


Fig.2.17. Photocatalytic oxidation of TCE as a function of illumination time on 1%Pd/TiO₂ and TiO₂ catalyst in the presence of oxygen. 1%Pd/TiO₂, prepared from physical mixture followed by treating at 430°C during 14 hours in H₂ flow. TiO₂, 430°C, H₂ 14 hours pretreatment. 15-W black light lamp, 600 ml of solution, initial pH = 5.4, 1.0 g cat./L, ~25°C.

of organochlorides in aerated systems suggests that the half-reaction occurring during the anodic process (*i.e.*, the adsorption of chloro-substrates onto photocatalyst surfaces and their reaction on them) be also a rate-controlling step, since Pd or Pt accelerates only the rate of the half-reaction occurring during the cathodic process.

The photocatalytic oxidation of dichloropropionic acid (sodium salt) (DCP) in aerated systems was also studied using the photocatalysts TiO_2 , Pd/TiO_2 and Pt/TiO_2 . The results are shown in Fig. 2.18 and 2.19, in which photocatalytic degradation yields CO_2 and Cl^- . According to Fig. 2.18, which shows the results of using TiO_2 and Pd/TiO_2 as photocatalysts, the best results were obtained by using native TiO_2 pretreated at 120°C . Using this TiO_2 , about 18% of DCP present at an initial concentration of 1,430 ppm was dechlorinated and 23% of this DCP was decarboxylated during an illumination period of three hours. Pretreatment of this photocatalyst at 500°C results in a lower conversion rate. 1% Pd/TiO_2 did not affect the degradation of dichloropropionic acid. During DCP degradation experiments, the solution pH increased from 0.2 to 0.4 during the first 20 minutes and then decreased during the illumination period (Fig. 2.18a). These variations in pH differ from those occurring during the oxidation of alcohols, chloroform and TCE, in which the pH always decreased. This is because during the first stage of the process intermediates of DCP of lower acidity are produced. This can occur when decarboxylation precedes dechlorination. According to Fig. 2.19, which shows the results of using TiO_2 and Pt/TiO_2 as photocatalysts, 1% Pt/TiO_2 showed the same changes in pH (Fig. 2.19a) as 1% Pd/TiO_2 but a different DCP degradation process. Regarding CO production, Pt/TiO_2 did not show a higher activity than native TiO_2 (Fig. 2.19b); regarding DCP dechlorination, it showed a 53% higher activity than TiO_2 (Fig. 2.19c); this might be due to processes occurring at the surface of Pt.

Since on Pt/TiO_2 and Pd/TiO_2 no rate-limiting cathodic steps occur and these photocatalysts show a lower oxidation activity towards chloroform and TCE compared to TiO_2 , some rate-controlling steps must be part of the anodic process, such as:

1. The adsorption of organochlorides onto the photocatalyst surface,
2. The transfer of electrons from organochlorides to photocatalyst surfaces,
3. The formation of $\bullet\text{OH}$ on photocatalyst surfaces,
4. The reaction of organochlorides with $\bullet\text{OH}$ on photocatalyst surfaces or in solution.

As $\bullet\text{OH}$ has a very high redox potential ($+2.02\text{ V}$)⁴⁷, it is thermodynamically capable of oxidizing alcohols, chloroform and TCE. If only step 3 or step 4 were rate-controlling, it would not explain why alcohols and not chloroform were oxidized faster by Pt/TiO_2 or Pd/TiO_2 than by native TiO_2 . It is likely that steps (1) or (2) are rate-controlling, because the lower activity of Pt/TiO_2 or Pd/TiO_2 during the photocatalytic oxidation of chloroform and TCE may be due to the slowness of adsorption and charge transfer on photocatalyst surfaces. This idea

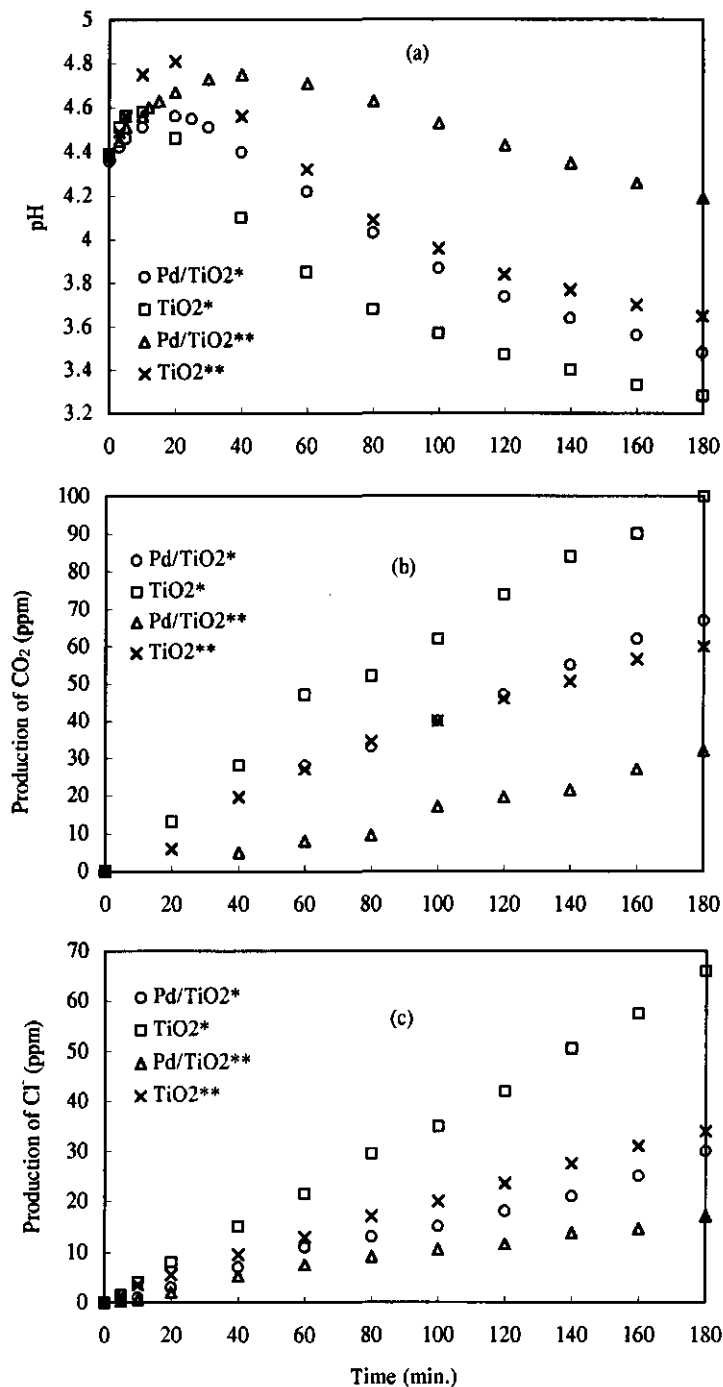


Fig. 2.18. Photocatalytic degradation of dichloropropionic acid as a function of illumination time in the presence of oxygen. Initial concentration of DCP: 1,430 ppm, 1%Pd/TiO₂, (photodeposited), 600 ml of solution, 1 g/L catalyst, temperature: ~25°C. *: The catalyst was pretreated in air for 6 hours at 120°C. **: The catalyst was pretreated in an H₂ flow for 14 hours at 500°C.

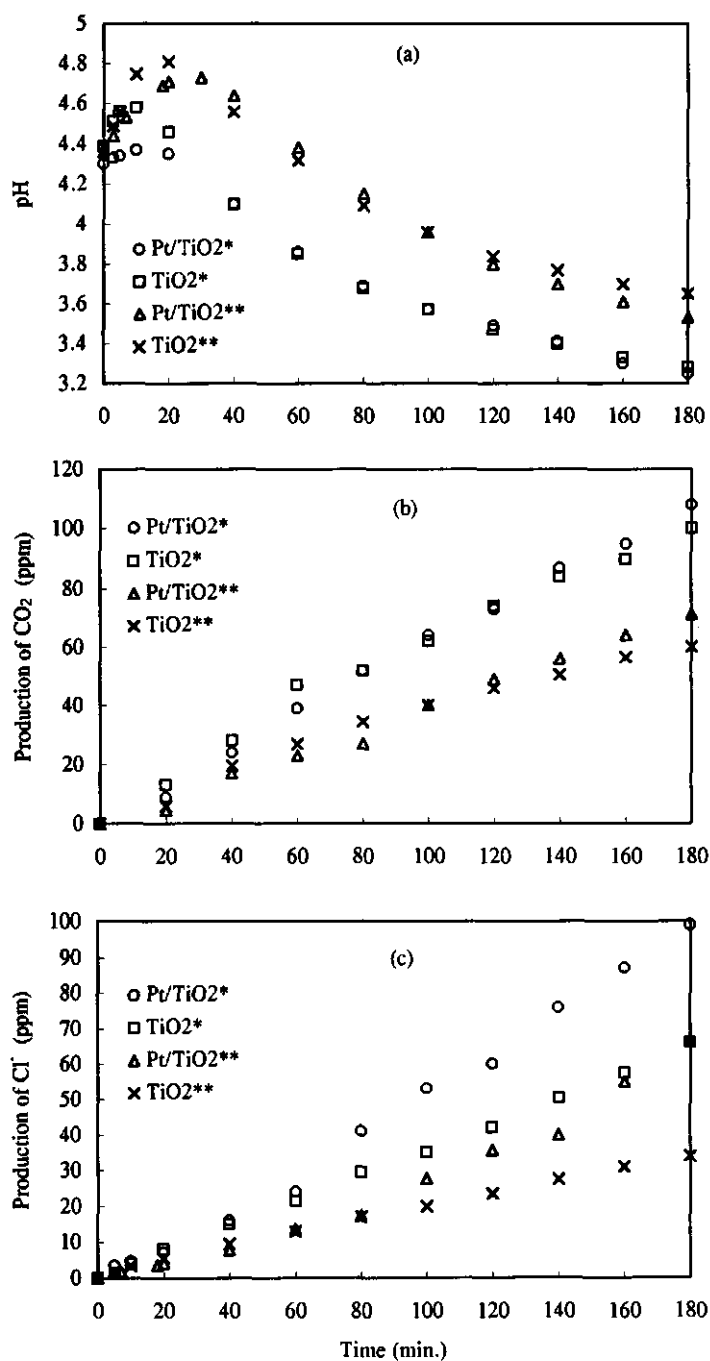


Fig.2. 19. Photocatalytic degradation of dichloropropionic acid as a function of illumination time in the presence of oxygen. Initial concentration of DCP: 1,430 ppm. 1%Pt/TiO₂, (photodeposited), 600 ml of solution, 1 g/L catalyst, Temperature: ~25°C. *: The catalyst was pretreated in air for 6 hours at 120°C. **: The catalyst was pretreated in an H₂ flow for 21 hours at 500°C for Pt/TiO₂, and for 14 hours for TiO₂.

also supports the above suggestion that pathway 1 is the main oxidation route where reaction substrates must absorb onto photocatalyst surfaces. It is also expected that, compared to native TiO_2 , Pt/TiO_2 and Pd/TiO_2 will play a less important role in deaerated systems during the photocatalytic oxidation of chloroform or TCE.

2.4 CONCLUSIONS

1. The photocatalytic oxidation of methanol and ethanol on aerated TiO_2 is accelerated by modifying the TiO_2 with Pt or Pd.
2. Compared to Pt, Pd has less effect on TiO_2 during the photocatalytic oxidation of methanol and ethanol in an aerated system.
3. The mineralization of methanol and ethanol (*i.e.*, the production of CO_2) is affected by the solution pH in an aerated system. If the solution pH is initially acidic, CO_2 is produced immediately during illumination, but if it is initially alkaline, the mineralization process can be seriously retarded.
4. In the case of photocatalytic oxidation of chloroform and trichloroethylene in an aerated system, metallization of TiO_2 with Pt or Pd results in a lower activity than when native TiO_2 is used.
5. In the case of photocatalytic oxidation of dichloropropionic acid (sodium salt) (DCP), metallization of TiO_2 with Pd results in a lower activity than when native TiO_2 is used, but metallization of TiO_2 with Pt results in a positive effect on the dechlorination of DCP.
6. The experimental data and the discussion of possible reaction pathways suggest the following:
 - a. During photocatalytic oxidation of alcohols and organochlorides in aerated systems, Pt and Pd can accelerate the cathodic process of oxygen reduction.
 - b. If a photocatalytic reaction has a rate-controlling step during the anodic process, modification of TiO_2 with Pt or Pd cannot affect the rate of this reaction except if Pt or Pd shows an anodic catalytic activity in relation to the reactant concerned.
 - c. The rate control exerted by anodic processes can be attributed mainly to the resistance of adsorption and electron transfer between the reactant and the anodic surface.
 - d. A favourable pathway for the anodic process comprises direct adsorption of reactants onto the photocatalyst surface and direct electron transfer from reaction substrates to holes in the surface, *i.e.*, direct oxidation reactions on this surface.

ACKNOWLEDGMENTS

Jian Chen wishes to express his gratitude for the financial support received from North Carolina State University and wishes to thank Dr Ed Wolfrum for the many interesting topical discussions held with him during this research.

2.5 REFERENCES

1. M. Barbeni, E. Pramauro, and E. Pelizzetti, "Photodegradation of pentachlorophenol catalyzed by semiconductor particles", *Chemosphere* **14**(2), 195-208, 1985.
2. X. Li, P. Fitzgerald, and L. Bowen, "Sensitized photo-degradation of chlorophenols in a continuous flow reactor system", *Wat.Sci.Tech.* **26**(1-2) 367-376, 1992.
3. T. Nguyen and D.F. Ollis, "Complete heterogeneously photocatalyzed transformation of 1,1-and 1,2-dibromoethane to CO_2 and HBr", *J. Phys. Chem.*, **88**, 3386-3388, 1984.
4. D. F. Ollis, "Contaminant degradation in water", *Environ. Sci. Technol.*, **19**(6), 480-484, 1985.
5. C. S. Turchi and D. F. Ollis, "Mixed reactant photocatalysis: Intermediates and mutual rate inhibition", *J. Catalysis*, **119**, 483-496, 1989.
6. B. Ohtani, M. Kakimoto, S. Nishimoto, and T. Kagiya, "Photocatalytic reaction of neat alcohols by metal-loaded titanium(IV) oxide particles", *J. Photochem. Photobiol. A: Chem.*, **70**, 265-272, 1993.
7. T. Kawai, T. Sakata, "Photocatalytic hydrogen production from water by the decomposition of poly-vinylchloride, protein, algae, dead insects, and excrement", *Chem. Lett.*, 81-84, 1981.
8. H. Dürr, S. Boßmann, and A. Beuerlein, "Biominetic approaches to the construction of supramolecular catalysts: titanium dioxide-platinum antenna catalysts to reduce water using visible light", *J. Photochem. Photobiol. A: chem.*, **73**, 233-245, 1993.
9. D. W. Bahnemann, J. Monig, and R. Chapman, "Efficient photocatalysis of the irreversible one-electron and two-electron reduction of halothane on platinized colloidal titanium dioxide in aqueous suspension", *J. Phys. Chem.*, **91**, 3782-3788, 1987.
10. I. Izumi, W. W. Dinn, K. O. Wilbourn, Fu-Ren F. Fan, and A. J. Bard, "Heterogeneous photocatalytic oxidation of hydrocarbons on platinized TiO_2 powders", *J. Phys. Chem.*, **84**, 3207-3210, 1980.
11. I. Izumi, Fu-Ren F. Fan, and A. J. Bard, "Heterogeneous photocatalytic decomposition of benzoic acid and adipic acid on platinized TiO_2 powder. The photo-kolbe decarboxylative route to the breakdown of the benzene ring and to the production of butane", *J. Phys. Chem.*, **85**, 218-223, 1981.
12. K. Tanaka, K. Harada, and S. Murata, "Photocatalytic deposition of metal ions onto TiO_2 powder", *Sol. Energy*, **36**, 159-161, 1986.
13. M. R. Prairie, L. R. Evans, and S. L. Martinez, "Destruction of organics and removal of heavy metals in water via TiO_2 photocatalysis", presented at the Symposium on Chemical Oxidation: Technology for the Nineties, Nashville TN, 1992.

14. R. Amadelli, A. Maldotti, S. Sostero and V. Carassiti, "Photodeposition of uranium oxides onto TiO_2 from aqueous uranyl solutions", *J. Chem. Soc. Faraday Trans.* **87**(19), 3267-3273, 1991.
15. D. F. Ollis, Ezio Pelizzetti, and Nick Serpone, "Photocatalysis-Fundamentals and Applications" (eds.) Ezio Pelizzetti, and Nick Serpone, John Wiley & Son, Inc. USA, 1989, pp. 619.
16. N. Serpone, D. Lawless, R. Terzian, C. Minero, and E. Pelizzetti, "Photochemical Conversion and Storage of Solar Energy" IPS-8, Italy, 1990, p. 466.
17. Dong Hyun Kim and Marc A. Anderson, "Photoelectrocatalytic degradation of formic acid using a porous TiO_2 thin-film electrode", *Environ. Sci. Technol.*, **28**, 479-483, 1994.
18. C.-M. Wang, A. Heller, and H. Gerischer, "Palladium catalysis of O_2 reduction by electrons accumulated on TiO_2 particles during photoassisted oxidation of organic compounds", *J. Am. Chem. Soc.*, **114**, 5230-5234, 1992.
19. T. Kobayashi, H. Yoneyama, and H. Tamura, "Role of Pt overlayers on TiO_2 electrodes in enhancement of the rate of cathodic processes", *J. Electrochem. Soc.* **130**, 1706-1711, 1983.
20. G. Nagomi, "Investigation of photocatalytic decomposition mechanism of organic compounds on platinized semiconductor catalyst by rotating ring disk electrode technique", *J. Electrochem. Soc.* **139**(12), 3415-3421, 1992.
21. I.M. Kolthoff, E.B. Sandell, "Textbook of quantitative analysis", 3rd ed., Macmillan, New York, 1952; p 542ff.
22. B. Kraeutler, and A. J. Bard, "Heterogeneous photocatalytic Preparation of supported catalysts. Photodeposition of platinum on TiO_2 powder and other substrates", *J. Am. Chem. Soc.*, **100**(13), 4317-4318, 1978.
23. P. Pichat, J.M. Hermann, J. Disdier, H. Courbon and M.N. Mozzanega, *Nouv. J. Chim.*, **5**, 627 1981
24. A. L. Pruden and D. F. Ollis, "Degradation of chloroform by photoassisted heterogeneous catalysis in dilute aqueous suspensions of titanium dioxide", *Environ. Sci. Technol.* **17**, 628-631, 1983.
25. Handbook of Chemistry and Physics, (ed.) Robert C. Weast, 60th Edition, B-104, 1979.
26. T. Sakata, T. Kawai, "Heterogeneous photocatalytic production of hydrogen and methane from ethanol and water", *Chem. Phys. Lett.*, **80**(2), 341-344, 1981.
27. H. Yoneyama, Y. Takao, H. Tamura, and A.J. Bard, "Factors influencing product distribution in photocatalytic decomposition of aqueous acetic acid on platinized TiO_2 ", *J. Phys. Chem.*, **87**, 1417-1422, 1983.
28. E. Borgarello, E. Pelizzetti, "UV/VIS. Light photocatalytic dihydrogen production from aliphatic alcohols over semiconductor particles", *La Chimica E L'Industria*, V. **65**, N. 7-8, 474-478, 1983.
29. M. Bideau, B. Claudel, L. Faure and H. Kazouan, "The photo-oxidation of acetic acid by oxygen in the presence of titanium dioxide and dissolved copper ions", *J. Photochem. Photobiol. A: Chem.*, **61**, 269-280, 1991.
30. M. Kaise, H. Kondoh, C. Nishihara, H. Nozoye, H. Shindo, S. Nimura, and O. Kikuchi, "Photocatalytic Reactions of Acetic Acid on Platinum-loaded TiO_2 : ESR Evidence of Radical Intermediates in the Photo-Kolbe Reaction", *J. Chem. Soc., Chem. Commun.*, 395-396, 1993.

31. P. Pichat, Marie-Noelle Mozzanega and H. Courbon, "Investigation of the mechanism of photocatalytic alcohol dehydrogenation over Pt/TiO₂ using poisons and labeled ethanol." *J. Chem. Soc., Faraday Trans. 1*, **83**, 697-704, 1987.
32. C. S. Turchi and D. F. Ollis, "Photocatalytic degradation of organic water contaminants: Mechanisms involving hydroxyl radical attack", *J. Catalysis*, **122**, 178-192, 1990.
33. C. Kormann, D. W. Bahnemann, and M. R. Hoffmann, "Photolysis of chloroform and other organic molecules in aqueous TiO₂ suspensions", *Environ. Sci. Technol.*, **25**, 494-500, 1991.
34. P. Clechet, C. Martelet, J. R. Martin, and R. Olier, *Electrochim. Acta*, **24**, 457, 1979.
35. M. Bideau, B. Claudel, L. Faure and H. Kazouan, "The photo-oxidation of propionic acid by oxygen in the presence of TiO₂ and dissolved copper ion". *J. Photochem. Photobiol. A: chem.*, **67**, 337-348, 1992.
36. J. Papp, H.-S. Shen, R. Kershaw, K. Dwight and A. Wold, "Titanium(IV) Oxide Photocatalysts with Palladium", *Chem. Mater.* **5**, 284-288, 1993.
37. D. F. Ollis, Chen-Yung Hsiao, L. Budiman, and Chung-Li Lee, "Heterogeneous photocatalysis: Degradation of dilute solutions of dichloromethane, chloroform, and carbon tetrachloride with illuminated TiO₂ photocatalyst", *J. Catalysis*, **82**, 418-423, 1983.
38. D. F. Ollis, Chen-Yung Hsiao, L. Budiman, and Chung-Li Lee, "Heterogeneous photoassisted catalysis: Conversions of perchloroethylene, dichloroethane, chloroacetic acids, and chlorobenzenes", *J. Catalysis*, **88**, 89-96, 1984.
39. J. R. Bolton, A Symposium on Advanced Oxidation Processes for the Treatment of Contaminated Water and Air, June 4-5, 1990, Toronto, ON, Canada, Wastewater Technology Centre, Burlington, ON, Canada, 1990.
40. D. F. Ollis, "Solar-assisted photocatalysis for water purification: issues, data, questions" and relative references, in "*Photochemical Conversion and Storage of Solar Energy*", (eds.) E. Pelizzetti and M. Schiavello, 1991, p. 593-622.
41. O. Micic I., Y. Zhang, K. R. Cromack, A. D. Trifunac, and M. C. Thurnauer, "Photoinduced hole transfer from TiO₂ to methanol molecules in aqueous solution studied by electron Paramagnetic resonance", *J. Phys. Chem.*, **97**(50), 13284-13288, 1993.
42. B. Kraeutler, and A. J. Bard, "Heterogeneous photocatalytic synthesis of methane from acetic acid-New kolbe reaction pathway", *J. Am. Chem. Soc.* **100**(7), 2239-2240, 1978.
43. B. Kraeutler, and A. J. Bard, "Heterogeneous photocatalytic decomposition of saturated carboxylic acids on TiO₂ powder. Decarboxylative route to alkanes". *J. Am. Chem. Soc.* **100**(19), 5985-5992, 1978.
44. S. Yamagata, R. Baba, and A. Fujishima, "Photocatalytic decomposition of 2-ethoxyethanol on titanium dioxide", *Bull. Chem. Soc. Jpn.*, **62**, 1004-1010, 1989.
45. K. Hashimoto, T. Kawai, and T. Sakata, "Photocatalytic reactions of hydrocarbons and fossil fuels with water. Hydrogen production and oxidation", *J. Phys. chem.* **88**, 4083-4088, 1984.
46. T. Sakata, T. Kawai, and K. Hashimoto, "Heterogeneous photocatalytic reaction of organic acids and water. New reaction paths besides the photo-kolbe reaction", *J. Phys. Chem.*, **88**, 2344-2350 1984.
47. Handbook of Chemistry and Physics, (ed.) David R. Lide, 73rd Edition, 8-17, 1992.

CHAPTER 3 KINETIC PROCESSES OF PHOTOCATALYTIC MINERALIZATION OF ALCOHOLS ON METALLIZED AND NATIVE TITANIUM DIOXIDE

This Chapter is based on:

1. Jian Chen, David F. Ollis, Wim H. Rulkens and Harry Bruning, "Kinetics of the Photocatalytic Oxidation of Alcohols," presenting on The Third International Conference on TiO_2 Photocatalytic Purification and Treatment of Water and Air, Orlando, Sep. 1997.
2. Jian Chen, David F. Ollis, presentation on First International Conference on Advanced Oxidation Technologies for Water and Air Remediation, Canada, 1994.
3. Jian Chen, Qixing Zhuang, presentation on The International Workshop on Electrocatalysis, Photoelectrocatalysis and Biomimetic Catalysis, sponsored by ESCO of United Nations, Xiamen, China, 1985.

KINETIC PROCESSES OF PHOTOCATALYTIC MINERALIZATION OF ALCOHOLS ON METALLIZED AND NATIVE TITANIUM DIOXIDE

3.1 INTRODUCTION

For nearly twenty years, photocatalysis has been studied intensively all over the world as a potential technique for the degradation and final mineralization of organic pollutants in aquatic environments^{1,2,3}. In photocatalytic systems, detoxification of more and more organic and inorganic pollutants has been observed. These pollutants include various organic compounds, such as halogen organics^{4,5,6,7,8}, insecticides^{9,10,11,12,13}, surfactants^{14,15}, and heavy metals^{16,17,18,19,20} (see Chapter 1), which occur on a large scale in rivers, lakes, groundwater, and industrial and domestic wastewater^{21,22,23,24}.

Titanium dioxide is one of the most interesting photocatalysts used in photocatalysis. It has been found to show a high photocatalytic activity during both oxidation and reduction for nearly all substrates investigated²⁵. Two mechanisms of photocatalysis have been suggested. One of them involves mainly free radicals. During this mechanism, hole-electron pairs (h^+ and e^- at the surface of the photocatalyst) oxidize OH^- in water (by h^+) or reduce O_2 (by e^-) to form $\bullet OH$ radicals in solution. Next, these radicals react with substrates in solution to yield oxidized products^{6,26,27}. During the other mechanism, the substrate is first adsorbed onto the catalyst surface and then reacts with h^+ , e^- or $\bullet OH$ to produce final products^{28,29,30,31}. Such direct photocatalytic processes can be expressed in a kinetic equation based on Langmuir adsorption^{26,32}, which is normally used to model heterogeneous catalytic processes on solid-gas interfaces. The mechanism of photocatalytic treatment of wastewater is not yet fully clear.

Metallization of TiO_2 with small amounts of noble metals (*e.g.*, platinum, palladium) not only accelerates the rate of photocatalytic degradation of some organic compounds²⁷, but also speeds up the photocatalytic deposition of inorganic metal ions in water onto the catalyst surface³³ (see Chapter 1). Metallization of semiconductors has been studied intensively, especially where TiO_2 is involved^{34,35,36,37,38}. However, many aspects have not yet been studied. In the case of the deaerated or aerated photocatalytic degradation of some nonchlorinated organic compounds (*e.g.*, alcohols) and the photocatalytic removal of certain metals in aerated systems (*e.g.*, Pb), the effect of metallization of the catalysts can be attributed to the acceleration of the dehydrogenation and the reduction of oxygen by noble metals (*e.g.*, platinum, palladium)³⁴. However, the effect of catalyst metallization is not yet fully clear for the photocatalytic removal of metals in deaerated systems (*e.g.*, uranium) and the degradation of organochlorides³⁹.

The redox activity of photocatalysts depends strongly on how they are prepared and pretreated, because these aspects affect the surface modification (*e.g.*, metallization), surface constitution, and crystal structure. In nature, TiO_2 occurs in two tetragonal crystal structures (anatase and rutile) and a rhombic form (brookite). It is extremely difficult to synthesize brookite in the laboratory, whereas both anatase and rutile can easily be prepared²⁵. For the most densely packed crystal faces (rutile 110 and anatase 001), calculations carried out by Woning and Van Santen⁴⁰ predict that at the surface of rutile the reducibility of the coordinatively unsaturated Ti^{4+} ions is higher than at that of anatase. They show that at the 110-face of rutile the intrinsic Lewis acidity (the ability to accept electrons) of the coordinatively unsaturated Ti^{4+} ions is higher than that at the 001-face of anatase. Thus, at the most densely packed crystal face, rutile may show a higher catalytic oxidation activity than anatase. However, anatase appears to be more active than rutile. This is probably due to differences in the extent and nature of the surface hydroxyl groups present in the low-temperature anatase structure. The higher photoactivity of anatase can also be explained from the fact that its Fermi level is higher than that of rutile⁴¹ by about 0.1 eV.

The surface constitution of a photocatalyst can be drastically changed by pretreating it for several hours to a flow of hydrogen, nitrogen or oxygen at a high temperature. A high temperature will promote the formation of a rutile structure in a TiO_2 catalyst, and in a flow of hydrogen it will increase the concentration of unsaturated Ti^{4+} ions on the TiO_2 surface. The photocatalytic activity of metallized TiO_2 can be raised by pretreating it to a flow of hydrogen at a high temperature (400°C and 700 °C), because at the TiO_2 surface strong metal-supporter interaction (SMSI) will occur rather than physical deposition of metals³⁵. SMSI will accelerate the velocity of electron transfer from the TiO_2 surface to metals and then the rate of reductive reactions. However, catalyst sintering at a high temperature will cause a sharp decrease in its specific surface area and activity. How to control and operate the catalyst pretreatment is the key to enhance the activity of photocatalysts.

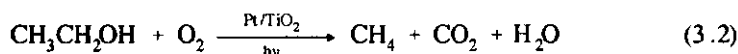
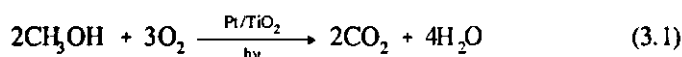
This chapter elaborates on the kinetics of photocatalytic oxidation of alcohols in solution. A theory of heterogeneous catalysis was applied in order to clarify the internal photocatalytic process and explain the photocatalytic phenomena observed during experiments. We chose methanol (MeOH) and ethanol (EtOH) as research probes rather than toxic organic compounds in wastewater. Methanol and ethanol can be easily oxidized at photocatalyst surfaces both with and without oxygen, and the intermediates resulting from the photocatalytic oxidizing process are relatively simple. We used an aerated system, because in such a system most organic compounds are more easily mineralized to CO_2 ($\Delta G^\circ > 0$) than in a deaerated system ($\Delta G^\circ < 0$). We investigated the effect of metallization of TiO_2 with platinum or palladium on the conversion process. For alcohol oxidation, the photocatalytic activity of metallized TiO_2 was compared with that of native TiO_2 . The distribution of Pt at the TiO_2 surface was measured using an electron beam probe. X-ray powder crystal diffraction was applied to investigate the

difference in crystal structure of metallized TiO_2 before and after pretreatment and whether during pretreatment any interaction had occurred between platinum and TiO_2 . To explain the photocatalytic process occurring on catalyst particles, it is important to use a photocatalytic model of powder photocatalyst. A photocatalytic micro-cell model for powder photocatalyst (Fig. 3.1a) has been used over the last fifteen or so years⁴². Based on the spectrum of X-rays excited at the surface, element analysis of the electron beam probe and a theoretical analysis, a new micro-cell model for a photocatalyst consisting of porous powder is discussed in which reactions occurred either at the outside surface or in pores. The difference between the old and the new micro-cell model, is that in the old one photocatalytic redox reactions occur only at the outside surface.

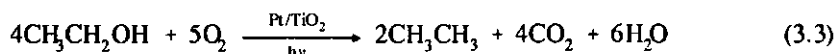
3.2 THE KINETIC PROCESSES OF HETEROGENEOUS CATALYSIS AND PHOTOCATALYSIS

3.2.1 Introduction

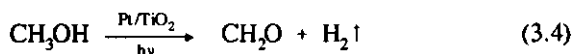
The net reactions of photocatalytic oxidation of methanol and ethanol in an aerated aqueous phase can be expressed as⁴³:



or:



In a deaerated system, the photocatalytic oxidation of methanol occurs according to:



Theoretically, the mathematical expressions regarding the kinetics of heterogeneous catalytic reactions in solution on the liquid-solid interface are far more complicated and unclear than those regarding the kinetics of such reactions in the gas phase on the gas-solid interface. As

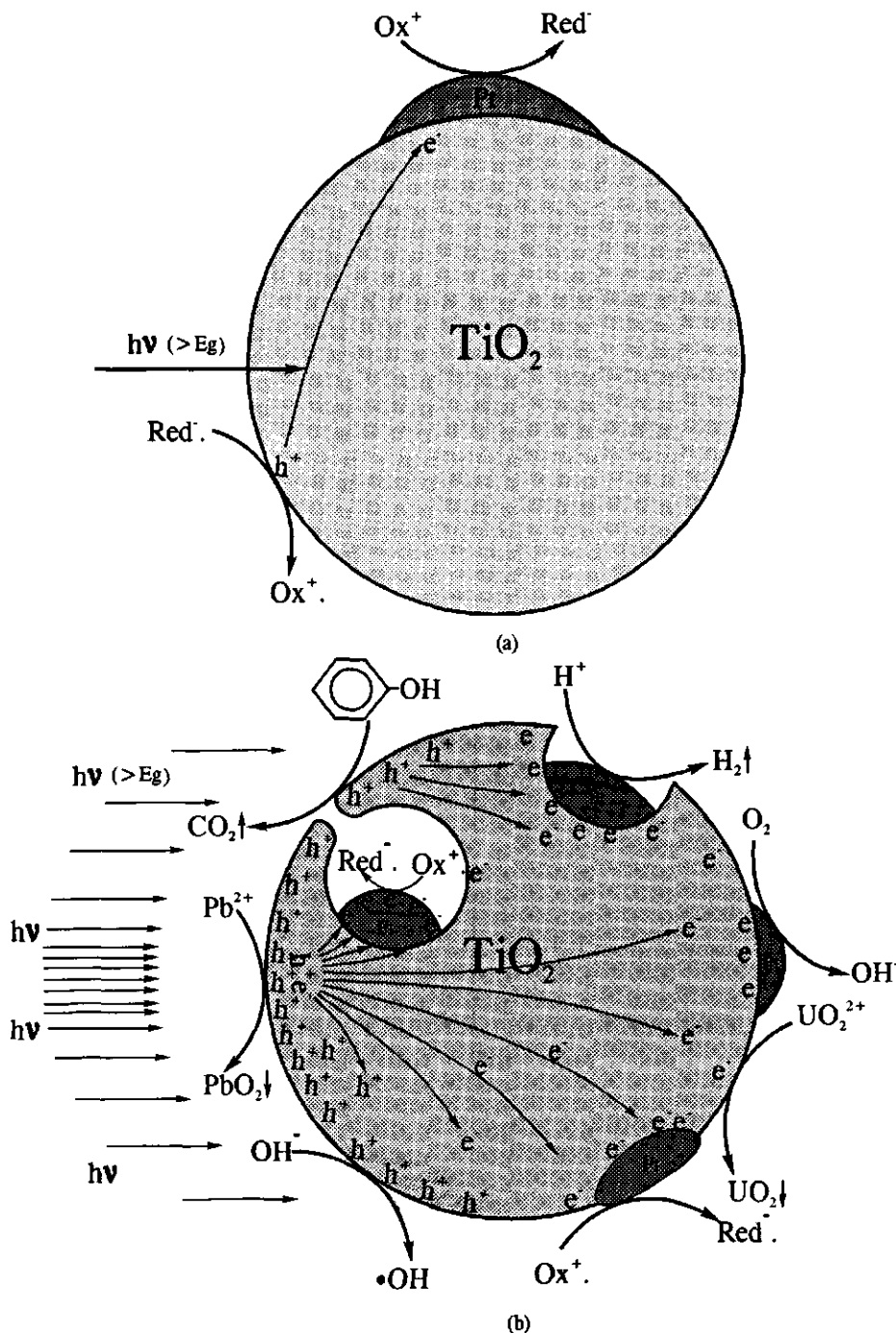


Fig.3.1 (a) A conventional simplified model of a micro-cell for a powder photocatalyst. (b) A suggested more detailed model of a porous micro-cell for a powder photocatalyst.

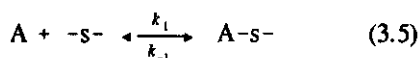
a simplification, the reaction in a dilute solution can be described using the theory of gas reactions. For this purpose, we assume that some kinetic equations of the heterogeneous catalysis theory^{44,45,46} (i.e., the Langmuir kinetic equations for gas reactions on heterogeneous catalyst surfaces) can be applied to describe the process of photocatalytic oxidation of alcohols. These equations are introduced below.

3.2.2 Langmuir adsorption isotherm for gas phase reactions

Because gas reactions occurring at the catalyst surface include the steps of diffusion, adsorption, surface reaction and desorption, we first describe the situation of adsorption and desorption. In this, θ is the surface percentage occupied by molecules adsorbed onto the surface (i.e., coverage, and $0 \leq \theta \leq 1$), and it is assumed that:

1. The solid surface contains a fixed number of adsorption sites. In a state of equilibrium, a fraction θ of the sites is occupied by adsorbed molecules, and a fraction $1 - \theta$ is unoccupied.
2. Each site can hold one adsorbed molecule.
3. The heat of adsorption is equal for all sites and does not depend on the fraction covered θ .
4. No interaction occurs among molecules located at different sites.

The chance that a molecule condenses at an unoccupied site or leaves an occupied site does not depend on whether or not neighbouring sites are occupied. According to the law of mass action, the rates of adsorption (v_1) and desorption (v_{-1}) processes of molecule A at the surface (-s-) of catalysts, which the processes are shown in following chemical equation:



can be expressed for adsorption as:

$$v_1 = k_1 P_A (1 - \theta_A) \quad (3.6)$$

and for desorption as:

$$v_{-1} = k_{-1} \theta_A \quad (3.7)$$

where P_A is the gas pressure of component A, k_1 the adsorption rate constant, and k_{-1} the desorption rate constant. When adsorption and desorption approach a state of equilibrium, the following applies:

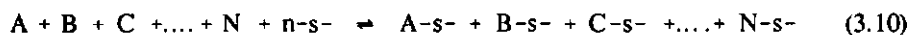
$$k_1 P_A (1 - \theta_A) = k_{-1} \theta_A \quad (3.8)$$

which can be rewritten as:

$$\theta_A = \frac{KP_A}{1 + KP_A} \quad (3.9)$$

where $K = k_i/k_{-i}$. K is called the adsorption coefficient (an equilibrium constant, also called the apparent binding constant), and the equation is called the Langmuir adsorption isotherm.

For the adsorption of n types of molecule (A to N):



the coverage of molecule i (θ_i) is given by:

$$\theta_i = \frac{K_i P_i}{1 + \sum_{j=1}^n K_j P_j} \quad (3.11)$$

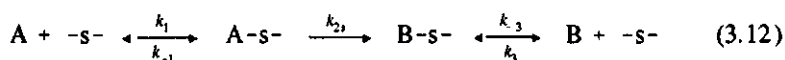
where the adsorption coefficient of component i is $K_i = k_i/k_{-i}$, and that of component j $K_j = k_j/k_{-j}$. k_i and k_j are the adsorption rate constants of component i and j , respectively, and k_{-i} and k_{-j} are the desorption rate constants of component i and j , respectively.

Based on the Langmuir adsorption isotherm, we can derive the kinetic equation for the adsorption reactions.

3.2.3 The kinetic equation for gas reactions in heterogeneous catalysis

If according to the theory of heterogeneous catalysis^{45,46} the gas diffusion (mass transfer) at the surface occurs very fast (which means that it is not the rate-determining step), the process occurring at the catalyst surface includes three steps: adsorption, surface reaction, and desorption.

The reaction of a single gas molecule can be expressed as:



where k_{2s} is the real rate constant of the surface reaction step, and B a reaction product. If the rate-determining step of the process expressed in Eq.3.12 is the reaction occurring at the surface, the total rate of the reaction occurring at the gas-solid interface γ is given by:

$$\gamma = k_{2s}\theta_A = \frac{k_{2s}K_A P_A}{1 + K_A P_A + K_B P_B} \quad (3.13)$$

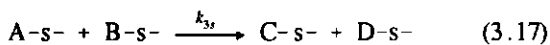
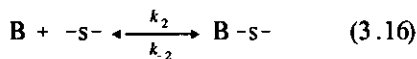
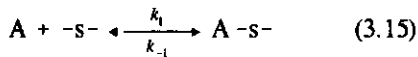
where K_A is the adsorption equilibrium constant of molecule A and K_B that of molecule B.

If $K_B P_B \ll 1$, we get:

$$\gamma = \frac{k_{2s}K_A P_A}{1 + K_A P_A} \quad (3.14)$$

k_{2s} represents the real rate constant of the overall reactions. Eq.3.13 is the Langmuir kinetic equation for the reaction of a single gas molecule at the surface. Although these equations concern the gas phase reactions at solid surface, we are here try to introduce these reactions in the liquid phase. As shown in Fig.3.2a, the maximum reaction rate (γ) of this system is equal to k_{2s} if P_A is high ($K_A P_A \gg 1$).

The rate of the catalytic reactions occurring between two gas molecules can be represented in two ways, if the reaction occurring at the surface is the rate-determining step. For the reaction occurring between two gas molecules (A and B) which are both adsorbed onto the surface, the equations can be written as⁴⁷



In these equations, C and D are reaction products of A and B. If C and D are not strongly adsorbed, the following can be derived for the reaction rate γ :

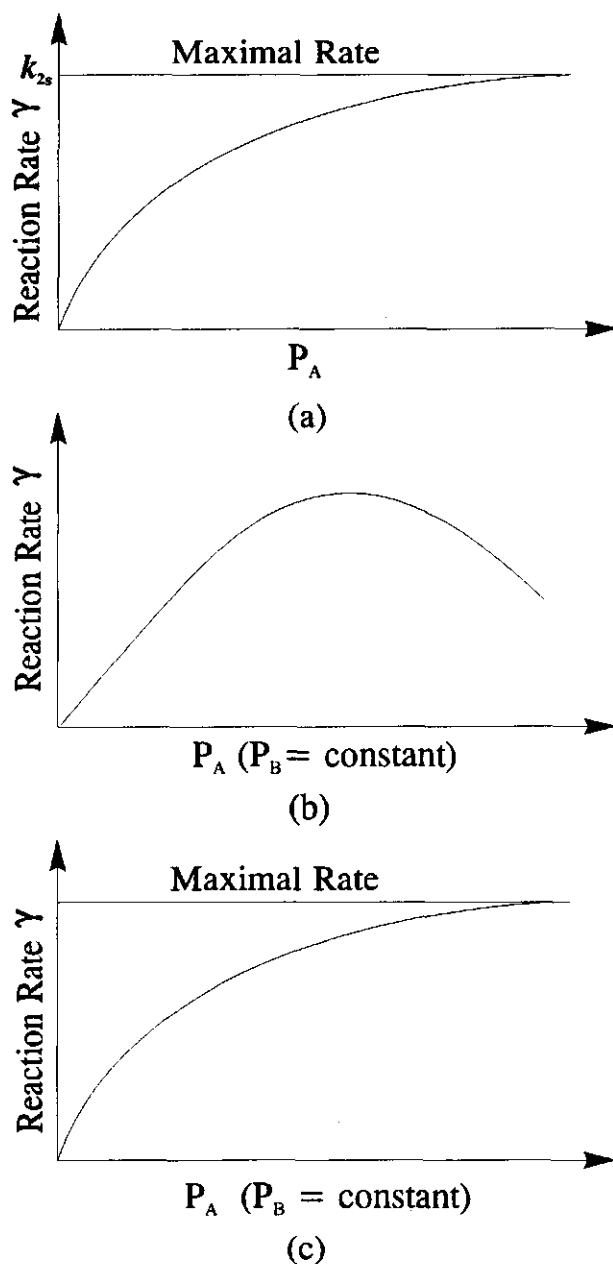
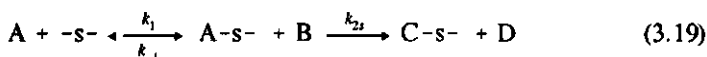


Fig. 3.2 (a). The variation of the reaction rate with reactant pressure P_A according to the Langmuir kinetic equation for single molecule reaction on catalyst surfaces (the controlling step of surface reaction, weak product adsorption). (b). The variation of reaction rate with reactant pressure P_A (or P_B) according to the Langmuir-Hinshelwood mechanism. P_B (or P_A) = constant. (c). The relationship of reaction rate with reactant pressure P_A according to Eley-Rideal mechanism, P_B = constant.

$$\gamma = k_3 \theta_A \theta_B = \frac{k_3 K_A K_B P_A P_B}{(1 + K_A P_A + K_B P_B)^2} \quad (3.18)$$

This mechanism for the reaction occurring between A and B, which are both adsorbed onto the catalyst surface, is called the Langmuir-Hinshelwood (L-H) process. If pressure P_B is kept constant, an increase in P_A will raise reaction rate γ up to a maximum; at a further increase in P_A , this reaction rate will decrease. If pressure P_A is kept constant, an increase in P_B will raise reaction rate γ up to a maximum; at a further increase in P_B , this reaction rate will decrease (Fig. 3.2b).

For the reaction occurring between two gas molecules (A and B) where A is adsorbed onto the surface and reacts with B present in the gas phase⁴⁸ (B may partly be adsorbed onto the surface, but A will react only with B in the gas phase, and product C will not be adsorbed strongly), we can derive:



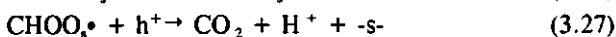
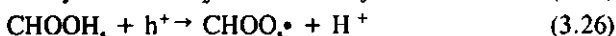
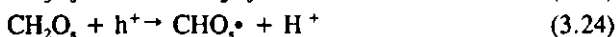
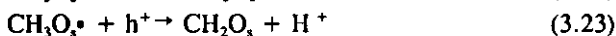
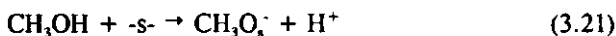
and

$$\gamma = k_2 P_B \theta_A = \frac{k_2 K_A P_A P_B}{1 + K_A P_A + K_B P_B} \quad (3.20)$$

This mechanism is called the Eley-Rideal (E-R) process. An E-R process is characterised by the fact that, at a constant pressure P_B and an increasing pressure P_A , reaction rate γ will reach a maximum value independent of a further increase in pressure P_A (Fig. 3.2c).

3.2.4 The mechanism of the photocatalytic oxidation of methanol

According to the assumptions made and our experimental results⁴⁹ given in Chapter 2, we suggest that the photocatalytic oxidation of methanol at the anodic surface occur mainly via surface reactions rather than via free radical reactions in the liquid phase:



Eq. 3.21 - 3.27 represent the half reactions of the oxidation occurring at the anodic area of TiO_2 ; the half reaction of the reduction of H_2O , O_2 or other reducible compounds occurring at the cathodic area of TiO_2 is given by Eq. 3.33. The total reaction is given by Eq. 3.1. If the methanol concentration is low, and the reaction product and oxygen are not strongly adsorbed onto the surface, we assume that the adsorption of methanol onto a photocatalyst surface in solution can be described as a simple Langmuir isotherm according to Eq. 3.9:

$$\theta_{\text{MeOH}} = \frac{K_{\text{MeOH}} C_{\text{MeOH}}}{1 + K_{\text{MeOH}} C_{\text{MeOH}}} \quad (3.28)$$

Here K_{MeOH} is the adsorption equilibrium constant and C_{MeOH} the methanol concentration in the liquid phase. Although the oxidation of methanol is a two-molecular reaction (Eq. 3.1), according to Eq. 3.21 - 3.27 its rate can be described by the rate equation for a one-molecular reaction (Eq. 3.13). Here it is assumed that the reaction occurring at the anodic area is the rate-determining step. Because illumination intensity I can change the distribution of surface charges and thus affect the adsorption of charged molecules onto the catalyst surface⁵⁰, the reaction rate is related to illumination intensity I . If the surface reaction step is the rate-controlling step, rate γ of the reaction occurring in an aqueous solution and given in Eq. 3.1 can therefore be represented by:

$$\gamma = k_2 \theta I = k_1 \theta I \quad (3.29)$$

where k_1 is the real rate constant of the overall reaction which it is related to illumination intensity I . If illumination intensity I is a constant, then, $k_1 I = k$, as during most experiments. According to eq. 3.28 and 3.29, we have:

$$\gamma = k\theta = \frac{kK_{\text{MeOH}} C_{\text{MeOH}}}{1 + K_{\text{MeOH}} C_{\text{MeOH}}} \quad (3.30)$$

or:

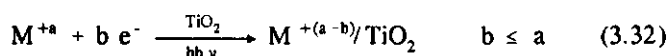
$$\frac{1}{\gamma} = \frac{1}{k} + \frac{1}{kK_{\text{MeOH}}} \frac{1}{C_{\text{MeOH}}} \quad (3.31)$$

where k is the real rate constant at a constant I . According to Eq. 3.31, k and K can be derived from a plot of the reciprocal reaction rate versus the reciprocal concentration of the reactant in the liquid phase. Under the same assumed conditions, Eq. 3.30 and 3.31 are not only valid for methanol but also for ethanol.

3.2.5 Powder micro-cell model of a photocatalyst in a slurry system

For a suspension of a powder catalyst in solution, a surface micro-cell model (Fig.3.1a) is often used to interpret the photocatalytic process⁴². In this model, all reactions occur at the surface of the photocatalyst, including oxidation (degradation of organics) and reduction (reduction of O_2 in an aerated system, and reduction of protons in a deaerated system). Below we describe a porous micro-cell model (Fig.3.1b), which is an improvement compared with the above model because it emphasizes the important role played by pores in photocatalysis according to a theoretical analysis carried out and the data on the X-ray exciting spectrum we obtained during electron beam probe microanalysis.

In this improved micro-cell model, most of surface of a porous catalyst is assumed to be inside particles, and the photocatalytic reductive reactions clearly happen not only at the outside surface of the particles but also in the pores inside particles. For example, the reductive photodeposition of metals occurring at the cathodic area of TiO_2 and described as:

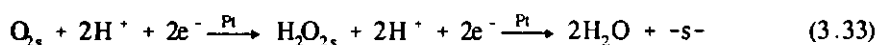


may take place inside pores. Only oxidative deposition (e.g., the reaction $Pb^{2+} + h^+ \rightarrow PbO_2 \downarrow$) takes place at the outside surface of the photocatalyst.

According to the semiconductor theory, with n-type semiconductors such as TiO_2 the anodic area, where an electron donor is adsorbed, must be an illuminated area, and the cathodic area, where an electron acceptor is adsorbed, a dark area. When a catalyst consisting of a fine powder suspended in solution is illuminated, the outside surface of particles may be illuminated, but the surface inside their pores will remain unilluminated. It will act as a permanent cathode, and if no mass transfer limitation occurs, the reductive reaction will happen mainly there.

3.2.6 The photocatalytic reduction of oxygen on TiO_2 and Pt/TiO_2

According to the possible reaction paths assumed, oxygen will not react directly with the substrate (e.g., methanol, ethanol) if the photocatalytic reaction occurs at the catalyst surface. Instead, the reactions will take place separately, as in an electrochemical cell. In the Pt area, oxygen will be reduced faster than at the TiO_2 surface. During these reductive processes, the electrons accumulated at the TiO_2 surface will be eliminated and H_2O will rapidly be formed via the intermediate H_2O_2 ^{34,51} according to the equation:



The mechanism of oxygen reduction is elaborated upon in Chapter 2.

3.3 EXPERIMENTAL

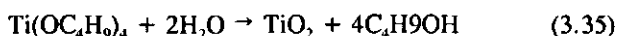
3.3.1 Reagents

The commercial titanium dioxide used during the experiments was Degussa P25 grade with a BET surface area of $\sim 50 \text{ m}^2 \text{ g}^{-1}$ and an average particle size of 30 nm. Some of the TiO_2 used for the preparation of metallized catalysts was prepared from titanium tetrachloride (TiCl_4) (analysis reagent, Shanghai Reagent Co.) and titanium butoxide ($\text{Ti}(\text{OC}_4\text{H}_9)_4$) (analysis reagent, Shanghai Reagent Co.). The methanol used was ALDRICH A.C.S. reagent, Lot No. 01707KX. The ethanol used was ethyl alcohol from AAPER Alcohol and Chem. Co. USP (Absolute - 200 Proof, DSP-KY-417) and an analysis reagent from Shanghai Reagent Co. The palladium dichloride used was Fisher purified product (Lot 915085) and an analysis reagent from Shanghai Reagent Co. The palladium black used was a product from Aldrich (Lot No. 06115BY). The chloroplatinic acid used ($\text{H}_2\text{PtCl}_6 \cdot 6\text{H}_2\text{O}$) was a reagent from Fisher A.C.S. (Lot No. 915412) and an analysis reagent from Shanghai Reagent Co. The glacial acetic acid used was a reagent from Fisher A.C.S. and an analysis reagent from Shanghai Reagent Co. These reagents were used without further purification.

3.3.2 Catalyst preparation

3.3.2.1 Preparation of TiO_2

Some TiO_2 samples were prepared by hydrolyzing TiCl_4 and $\text{Ti}(\text{OC}_4\text{H}_9)_4$ according to the following hydrolysis reactions:



Because hydrolysis of TiCl_4 with water occurs very rapidly and violently and produces immediately a huge amount of toxic HCl smoke, the preparation should be carried out very carefully in a draft hood, and the water should be added drop by drop. After the hydrolysis, the sample was centrifuged at 3,000 rpm for 15 minutes, the supernatant was decanted, and the solid sample was washed with water to remove all chloride. The procedure (*i.e.*, centrifuging and washing) was repeated ten times. After three hours of drying at 120°C , the specific surface of the TiO_2 was $54 \text{ m}^2/\text{g}$ according to the results of a BET calculation.

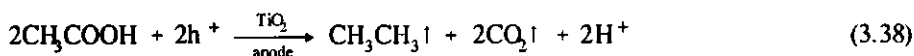
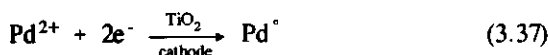
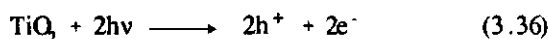
Hydrolysis of $\text{Ti}(\text{OC}_4\text{H}_9)_4$ with water occurs smoothly, and all hydrolyzed products, including butanol, remain in solution (see the equations above). To obtain very fine TiO_2 particles and a large specific surface area, water had to be added slowly during stirring. After water was added to the $\text{Ti}(\text{OC}_4\text{H}_9)_4$ and the hydrolyzed solution was stirred for 24 hours, the solution was centrifuged at 3,000 rpm for 15 minutes, the supernatant was decanted, and the solid sample was washed with ethanol in order to remove butanol as far as possible. The procedure (*i.e.*, centrifuging and washing) was repeated ten times. Then the sample was dried at 200°C for 15 hours to remove any remaining butanol. The specific surface of the TiO_2 was $130 \text{ m}^2/\text{g}$ according to the results of a BET calculation.

3.3.2.2 Preparation of 1% wt. Pd/ TiO_2

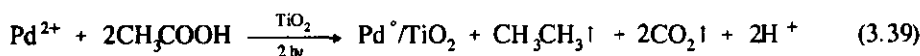
A photocatalyst consisting of 1% wt. Pd/ TiO_2 was prepared by employing two methods: physical mixing and photodeposition⁵.

Preparation of Pd/ TiO_2 by physical mixing occurred by putting 1% wt. palladium black and TiO_2 into a mortar, carefully grinding the contents, and pretreating the resultant mixture consecutively in nitrogen flow at 240°C for about one hour, and then in hydrogen flow at 430°C and 700°C for about twenty hours.

Photodeposition of 1% wt. Pd on TiO_2 was achieved by dissolving 0.333 g of PdCl_2 in 13.33 ml of glacial acetic acid. The sample was diluted to 270 ml in a 600-ml photoreactor with a quartz window 12 cm in diameter at the top. 20.0 g of TiO_2 was added and the solution was stirred. The reactor was closed, sealed and then illuminated for 17 hours using a 100-W medium-pressure mercury lamp (Sylvania, Par 38) with a near-UV filter. The following reactions occurred during the deposition (reduction) of Pd^{2+} on TiO_2 :



The overall reaction is therefore:

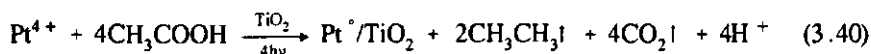


When the Pd^{2+} began to be reduced by TiO_2 and was deposited on TiO_2 under UV light, the slurry gradually turned from dark brown (the colour of Pd^{2+}) to grey. After all Pd^{2+} in the solution was reduced and deposited on TiO_2 (after 17 hours during our experiment), the dark grey slurry of suspended 1% Pd/TiO_2 particles was centrifuged at 3,000 rpm for 30 minutes; next, the supernatant was decanted and the solid (Pd/TiO_2) was washed with water. The procedure of centrifuging and washing was repeated eight times to remove ions such as acetate as far as possible. After cleaning, the solid was dried at ambient temperature, or at 120°C for about 3 hours.

3.3.2.3 Preparation of 1% Pt/TiO_2

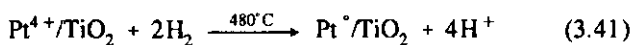
1% Pt/TiO_2 was prepared by photodeposition⁴³ and chemical deposition⁵²:

Several batches of photo-deposited Pt/TiO_2 were prepared in the same way. A 467-ml slurry containing 34.6 g of TiO_2 , 0.923 g of $\text{H}_2\text{PtCl}_6 \cdot 6\text{H}_2\text{O}$ and 25 ml of glacial acetic acid was put into a sealed 600-ml photoreactor with a quartz window of 12 cm in diameter at the top. The slurry was stirred and illuminated with UV light for 38 hours. The overall equation for the deposition (reduction) of Pt^{4+} on TiO_2 in this system is:



During the illumination, the slurry gradually turned from orange (the colour of PtCl_6^{2-}) to grey, which means that Pt^{4+} was reduced to Pt^0 . This reduction occurred slower than that of Pd^{2+} , because the higher reduction potential of Pt^{4+} is required to produce Pt^0 . After illumination (for 38 hours), the dark grey slurry was centrifuged at 3,000 rpm for 30 minutes and then the solid (Pt/TiO_2) was washed. This procedure was repeated eight times. The dark grey solid was dried at ambient temperature, or at 120°C for about 3 hours.

Chemical deposition of Pt on TiO_2 occurred by putting 37.7 g of TiO_2 into 500 ml of water containing 1 g of chloroplatinic acid ($\text{H}_2\text{PtCl}_6 \cdot \text{H}_2\text{O}$). The slurry was stirred in a rotary vacuum evaporator for 3 hours at 75°C in order to thoroughly mix the Pt^{4+} ions and TiO_2 . The solid mass was dried in an air oven at 110°C , heated to 200°C in a flow of nitrogen, and then reduced in a flow of hydrogen at 480°C for 2 hours so that all Pt^{4+} present at the surface of TiO_2 was reduced to Pt^0 by hydrogen:



3.3.3 The apparatus used and procedure of the photocatalytic experiments

3.3.3.1 The apparatus of the photocatalytic experiments

The experiments were carried out in a liquid-phase recycle photoreactor similar to the one used early by Pruden and Ollis⁵³ (see Fig.2.1b). A 0.1 wt% slurry of photocatalyst in water was recycled through a quartz annular photoreactor using a polypropylene/ceramic pump. An illumination of 3.08×10^{-4} Einstein/min was provided by a black light fluorescent bulb (GE BLB - 15 W) fixed in the centre of the photoreactor. The predominant emission wave length band of this lamp ($320 \leq \lambda \leq 400$ nm) is sufficient to photo-excite TiO_2 ($\lambda \leq 410$ nm) and causes no homogeneous photolysis of the reactants (if $\lambda \leq 300$ nm). A pressure gauge scaled from 0-60 in. H_2O (inch of water column) was fixed at the top of the reservoir to monitor the changes in pressure occurring in the reactor and to measure the oxygen consumption. The total reactor volume was ~ 930 cm³, including a 280-cm³ quartz annular photoreactor and a reactor reservoir (made from a 500-ml, 3-neck flask). The total liquid volume in the reactor was fixed at ~ 600 cm³, with a ~ 330 -cm³ reservoir headspace during each run.

3.3.3.2 The procedure and conditions of the photocatalytic experiments

During the photocatalytic oxidation experiments with oxygen, 550 ml of water and 0.600 g of photocatalyst (M/TiO_2 or plain TiO_2) were put into the reservoir. The solution was pumped through the recycling system and stirred in the reservoir. The liquid slurry (~ 550 cm³) was sparged with pure oxygen for 30 minutes. Then the reactor was closed and substrate added. The solution pH was adjusted using HNO_3 or NaOH , and the solution was diluted to 600 ml. 40 cm³ of pure oxygen was syringed to maintain excess pressure (about 20 in. H_2O) in the reactor. After 5 minutes of stirring, during which no gas leaking was observed, the light was turned on for illumination, and at fixed periods gas and liquid samples (0.5-1 ml) were taken for analysis. The reaction temperature was kept at $25 \pm 2^\circ\text{C}$ using cooling water. The slurry was recycled through the photoreactor at 1,500 ml/min. In accordance with the variations in reactor pressure occurring during illumination, pure O_2 was replenished constantly.

3.3.3.3 X-ray powder crystal diffraction of M/TiO_2 photocatalyst

X-ray powder crystal diffraction was applied to identify the crystal structure of the catalyst and the state of the platinum present at the surface of TiO_2 : whether the platinum was deposited on TiO_2 without any interaction with TiO_2 or including the formation of chemical bonds (Pt-Ti).

As much as 5% wt. platinized TiO_2 was prepared for X-ray analysis to ensure sufficiently clear diffraction peaks for platinum. An automatic X-ray powder crystal diffractometer was used. Around 1 g of Pt/TiO_2 in the form of a powder sample was pressed onto the diffractometer's

sample holder. The diffractometer's recorder recorded relative diffraction intensity versus diffraction angle 2θ . By comparing 2θ of the sample data peaks with the data published on standard samples, we could identify the components and sample structure.

3.3.3.4 The Electron Beam Probe (X-ray exciting spectrum) for surface element analysis of an M/TiO₂ photocatalyst

In order to examine the distribution and content of a metal (such as platinum) deposited on the surface of TiO₂, an electron probe microanalysis⁵⁴ was carried out. This technique gives a surface component analysis to a depth of 1-2 μm in a sample and over a diameter range of 1 μm at the surface of a sample. When a beam of electrons is focused on a fine pencil of 0.1-1 μm cross section and directed at the specimen surface exactly at the spot to be analyzed, this electron bombardment excites characteristic X-rays essentially from a point source and at considerably high intensities. Detection and measurement of these characteristic X-ray spectra reveal what components are present at the sample surface. During the experiments, the electron beam probe microanalyzer was combined with an electron microscope. The latter was used to locate a spot at the specimen surface interesting for electron beam probe microanalysis. The detection limit (in a 1- μm size region) is about 10^{-14} gram. The relative accuracy is 1-2%, if the concentration of an element (Pt) at a surface (TiO₂) is higher than a few percent and if adequate standards are available.

As an electron probe microanalyzer, a tunnel electron microscope (8×10^5 times) with an electron probe microanalyzer was used. Powder samples of Pt/TiO₂ (approximately 50 mg) must be fixed firmly on the metal sample-supporter (diameter ~ 2 cm) in order to ensure that they do not move while they are bombarded by high-energy electron beams. The screen of the electron microscope allowed continuous visual observation of the exact sample area hit by the electron beam. The possible elements and contents of the sample surface (to a depth of 100 Å) were calculated automatically by the instrument's software.

3.3.4 Analytic method

3.3.4.1 pH

pH was measured using an *in-situ* pH electrode (Fisher, 13-620-93) connected to an ORION 701A digital pH/mv meter. Standard buffer solutions (pH = 4, 7 and 10) were used to calibrate the pH electrode before each run.

3.3.4.2 Methanol and ethanol concentrations

Reaction-solution samples of methanol and ethanol were taken periodically, put into a centrifuge cup and centrifuged in order to remove photocatalyst. 1 μl of supernatant was injected directly into an HP 5890A Gas Chromatograph (capillary column, J & W Scientific Cat. No. 125-1334) fitted with a Flame Ionization Detector (FID). Standard methanol and ethanol solutions were used to calibrate the GC for each experiment.

3.3.4.3 Carbon dioxide analysis

The production of carbon dioxide in the gas phase was measured by injecting a gas sample of 0.5 or 1 ml directly into an absorption tube fixed on an infrared carbon dioxide analyzer (Horiba, PIR-2000). To measure the production of CO_2 dissolved in the reaction solution, a liquid sample of 0.5 or 1 ml was taken and injected into the absorption tube, which contained a solution of 1 N H_2SO_4 , in order to convert all CO_2 present in the solution (carbonate, bicarbonate) to gaseous CO_2 , which was tripped by helium carry gas. Weekly, a sodium carbonate solution was used as a standard sample to calibrate the instruments.

3.3.4.4 Oxygen analysis

The consumption of oxygen can be calculated from the difference of the pressure change and the rectification resulted from the production of CO_2 and other gas (*i.e.*, methane). The saturation concentration of pure oxygen in water amounts to 41.36 ppm (25°C)⁵⁵. If 330 cm^3 of pure O_2 in the reservoir headspace completely dissolves in 600 cm^3 of water, the total concentration of O_2 is ~ 760 ppm (23.8 mM).

3.4 RESULTS AND DISCUSSION

3.4.1 The results of X-ray powder crystal diffraction of powder Pt/TiO₂ catalysts

As mentioned above, pretreatment of Pt/TiO₂ by hydrogen reduction at a temperature of between 400°C and 700°C increases its photocatalytic activity⁵⁵. It is therefore interesting to investigate why such pretreatment can raise the photoactivity of the catalyst. We applied X-ray powder crystal diffraction to investigate the difference in crystal structure before and after pretreatment. Fig. 3.3a and 3.3b show the results of X-ray powder crystal diffraction for TiO₂ and Pt/TiO₂. These results reveal that in Pt/TiO₂ a small quantity of a rutile component of TiO₂ appeared (Fig. 3.3b) after treatment with hydrogen at a high temperature. Furthermore, the peak indicated with an asterisk at the diffraction angle of $2\theta = 40^\circ$ increased. Although some weaker diffraction peaks may be covered by those of the main crystal structure, $2\theta = 40^\circ$ may

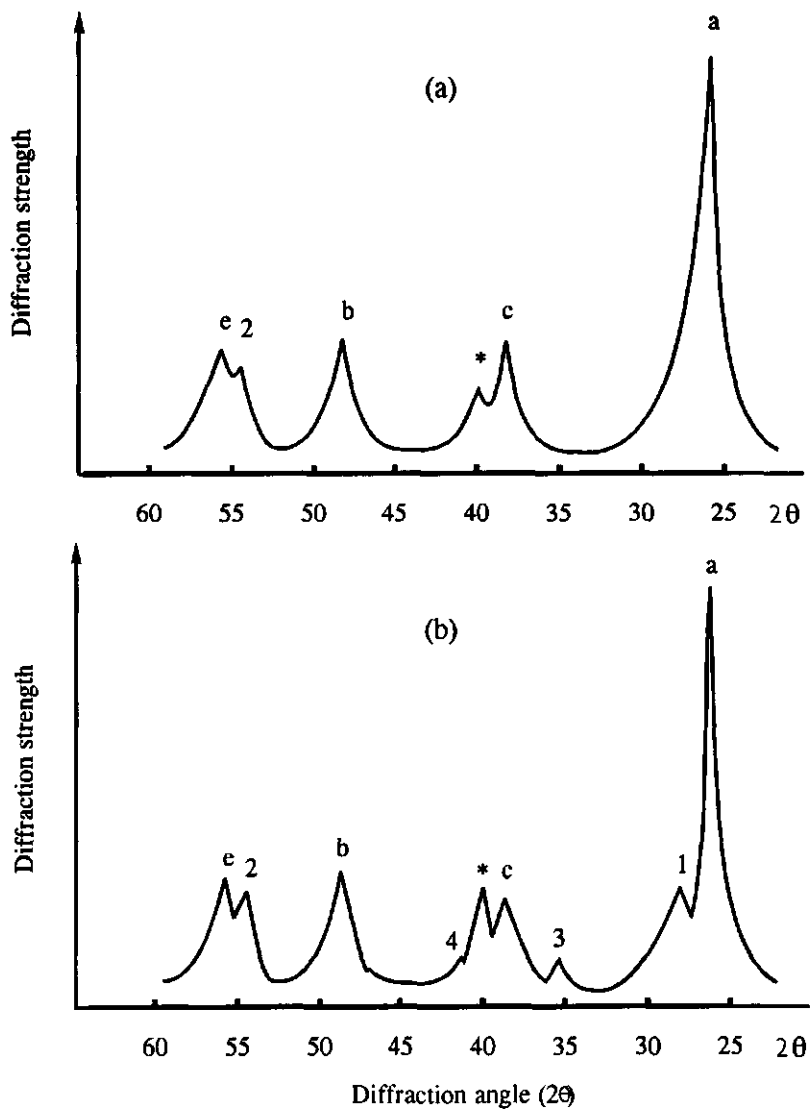


Fig. 3.3 The figures of X-Ray powder crystal diffraction of Pt/TiO₂. The diffraction angle strength for anatase are given by a, b, c and e, and those for rutile are given by 1, 2, 3 and 4 respectively. *: The diffraction angle may be due to the Ti-Pt interaction. (a). The photocatalyst Pt/TiO₂ without pretreatment. (b). The photocatalyst Pt/TiO₂ with pretreatment in an hydrogen flow for four hours at 700°C.

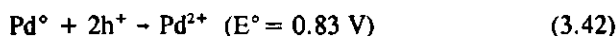
be the strongest Bragg angle of a Pt-Ti intermetallic compound. According to the principle of strong metal-supporter interaction ³⁵(SMSI), strong interaction (*i.e.*, a chemical bond) will occur between a deposited metal and the support (*i.e.*, carrier) when a metallized catalyst is treated at a high temperature. Therefore, the peak at $2\theta=40^\circ$ should be the result of the diffraction of Pt-Ti intermetallic compounds (*i.e.*, alloys), which was strengthened by hydrogen reduction at a high temperature, although it is hard to identify a specific compound based on only one Bragg-angle peak. According to the X-ray diffraction analysis carried out, in the Pt/TiO₂ with a structure consisting almost completely of anatase some rutile had emerged, and the interaction between Pt and TiO₂ had increased by pretreatment at a high temperature.

Although the results of X-ray diffraction analysis showed the existence of a rutile structure and the occurrence of Pt-TiO₂ interaction (SMSI), it is not to be expected that the photocatalytic activity of a photocatalyst will always increase as a result of pretreatment by hydrogen reduction at a high temperature. In spite of the positive effect created by SMSI in the form of a higher catalyst activity, the sintering of catalysts at a high temperature has a disadvantage in that it drastically reduces their photocatalytic activity. Comparing the activity of a catalyst before and after pretreatment is justified only if the particle size does not change. The particle size of a photocatalyst is an important aspect of photocatalytic activity: the smaller the particle, the higher the activity. During our experiments, using the same Pt/TiO₂ from different pretreatment batches resulted in different results, although the pretreatment conditions were the same in each batch. This is because in the various batches the catalyst was not sintered to the same degree. Some of the catalysts were well dispersed in solution, and others not. Sintering makes the catalyst particles size much larger than that before pretreatment, and most of the catalyst particles precipitate on the bottom of the reactor. If little catalyst is suspended in solution, there is little photocatalytic activity. How to control the sintering of catalyst during high temperature pretreatment is still a poser; it is a sophisticated experimental skill.

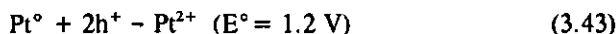
3.4.2 The results of the X-ray exciting spectrum, and a discussion of a porous micro-cell model

The X-ray exciting spectrum of Pt/TiO₂ resulting from an electron beam probe microanalysis showed only signals created by Ti and oxygen, not any signal created by Pt in the first 100-Å layer at a certain surface area of Pt/TiO₂. Checking a large number of spots at the surface and visually analysing them using an electron microscope had the same result. This can be attributed to the deposition of platinum like an island at the surface (island distribution), or assumes that some of the platinum could be deposited inside the pores of TiO₂. Another experiment of XPS (X-ray Photoelectron Spectroscopy) also confirmed this assumption (see Chapter 6, § 6.3.5).

As shown in Fig.3.1b, when TiO_2 catalyst particles are irradiated in suspension, the modified palladium or platinum outside the TiO_2 particles may become a "transient" anode. The following oxidation reactions may take place:



or



Because of the restriction imposed by the Schottky barrier (Fig.1.9b), Eq.3.42 or 3.43 seems to be impossible at semiconductor surfaces for electron transport in the opposite direction. However, there are three reasons for the occurrence of Eq.3.42 or 3.43 at the surface of powder photocatalysts. First, if the deposited metal particles are so small that they provide insufficient capacity (atomic orbits) for maintaining their Fermi level when electrons flow from semiconductor to metal after their contacting, the height of Schottky barrier will decrease greatly. It may result in electrons flowing from metal to semiconductor. Secondly, after pretreatment at a high temperature the metal and semiconductor are no longer in physical contact with each other due to the role played by SMSI. Between the metal and semiconductor, chemical bonds of various types exist rather than a Schottky barrier. Thirdly, the oxidation capability of TiO_2 (Fig.1.7) is sufficiently high to oxidize Pd or Pt. Therefore, photocatalytic oxidation probably also occurs where $\text{Pd}^\circ/\text{Pd}^{2+}$ is located; for example, Pd^{2+} can oxidize alcohol and is then reduced to Pd° .

On the other hand, some of the palladium deposited in pores acts as a "permanent" cathode which cannot be irradiated, meaning the efficiency of reductive sites on the total surface being increased. The palladium or platinum deposited at the outside of TiO_2 is not only a reductive but also an oxidative catalyst. The catalyst can therefore perform two functions.

3.4.3 Application of the heterogeneous catalysis theory on gas reactions to photocatalytic reactions in aqueous liquids: The Langmuir form of photocatalytic kinetic processes

During the studies conducted earlier by Ollis *et al.*^{4,26,28}, photocatalytic oxidation of organic halogen compounds in a dilute aqueous solution was described satisfactorily using kinetic equations in a Langmuir form normally used in relation to heterogeneous systems in which gas reactions occur at catalyst surfaces. This section presents detailed experimental measurements of the photocatalytic oxidation of aqueous solutions of methanol and ethanol. The alcohol concentration ranged from 100 to 400 ppm. Fig.3.4 and 3.8 show alcohol concentration as a function of illumination time and compare the results found at different initial concentrations of methanol and ethanol. The slope of the tangent line at each experimental data point located on the curves in Fig.3.4 and 3.8 indicates relative reaction rate γ . Fig.3.5 and 3.9 show the relationship between photocatalytic oxidation rate and concentration for methanol and ethanol.

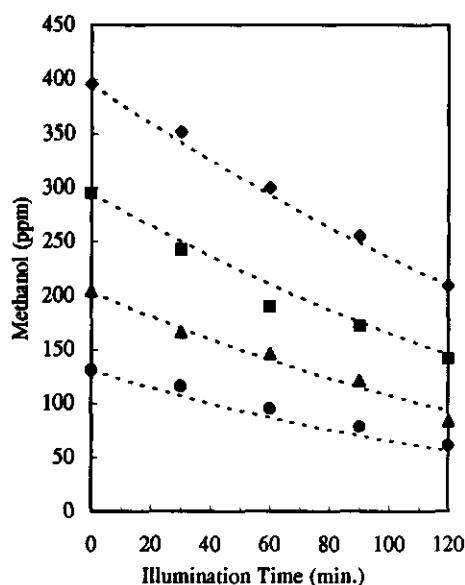


Fig.3.4 Methanol photocatalytic oxidation as a function of illumination time for various initial concentrations. Catalyst: 1%Pt/TiO₂, 1 g/L. Initial pH=5.1. 25°C. The markers in the graph indicate experimental data. The dashed lines indicate the fit by the Langmuir equation.

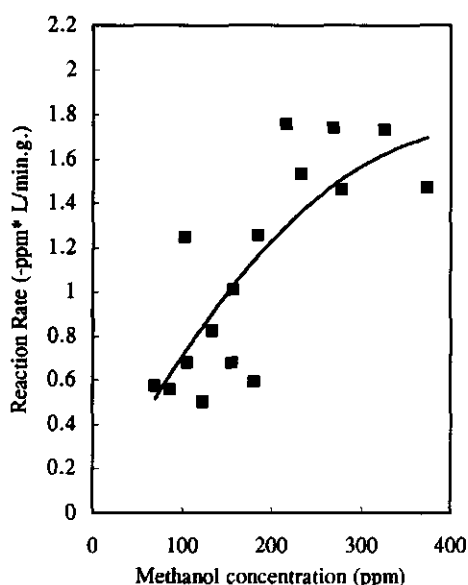


Fig.3.5 The relationship between rate of photocatalytic methanol oxidation and methanol concentration. Conditions: see Fig.3.4.

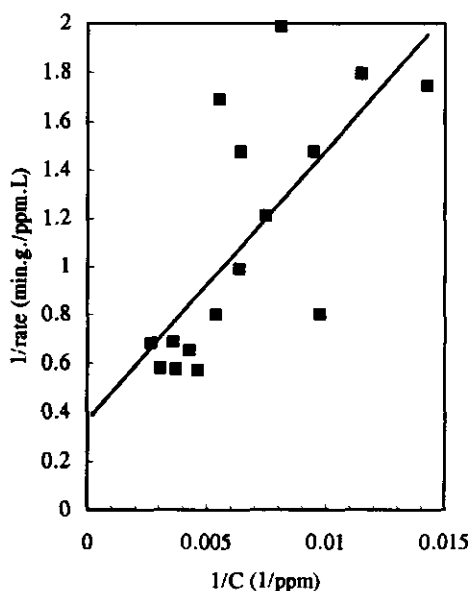


Fig.3.6 Reciprocal rate vs. reciprocal methanol concentrations. Conditions: see Fig.3.4.

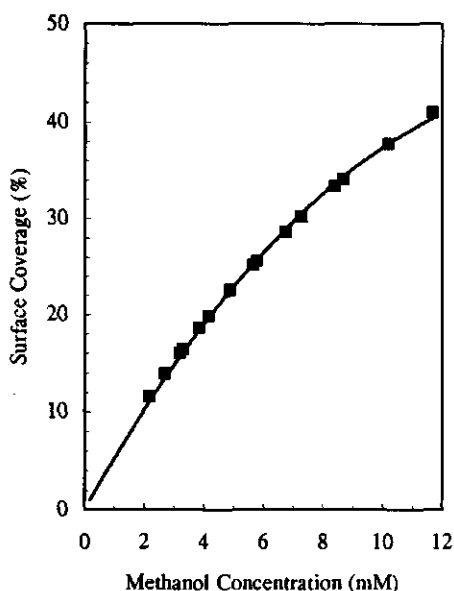


Fig.3.7 The methanol coverage at various concentrations. Conditions: see Fig.3.4

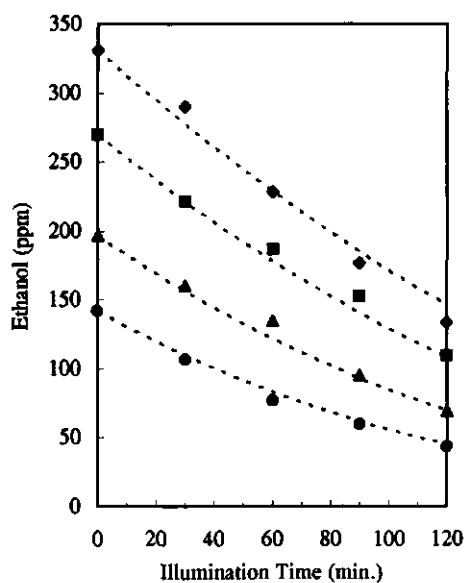


Fig.3.8 Ethanol photocatalytic oxidation as a function of illumination time for various initial concentrations. Catalyst: 1%Pt/TiO₂, 1g/L. Initial pH=5.1. 25°C. The markers in the graph indicate experimental data. The dashed lines indicate the fit by the Langmuir equation.

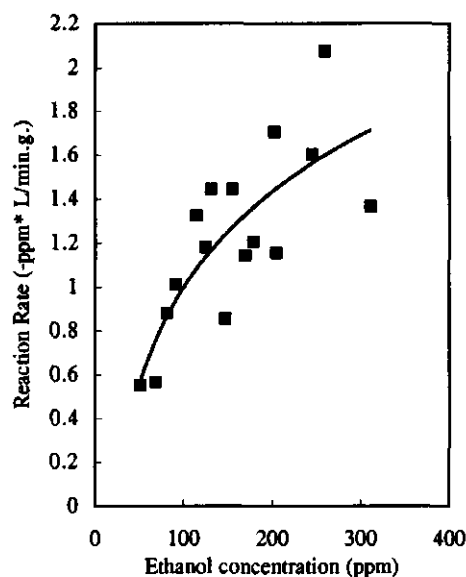


Fig.3.9 The relationship between rate of photocatalytic ethanol oxidation and ethanol concentration. Conditions: see Fig.3.8.

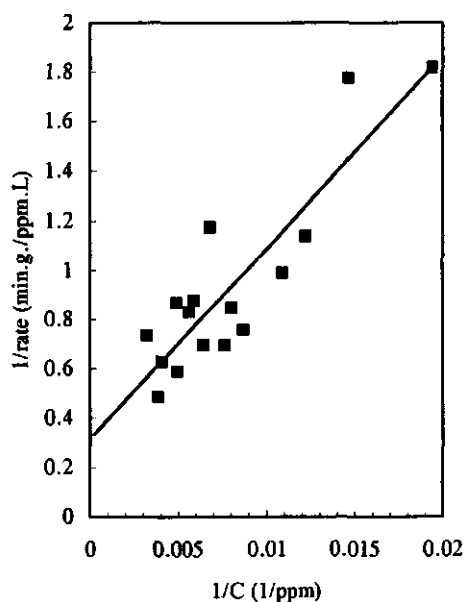


Fig.3.10 Reciprocal rate vs. reciprocal ethanol concentrations. Conditions: see Fig.3.8.

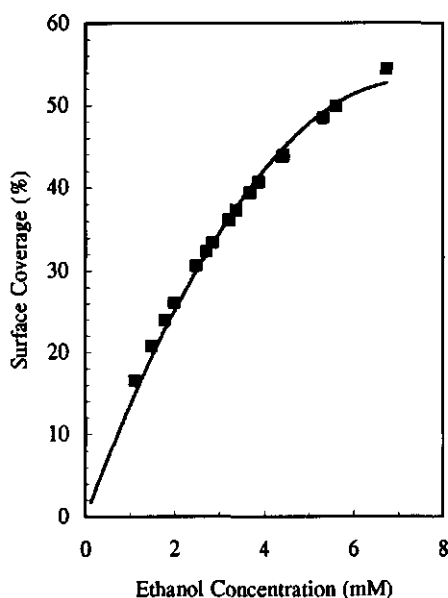


Fig.3.11 The ethanol coverage at various concentrations. Conditions: see Fig.3.8.

Fig. 3.5 and 3.9 were derived from Fig. 3.4 and 3.8 by taking the slope of each pair of adjacent experimental points (concentrations) as the reaction rate at the average concentration at these two points. Fig. 3.6 and 3.10 show the linear regression of reciprocal reaction rates with reciprocal concentrations of methanol and ethanol, respectively. They represent the linear relationship of the Langmuir kinetic equation for single-molecule reaction at photocatalyst surfaces (Eq. 3.31); from this, rate constant k and adsorption equilibrium constant K can be calculated. Table 3.1 gives Langmuir equation parameters derived from experimental data. These values were obtained by fitting the integrated Langmuir equation to the experimental concentrations (Fig. 3.4 and 3.8). The error of the fit is within 10%, which is the experimental error.

Table 3.1 The kinetic parameters of the Langmuir model for methanol and ethanol photocatalytic oxidation.

	Methanol	Ethanol
k (ppm/min.g)	4.4	3.3
K (ppm ⁻¹)	1.9×10^{-3}	3.8×10^{-3}
kK (1/min.g)	8.2×10^{-3}	1.3×10^{-2}

The surface coverages θ on TiO_2 for methanol and ethanol were calculated based on the data given in Table 3.1 and the Langmuir isotherm equation (Eq. 3.28), and are represented in Fig. 3.7 and 3.11. As shown in these figures, at the same molar concentration the coverage shown by ethanol is twice as high as that shown by methanol. It means that at low concentrations ethanol will occupy twice as much space at the TiO_2 surface as methanol. According to our assumption made in Chapter 2 regarding the adsorption pattern, ethanol and methanol have the same end-group (hydroxyl group) adsorption pattern. When the hydroxyl group of an ethanol molecule is adsorbed onto the TiO_2 surface, this molecule occupies more space at the catalyst surface than a methanol molecule as a result of sp^3 hybridization of carbon atomic orbits. Although at the same low molar concentration the number of ethanol molecules present at a TiO_2 surface is half that of methanol molecules, the overall reaction rate constant (k) of ethanol is only 25% lower than that of methanol. This means that, compared with methanol, the reaction rate constant for a single reactant molecule of ethanol (k') is higher, because k can be considered the sum of the k' of all reactants adsorbed onto the surface.

$$k = k'N_{\text{ads}} \quad (3.44)$$

where N_{ads} is the total number of reactant molecules adsorbed onto TiO_2 surfaces.

Based on Eq.3.28, Fig.3.12 gives the calculated surface coverage of the reactants present on TiO_2 as a function of their concentration, where K is a parameter. Equilibrium constant K for alcohol was derived from our experiments (Table 3.1), whereas the K value for organic chlorides was derived from research carried out earlier by Ollis *et al.*⁴ If the k and K of compounds can be derived from experiments, the reaction rate in a photocatalytic system for various organic and inorganic compounds can be estimated based on the relationships between coverage and concentration, and on the reaction rate constant. As shown in Fig.3.12, occupying 90% anodic surface of 1 gram of TiO_2 requires around 5,000 ppm (156 mM) of methanol ($K=0.00185$), 2,500 ppm (54 mM) of ethanol ($K=0.0038$), 3,000 ppm of chloroform ($K=0.003$), 900 ppm of TCE ($K=0.01$) or only 450 ppm of dichloromethane or PCE ($K=0.02$). If a surface reaction is a rate-controlling step, the reaction rate will not increase with concentration after the surface is fully covered. According to Eq.3.30, the maximum rate of photocatalytic oxidation is indicated by rate constant k (see Table 3.1), which for methanol is 4.4 ppm/min.g and for ethanol 3.3 ppm/min.g.

There are different Langmuir kinetic equations which describe different reaction mechanisms. Different assumptions of mechanism processes for a reaction result in different descriptions of kinetic equations. According to the surface mechanism proposed in Eq.3.21 - 3.27 and Eq.3.30, a rate expression for a single-molecular reaction in solution can be used to describe the two-molecular photocatalytic reactions given in Eq.3.1. If assuming that the mechanism of the reactions given in Eq.3.1 is a two-molecular adsorption reaction at a surface, such as the reaction occurring between methanol and hydroxyl groups both adsorbed onto a surface (as is the case in Eq. 2.23 - 2.30 given in § 2.3.5.2), this mechanism can be described as an L-H two-molecular process. The E-R process can also be used to describe Eq.3.1, if assuming that methanol or ethanol was adsorbed onto a surface and reacted with free hydroxyl radicals in solution.

3.4.4 The effect of oxygen concentration on the photocatalytic degradation of methanol and ethanol

The oxygen concentration affects the oxidation of alcohol. If the rate- controlling step of the overall reaction (Eq.3.1) is the anodic surface reaction of alcohol oxidation, the oxygen pressure in the system should be kept constant to eliminate the effect of oxygen concentration on alcohol oxidation, meaning that a continuous supply of oxygen is necessary. Fig. 3.13 shows total oxygen consumption versus illumination time at various initial alcohol concentrations,

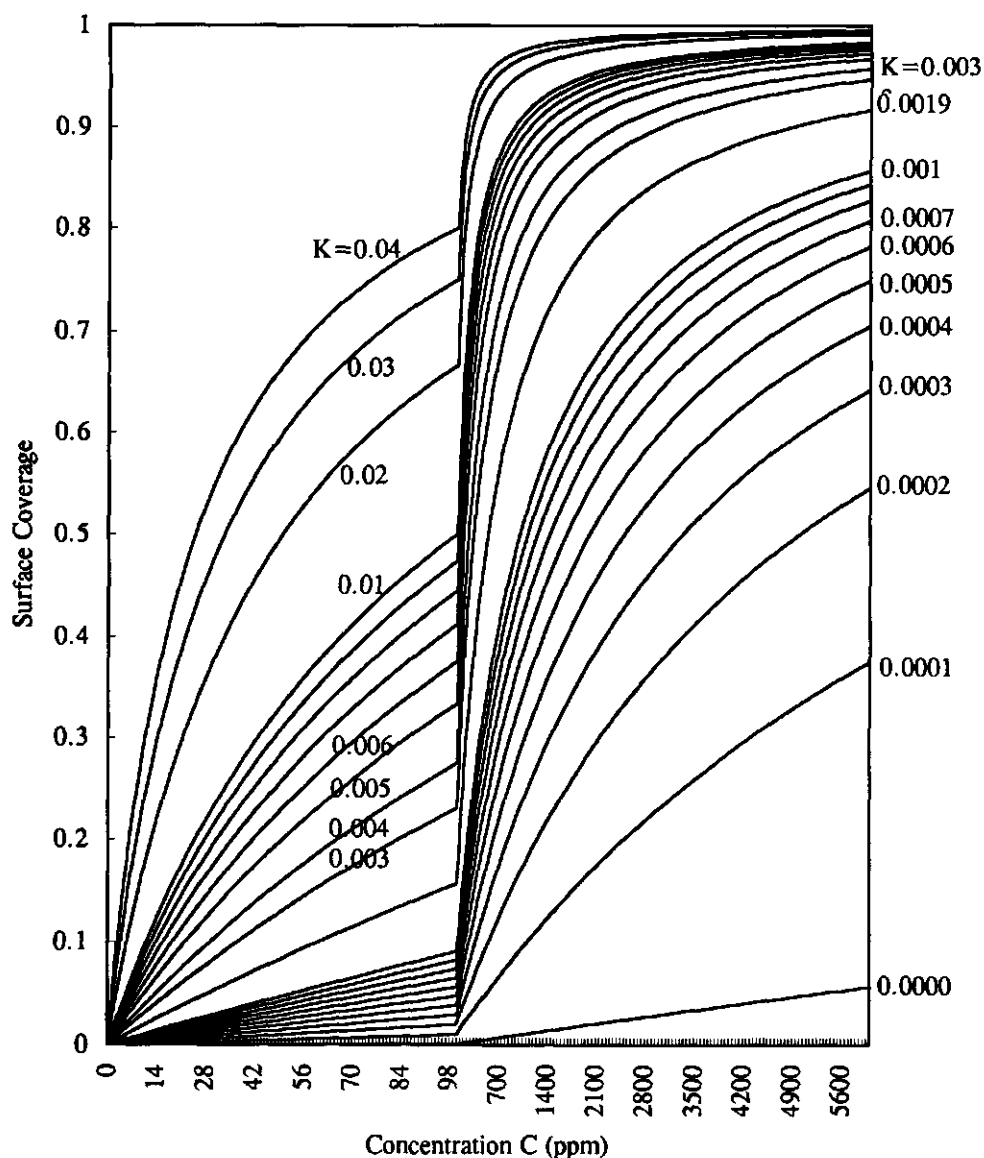


Fig.3.12. The Langmuir relationship for surface coverage on TiO_2 surfaces as a function of reactant concentration, where $K=0.0019$ and $K=0.0038$ are the adsorption equilibrium constants for methanol and ethanol on the surface of TiO_2 , and $K=0.003$ that for chloroform, $K=0.01$ that for TCE and $K=0.02$ that for PCE⁽⁴⁾. The experiment conditions are shown in Fig.3.4 and Fig.3.8.

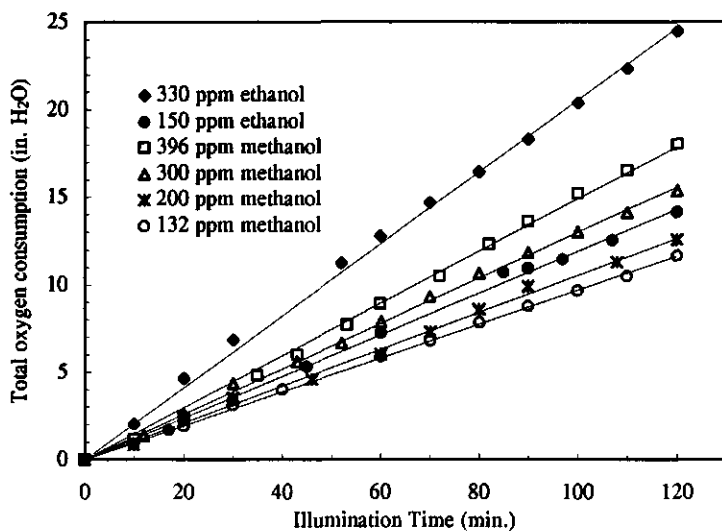


Fig.3.13 Total oxygen consumption as a function of illumination time. Conditions are similar to those given in Fig.3.4.

when the 30-inch H_2O pressure of oxygen in the photoreactor was fixed by continuous oxygen supply. All plots of oxygen consumption in Fig.3.13 show an almost linear but different slope. It means that, under conditions existing during our experiments, the oxygen consumption was nearly of zero order. Table 3.2 gives values for the oxygen consumption rate calculated from Fig.3.13. It shows clearly that at similar concentrations ethanol oxidation required a higher oxygen reduction than methanol oxidation.

Table 3.2. The reaction rate of oxygen reduction at various initial substrate concentrations

Reactant	Reactant initial concentration (ppm)	Oxygen reduction rate γ (-ppm/min.g)
methanol	132	0.104
	200	0.105
	300	0.137
	396	0.138
ethanol	150	0.121
	330	0.221

3.5 CONCLUSION

1. X-ray diffraction revealed a diffraction peak ($2\theta=40^\circ$) not belonging to the anatase or rutile crystal structure of TiO_2 in a Pt/TiO_2 sample pretreated at a high temperature. According to diffraction data of Pt-Ti intermetallic compounds (alloys), it is assumed to be the diffraction peak of these compounds.
2. An improved porous micro-cell model is proposed to explain the photocatalytic elimination of pollutants at the surface of such powder catalysts as Pt/TiO_2 . According to this model, only the surface outside particles can be illuminated, not that of particle pores. This inner surface acts as a permanent cathode at which Pt is also photodeposited.
3. Photocatalytic oxidation of methanol and ethanol in a dilute aqueous solution is clearly expressed by the kinetic equation of the Langmuir isotherm.
4. Compared to methanol, at low concentrations the coverage shown by ethanol at the photocatalyst surface of Pt/TiO_2 is twice as high. The maximum rate and efficiency of photocatalytic oxidation of methanol and ethanol on catalyst surface can be estimated by the results of the calculation.
5. An end-group adsorption of methanol and ethanol on catalyst surfaces is proposed to express the processes of the surface mechanisms of photocatalytic oxidation of alcohols.
6. In the aerated reactor system used for ethanol and methanol reactions, the oxygen consumption is of zero order.

ACKNOWLEDGMENTS

Jian Chen wishes to express his gratitude for the financial support received from North Carolina State University and wishes to thank Dr. Ed Wolfrum for the many interesting topical discussions held with him during this research.

3.6 REFERENCES

1. D. F. Ollis, H. Al-Ekabi, Eds., *Photocatalytic Purification and Treatment of Water and Air*, Elsevier Science Publishers, Amsterdam, 1993.
2. E. Pelizzetti, M. Schiavello, Eds., *Photochemical Conversion and Storage of Solar Energy*, Kluwer, Dordrecht, The Netherlands, 1991.
3. N. Serpone, Ezio Pelizzetti, Eds., *Photocatalysis Fundamentals and Applications*, John Wiley & Sons, New York, 1989.
4. (a). T. Nguyen and D. F. Ollis, "Complete heterogeneously photocatalyzed transformation of 1,1-and 1,2-dibromoethane to CO_2 and HBr ," *J. Phys. Chem.*, **88**, 3386-3388, 1984. (b). C. S. Turchi and D. F. Ollis, "Photocatalytic degradation of organic water contaminants: Mechanisms involving hydroxyl radical attack," *J. Catalysis*, **122**, 178-192, 1990.
5. C.-M. Wang, Adam Heller, and Heinz Gerischer, "Palladium catalysis of O_2 reduction by electrons accumulated on TiO_2 particles during photoassisted oxidation of organic compounds," *J.A.C.S.*, **114**, 5230-5234, 1992.
6. C. Kormann, D. W. Bahnemann, and M. R. Hoffmann, "Photolysis of chloroform and other organic molecules in aqueous TiO_2 suspensions," *Environ. Sci. Technol.*, **25**, 494-500, 1991.
7. M. Barbeni, E. Pramauro, and E. Pelizzetti, E. Borgarello, and N. Serpone, "Photodegradation of pentachlorophenol catalyzed by semiconductor particles," *Chemosphere*, **14**(2), 195-208, 1985.
8. X. Li, P. Fitzgerald and L. Bowen, "Sensitized photo-degradation of chlorophenols in a continuous flow reactor system," *Wat.Sci.Tech.*, **26**(1-2), 367-376, 1992.
9. (a). C. K. Grätzel, M. Jirousek and M. Grätzel, "Accelerated Decomposition of Active Phosphates on TiO_2 Surfaces," *J. Mol. Cat.*, **39**, 347-353, 1987. (b). C. K. Grätzel, M. Jirousek and M. Grätzel, "Decomposition of Organophosphorus Compounds on Photoactivated TiO_2 surfaces," *J. Mol., Cat.* **60**, 375-387, 1990.
10. W. Klöpffer, "Photochemical degradation of pesticides and other chemicals in the environment: a critical assessment of the state of the art," *The Science of the Total Environment*, **123/124**, 145-159, 1992.
11. H. Hidaka, Kayo Nohara and Jincui Zhao, Nick Serpone, Ezio Pelizzetti, "Photo-oxidative degradation of the pesticide permethrin catalysed by irradiated TiO_2 semiconductor slurries in aqueous media," *J. Photochem. Photobiol. A. Chem.*, **64**, 247-254, 1992.
12. S. T. Hung, Mark K. S. Mak, "Titanium dioxide photocatalysed degradation of organophosphate in a system simulating the natural aquatic environment," *Environ. Technol.*, **14**, 265-269, 1993.
13. E. Pelizzetti, C. Minero, E. Borgarello, L. Tinucci, N. Serpone, "Photocatalytic Activity and Selectivity of Titania Colloids and Particles Prepared by the sol-Gel Technique: Photooxidation of Phenol and Atrazine," *Langmuir*, **9**, 2995-3001, 1993.

14. H. Hidaka, J. Zhao, K. Nohara, K. Kitamura, Y. Satoh, E. Pelizzetti, and N. Serpone, "Photocatalyzed mineralization of non-ionic, cationic, and anionic surfactants at $\text{TiO}_2/\text{H}_2\text{O}$ interfaces," in *Photocatalytic Purification and Treatment of Water and Air*, D. F. Ollis, H. Al-Ekabi, Eds., Elsevier Science Publishers, Amsterdam, 1993, p.251-259.
15. E. Pelizzetti, C. Minero, H. Hidaka, and N. Serpone, "Photocatalytic processes for surfactant degradation," in *Photocatalytic Purification and Treatment of Water and Air*, D. F. Ollis, H. Al-Ekabi, Eds., Elsevier Science Publishers, Amsterdam, 1993, p.261-273
16. E. Borgarello, N. Serpone, G. Emu, R. Harris, E. Pelizzetti and C. Minero, "Light-induced reduction of rhodium(III) and palladium(II) on titanium dioxide dispersions and the selective photochemical separation and recovery of gold(III), platinum(IV), and rhodium(III) in chloride media," *Inorg. Chem.*, 25, 4499-4503, 1986.
17. N. Serpone, Y. K. Ah-you, T. P. Tran, R. Harris, E. Pelizzetti and H. Hidaka, "AM1 simulated sunlight photoreduction and elimination of Hg(II) and organic $\text{CH}_3\text{Hg(II)}$ chloride salts from aqueous suspensions of titanium dioxide," *Solar Energy*, 39(6), 491-498, 1987.
18. J. Sabate, M. A. Anderson, M. A. Aguado, J. Giménez, S. Cervera- March, C. G. Hill, Jr., "comparison of TiO_2 powder suspensions and TiO_2 ceramic membranes supported on glass as photocatalytic systems in the reduction of chromium(VI)," *J. Molecular Catalysis*, 71, 57-68, 1992.
19. Y. Inel and Durata Ertek (Hacı), "Photocatalytic deposition of bismuth(III) ions onto TiO_2 powder," *J. Chem. Soc. Faraday Trans.*, 89, 129-133, 1993.
20. M. R. Prairie, B. M. Stange, and L. R. Evans, " TiO_2 photocatalysis for the destruction of organics and the reduction of heavy metals," in *Photocatalytic Purification and Treatment of Water and Air*, D.F.Ollis, H. Al-Ekabi, Eds., Elsevier Science Publishers, Amsterdam, 1993, p.353-363.
21. J. H. Stacha and F. W. Pontius, "An overview of water treatment practices in the United States," *J. Am. Water Works Assoc.*, 76(10), 73-85, 1984.
22. D. M. Mackay, P. V. Roberts and J. A. Cherry, "Transport of organic contaminants in groundwater," *Environ. Sci. Technol.*, 19(5), 384-392, 1985.
23. Y. Cohen, "Organic pollutant transport," *Environ.Sci.Technol.*, 20(6), 538-544, 1986.
24. T. C. Voice and W. J. Weber Jr, "Sorption of hydrophobic compounds by sediments, soils and suspended solids-I," *Water Res.*, 17(10), 1433-1441, 1983.
25. A. Wold, "Photocatalytic properties of TiO_2 ," *Chem. Mater*, 5, 280-283, 1993.
26. D. F. Ollis, "Contaminant degradation in water," *Environ. Sci. Technol.*, 19(6), 480-484, 1985.
27. I. Izumi, W. W. Dunn, K. O. Willbourn, Fu-Ren F. Fan, and A. J. Bard, "Heterogeneous photocatalytic oxidation of hydrocarbons on platinized TiO_2 powders," *J. Phys. Chem.*, 84, 3207-3210, 1980.
- 28.. D. F. Ollis, Chen-Yung Hsiao, L. Budiman, and Chung-Li Lee, "Heterogeneous photoassisted catalysis: Conversions of perchloroethylene, dichloroethane, chloroacetic acids, and chlorobenzenes," *J. Catalysis*, 88, 89-96, 1984.

29. S. Yamagata, R. Baba, and A. Fujishima, "Photocatalytic decomposition of 2-ethoxyethanol on titanium dioxide," *Bull. Chem. Soc. Jpn.*, **62**, 1004-1010, 1989.
30. O. I. Micic, Y. Zhang, K. R. Cromack, A. D. Trifunac, and M. C. Thurnauer, "Photoinduced hole transfer from TiO_2 to methanol molecules in aqueous solution studied by electron Paramagnetic resonance," *J. Phys. Chem.*, **97**, 13284-13288, 1993.
31. M. Bideau, B. Claudel, L. Faure and H. Kazouan, "The photo-oxidation of propionic acid by oxygen in the presence of TiO_2 and dissolved copper ion," *J. Photochem. Photobiol. A: Chem.*, **67**, 337-348, 1992.
32. A. P. Davis, Oliver J. Hao, "Reactor dynamics in the evaluation of photocatalytic oxidation kinetics," *J. Catalysis*, **131**, 285-288, 1991.
33. D. Lawless, A. Res, R. Harris, N. Nerpone, C. Minero, E. Pelizzetti, H. Hidaka, "Removal of toxic metal from solutions by photocatalysis using irradiated platinized titanium dioxide: removal of lead," *La Chimica & L'industria*, **72**, 139-146, 1990.
34. G. Nagomi, "Investigation of photocatalytic decomposition mechanism of organic compounds on platinized semiconductor catalyst by rotating ring disk electrode technique," *J. Electrochem. Soc.*, **139**(12), 3415-3421, 1992.
35. B.-H. Chen, J. M. White, Lyle R. Brostrom, and M. L. Deviney, "Electron microscopy investigation of platinum supported on TiO_2 and TiO ," *J. Phys. Chem.*, **87**(13), 2423-2425, 1983.
36. H. Courbon, Jean-Marie Herrmann, and Pierre Pichat, "Effect of platinum deposits on oxygen adsorption and oxygen isotope exchange over variously pretreated, Ultraviolet-Illuminated powder TiO_2 ," *J. Phys. Chem.*, **88**(22), 5210-5214, 1984.
37. J.-M. Herrann, and Jean-Louis Mansot, "Analytical TEM study of the selective photocatalytic deposition of platinum on titania-silica mixtures and silica-supported titania," *J. Catalysis*, **121**, 340-348, 1990.
38. J. M. Kesselman, Gary A. Shreve, Michael R. Hoffmann, and Nathan S. Lewis, "Flux-matching conditions at TiO_2 photoelectrodes: Is interfacial electron transfer to O_2 rate-limiting in the TiO_2 -catalyzed photochemical degradation of organics?" *J. Phys. Chem.*, **98**, 13385-13395, 1994.
39. T. Hisanaga, Kenji Harada, and Keiichi Tanaka, "Photocatalytic degradation of organochlorine compounds in suspended TiO_2 ," *J. Photochem. Photobiol., A: Chem.*, **54**, 113-118, 1990.
40. J. Woning, and R. A. van Santen, "Electrostatic potential calculations on crystalline TiO_2 : The surface reducibility of rutile and anatase," *Chemical Physics Letters*, **101**(6), 541-547, 1983.
41. H.P. Maruska, A.K. Gosh, *Sol. Energy*, **20**, 443, 1978.
42. A. J. Bard, "Photoelectrochemistry and heterogeneous photocatalysis at semiconductors," *Journal of Photochemistry*, **10**, 59-75, 1979.
43. B. Kraeutler, and A.J. Bard, "Heterogeneous photocatalytic Preparation of supported catalysts. Photodeposition of platinum on TiO_2 powder and other substrates," *J.A.C.S.*,

100(13), 4317-4318, 1978.

44. W. J. Moore, "Physical Chemistry", Fifth edition, Longman Group Limited, Englewood Cliffs, 1972.

45. M. Boudart, and G. Djéga-Mariadassou, "Kinetics of Heterogeneous Catalytic Reactions," 1984.

46. P. W. Atkins, J. S. E. Holker, A. K. Holliday, *Heterogeneous Catalysis*, 1987.

47. I. M. Campbell, *Catalysis at Surfaces*, 1988, p37.

48. B. C. Gates, *Catalytic Chemistry*, 1992, p223.

49. J. Chen, D. F. Ollis, "Photocatalytic Oxidation of Alcohols and Organochlorides by O_2 on Suspended Pt/TiO_2 and Pd/TiO_2 ," preparation for publication.

50. C.-Y. Hsiao, Chung-Li Lee, and David F. Ollis, "Heterogeneous photocatalysis: Degradation of dilute solutions of dichloromethane, chloroform, and carbon tetrachloride with illuminated TiO_2 photocatalyst," *J. Catalysis*, **82**, 418-423, 1983.

51. T. Kobayashi, H. Yoneyama, and H. Tamura, "Role of Pt overlayers on TiO_2 electrodes in enhancement of the rate of cathodic processes," *J. Electrochem.Soc.: Electrochemical Science and Technology*, **130**(8), 1706-1711, 1983.

52. P. Pichat, J-M. Herrmann, J. Disdier, H. Courbon and M-N. Mozzanega, *Nouv. J. Chim.*, **5**, 627, 1981.

53. A.L. Pruden and D.F. Ollis, "Degradation of chloroform by photoassisted heterogeneous catalysis in dilute aqueous suspensions of titanium dioxide," *Environ. Sci. Technol.*, **17**, 628-631, 1983.

54. H. H. Willard, Lynne L. Merritt, JR., John A. Dean, and Frank A. Settle, Jr., *Instrumental Methods of Analysis*, Wadsworth Publishing Company, Belmont, California, 1981.

55. R. C. Weast, *Handbook of Chemistry and Physics*, 60th Edition, CRC Press, Inc., Boca Raton, Florida, 1980, B-104.

CHAPTER 4 THE ELIMINATION OF PHENOLS AND COD FROM INDUSTRIAL WASTEWATER BY EMPLOYING PHOTOCHEMICAL METHODS

This Chapter is based on:

1. Jian Chen, Wim Rulkens and Harry Bruning. "Photochemical Elimination of Phenol and COD in Industrial Wastewaters," *Water Science and Technology*, **35**(4), 231-231, 1997, and The International conference of Oxidation Technologies for Water and Wastewater Treatment, Goslar, Germany, May 12-15, 1996.
2. Jian Chen, Qixing Zhuang, and Jing-Yin Fu, "A Photochemical Method for Wastewater Treatment", China Patent ZL 88 1 06599.4, March 1995.
3. Jian Chen, Jing-Yin Fu, Qixing Zhuang, "An Improved Photochemical Method for Wastewater Treatment", China Patent Application 89 1 05630.0, August 1989.

THE ELIMINATION OF PHENOLS AND COD FROM INDUSTRIAL WASTEWATER BY EMPLOYING PHOTOCHEMICAL METHODS

4.1 INTRODUCTION

Photochemical methods, including photolysis and photocatalysis, are attractive environmental remediation technologies for the degradation and final mineralization of organic pollutants in an aquatic environment and the air, and have extensively been researched for many years^{1,2,3,4}. The photo-Fenton reaction (based on $UV/H_2O_2/Fe^{2+}$) is an example of photolysis and has been studied in detail⁵. It promises to become an important pathway for the treatment of wastewater contaminated with various organic compounds^{6,7}. Heterogeneous photocatalysis, which uses various semiconductor photocatalysts such as titanium dioxide, zinc oxide and ferric oxide, is also a feasible method for the detoxification of water containing various organic and inorganic pollutants, such as halogenated organic compounds^{8,9,10}, insecticides^{11,12,13}, surfactants^{14,15}, and heavy metals^{16,17,18}.

In contrast to photocatalytic methods that use a catalyst in suspension, homogeneous photolysis methods do not require separation of powder catalysts after treatment. For effective treatment, photolysis requires short wavelengths of high-energy UV light and chemical oxidants such as hydrogen peroxide and ozone. However, photocatalysis can use long wavelengths of lower energy near UV and visible light, such as sunlight, for effective elimination of pollutants^{19,20,21} without extra chemical oxidants. If a photocatalyst is fixed on a supporter, it does not have to be separated as a slurry from the process water, but so far this type of process has shown less photocatalytic activity (about twice as slow) than suspension systems²².

A sophisticated combination of methods for homogeneous photolysis and photocatalysis can raise the treatment efficiency, because it promotes the utilization of sunlight or the light of lamps at various wavelengths in the presence of H_2O_2 and a photocatalyst. A combined system may consist of a photocatalyst together with high-energy UV light, or together with H_2O_2 or even a photo-Fenton reaction. Such systems can simultaneously photocatalyze and photolyze toxic substrates. Some studies report the use of a combination of photolysis and photocatalysis for wastewater treatment^{23, 24, 25}.

Many wastewaters are characterized by the presence of phenol and its derivatives. These substances are present in large quantities in wastewaters from oil refining, pharmacy, electroplating, paper, coking and iron-smelting industry, etc. Some industrial wastewaters contain various substituted phenols and have a COD of several thousands of ppm. Typical components of such industrial wastewaters are listed in Table 4.1.

Table 4.1. Typical components of some industrial wastewaters

Type of wastewater	pH	Pollutants in wastewater		
		Phenols (ppm)	COD (ppm)	Other components
Phenolic resin	1	400	~	Pink colour, resin, formaldehyde, Cu^{2+} , HCl
Petroleum refining	7	50	500	No colour, organic sulphide
Naphthenic acid	6	12	1,300	No colour, organic sulphide
Dry distillation of shale oil	8	200	16,000	Dark brown colour, aromatics, cyanide, hydrocarbons, etc.

The wastewaters from industrial sources shown in Table 4.1 normally contain many toxic compounds in addition to phenols. In wastewater containing phenolic resins, these resins are pink, soluble and of low molecular weight. The COD of wastewaters from petroleum refining and the recovery of naphthenic acid is attributed mainly to hydrocarbons and organic sulphide compounds. Wastewater from the dry distillation of shale oil is a very complicated type of wastewater with a dark brown colour and a COD ranging from ~7,000 to ~24,000 ppm. In addition to phenols of several hundreds of ppm, it contains large quantities of various organic compounds, such as nitro- and sulpho-organics, aromatics and hydrocarbons, as well as inorganic compounds (*e.g.*, cyanides).

The treatment of phenol containing wastewater to a harmless level of 0.5 ppm phenol is a difficult process for many chemical and biological methods because of the high solubility and stability of phenols²⁶. There are many reports on photolysis^{27,28} and photocatalysis^{29,30,31} for the treatment of phenol-containing wastewaters. Most experiments of the photocatalytic treatment of phenol-containing wastewaters use slurry TiO_2 as a photocatalyst, because until now it has proven to be the most efficient photocatalyst and it is also nontoxic. In practice, however, the problem of how to separate suspended particles from wastewater still has to be solved. There are some reports on investigations carried out into the photoactivity of other materials, such as ZnO , WO_3 , CdS and Fe_2O_3 , which also proved to affect various pollutants^{32,33,34}.

The PB report from the American government³⁵ discusses the possibility of applying photocatalytic oxidation for the remediation and recovery of several wastewaters. The report details the use of semiconductors consisting of titanium dioxide, zinc oxide and ferric oxide as photocatalysts. By using titanium dioxide and zinc oxide, photocatalytic degradation of 30% to 50% of chloroform, dimethylamine, methanol and some phenolic and nitric compounds

(except amine) could be attained after six hours of illumination. However, ferric oxide did not show any photoactivity in relation to these compounds.

Another PB report from the American government³⁶ discusses the photocatalytic oxidation of organic pollutants. From this report, which details the use of non-oxide soluble inorganic compounds as homogeneous photocatalysts, it appears that ferrous nitrate showed the highest photocatalytic activity during the treatment of phenol.

Hokayisu and Sawujiyi³⁷ report the photocatalytic oxidation of phenol using the semiconductor zinc oxide. It was observed that 50 ppm of phenol in an aerated solution decreased to a level of 3.5 ppm when the solution was illuminated for three hours using a 400-W mercury lamp.

Izumi and Ohnishi³⁸ report the photocatalytic degradation of phenol and 2, 4, 6-trichlorophenol (TCE) using a semiconductor photocatalyst. When 15 mg of 12% Pt/TiO₂ was suspended in a 3-ml solution containing 50 ppm of TCE and this solution was illuminated using a 500-W mercury lamp, the TCE was degraded by 90% in 2.5 minutes, and by 95% in 5 minutes. However, when a solution containing 150 or 300 ppm of TCE was used, only 70% of the pollutant was degraded in 3 hours. When 15 mg of native TiO₂ was suspended in a 3-ml solution, 90% of the TCE in a solution with a TCE concentration of 50 ppm was degraded in 3 hours. Under the same conditions, 95% of the phenol contained in a solution with a phenol concentration of 50 ppm was degraded in 5 minutes, but only 92% of the phenol contained in a solution with a phenol concentration of 94 ppm was degraded in 3 hours.

Okamoto and Yamamoto *et al.*³¹ report heterogeneous photocatalytic degradation of phenol in the presence of TiO₂, ZnO and Fe₂O₃ as photocatalysts. Pure Fe₂O₃ did not show any photocatalytic activity. The best result was obtained by using anatase TiO₂ pretreated in hydrogen gas at 520 °C for six hours. By using 2.5 grams of this TiO₂ in a 400-ml solution, phenol was degraded to 10 ppm in a solution with a phenol concentration of 94 ppm, when the solution was illuminated for half an hour with a 100-W mercury lamp. The use of ZnO resulted in phenol degradation to 2 ppm in a solution with a phenol concentration of 94 ppm, when the solution was illuminated for one hour, but at the same time ZnO decomposed proportionally to the quantity of phenol degraded.

Peral and Doménech *et al.*³⁹ report light-induced oxidation of phenol using ZnO powder as a photocatalyst, during which 95% of the phenol contained in a solution with a phenol concentration of 9 ppm was removed, when the solution was illuminated for 10 minutes with UV light. At the same time, ZnO dissolved.

L. Palmisano *et al.*^{32,40} report the use of titanium photocatalysts for the photodegradation of acetic acid and phenol, in which various semiconductor photocatalysts were employed to

degrade a 90-ppm solution of phenol at a pH of 3, 6 and 13 using a 1500-W xenon lamp for illumination. Pure ferric oxide showed a higher photocatalytic activity during the oxidation of acetic acid in aerated systems, but did not show photoactivity during phenol oxidation in deaerated systems.

All experiments mentioned in the above reports during which phenol and other organic compounds were degraded photocatalytically were carried out on a laboratory scale with artificial solutions of pure compounds in water. The photocatalyst with the highest activity was 12% Pt/TiO₂ obtained by pretreatment for a long time at a high temperature in hydrogen gas. Ferric oxide did not show any photoactivity in relation to phenols.

Photolytic or photocatalytic oxidation of phenol-containing wastewater requires oxygen and is pH-dependent. In the acidic range, it is pH-dependent only in a very narrow pH range, namely $\sim 3.5 \pm 0.5$, where it shows a very high degradation rate⁴¹. The degradation rate is slowest around neutral pH and increases gradually with increasing pH. To obtain a suitable rate in practice, adjusting the reaction pH to the alkaline range is more convenient than doing so to the narrow acidic range of $\sim 3.5 \pm 0.5$.

In this chapter, ferric compounds (especially tri-iron tetroxide) and aluminium oxide are discussed as photocatalysts. Because iron-containing compounds have magnetic properties, the suspended catalyst powder can be recovered from wastewaters by employing magnetic methods. From an economic point of view, the use of related ores as alternatives to pure compounds is very interesting. The use of magnetite as a ferric photocatalyst is a good choice, because its main component is magnetic tri-iron tetroxide. With respect to the use of aluminium oxide as a photocatalyst, it is interesting to look at the possibilities for using its ores bauxite and kaolin as photocatalysts. In our study, the effect of combining photolysis (*i.e.*, the use of high-energy UV light) and photocatalysis (*i.e.*, the use of magnetite and dialuminium trioxide as photocatalysts) was investigated for the treatment of various types of industrial wastewaters. Calcium oxide was chosen as a promoter of photocatalysts to control the reaction pH and to deposit the final gas product (CO₂) as a solid (CaCO₃). A special method that combines photocatalysis and the photo-Fenton reaction was investigated, in which a double-function compound was used for the first time. This compound (ferric oxide) can act both as a photocatalyst and as a solidified Fenton reagent. This combination is expected to increase the efficiency of photochemical systems in the elimination of various organic pollutants.

4.2 EXPERIMENTS CARRIED OUT WITH PHOTOCATALYSTS

4.2.1 Introduction

Three combined methods of heterogeneous photochemistry in aerated systems were used to treat phenol-containing wastewater: 1. UV light ($313 \leq \lambda \leq 456$ nm) and the use of a photocatalyst consisting of a ferric or aluminium compound under alkaline conditions. In such a system, phenol can be degraded by direct photolysis and by photocatalysis; 2. UV light ($313 \leq \lambda \leq 456$ nm) and the use of a photocatalyst consisting of a ferric or aluminium compound and calcium oxide. The latter was used as a promoter, for adjusting the reaction pH to around 12 (and maintaining it at this level), and for removing (*i.e.*, precipitating) the produced CO_2 from the liquid phase; 3. UV light ($313 \leq \lambda \leq 456$ nm) combined with the use of a solid ferric compound as a photocatalyst, calcium oxide as a promoter, and hydrogen peroxide as an oxidant. In this system, solid ferric oxides act either as a photocatalyst or as a solidified Fenton reagent, and phenol or other organic pollutants would be degraded by the combination of direct photolysis, photocatalysis and the photo-Fenton reaction.

4.2.2 Experimental procedure for a heterogeneous system of UV/ferric or aluminium compound photocatalyst

In general, experiments can be carried out as follows. The pH of a solution of pure phenol in water (≤ 300 ppm) or phenol-containing industrial wastewater (30 - 400 ppm of phenol) is adjusted to alkaline conditions using sodium hydroxide. After filtering to remove solids (in the case of industrial wastewater), the sample is placed in a photoreactor ($\phi 30 \times 170$ mm) (Fig.4.1). A photocatalyst consisting of a ferric or aluminium compound is added to the solution. Air is sparged to suspend the catalyst powder and supply the oxygen required. The wastewater is illuminated using a UV lamp. After being illuminated for a period of between 30 minutes and 4 hours, the solution is centrifuged. The total concentration of volatile phenols, including substitutive phenols, in the supernatant is analyzed directly by colorimetric analysis using 4-AAP (4-aminoantipyrine) at 500 nm. In the case of coloured industrial wastewaters, samples have to be pretreated by distillation to remove all volatile phenols before analysis. COD is analyzed by potassium dichromate oxidation. Detailed information on the procedures followed for the analysis of phenol and COD can be found in the Standard Methods for the examination of water and wastewater⁴².

An example of a UV/photocatalyst experiment is as follows. After being filtered (using a paper filter), 60 ml of wastewater from a phenol resin factory (pH = 1, the wastewater contained 400 ppm of phenol as well as soluble phenol resins of low molecular weight, formaldehyde, Cu^{2+} , HCl, etc.) was placed in a quartz photoreactor with a cooling-water thimble (Fig.4.1). The wastewater pH was adjusted to 13.7 using sodium hydroxide. 400 mg of 320-mesh magnetite

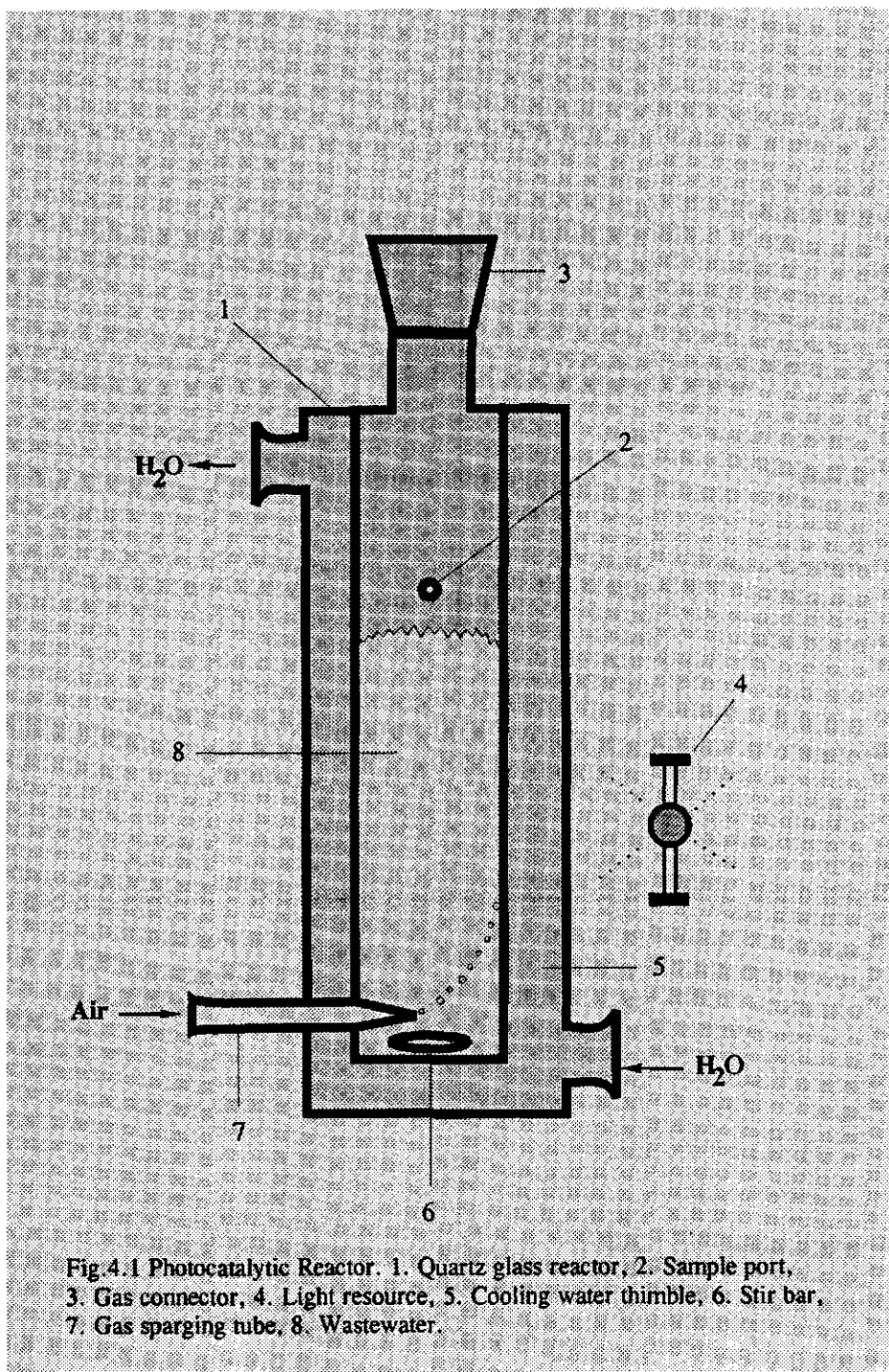


Fig.4.1 Photocatalytic Reactor. 1. Quartz glass reactor, 2. Sample port, 3. Gas connector, 4. Light resource, 5. Cooling water thimble, 6. Stir bar, 7. Gas sparging tube, 8. Wastewater.

particles extracted from beach sand using a magnetic separator were added to the wastewater. The main component in magnetite is tri-iron tetroxide. Air (1.3 L/min.) was sparged into the wastewater to suspend the magnetite powder. The wastewater was illuminated using a 200-W mercury lamp ($313 \leq \lambda \leq 456$ nm) mounted at a distance of 5 cm from the reactor wall. After illumination for one hour, a sample of 3 ml was taken and centrifuged at 4,000 rpm for 5 minutes. The supernatant was distilled in order to remove volatile phenols, and then analyzed by colorimetric analysis using 4-AAP.

4.2.3 Experimental procedure for a heterogeneous system of UV/ferric or aluminium compound photocatalyst/calcium oxide or hydroxide as a promoter

In general, experiments can be carried out as follows. The required quantities of a promoter and photocatalyst powder consisting of a ferric or aluminium compound are suspended in wastewater by mechanical stirring and air bubbling. The photochemical promoter used is a calcium compound: calcium oxide (CaO) or calcium hydroxide ($\text{Ca}(\text{OH})_2$). The weight ratio between promoter and photocatalyst may vary from 1/10 to 4/1, and the mass quantity of promoter present in the wastewater should be at least as high as that of the wastewater COD. The photocatalyst and promoter powder should be suspended completely by air bubbling. The air flow rate may vary from 500 to 1,500 ml/min. The photochemical reactions may be carried out at ambient temperature and normal pressure (ambient $\leq T \leq 100$ °C, $P = 1$ atm.), or at a high temperature and high pressure ($T \geq 100$ °C, $P \geq 1$ atm.). The other experimental conditions are similar to those detailed in § 4.2.2.

As an example of a UV/photocatalyst/promoter experiment, 60 ml of filtered wastewater from an oil refinery (containing 40 ppm of phenol, 1,500 ppm of COD and such compounds as cyanide and sulphide) were put into a quartz photoreactor with a cooling-water thimble. 400 mg of 250 to 300 mesh magnetite and 300 mg of CaO (as a promoter) were added to this wastewater. The wastewater pH remained at 12 because of the dissolution of CaO. Air (1.3 L/min.) was sparged into the wastewater in order to suspend the magnetite and promoter powder. The wastewater was illuminated using a 200-W mercury lamp ($313 \leq \lambda \leq 456$ nm) mounted at a distance of 5 cm from the reactor wall. After illumination, the wastewater was filtered (using a paper filter). A certain quantity of clarified solution was distilled and then analyzed. The other conditions were similar to those detailed in § 4.2.2. For the control experiment without promoter, a similar quantity of wastewater (60 ml) was put into the reactor. In this case, the pH was adjusted to 13.4 using sodium hydroxide. All other conditions were similar to those detailed in § 4.2.2.

As another example, 20 ml of wastewater from the dry distillation of shale oil were put into the reactor and diluted to 60 ml. The diluted wastewater contained 63 ppm of phenol, 2500 ppm of COD, cyanide, sulphide, and many other organic compounds. 300 mg of magnetite and

600 mg of CaO as a promoter were added to this wastewater, and the wastewater pH was adjusted to 12 and remained at this level because of the dissolution of CaO. All other conditions were similar to those detailed in § 4.2.2.

4.2.4 Experimental procedure for a heterogeneous system of UV/ferric compound photocatalysts/promoter/ hydrogen peroxide

In general, experiments can be carried out as follows. The required quantities of the ferric compounds used as photocatalysts and as solidified Fenton-reagents are either suspended in water by mechanical stirring and air sparging, or mounted on a supporter in water. A certain quantity of the calcium compound used as a photochemical promoter and hydrogen peroxide are added to this water. The mass quantity of hydrogen peroxide present in the water is 0.1 to 5 times higher than that of the pollutants present in the water. These pollutants include various organic and inorganic compounds, such as phenols, halo-, nitric- and phospho-organics, aromatic compounds, and cyanides. The ferric compounds include ferric oxide, ferrous oxide, tri-iron tetroxide, ferrous oxide, ferrous sulphide, etc. These compounds can be either natural ores such as magnetite, hematite and iron pyrite, or manmade pure compounds and mixtures containing ferric compounds. The weight ratio between the photocatalyst or photo Fenton-reagent and the wastewater may vary from 1/1000 to 20/1000. The wastewater pH should be made alkaline or close to neutral. The photochemical promoter used is a calcium compound: calcium oxide (CaO) or calcium hydroxide ($\text{Ca}(\text{OH})_2$). The weight ratio between the promoter and photocatalyst may vary from 1/10 to 4/1, and the quantity of promoter should be at least as high as that of the wastewater COD. The promoter may be either first mixed with the photocatalyst and then added to the water, or directly added to the water. The air flow rate may vary from 500 to 1,500 ml/min. The photochemical reactions are carried out at ambient temperature and normal pressure (ambient $\leq T \leq 100^\circ\text{C}$, $P = 1 \text{ atm.}$), at a high temperature and high pressure ($T \geq 100^\circ\text{C}$, $P \geq 1 \text{ atm.}$), or in other combinations. The illumination resource consists of either sunlight or various lamps emitting ultraviolet light, near-ultra-violet light or visible light. The light resource should be as close to the water as possible.

As an example of a UV/photocatalyst/promoter/hydrogen-peroxide experiment, 60 ml of wastewater from an oil refinery (containing 40 ppm of phenol, 1,500 ppm of COD and such compounds as cyanide and sulphide) were put into a quartz photoreactor with a cooling-water thimble. 100 mg of 30% hydrogen peroxide and 400 mg of 250 to 300 mesh magnetite particles (the main component is tri-iron tetroxide) and 300 mg of CaO (as a promoter) were added to this wastewater. Air was sparged into the wastewater (1.3 L/min.) in order to suspend the magnetite and promoter powder. The wastewater was illuminated using a 200-W mercury lamp ($313 \leq \lambda \leq 456 \text{ nm}$) mounted at a distance of 5 cm from the reactor wall. After illumination, the wastewater was filtered (using a paper filter), distilled, and then analyzed.

4.2.5 Results and Discussion

4.2.5.1 Elimination of phenols and COD from industrial wastewater by a heterogeneous system of UV/photocatalyst of Fe_3O_4 or Al_2O_3

Phenols contained in the types of industrial wastewater listed in Table 4.1 can be effectively eliminated by the combination of high-energy UV and the photocatalyst of magnetite powder or aluminum oxide ($\gamma\text{-Al}_2\text{O}_3$). This may be the result of the combined effect of photolysis and photocatalysis. The experimental results are summarized in Table 4.2. The wastewaters of type 1(a), 1(b), 4(a) and 4(b) were executed under the same conditions, except for illumination time. Assuming a first-order reaction ($C/C_0 = \exp(-kt)$), where C_0 is the initial concentration, C the concentration at time t , and k a reaction rate constant, the reaction constant $k_{1(a)} = 1.5 \text{ h}^{-1}$ and reaction constant $k_{1(b)} = 2.4 \text{ h}^{-1}$. The difference of 46% between $k_{1(a)}$ and $k_{1(b)}$ may be due to the various competitive photoreactions occurring in industrial wastewaters. The difference of 26% between $k_{4(a)} = 4.6 \text{ h}^{-1}$ and $k_{4(b)} = 6.0 \text{ h}^{-1}$ in the case of a pure phenol solution may be due to either the combined effect of photocatalytic and photolytic reactions, or experimental errors.

The use of high-energy UV light not only induces photocatalytic elimination of phenols and other organic compounds at photocatalyst surfaces, but also photolyzes them directly. Phenol can be eliminated more effectively by using the combination of UV light and aluminium oxide than by using UV light and ferric oxide because of the higher band gap of aluminium oxide. The data given in Table 4.2 also show that the initial alkaline pH of solutions strongly affects the elimination of phenols. The higher the initial pH, the faster the elimination of phenols. It should be noted that during the reaction the pH will decrease as a result of the production of higher oxidative products (organic acids) and CO_2 .

During the experiments mentioned in Table 4.2, the effects of pH, catalysts and illumination time on the elimination of phenols were studied. During separate experiments in which the same wastewaters were used, both phenol elimination and COD elimination were studied. The data given in Table 4.3 show that ferric oxides (magnetite) used as a photocatalyst can to a large extent eliminate organic compounds (in terms of COD) other than phenol from industrial wastewaters. A COD concentration of 2,500 ppm in wastewater from the dry distillation of shale oil can be reduced by 62%, when the wastewater is illuminated for one hour. It is very probable that the pollutants are finally mineralized to carbon dioxide and water.

Table 4.2. The photochemical elimination of phenols from industrial wastewaters by a combined method of UV/Photocatalyst. 1: phenolic resin, 2: petroleum refining, 3: dry distillation of shale oil, 4: pure phenol in water. The experimental conditions are given in § 4.2.2.

Type of industrial wastewater	Initial solution pH	Concentration of phenols Before illumination (ppm)	Concentration of phenols After illumination (ppm)	Illumination time (hours)	Photocatalyst
1(a)	13.7	400	90	1	magnetite
1(b)	13.7	400	0.3	3	magnetite
2	13	40	0.2	2	magnetite
2	12.4	40	0.8	2	magnetite
2	13	40	0.2	1	$\gamma\text{-Al}_2\text{O}_3$
3	12.6	8	0.3	2	magnetite
3	13.7	8	0	1	magnetite
4(a)	13	30	0.3	1	$\gamma\text{-Al}_2\text{O}_3$
4(b)	13	6	0.3	0.5	$\gamma\text{-Al}_2\text{O}_3$
4	13.3	300	1.3	3	$\gamma\text{-Al}_2\text{O}_3$
4	13.3	300	2	3	magnetite

Table 4.3. Photochemical elimination of phenols and COD from industrial wastewaters by a combined method of UV/Magnetite. Initial pH = 13.3. The experimental conditions are given in § 4.2.2.

Type of wastewater	Initial concentration (ppm)		Treatment time (hours)	Elimination efficiency (%)	
	[phenols]	[COD]		Phenol	COD
Phenolic resin	40	~	2	99	~
Dry distillation of	63	2,500	1	52	62
Petroleum refining	35	600	4	100	70
Petroleum refining	40	280	4	100	70
Naphthenic acid	~	1,300	4	~	68

4.2.5.2 Elimination of phenols and COD from industrial wastewater by a heterogeneous system of UV/photocatalyst of Fe_3O_4 or Al_2O_3 /promoter

The effect of the addition of fine-powdered calcium oxide to wastewater as a pH adjuster rather than sodium hydroxide on the promotion of the photocatalytic activity of the photocatalysts magnetite and aluminium oxide was investigated. The results given in Table 4.4 show that calcium oxide clearly promotes the elimination of phenols. In various wastewaters, complete (100%) elimination of phenols can be achieved. One of the advantages of adding calcium oxide is that an over dose of calcium oxide in wastewater prevents a decrease in solution pH with illumination time, because this substance is continuously dissolving during the photodegradation process. Another advantage of the use of this substance is its lower cost compared with the cost of sodium hydroxide.

Table 4.4. The effect of the use of calcium oxide for promoting the photocatalytic elimination of phenol in industrial wastewaters, when a photocatalyst and UV light are used. (a) is $\gamma\text{-Al}_2\text{O}_3$, (b) is magnetite. The experimental conditions are given in § 4.2.3.

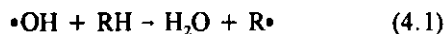
Type of wastewater	Promoter CaO (mg)	Photocatalyst (mg)	Initial Solution pH	Concentration of phenols before illumination (ppm)	Concentration of phenols after illumination (ppm)
Phenol	0	400 (a)	13*)	30	0.3 (1 hr.)
Phenol solution	300	400 (a)	12	30	0 (1 hr.)
Petroleum refining	0	400 (b)	13.4*)	40	13 (1 hr.)
Petroleum refining	300	400 (b)	12	40	0 (1 hr.)
Dry distillation of shale oil	600	300 (b)	12	63	0 (2 hr.)

*) In these cases, sodium hydroxide was used

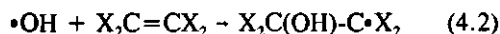
4.2.5.3 Elimination of phenols and COD from industrial wastewater by a heterogeneous system of UV/photocatalyst of Fe_3O_4 /promoter/hydrogen peroxide

The combination of photocatalysis, employing suspended ferric oxide as a photocatalyst, and the photo-Fenton reaction can circumvent the chemical limitations of hydroxyl radical reactions. The photo-Fenton reaction (*i.e.*, hydrogen peroxide oxidation with an iron catalyst such as ferrous chloride) is one of the most promising photochemical methods for practical application^{5,27}. The hydroxyl radical produced during this reaction is one of the most reactive radicals known. However, this method introduces inorganic ions (ferric, chloride) into water, and what is even more important, it has proved to be not yet suitable for the treatment of some organic pollutants such as organochlorides (poly-, or perfluorinated alkanes). This is due to the chemical limitations of hydroxyl radical reactions (*e.g.*, the reactions of $h\nu/\text{H}_2\text{O}_2$, $h\nu/\text{H}_2\text{O}_2/\text{Fe}$ or $h\nu/\text{O}_3$), as described below. Organic pollutants can be oxidized by hydroxyl radicals according to one of the following three mechanisms^{43,44}:

Hydrogen abstraction:

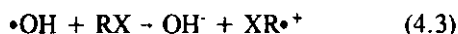


Addition of a hydroxyl radical:

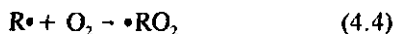


where $\text{X} = \text{Cl}, \text{F}$.

Electron transfer:



The capturing of C-centred radicals by dissolved molecular oxygen, resulting in the production of key intermediates of organic peroxy radicals (Eq.4.4) is essential to accelerate the oxidative degradation and mineralization of organic substrates to CO_2 ⁴⁵.



Hydroxyl radical reactions have a disadvantage in that hydroxyl radicals cannot generate C-centred radicals by halogen abstraction, and produce unsaturated alkenes. This is because of the strong negative inductive effects of poly-halogenated hydrocarbons preventing electrophilic addition. As a result of such chemical limitations, poly-halogenated hydrocarbons cannot be oxidized by means of hydroxyl radical reactions.

However, such chemical limitations do not apply in the case of photocatalytic reactions. Many experiments have shown that such halogenated compounds can be very efficiently degraded by photocatalytic oxidation. Employing the method of combining photolysis, the photo-Fenton reaction and photocatalysis can circumvent these problems and raise the treatment efficiency by promoting light absorption at various wavelengths. The use of magnetic ferric oxide as a photocatalyst is a good choice, because this substance can be easily separated from water or can act as a solidified Fenton reagent, thus reducing the quantity of inorganic ions in solution. Table 4.5 gives the first experimental data available on phenol elimination attained by employing the combined method of UV/photocatalyst/promoter/hydrogen peroxide. It was observed that by adding H_2O_2 the minimum time required for complete reduction of all the phenol present in the solution decreased from about one hour to about 20 minutes.

Table 4.5. The results of using UV/magnetite/promoter/ H_2O_2 for the photocatalytic elimination of phenol in industrial wastewater. The experimental conditions are given in § 4.2.4.

Type of wastewater	Photocatalyst magnetite (mg)	Promoter CaO (mg)	Solution of 30% H_2O_2 (mg)	Initial solution pH	Concentration of phenols before illumination (ppm)	Concentration of phenols after illumination (ppm)
Petroleum refining	400	300	0	12	40	~0* (1 hour)
Petroleum refining	400	300	100	12	40	~0 (20 minutes)

*: ~0 ppm means that the phenol concentration had decreased to an undetectable level after a certain period of illumination.

4.3 EXPERIMENTS USING PHOTOLYSIS

4.3.1 Introduction

The following homogeneous photochemical systems for the treatment of an aqueous solution of pure phenol under aerated conditions were investigated: 1. Photolysis using UV light ($313 \leq \lambda \leq 456$ nm). In this system, phenol is degraded by direct photolysis; 2. UV/ H_2O_2 system. In this system, UV not only photolyzes phenol directly but also decomposes hydrogen peroxide to form more hydroxyl radicals, thus indirectly accelerating the phenol decomposition; 3. UV/ $FeCl_3/Fe^{2+}$ system (Fe^{2+} in the form of $Fe(NH_4)_2(SO_4)_2$). In this system, ferric chlorides adsorb UV light to produce radicals; next, phenol is oxidized in solution; 4. UV/ $H_2O_2/FeCl_3$ system (photo-Fenton reaction). In this system, UV and the Fenton reagent associate and

catalyze simultaneously the decomposition of hydrogen peroxide resulting in more hydroxyl radicals, which may greatly increase the rate of phenol degradation.

4.3.2 Experimental procedures of a homogeneous photolytic system

Except where indicated otherwise in the text or graphs, the procedures followed and conditions existing during the experiments were as follow: Exactly 60 ml of an aqueous solution of pure phenol (phenol concentration ≤ 80 ppm) were put into the photoreactor (Fig.4.1). The pH was adjusted using sodium hydroxide or hydrochloric acid, if necessary. A certain quantity of ferric chloride and/or hydrogen peroxide was added to the solution. Air was sparged to supply the oxygen required. The solution was illuminated using a UV lamp (the same as the one mentioned in § 4.2.2). The solution was kept at ambient temperature. After illumination for 5 or 10 minutes, samples were taken from the solution and analyzed directly by colorimetric analysis using 4-AAP (4-aminoantipyrine) at 500 nm. Detailed information on the procedures followed for analysing phenol can be found in the Standard Methods for the examination of water and wastewater⁴².

4.3.3 Results and Discussion

4.3.3.1 UV photolytic degradation of phenol

The photolytic degradation of phenol (initial concentration $C_0 = 25$ ppm) in an aerated solution with an initial pH of 3.5 and using UV light for illumination is given as a function of time in Fig.4.2. The figure shows an apparent first-order reaction-rate relationship given by:

$$\gamma = k_{app} [\text{Phenol}] \quad (4.5)$$

where γ is the reaction rate and k_{app} the apparent reaction rate constant. The degradation of phenol is strongly pH-dependent. Apparent rate constant k_{app} versus pH is given in Fig.4.3. The curve shown in Fig.4.3 has a sharp peak around pH = 3.5. Above pH = 9, k_{app} increases with increasing pH. This proves that the photolytic degradation of phenol is strongly pH-dependent. The degradation rate constant is highest in a narrow pH range, namely pH = ~3.5.

4.3.3.2 UV/H₂O₂ destruction of phenol

The combination of UV and a small quantity of H₂O₂ strongly raises the efficiency of phenol degradation under aerated conditions. Fig.4.4 gives the photolytic conversion rate of a solution with an initial phenol concentration C_0 of 25 ppm as a function of the concentration of H₂O₂;

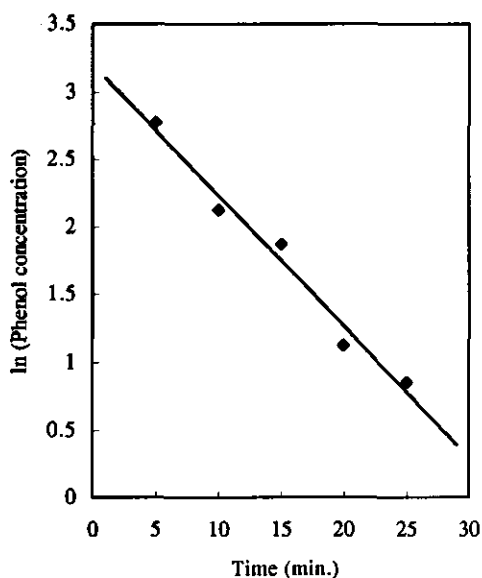


Fig.4.2 The relationship between phenol concentration and illumination time. Initial concentration of phenol $C_0=25$ ppm, Initial pH = 3.5

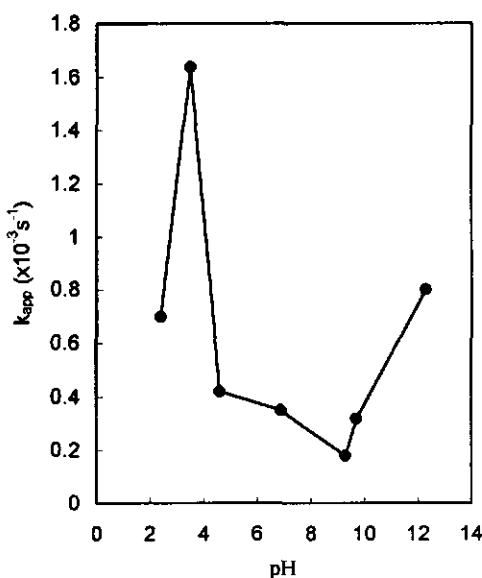


Fig.4.3 The apparent rate constants of phenol photolysis as a function of initial solution pH. Initial concentration of phenol $C_0=25$ ppm. Illumination time is 10 minutes.

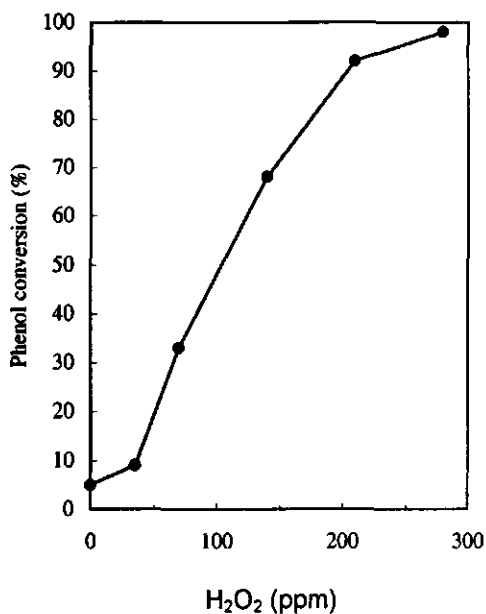


Fig. 4.4 The photolytic conversion rate of a phenol solution as a function of H_2O_2 concentration. Initial concentration of phenol $C_0=25$ ppm. Illumination time is 5 minutes. Initial pH = 12.2.

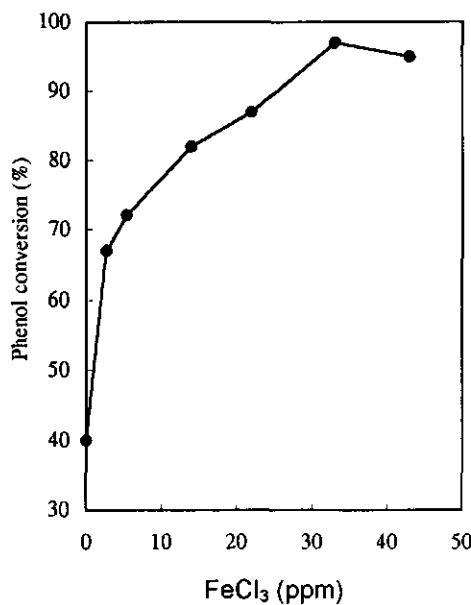


Fig.4.5 The photolytic conversion rate of a phenol solution as a function of $FeCl_3$ concentration. Initial concentration of phenol $C_0=25$ ppm. Illumination time is 10 minutes. Initial pH \approx 3.5.

the initial pH was 12.2 and the UV illumination time was 5 minutes. The figure shows clearly that, at an illumination time of 5 minutes and without the addition of H_2O_2 , only 5% of the phenol is eliminated. However, the elimination of phenol can be increased to 95% by adding 200 ppm of H_2O_2 to the solution. However, at a H_2O_2 concentration in solution of less than 35 ppm, hardly any increase in phenol conversion occurs.

4.3.3.3 UV/ FeCl_3 / Fe^{2+} destruction of phenol

FeCl_3 has an absorption peak in the range of 300-400 nm. It is photolyzed and produces Cl^\bullet and $^\bullet\text{OH}$ radicals under the illumination of UV light (see § 1.1.1.3). Fig. 4.5 gives the photolytic conversion rate of phenol in a solution as a function of the concentration of FeCl_3 ; the initial phenol concentration was 25 ppm, the initial pH 3.5, and the UV illumination time 10 minutes. The figure shows clearly that FeCl_3 accelerates the photodegradation of phenol. In addition, experimentally it was found that Fe^{2+} (in the form of $\text{Fe}(\text{NH}_4)_2(\text{SO}_4)_2$) raises the efficiency of UV/ FeCl_3 during the degradation of phenol. For example, 2.3 ppm of Fe^{2+} added to a solution containing 25 ppm of phenol and 8.1 ppm of FeCl_3 accelerates the degradation of phenol from 72% to 92%, as shown in Table 4.6.

Table 4.6. The promotive effect of Fe^{2+} in a UV/ FeCl_3 system for phenol elimination. Illumination time = 10 minutes, Initial pH = 3.5.

Initial phenol concentration (ppm)	FeCl_3 concentration (ppm)	Fe^{2+} concentration (ppm)	Phenol concentration after 10 min. (ppm)	Phenol conversion (%)
25	8.1	0	7	72
25	8.1	1.1	5	80
25	8.1	2.3	2	92

4.3.3.4 UV/ H_2O_2 / FeCl_3 destruction of phenol

The decomposition of hydrogen peroxide into hydroxyl radicals, which can activate the degradation of organic compounds in solution, will occur slowly if no photocatalyst or UV irradiation is applied. The introduction of a Fenton reagent (Fe^{2+} or Fe^{3+}) into the solution will catalyze the decomposition of hydrogen peroxide. Certain wavelength UV light also accelerates this process. Table 4.7 gives the photolytic conversion rate for phenol decomposition in a

solution with an initial phenol concentration of 25 ppm, an initial pH of 3.5, and a UV illumination time of 10 minutes. This table shows that all the phenol present in the solution was degraded after 10 minutes of UV illumination at an FeCl_3 concentration of 8.1 ppm and an H_2O_2 concentration of 70 ppm. This is much higher than the 72% conversion obtained in a UV/ FeCl_3 system. It is expected that it will also be much higher than the degree of conversion obtained in a UV/ H_2O_2 system (Fig. 4.4), even though the initial pH values are different. Therefore, the combination of high-energy UV with Fenton reaction will be the best photochemical method for phenol degradation, as well as for other organic compounds.

Table 4.7. The results of phenol elimination in a UV/ H_2O_2 / FeCl_3 system. Illumination time = 10 minutes, initial pH = 3.5.

Initial phenol concentration (ppm)	H_2O_2 concentration (ppm)	FeCl_3 concentration (ppm)	Phenol concentration after 10 min. (ppm)	Phenol conversion (%)
25	0	8.1	7	72
25	70	8.1	~0	100

4.4 CONCLUSIONS

1. Phenols and other organic pollutants (in terms of COD) present in industrial wastewaters can be eliminated efficiently by a combination of UV photolysis and heterogeneous photocatalysis using magnetite or aluminium oxide.
2. An alkaline reaction pH is required for the effective elimination of phenols and COD in above-mentioned industrial wastewaters.
3. Powdery calcium oxide or calcium hydroxide may be used to promote the elimination of phenols at high pH values. Compared with sodium hydroxide, calcium oxide is cheap and removes the final oxidation product (CO_2) from wastewater via the precipitation of CaCO_3 .
4. Combining the use of magnetite as a photocatalyst and also as a solidified Fenton reagent forms a sophisticated photochemical method for combining photocatalysis with the photo-Fenton reaction.

5. UV photolysis of phenol is pH-dependent. The reaction rate is highest at an initial pH of ~3.5.
6. The addition of small quantities of hydrogen peroxide or iron ions ($\text{Fe}^{3+}/\text{Fe}^{2+}$) to a phenol solution can strongly raise the rate of UV photolytic elimination of phenol.
7. The homogeneous system of $\text{UV}/\text{H}_2\text{O}_2/\text{Fe}$ (soluble photo Fenton reagent) gives highest photochemical elimination rate of phenol, as well as other organic compounds.

ACKNOWLEDGMENTS

Jian Chen wishes to express his gratitude for the financial support received from China Maoming Petroleum Company and Wageningen Agricultural University, and wishes to thank Prof. Fu, Jing Yin, Prof. Zhuang, Qi Xing for the helpful discussions held with them, and Lecturer Yang, Ru for the analysis of samples.

4.5 REFERENCES

1. O. Legrini, E. Oliveros, and A. M. Braun, *Chem. Rev.*, **93**(2), 671-698, (1993).
2. (a). D.F. Ollis, *Comparative Aspects of Advanced Oxidation Processes*, presented at: ACS Symposium, "Emerging Technologies for Hazardous Wastes", Atlanta, Georgia, October 1991.
(b). D.F. Ollis, H. Al-Ekabi(eds.) *Photocatalytic Purification and Treatment of Water and Air*, Elsevier Science Publishers, Amsterdam, 1993.
3. W. Klöpffer, *The Science of the Total Environment*, **123/124**, 145-159, 1992.
4. G.R. Peyton, *Oxidative Treatment Methods for Removal of Organic Compounds from Drinking Water Supplies*, Chapter 14, p.313-362, in *Significance and Treatment of Volatile Organic Compounds in Water Supplies*, (eds.) N.M. Ram, R.F. Chrisman, K.P. Cantor, Lewis Publishers, 1990.
5. R.G. Zepp, B.C. Faust, and J. Holgné, *Environ. Sci. Technol.* **26**(2), 313-319, 1992.
6. K.W. Yost, *43rd. Purdue Industrial Waste Conference. Proceedings*, Lewis Publishers, Inc., Chelsea, Michigan, 1989.
7. M.R. Matsumoto, J.N. Jensen, P. McGinley, B.E. Reed, *Water Environ. Research*, **66**(4), 309-324, 1994.
8. C. S. Turchi and D. F. Ollis, *J. Catalysis*, **122**, 178-192, 1990.
9. C. Kormann, D. W. Bahnemann, and M. R. Hoffmann, *Environ. Sci. Technol.* **25** 494-500, 1991.
10. X. Li, P. Fitzgerald and L. Bowen, *Wat. Sci. Tech.* **26**(1-2) 367-376, 1992.
11. C. K. Grätzel, M. Jirousek and M. Grätzel, *J. Mol. Cat.* **60**, 375-387, 1990.
12. S.T. Hung, M.K.S. Mak, *Environ. Technol.* **14**, 265-269, 1993.
13. E. Pelizzetti, C. Minero, E. Borgarello, L. Tinucci, N. Serpone, *Langmuir*, **9**, 2995-3001, 1993.
14. H. Hidaka, J. Zhao, K. Nohara, K. Kitamura, Y. Satoh, E. Pelizzetti, and N. Serpone in "Photocatalytic Purification and Treatment of Water and Air" D. F. Ollis, H. Al-Ekabi (eds.), ISBN: 0-444-89855-7, 251-259, 1993.
15. E. Pelizzetti, C. Minero, H. Hidaka, and N. Serpone in "Photocatalytic Purification and Treatment of Water and Air" D. F. Ollis, H. Al-Ekabi(eds.), Elsevier Science Publishers, Amsterdam, 261-273, 1993.
16. N. Serpone, Y. K. Ah-you, T. P. Tran, R. Harris, E. Pelizzetti and H. Hidaka, *Solar Energy* **39**, 491-498, 1987.
17. J. Sabate, M. A. Anderson, M. A. Aguado, J. Giménez, S. Cervera- March, C. G. Hill, Jr. *J. Molecular Catalysis* **71**, 57-68, 1992.
18. M. R. Prairie, B. M. Stange, and L. R. Evans, "Photocatalytic Purification and Treatment of Water and Air" D.F.Ollis, H. Al-Ekabi(eds.), Elsevier Science Publishers, Amsterdam, 353-363, 1993.

19. E. Pelizzetti, E. Pramauro, C. Minero, and N. Serpone, *Waste Management*, **10**, 65-71, 1990.
20. S. Das, M. Muneer, and K. R. Gopidas, *J. Photochem. Photobiol. A: Chem.*, **77**, 83-88, 1994.
21. H. Hidaka, K. Nohara and J. Zhao, N. Serpone, E. Pelizzetti, *J. Photochem. Photobiol. A. Chem.* **64** 247-254, 1992.
22. R. W. Matthews and S.R. McEvoy, *J. Photochem. Photobiol. A. Chem.* **64**, 231-246, 1992.
23. (a) J. Kiwi, *Environmental toxicology and Chemistry*, **13**(10), 1569-1575, 1994. (b) N.N. Lichtin, J. Dong, and K. M. Vijayakumar, *Water Poll. Res. J. Canada*, **27**(1), 203-210, 1992. (c) T.-Y. Wei, C.-C. Wan, *J. Photochem. Photobiol. A: Chem.* **69**, 241-249, 1992. (d) A. Sclafani, L. Palmisano and E. Davì, *New J. Chem.* **14**(4), 265-268, 1990.
24. (a) K. Tanaka, T. Hisanaga, and K. Harada, *New J. Chem.*, **13**, 5-7, 1989. (b) Teruaki Hisanaga, Kenji Harada, and Keiichi Tanaka, *J. Photochem. Photobiol., A: Chem.*, **54**, 113-118, 1990.
25. J. CHEN, J.-Y. Fu, Q.-X. ZHUANG, China Patent No. ZL 88106599.4, 1995.
26. X.-Q. Zhang, *The Treatment and Application of Phenol Wastewater*, Peijing, 1980.
27. H.M. Castrantas, and R.D. Gibilisco, *Emerging Technologies in Hazardous Waste Management*, ACS Symp. Ser., pp.77-99, 1990
28. E. Lipczynska-Kochany, *Water Poll. Res. J. Canada*, **27**(1), 97-122, 1992.
29. (a) J.-C. D'Oliveira, C. Minero, E. Pelizzetti, and P. Pichat, *J. Photochem. Photobiol.* **72**, 261-267, 1993. (b) C. Pelizzetti, E. Minero, E. Borgarello, L. Tinucci, N. Serpone, *Langmuir* **9**, 2995-3001, 1993. (c) V. Augugliaro, L. Palmisano, and A. Sclafani, C. Minero, and E. Pelizzetti, *Toxicological and Environmental Chemistry*, **16**, 89-109, 1988.
30. (a) J. Tseng, and C. P. Huang, *Emerging Technologies in Hazardous Waste Management*, ACS symp. Ser. 1990. pp. 12-39. (b) A.P. Davis, and C. P. Huang, *Wat. Res.* **24**(5), 543-540, 1990. (c) A.P. Davis, and C. P. Huang, *Wat. Sci. Tech.*, **21**, 455-464, 1989.
31. (a) K.-I. Okamoto, Y. Yamamoto, H. Tanaka, M. Tanaka, and A. Itaya, *Bull. Chem. Soc. Jpn.*, **58**(7), 2015-2022, 1985. (b) K.-i. Okamoto, Y. Yamamoto, H. Tanaka, and A. Itaya, *Bull. Chem. Soc. Jpn.*, **58**(7), 2023-2028, 1985.
32. L. Palmisano, V. Augugliaro, M. Schiavello, and A. Sclafani, *J. Molecular Catalysis*, **56**, 284-295, 1989.
33. C. Guillard, H. Delprat, C. Hoang-van and P. Pichat, *J. Atmospheric Chemistry* **16**, 47-59, 1993.
34. R. Borello, C. Menero, E. Pramauro, E. Pelizzetti, N. Serpone, H. Hidaka, *Environmental Toxicology and Chemistry*, **8**, 997-1002, 1989.
35. PB report, No. 82-108457, National Technical Information Service/U.S. Department of Commerce, 1982.
36. PB report, No. 83-173179, National Technical Information Service/U.S. Department of Commerce, 1983.

37. Hokayisu and Sawujiyi, *Jpn. Chem. Eng. Thesis P. (1)*, 1983.
38. I. Izumi and Y. Ohnishi, *Mizu Shori Gijutsu*, 26(4), 233-237, 1985.
39. J. Peral, J. Casado, and J. Doménech, *J. Photochem. Photobiol. A: Chem.*, 44(2), 209-217, 1988.
40. V. Augugliaro, L. Palmisano, and A. Sclafani, C. Minero, and E. Pelizzetti, *Toxicological and Environmental Chemistry*, 16, 89-109, 1988.
41. J. Chen, W. Rulkens and H. Bruning. *The Elimination of Phenol and COD in Industrial Wastewater Using Photochemical Methods*, paper in The International conference of Oxidation Technologies for Water and Wastewater Treatment, Goslar, Germany, May 12-15, 1996.
42. *Standard methods for the Examination of Water and Wastewater*, p.556-561 for phenol, p.532-538 for COD. Published by American Public Health Association, 16th Edition, 1985.
43. A.M. Braun, "How to evaluate photochemical methods for water treatment", paper in International Conference - Oxidation Technologies for Water and Wastewater Treatment, Clausthaler Umwelttechnik-Institut GmbH, Goslar, Germany, May 1996.
44. C. von Sonntag and H.P. Schuchmann, *Angew. Chem. Int. Ed. Engl.* 30, 1229-1253, 1991.
45. L. Jälob, T.M. Hashem, S. Bürki, M.N. Guindy and A.M. Braun, *J. Photochem. Photobiol. A: Chem.*, 75, 97-103, 1993.

CHAPTER 5 PHOTOCATALYZED DEPOSITION AND CONCENTRATION OF SOLUBLE URANIUM(VI) FROM AQUEOUS SOLUTIONS SUSPENDING TiO_2 OR Pt/TiO_2

This Chapter is based on:

J. CHEN, D.F. Ollis, W.H. Rulkens and H. Bruning, "Photocatalyzed deposition and concentration of soluble uranium(VI) from wastewater using suspended TiO_2 or Pt/TiO_2 ", to be presented on The International Conference of Interfaces Against Pollution 1997, Wageningen, the Netherlands, August 10 - 13, 1997, organized by Sub-Committee of the IUPAC on Colloid and Surface Chemistry Including Catalysis, and submitted to *Colloids and Surfaces A*, 1997.

PHOTOCATALYZED DEPOSITION AND CONCENTRATION OF SOLUBLE URANIUM(VI) FROM AQUEOUS SOLUTIONS SUSPENDING TiO_2 OR Pt/TiO_2

5.1 INTRODUCTION

5.1.1 Traditional treatment of radioactive wastewater

In water, uranium (normally uranium(VI) (or U(VI)) in the form of uranyl (UO_2^{2+})) is a hazardous substance due to its chemical toxicity and sometimes also radioactive¹. Periodic decontamination of various parts of a nuclear power plant produces aqueous wastewater flows containing dilute levels of radioactivity. The radioactive species contained in these wastewaters are typically metal ions with chelating agents and their complexes. They are typically complexants and organic acids, such as ethylenediaminetetraacetic acid (EDTA), hydroxyethylenediaminetriacetic acid (HEDTA), oxalic and citric acid and the associated degradation products, many of which have not been characterized. Such wastewaters must be processed to reduce the radiation level of the aqueous phase and to bring the radioactive compounds in a physicochemical state suitable for long-term, safe disposal, which is usually a solid phase. At the Hanford plant in the State of Washington in the US, the final objective is to convert the high-level and/or transuranic radioactive waste into glass for disposal at a geological repository².

The methods currently employed for the removal of radioactive uranium from contaminated water include three basic processes: evaporation, precipitation, and ion exchange. Evaporation requires a long retention time and high costs of energy. Precipitation is the most attractive option for treating a concentrated solution, although it can also be applied to dilute solutions. Ion exchange is the method generally used in current commercial practice³.

5.1.2 Application of photocatalysis on metal-ion deposition

Photocatalysis has been studied extensively as a potential method for wastewater treatment^{4,5}, not only for the oxidation of organic contaminants but also for the removal and recovery of various dissolved metals^{6,7,8,9,10,11,12}. An example of the application of metal-ion deposition is the deposition of gold(III) by photocatalyzed reduction of a deoxygenated gold(III) solution containing 4 vol. % methanol. The reported quantum yields are about 3% at $\text{pH} = 14$, and about 15% at $\text{pH} = 5-6$ ⁷. The addition of methanol was found to assist also the release of gold from the complexing agent cyanide (CN^-). An aqueous cyanide solution containing 155 ppm gold(III) (tenfold excess of cyanide) did not show depositing upon photocatalyst illuminated, but 80% recovery via deposition was achieved upon addition of methanol and subsequent

illumination. Other photocatalyst studies showing good possibilities for metal recovery include those examining aqueous solutions⁸ of manganese (Mn), thallium (Tl) and cobalt (Co), solutions of mercury and methylmercury⁹, and the selective, serial deposition of platinum, gold and rhodium from a chloride solution⁷.

In the given examples of reductive photodeposition of metals in deaerated systems or systems in which very little oxygen is dissolved, the primary electron acceptor consists of a metal ion (rather than molecular oxygen). Another interesting application of photocatalysis for the treatment of metal ions is oxidative deposition on photocatalyst surfaces in aerated systems. A typical example is the oxidative deposition of Pb^{2+} ions occurring when an aerated aqueous solution with a Pb^{2+} concentration of 90 ppm and a 5%Pt/TiO₂-photocatalyst concentration of 2 g/L is illuminated using near-UV radiation. The photocatalytic removal efficiency proved to be 90% Pb^{2+} (in the form of PbO_2) deposited on the Pt/TiO₂ surface at pH = 3.7 after illumination for four hours^{8,13}.

The application of photocatalysis for the removal of dissolved radioactive uranium ions has some advantages. Normally, the treatment of wastewater containing radioactive uranium from a nuclear power plant includes the processes of concentration and solidification. Photocatalysis can combine these two processes in one step, since it has shown to be capable of reducing and depositing metal ions from aqueous solutions¹⁴. In addition, wastewaters polluted with transuranic and other radioactive materials already contain chelating agents (*e.g.*, EDTA, HEDTA, citric acid, oxalic acid) after being pretreated. Photocatalysts can oxidize such complexes simultaneously with the reductive deposition of radioactive ions on the photocatalyst surface. The complexes can be partially or completely mineralized. Studies of the phototreatment of uranium have been focused on photoreduction by only illumination^{15,16,17}. It is, in fact, a photolytic process, and the reduced uranium ion normally remains in solution. So far, not many studies of the treatment of dissolved uranium by photocatalysis¹⁸ have been reported, and some of them were only preliminary.

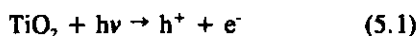
This chapter deals with reversible, photocatalyzed, reductive deposition of uranium(VI), the destruction of radioactive metallo-EDTA complexes, and the associated partial decarboxylation of EDTA at plain TiO₂- and Pt/TiO₂ surfaces in deaerated aqueous solutions. We used uranyl (UO_2^{2+}) as a substrate in aqueous solutions of uranium(VI) at a concentration of 50 ppm.

5.1.3 Basic principles of photocatalysis for the removal of metal ions in aqueous solutions

Photocatalyzed reductive or oxidative deposition of metal ions from an aqueous solution (*i.e.*, a redox reaction occurring at photocatalyst surfaces) involves simultaneous participation by an electron donor (ED) (*e.g.*, an oxidizable metal ion, or ethanol) and an electron acceptor (*e.g.*,

a reducible metal ion, or dissolved oxygen). In general, deposition of metal ions from an aqueous solution on the surface of a photocatalyst (such as TiO_2) can be expressed in the following equations.

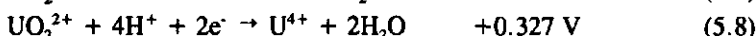
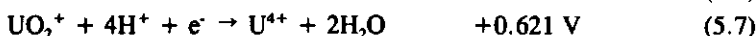
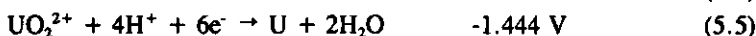
First, illumination results in:



Reductive deposition of metal ions occurs as follows. Here, a uranyl ion (UO_2^{2+} or simply U(VI)) is given as an example; this ion is reduced to uranium oxide (UO_2).



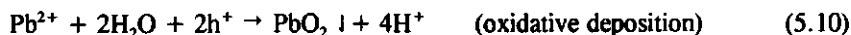
In eq.5.3, n is the number of holes. The reaction can take place thermodynamically if suitable electropotentials exist at the photocatalyst surface. After illumination, TiO_2 surfaces will have two electropotentials: one in the cathodic area with a conductor band electropotential of around -0.1 volts (vs. NHE), and the other in the anodic area with a valence-band electropotential of around $+3.0$ volts (vs. NHE) (see Fig.1.7 in Chapter 1). In the case of uranium, possible redox electropotentials are listed below¹⁹.



If an aqueous solution contains only uranyl (UO_2^{2+}), the photocatalyst TiO_2 will allow only the reactions given by Eq.5.7 to 5.9 to occur, because a maximum flat-band potential of n-type TiO_2 is equal to or larger than -0.1 V (vs. NHE)²⁰. Thermodynamically, TiO_2 cannot reduce uranium(VI)(uranyl) to a valence below $+4$ (Eq.5.4 - 5.6).

It is not clear what effects of platinization of TiO_2 creates on the reductive deposition of uranium. The oxidative deposition of certain metal ions (e.g., Pb^{2+} , Mn^{2+} , Ti^+) occurs much faster on a Pt/TiO_2 surface than on a native TiO_2 surface⁸. It is well known that the platinization of TiO_2 can accelerate the cathodic processes of proton or oxygen reduction occurring at the surface of TiO_2 ^{21,22,23}, because at the site of platinum, there is a much lower

adsorption energy than at the non-platinized site. It is clear that during oxidative deposition of metal ions at TiO_2 surfaces the Pt located on TiO_2 accelerates the oxygen reduction, which in general is the rate-determining step of metal deposition. An example is oxidative deposition during which Pb^{2+} is oxidized to PbO_2 :



Because the deposition of uranium is a reductive process rather than an oxidative one, it needs to be investigated whether platinum has a positive effect.

5.2 EXPERIMENTAL

5.2.1 Reagents

The titanium dioxide (TiO_2) used during the experiments is Degussa P25 grade with a BET surface area of $\sim 50 \text{ m}^2 \text{ g}^{-1}$ and an average primary particle size of 30 nm. The 5-Br-PADAP (2-(5-Bromo-2-Pyridylazo)-5-(diethylamino)phenol) used is SIGMA, No.63H3486. The 5-Sulfosalicylic Acid used is SIGMA, No.64H0320, ACS reagent. The chloroplatinic acid ($\text{H}_2\text{PtCl}_6 \cdot 6\text{H}_2\text{O}$) used is Fisher, No.915412, ACS reagent. The CyDTA (trans-1,2-diaminocyclohexane- $\text{N},\text{N},\text{N}',\text{N}'$ -tetraacetic acid) used is SIGMA, No.73H2608, assay > 99%. The EDTA disodium salt (ethylenediaminetetraacetic acid disodium salt, $\text{Na}_2\text{EDTA} \cdot 2\text{H}_2\text{O}$, M.W. = 372.24) used is Baker, No.640395. The ethanol used is AAPER Alcohol and Chem. Co., USP ethyl alcohol, Absolute - 200 Proof, DSP-KY-417. The perchloric acid (HClO_4) used is Fisher, No.SP339-500, 0.1N. The sodium fluoride (NaF) used is Fisher, 936904. The triethanolamine used is SIGMA, No.73H5761, assay > 99.5%. The uranyl nitrate ($\text{UO}_2(\text{NO}_3)_2$) used is Fluka, 94270, assay > 99%. The other, common reagents (*e.g.*, acetic acid) are mentioned in the text. These reagents were used without further purification.

5.2.2 Catalyst preparation

Photo-deposited Pt/ TiO_2 was prepared by near-UV illumination for 38 hours of 467 ml of a slurry containing 34.6 g of TiO_2 , 0.923 g of $\text{H}_2\text{PtCl}_6 \cdot 6\text{H}_2\text{O}$ and 25 ml of glacial acetic acid. After illumination, the dark grey slurry was centrifuged for 30 min at 3,000 rpm (Sorvall Instruments, Model RC5C, Du Pont) and then washed. The process was repeated eight times to remove all inorganic and organic ions. The dark grey solid was dried for about three hours at 120°C .

5.2.3 Apparatus and procedures of experiments

All experiments were conducted in a liquid-phase recycle photoreactor similar to the one described in Chapter 2 (Fig.2.1b). A 0.1 wt. % slurry containing 1 wt. % Pt/TiO₂ in water was recycled through a quartz annular photoreactor using a polypropylene/ceramic pump. Illumination of 3.08×10^{-4} Einstein/min was provided using a black-light fluorescent bulb (GE BLB - 15 W) mounted in the centre of the photo-reactor. The predominant emission wavelength band of this lamp ($320 \leq \lambda \leq 400$ nm) is sufficient to photo-excite TiO₂ ($\lambda \leq 410$ nm). This wavelength band is longer than the wavelengths of 254 and 308 nm and shorter than that of around 420 nm, which are required for photolysis^{15,24}, especially for the photoreduction of uranium(VI) to uranium(V)^{25,26}. The total reactor volume was $\sim 1,480$ cm³, including a 280-cm³ quartz annular photoreactor and a reactor reservoir made from a 1000-ml, 3-neck flask. The total fluid volume in the reactor was fixed at ~ 600 cm³, with a ~ 880 -cm³ gas headspace in the reservoir during each run.

To confirm that the deposition of uranium(VI) is caused only by photocatalysis, control (blank) experiments were carried out involving photolysis, a chemical reaction in the dark, and physical adsorption. Five types of experiment (including the above-mentioned types) were carried out during this research, namely:

(1). *Photocatalysis*. Before illumination, uranyl, EDTA (as an electron donor) and a photocatalyst were added, and the liquid was sparged with pure N₂ for 30 minutes. Then the reactor was closed. Next, another 40 cm³ of pure N₂ were added using a gas syringe to maintain a positive pressure (20 in.H₂O) in the reactor. A pressure gauge (0-60 in.H₂O) was mounted on the reservoir to detect any change in pressure in the reactor.

(2). *Photolysis without a photocatalyst*. To investigate whether photolytic deposition of uranium(VI) also occurs if only near-UV illumination is applied, no photocatalyst was added to the reaction solution during this experiment. The other experimental conditions were similar to those existing during process (1).

(3). *A chemical reaction in the dark*. During this experiment, a photocatalyst was added to the reaction solution but no illumination was applied. The aim of this experiment was to find out whether any chemical deposition of uranium(VI) occurs in the presence of the catalyst TiO₂. The other experimental conditions were similar to those existing during process (1).

(4). *Physical adsorption*. Because the photocatalyst TiO₂ has a large specific surface area, in addition to a chemical dark reaction, physical adsorption of uranyl on TiO₂ surfaces in the dark may also occur, resulting in a decrease in the uranium(VI) concentration in the solution.

During this experiment, photocatalyst was added to the reaction solution but no illumination was applied. The solution was exposed to air and stirred for 150 minutes. The amount of uranium(VI) adsorbed onto TiO_2 surfaces was determined by analysing the solution.

(5). *Reoxidation*. Literature²⁷ shows that uranium reduced by photolysis (*e.g.*, U(V), U(IV)) can be easily reoxidized in air. To check this in a photocatalytic system, after a U(VI)-EDTA solution containing suspended TiO_2 was illuminated in a deaerated system for some time, this solution was exposed to air to examine whether any reduced uranium could be reoxidized to U(VI) in the dark or while UV illumination occurred.

5.2.4 Analysis

5.2.4.1 Uranium(VI) (uranyl)

The standard methods for uranium analysis are radiochemical or fluorometric method²⁸. Because such methods require special, expensive instruments and materials, overelaborate sample pretreatment and an analysis process, they cannot be applied daily for the analysis of large quantities of samples that rapidly need to be analysed during experiments. Therefore, we used one of the new photometric methods for uranium analysis recently reported by H. Onishi²⁹. This method includes convenient use of the complexing agent 2-(5-Bromo-2-Pyridylazo)-5-(diethylamino) phenol (5-Br-PADAP)³⁰.

This analytical method is highly sensitive to uranium ($0.003 \mu\text{g U/cm}^2$) and shows a high selectivity in the presence of masking agents (trans-1,2-diaminocyclohexane-N,N,N',N'-tetraacetic acid (CyDTA), NaF, and sulfosalicylic acid)^{31,32}. 5-Br-PADAP can only form a complex with uranium(VI) (uranyl), resulting in a deep-red colour with maximum absorbance at 578 nm at pH = 7.6. During colorimetric analysis of most substances, always compounds are present that seriously interfere with the analytical accuracy. In the presence of the above masking agents, the maximum permissible quantities (in mg) of interfering ions during the determination of 50 μg of uranium(VI) in 25 ml are for arsenic(V) 0.5, for cobalt (any valence) 4, for chromium(III) 3, for copper (any valence) 3, for nickel (any valence) 3, for vanadium(V) 0.01, for vanadium(VI) 1.0, for zirconium (any valence) 0.5, and for PO_4^{3-} 0.5²⁸.

The following reagents are required for this method: (1). A standard stock solution of uranium containing 0.1N HNO_3 and 1,000 ppm of uranium(VI) from uranium nitrate ($\text{UO}_2(\text{NO}_3)_2$) (stock in the dark) (2). A complexing solution containing 25 g of CyDTA, 5 g of NaF and 65 g of sulphosalicylic acid in 800 ml of water, neutralized to a pH of 7.85 with 40% NaOH, and diluted to one litre. (3). A buffer solution consisting of 149 g of triethanolamine dissolved in 800 ml of water, neutralized to a pH of 7.85 with HClO_4 (if triethanolamine-HCl is used, the

solution should first be neutralized to a pH of ~ 7 using NaOH), and then diluted to 1 litre. (4). 0.05% 5-Br-PADAP in ethanol, which should be prepared weekly.

The analysis is carried out as follows: Take a 1-ml sample from the slightly acidic or neutral reaction solution, and immediately centrifuge it for 10 min at 5,000 rpm. Transfer 0.5 ml of supernatant (containing 5-50 μg of uranium(VI)) at once into a 25-ml volumetric flask. Add 2.0 ml of a complexing solution, 2.0 ml of a buffer solution, 10.0 ml of ethanol, and 2.0 ml of a 5-Br-PADAP solution. Mix and dilute with water to 25 ml. Allow it to stand for 40 minutes, and then measure the absorbance at 578 nm in a photometer (Spectronic 21D, MILTON ROY) against a reagent blank using a 1-cm cell. The maximum concentration still showing proportional absorbance is 100 μg of U(VI)/25 ml.

5.2.4.2 CO_2 and pH

The carbon dioxide produced in the liquid and gas phases was measured by injecting liquid and gas samples directly into a 1 N H_2SO_4 absorption liquid contained in an infrared carbon dioxide analyzer (Horiba, PIR-2000). The instrument was calibrated weekly.

The pH of solutions was measured using an *in-situ* pH electrode (Fisher, 13-620-93) connected to an ORION 701A digital pH/mV meter. Before each experiment, the pH electrode was calibrated at two points (pH = 4 and 10) with standard pH buffers.

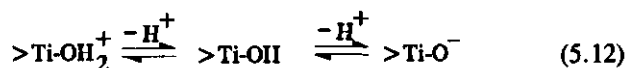
5.3 RESULTS AND DISCUSSION

5.3.1 Uranium adsorption on TiO_2

In an acidic solution, physical adsorption of uranyl onto TiO_2 increased with pH, as shown in Table 5.1. Such a trend was also reported by Amadelli *et al.*¹⁸ and Ho *et al.*³³ They state that in this situation different hydrolysis products (species) of UO_2^{2+} are present, and that one or more of these species, such as $(\text{UO}_2^{2+})_2(\text{OH})_2^{2+}$ and subsequently $(\text{UO}_2^{2+})_3(\text{OH})_4^+$, are possibly involved in the adsorption process. This large species, which has a trimeric structure, is expected to be less solvated and therefore more easily adsorbed than UO_2^{2+} .³³ The difference between the experiments carried out by Amadelli *et al.*¹⁸ and Ho *et al.*³³ and ours is that during our experiments EDTA (EDTA/ U^{6+} mole ratio = 4:1) was added to the solution. Because uranyl (UO_2^{2+}) is chelated by EDTA, the chelate $[\text{UO}_2\text{EDTA}]^{2-}$ is formed. The uranyl-EDTA chelate has one uranyl ion and one EDTA ligand³⁴. Because we added extra EDTA, hardly any or no free cations of uranyl (UO_2^{2+}) were expected to occur in the solution during our

experiments. Therefore, the adsorbed species should be the chelate anion $[\text{UO}_2\text{EDTA}]^{2-}$ rather than the cation UO_2^{2+} or its hydrolysis products.

The charge of TiO_2 particles is known to be pH-dependent through protonation-dissociation equilibria of the surface hydroxyl groups:



According to the discussions presented by Amadelli *et al.*¹⁸ Ohtani *et al.*³⁵, in an EDTA-free solution the positively charged uranium species will interact favourably with the surface while the pH increases toward the isoelectric point, which is electrically neutral on TiO_2 surfaces (at $\text{pH} = \sim 6.4$). This means that adsorption of the positively charged uranium species (UO_2^{2+}) onto TiO_2 surfaces is highest only around the isoelectric point. From our data, we can conclude that a negatively charged uranium species (*e.g.*, uranium chelate $[\text{UO}_2\text{EDTA}]^{2-}$) should also adsorb favourably onto TiO_2 surfaces around the isoelectric point.

Table 5. 1 Physical adsorption of uranium(VI) onto TiO_2 in water with a uranium(VI) concentration of 50 ppm and an EDTA concentration of 310 ppm at different pH values.

pH	0.90	3.18	5.05	6.81
Amount (%)	2%	15%	31%	37%

Conditions: Aerated solution, a reaction temperature of 25°C, a reaction time of 150 minutes, initial solution pH adjusted with HNO_3 , 1 g/L TiO_2 , no UV illumination.

5.3.2 Photocatalytic reduction of uranyl on TiO_2

Fig. 5.1 shows a photolysis reaction (illumination, no TiO_2 present, deaerated solution), a dark reaction (TiO_2 , no illumination, deaerated solution) and the photocatalytic reductive deposition of uranyl on plain TiO_2 (initial pH of the solution = 2.7, the uranium:EDTA molar ratio = 1:8). Nearly 100% uranyl was still found to be present in solution after reactions had occurred for a total of six hours in region (a) (photolysis, 5 hours) and in region (b) (dark reaction, 1 hour). These results show that neither any photolytic reactions nor any dark reactions occurred in the photocatalytic system. According to literature^{36,37}, although a homogeneous uranyl photolytic reduction could occur if UV light of suitable wavelengths is applied, it would

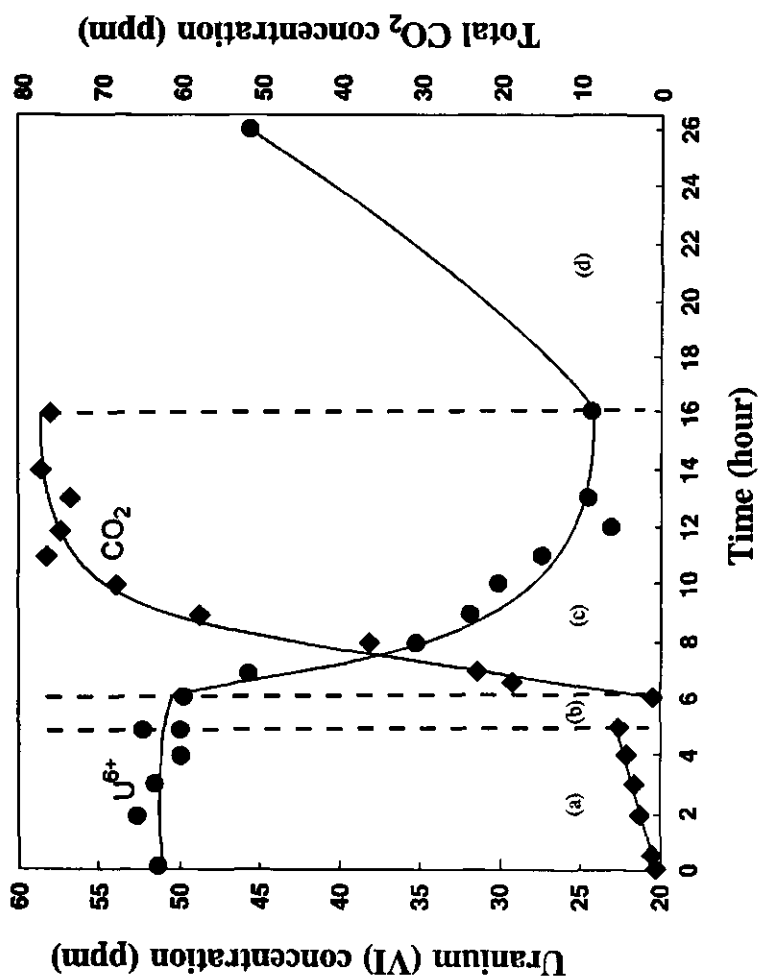


Fig. 5.1. The photocatalyzed reductive deposition of uranium from an aqueous solution containing 50 ppm (initial concentration) of uranium(VI) on plain TiO₂ as a function of time. Concentration of EDTA is 620 ppm. The molar ratio U⁶⁺:EDTA = 1:8, solution volume: 600 ml, catalyst: 1 g/l, pH = 2.7. Region (a): illumination, no TiO₂, deaerated, (b): dark, TiO₂, aerated, (c): illumination, TiO₂, deaerated, (d): dark, TiO₂, aerated.

● : Uranium(VI) concentration, ◆ : Total CO₂ concentration.

be difficult to recover the reduced uranyl species because they are still dissolved in solution, and will reoxidize easily in the presence of air²⁷. Only a small amount of CO₂ was released (~5 ppm) during 5 hours of near-UV photolysis (region (a)). This negligible amount formed by photolytic mineralization is assumed to be the result of photolysis of a uranyl-EDTA complex at the near-UV wavelength used.

During the experiments the results of which are shown in Fig.5.1, the pH of the aqueous solution remained constant. It was observed that, when near-UV illumination was applied in the presence of suspended TiO₂, the catalyst, which was originally white, turned grey in region (c) shown in Fig.5.1. This region shows that uranyl can be photocatalytically reduced. It was observed that, when the TiO₂ suspension was centrifuged immediately after sampling (preventing air contact) in order to separate the TiO₂ catalyst, the uranyl concentration in the supernatant remained low and constant. If, however, the suspension was left in an aerated atmosphere (region(d)), the uranyl concentration in the solution regained its original value. Thus, it can be concluded that during the experiments most of the reduced uranium deposited on TiO₂ surfaces, and that it can be restored to uranyl. During the photocatalyzed reduction of uranyl, EDTA is necessary as an electron donor; it is partially oxidized and converted to CO₂ (region (c)). The presumed decarboxylation reaction stopped after 26 ppm of uranium had been removed from solution. At this point, about 53% of 50 ppm (0.21 mM) of uranium(VI) was reduced and deposited in six hours and about total 78 ppm of CO₂ was released. This amount of CO₂ corresponds to a complete single decarboxylation of a 620-ppm (1.67 mM) EDTA solution.

Photocatalyzed reduction of uranyl is sensitive to the presence of oxygen. Fig.5.2 compares the results of photocatalyzed deposition of 50 ppm of uranium(VI) on plain TiO₂ in aerated and deaerated systems (the initial solution pH = 2.7, the uranium/EDTA molar ratio = 1:4). In region (a) or (b) with an aerated solution, hardly any or no uranyl can be reduced and deposited on TiO₂ by UV illumination. Although little uranyl was reduced (in region (a)), CO₂ was still released and it occurred at a much faster rate than would have happened in a deaerated system. This release of CO₂ must have been due to fast decarboxylation of EDTA in the presence of air. Dissolved oxygen is apparently either a better electron scavenger than uranyl, or a strong oxidant by which the reduced uranyl species can be rapidly reoxidized. After illumination for more than three hours in the presence of air, all air was displaced by N₂, and the suspension was illuminated again. About 50% of 50 ppm of dissolved uranium(VI) was now reduced and deposited on TiO₂ in four hours (region (c)). The total amount of CO₂ released (0.66 mM) in region (c) corresponds reasonably with the total initial EDTA concentration (0.83 mM), which again suggests the occurrence of single decarboxylation of EDTA. The delay in the decrease in uranium concentration occurring in the water phase

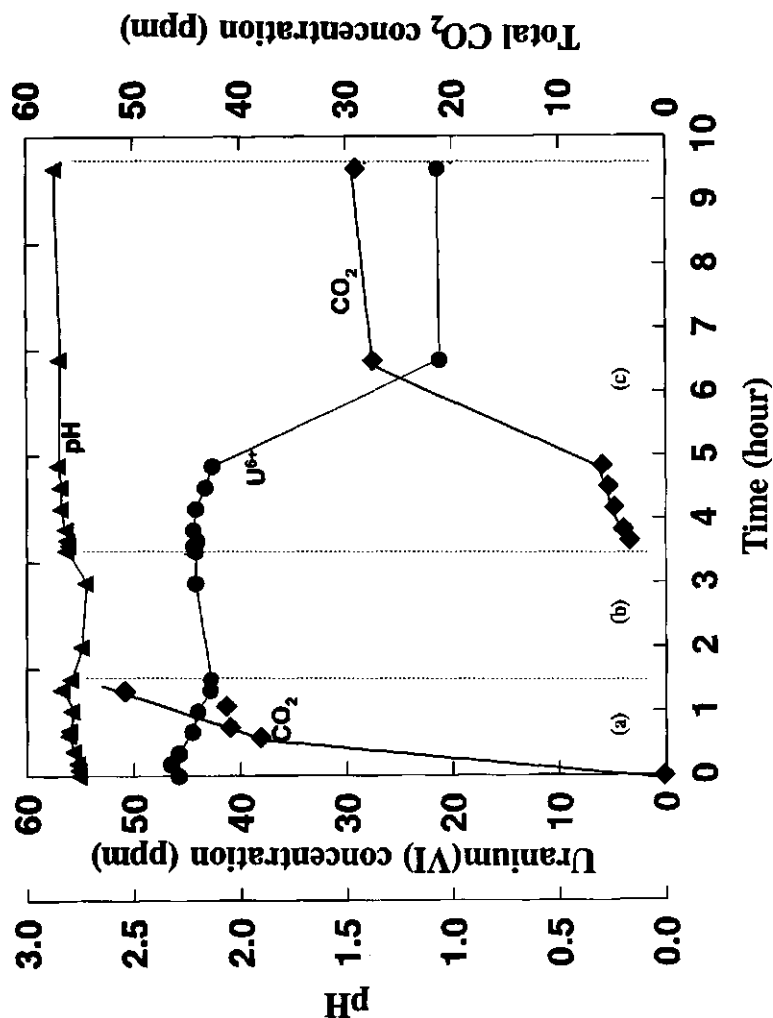


Fig. 5.2. The photocatalyzed reductive deposition of uranium from an aqueous solution containing 50 ppm (initial concentration) of uranium(VI) on plain TiO_2 as a function of time. Concentration of EDTA is 310 ppm. The molar ratio U^{6+} : EDTA = 1:4, solution volume: 600 ml, catalyst 1 g/l. Region (a): illumination, aerated, closed, (b): illumination, aerated, open, (c): illumination, deaerated, closed, (d): illumination, deaerated, open.

(region (c)) is probably due to the consumption of residual adsorbed oxygen completing the deaeration. The acidic solution pH remained almost constant during illumination.

Comparing the results of the photocatalyzed reduction of 50 ppm of uranium(VI) in U-EDTA solutions using plain TiO_2 at a $\text{U}^{6+}/\text{EDTA}$ ratio of 1:8 (region (c) in Fig. 5.1) with those obtained at a 1:4 ratio (region (c) in Fig. 5.2), shows that in both cases the maximum conversion rate of uranium(VI) was around 50% in five hours, and in both cases single decarboxylation should have occurred. The ratio between metal and ligand in the uranyl/EDTA chelate is 1:1. Although the solution with a ratio of 1:8 contains far more EDTA than that with a ratio of 1:4, this apparently does not affect the reduction of uranyl.

5.3.3 Photocatalytic reduction of uranyl on Pt/TiO_2

Using platinized TiO_2 , we investigated the repeated deposition of uranyl in a deaerated system during illumination, the subsequent recovery of uranyl in an aerated system, the effect of the initial uranyl concentration, and whether the modified platinum present at TiO_2 could accelerate the reductive deposition of uranyl.

5.3.3.1 Initial concentration of uranium(VI) 50 ppm

For a solution with an initial uranium(VI) concentration of 50 ppm and a $\text{U(VI)}/\text{EDTA}$ ratio of 1:8, Fig. 5.3 shows the concentrations of uranium(VI) and CO_2 in the reactor plotted against illumination time. The figure shows a strong increase in CO_2 concentration and a strong decrease in uranium(VI) concentration in the solution (region (a)). After four hours of illumination, about 62% of the initial amount of uranium(VI) was deposited, about 90% of the EDTA was degraded involving single decarboxylation, and the rates of both processes dropped to zero. These results are similar to those obtained using plain TiO_2 (Fig. 5.1). To check that the reduced uranium(VI) compounds could be reoxidized, 50 ml of air was injected into the closed reactor containing N_2 after 23 hours of illumination. It was found that during two hours of aerated illumination about 42% of the reduced products of uranium(VI) present on Pt/TiO_2 were reoxidized and dissolved again (region (b) of Fig. 5.3).

Little pH change was observed in region (a) during illumination. This had already been found during the experiments illustrated in Figures 5.1 and 5.2. It seems that the oxidation of EDTA (decarboxylation) and the resultant production of CO_2 (in the form of carbonate, bicarbonate or carbonic acid) in aqueous solutions do not cause enough acidity to change the solution pH.

To investigate the reversible character of uranium deposition on Pt/TiO_2 , we alternately illuminated and aerated (after deaeration) a solution containing 50 ppm of uranium(VI), 620

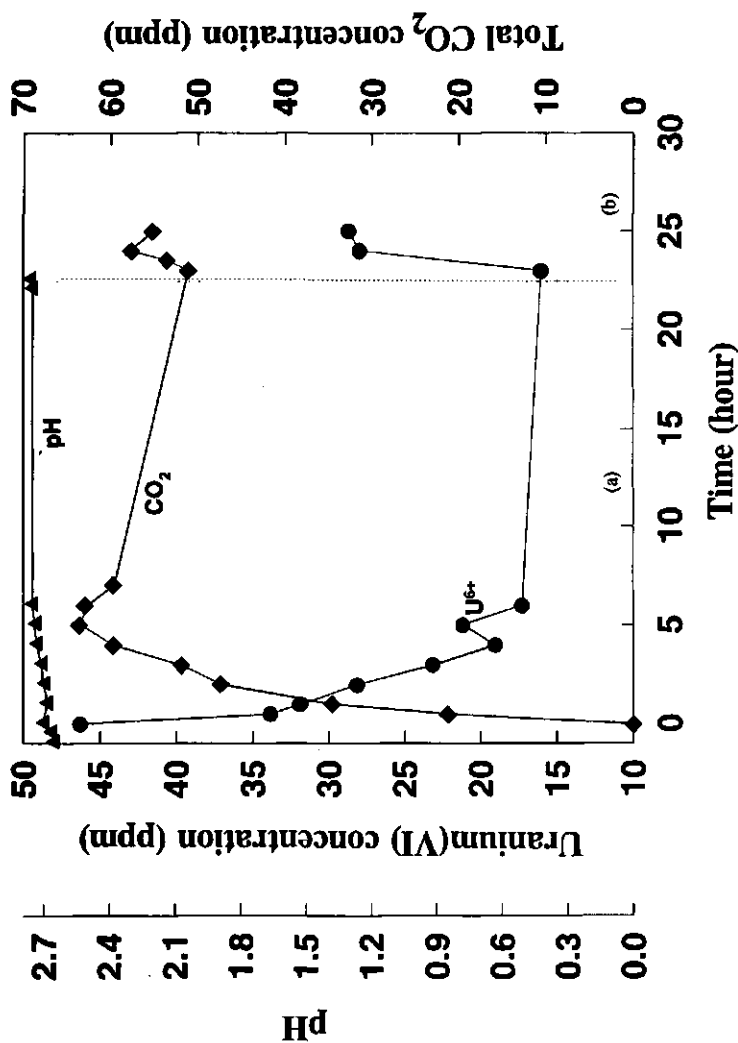


Fig.5.3. The photocatalyzed reductive deposition of uranium from an aqueous solution containing 50 ppm (initial concentration) of uranium(VI) on 1%Pt/TiO₂ as a function of time. Concentration of EDTA is 620 ppm. The molar ratio U⁶⁺:EDTA = 1:8, solution volume: 600 ml, catalyst 1 g/l. Region (a): illumination, Pt/TiO₂, deaerated, (b): illumination, Pt/TiO₂, aerated, closed.

ppm of EDTA and 1 g/l 1%Pt/TiO₂ at an initial pH of 2.8. All concentration data on uranium(VI) are shown in Fig.5.4. In region (a) (dark and deaerated), nearly 18% of the uranyl was adsorbed onto Pt/TiO₂ after one hour. Region (b) is the first illumination region with an N₂ atmosphere, resulting in the deposition of a total of nearly 54% uranyl (including the 18% dark adsorption in (a)) on Pt/TiO₂ in 2 hours. Region (c) is the first region where aerated exposure occurred after illumination, and nearly 100% of the deposited uranyl was reoxidized. The deaerated region (d) is the second illumination region with an N₂ atmosphere, and again about 54% uranyl was deposited. Region (e) is the second region where aerated exposure occurred; here about 60% of the deposited uranium(VI) was released into solution by reoxidization. Region (f) is the third illumination period with an N₂ atmosphere. In view of the high consumption of EDTA occurring during such prior illumination, an extra amount of EDTA amounting to one mmol was injected into the reactor at the beginning of the third illumination period. In this region, 62% uranyl deposited on Pt/TiO₂ in nearly 24 hours. During the third aerated period (region (g)), about 62% redeposited uranyl was reoxidized into solution in two hours. From regions (b) and (d) in Fig.5.4, it is apparent that the photocatalyzed deposition (reduction) and dissolution (oxidation) of uranyl on Pt/TiO₂ is largely reversible. It indicates that photocatalysis can be applied to recover complexed uranyl from wastewater, after which it can be concentrated.

Fig.5.5 shows the corresponding variations in CO₂ concentration and solution pH occurring during the experiment illustrated in Fig.5.4. During the first illumination period (region (b)), EDTA was quickly decarboxylated to yield CO₂, and uranyl was reduced and deposited. During the second illumination period in region (d), only little CO₂ (~10 ppm) was produced. Yet approximately the same amount of uranyl ions was reduced and deposited quickly. It is possible that, after the first deposition, the reaction products of EDTA that had remained in solution were not as easily oxidized or decarboxylated to CO₂ as the EDTA itself. Therefore, another mmol of EDTA was injected into the system at the beginning of the third illumination period (region (f)). It was observed that initially much CO₂ was produced during this period. Fig.5.5 shows that the pH increased with illumination time. This increase should be consistent with the occurrence of more decarboxylation in EDTA molecules. However, this deviates from the result of the experiment illustrated in Fig.5.3. This is probably because, in the case of a long period of illumination, EDTA molecules are decarboxylated more than once. The acidity of the solution is caused by the four carboxyl groups present in each EDTA molecule (see Eq.5.13). The more decarboxylation occurs in an EDTA molecule, the more acidity results.

5.3.3.2 Initial concentration of uranium(VI) 25 ppm

For a solution with an initial uranium(VI) concentration of 25 ppm and a U(VI)/EDTA ratio of 1:8, Fig.5.6 shows the photocatalyzed deposition of uranium(VI) and the release of CO₂

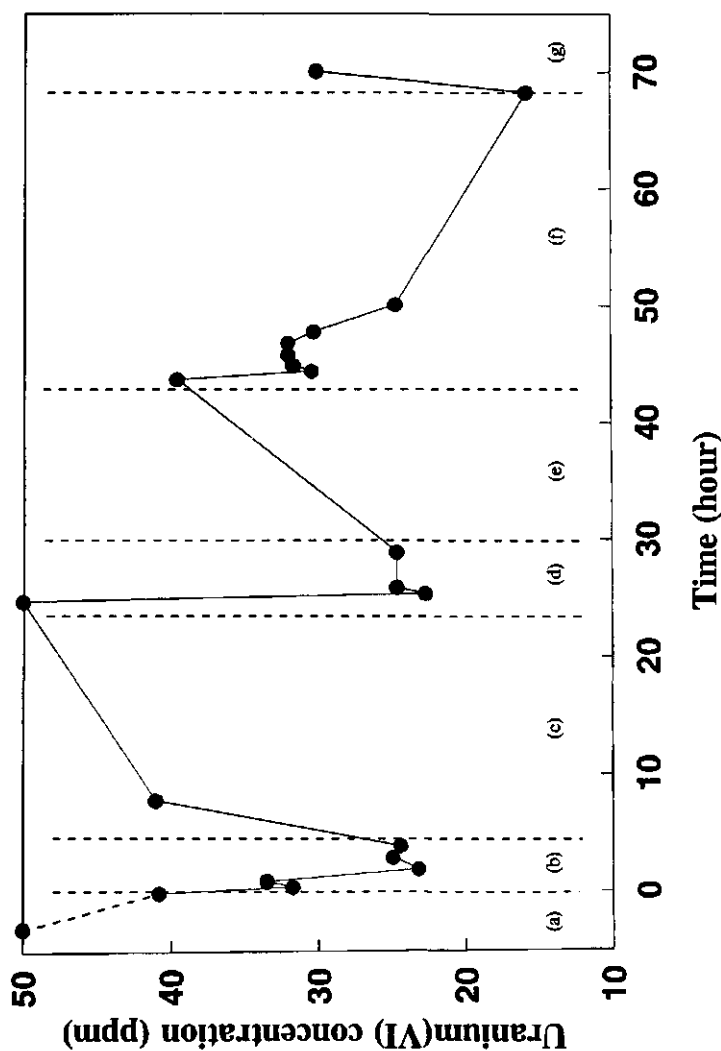


Fig.5.4. The repeatable photocatalyzed reductive deposition and reoxidation of uranium from an aqueous solution containing 50 ppm (initial concentration) of uranium(VI) on 1%Pt/TiO₂ as a function of time. Concentration of EDTA is 620 ppm. The molar ratio U⁶⁺: EDTA = 1:8, (another 1 mmol of EDTA corresponding with 223 ppm in the reaction solution was added at the 43rd hour). Solution volume: 600 ml, catalyst: 1 g/l in all regions, solution pH is given in Fig.5.5. Region (a): dark, deaerated, (b): illumination, deaerated, (c): dark, aerated, (d): illumination, deaerated, (e): dark, aerated, (f): illumination, deaerated, (g): dark, aerated.

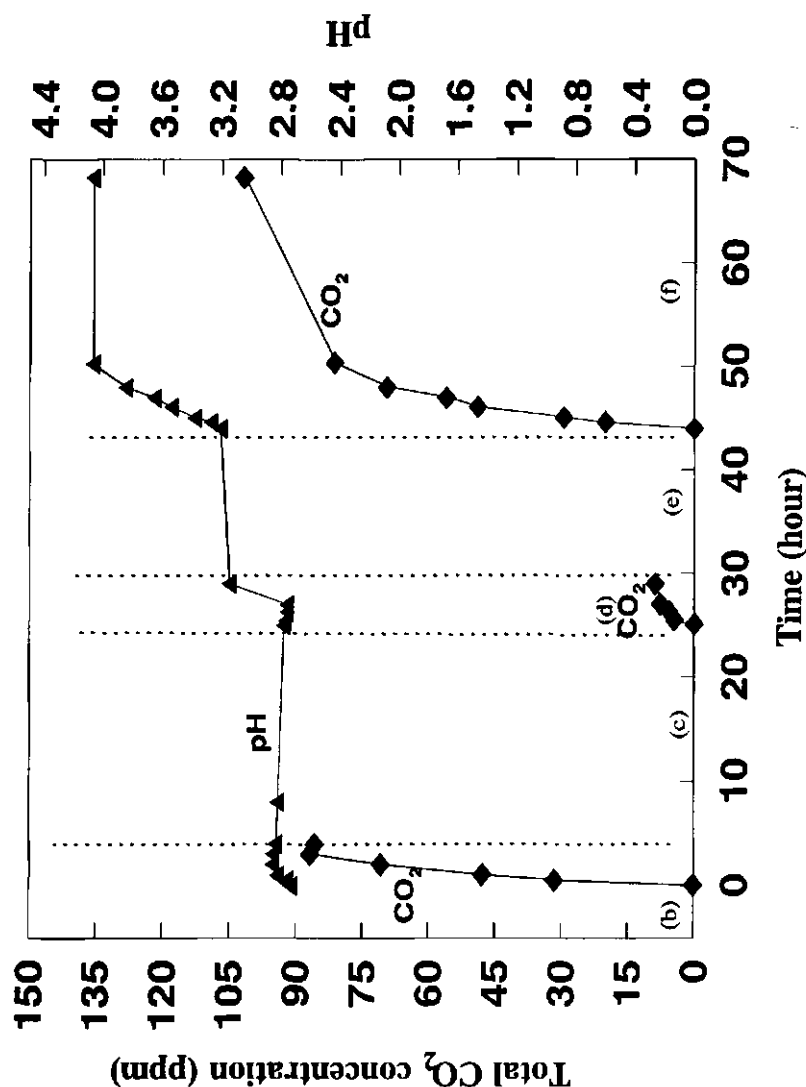


Fig. 5.5. The CO₂ and pH changes during the photocatalyzed reduction of uranium in an aqueous solution containing 50 ppm (initial concentration) of uranium(VI) on 1%Pt/TiO₂ as a function of time (the same experiment as that represented in Fig. 5.4). Concentration of EDTA is 620 ppm. The molar ratio U⁶⁺: EDTA = 1:8; (another 1 mmol EDTA corresponding with 223 ppm in the reaction solution was added at the 43rd hour). Solution volume: 600 ml, catalyst: 1 g/l in all regions. Region (b): illumination, deaerated, (c): dark, aerated, (d): illumination, deaerated, (e): dark, aerated, (f): illumination, deaerated.

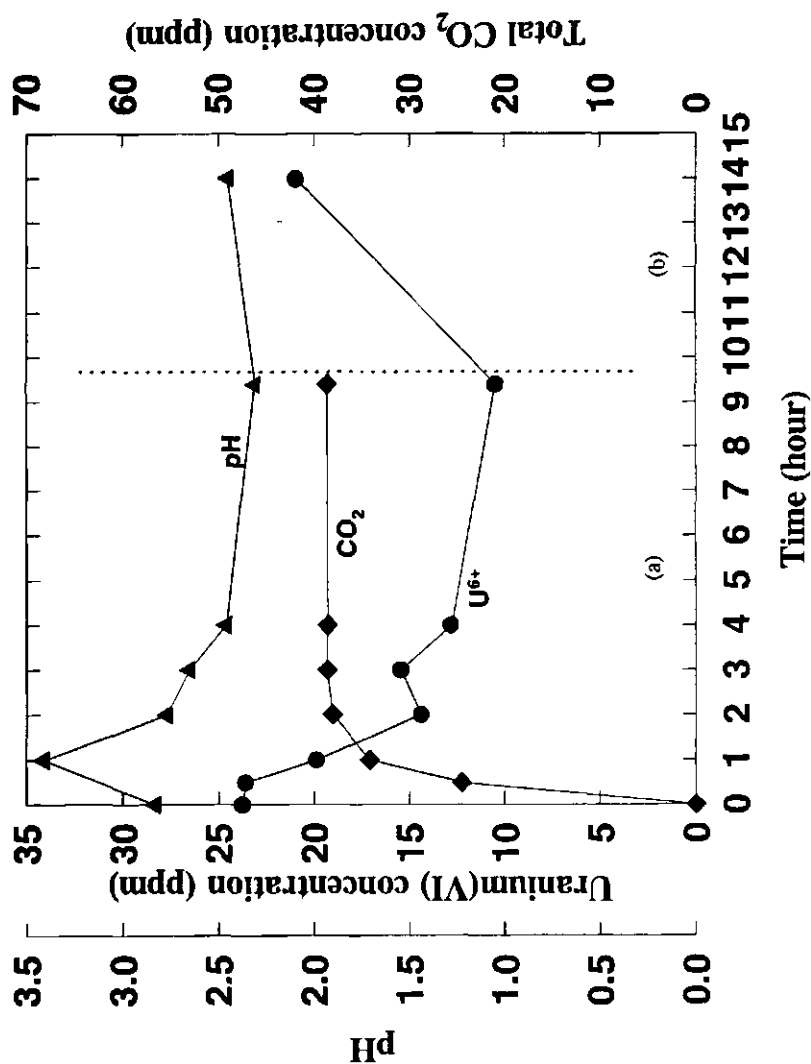


Fig.5.6. The photocatalyzed reductive deposition of uranium in an aqueous solution containing 25 ppm (initial concentration) of uranium(VI) on 1 %Pt/TiO₂ as a function of time. Concentration of EDTA is 310 ppm. The molar ratio U⁶⁺:EDTA = 1:8, solution volume: 600 ml, catalyst: 1 g/l. Region (a): illumination, deaerated, (b): dark, aerated.

as a function of time. It was observed that, after four hours of illumination, about 48% of the uranyl had deposited on Pt/TiO_2 , and this increased to about 58% in a total of nine hours. After five hours of subsequent aeration, 72% of the deposited uranium was reoxidized and dissolved in solution. With the decrease of uranyl concentration in the solution, the CO_2 release follows the uranyl deposition at a fast rate first, and no increasing at the end. During this experiment, the release of CO_2 expressed in mole corresponded with a complete (100%) single-step decarboxylation of EDTA in two hours. This corresponds with the situation where the uranium(VI) concentration is 50 ppm.

Fig. 5.7 confirms the reversibility of deposition and dissolution of 25 ppm of uranium(VI) in the presence of Pt/TiO_2 . During the two periods, region (a) (illumination, deaerated) and region (b) (dark, aerated) were similar to those presented in Fig. 5.6. During the second illumination period (region (c)), there was initially 21.3 ppm of uranium(VI) in solution, of which 28% was deposited in nine hours and 35% in about twenty-four hours. This deposition rate is slower than the one occurring during the first illumination period. The release of CO_2 in region (c) corresponds with as little as 70% single decarboxylation of EDTA in twenty-four hours, and is also much slower than the release of CO_2 occurring during the first illumination period. In region (d), 55% of the redeposited amount was reoxidized and dissolved in five hours, and 69% in twenty-three hours.

5.3.4 The most relevant factors that affect uranyl deposition and EDTA mineralization on TiO_2 or Pt/TiO_2

The highest percentages of uranium(VI) deposition observed are given in Table 5.2. From this table, it can be calculated that the highest percentage of deposition is around 50-60%; at a uranyl/EDTA ratio of 1:8, it is slightly higher than at one of 1:4. Table 5.2 also shows that platinization of titanium dioxide has only little effect on the deposition of uranyl on TiO_2 .

According to the literature, platinization of titanium dioxide results in strongly accelerated deposition of some metals⁸, such as Pb^{2+} , Mn^{2+} and Ti^{+} . However, no obvious acceleration of the deposition of uranium was observed. The reason for this difference is clear: in the former case, oxidative deposition occurs and during such deposition oxygen is normally needed as an electron scavenger. Platinum can accelerate the reduction of oxygen. The deposition of uranyl is reductive, and platinum seems unable to accelerate the electron transfer to uranyl. Figures 5.1 and 5.3 show that no more CO_2 is released after about six hours, and EDTA is almost completely converted by single decarboxylation with or without platinum.

A very important factor influencing uranyl deposition is oxygen. If any dissolved oxygen appears in the reactor, the reductive deposition stops immediately and the deposited forms of

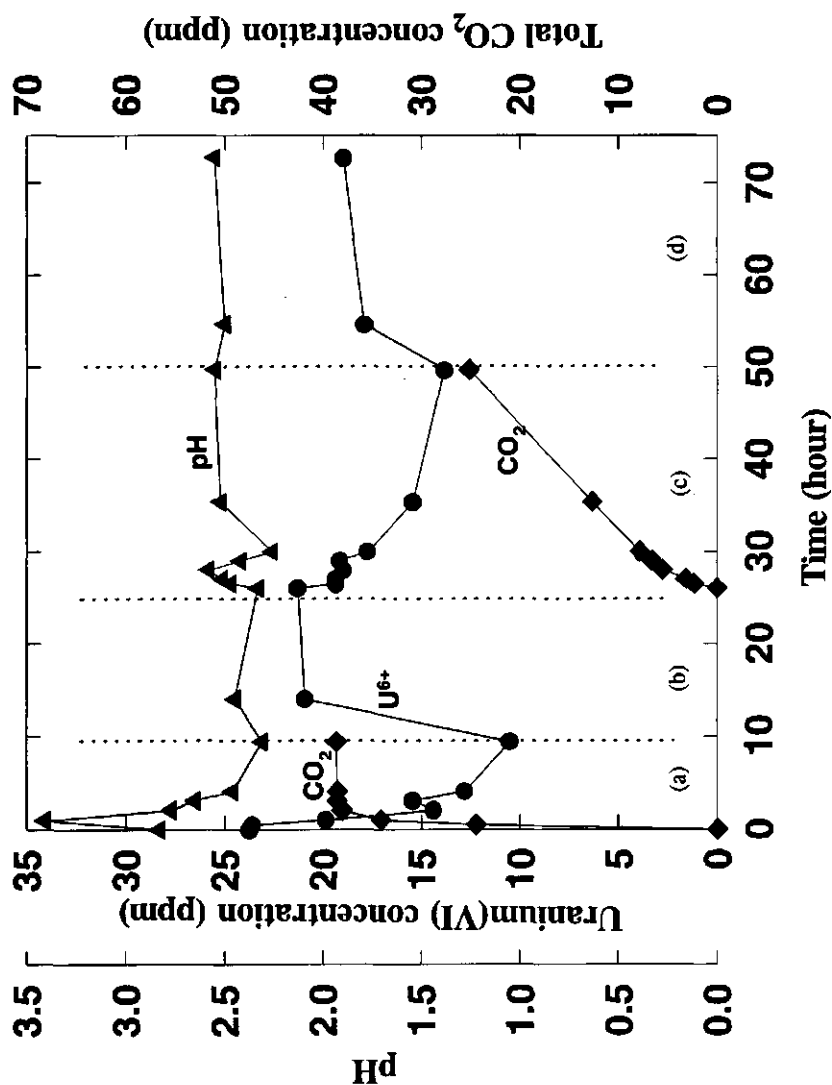


Fig. 5.7. The repeatable photocatalyzed reductive deposition of uranium in an aqueous solution containing 25 ppm (initial concentration) of uranium(VI) on 1% Pt/TiO₂ as a function of time. Concentration of EDTA is 310 ppm. The molar ratio U⁶⁺:EDTA = 1:8, solution volume: 600 ml, catalyst: 1 g/l. Region (a): illumination, deaerated, (b): dark, aerated, (c): illumination, deaerated, (d): dark, aerated.

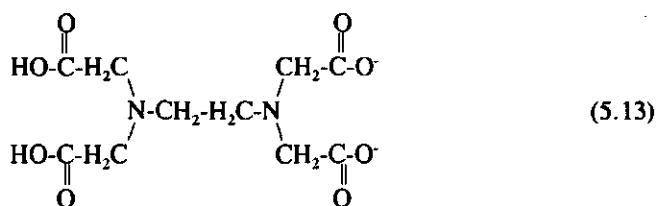
uranium are reoxidized. Therefore, oxygen seems to be a better permanent electron acceptor than uranyl: it prevents uranyl from receiving electrons and remaining on the TiO_2 surface, and reoxidizes any reduced products of uranyl deposited on TiO_2 , so these dissolve.

Table 5.2. The highest percentages of uranium(VI) deposition observed using TiO_2 and Pt/TiO_2 , and the calculated corresponding single-decarboxylation percentage of EDTA. *: the time required for reaching maximum deposition (or single decarboxylation). **: the data applying to uranium(VI) concentration obtained with the molecular uranyl/EDTA ratio as a parameter.

Catalyst	Uranium initial concentration (ppm)	Uranium deposition (%) uranyl/EDTA ratio**		Single decarboxylation of EDTA (%) uranyl/EDTA ratio	
		1:8	1:4	1:8	1:4
TiO_2	50	53%(6hrs)*	50%(4hrs)*	100%(5hrs)*	80%(4hrs)*
Pt/TiO_2	50	62%(4hrs)*	54%(5hrs)*	90%(4hrs)*	90%(4hrs)*
Pt/TiO_2	25	58%(9hrs)*		100%(2hrs)*	

5.3.5 Decarboxylation of EDTA

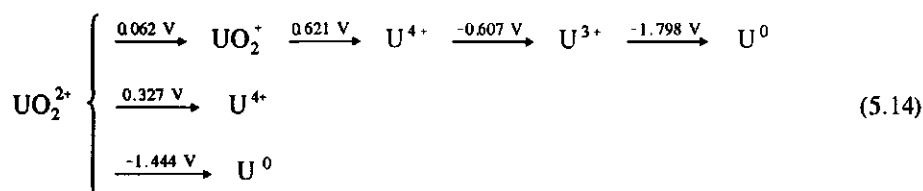
Figures 5.1, 5.2, 5.3 and 5.6 show that during most of the experiments carried out the total molar production of CO_2 was always equal to or nearly equal to the total molar amount of EDTA added to the reactor. To give a reasonable explanation for the mechanism of EDTA oxidation based on this experimental result, we propose that single decarboxylation of EDTA occurs, which may occur fully (Table 5.2) regardless of the molar $\text{U}^{6+}/\text{EDTA}$ ratio or the initial concentrations of uranium(VI) and EDTA. In spite of the fact that EDTA, the chemical structure of which is shown below, has 10 carbon atoms, the release of CO_2 shown in Table 5.2 corresponds with single decarboxylation of EDTA.



To confirm this, a blank experiment was carried out with only EDTA and Pt/TiO₂ in solution and without aeration. The results are given in Fig. 5.8, which shows the solution pH and total CO₂ production as a result of the photocatalyzed oxidation of 620 ppm of EDTA on 1% Pt/TiO₂ plotted against illumination time. The release of approximately 85 ppm or 1.93 mmol of CO₂, mentioned in this figure, approaches the total amount of EDTA present in the solution, being 1.7 mmol. The result of this "photo-Kolbe" experiment shows clearly that the maximum CO₂ production still corresponds to complete (100%) single-step decarboxylation of EDTA. Because no uranyl or other reducible reactant was present in the solution, one of the products assumed to be formed is singly decarboxylated EDTA, which may be associated with the reduction of protons (for the mechanisms, see below). According to the results of this control experiment, the reason for the limited reductive deposition of uranyl (about 50-60%) may be the complete single decarboxylation of EDTA. The resulting tricarboxylic acid can possibly not be easily oxidized further, and it renders any further reductive process of UO₂²⁺ on the negative charged cathodic area on the TiO₂ surface.

5.3.6 The possible reductive products of uranyl, and the reduction mechanism

Whether a photocatalyzed redox reaction can occur at the surface of TiO₂ depends at first on its thermodynamic properties. Reduction of uranium ions would energetically match with the band gap of TiO₂. According to the discussion given in the introduction and the possible redox electropotential of uranium compounds, we propose the following reduction scheme:



It is important to figure out what kind of reduced uranyl compound is deposited on the TiO₂ surface. Based on scheme 5.14, the only reduced products that can deposit on TiO₂ are uranium(V) (UO₂⁺) and U⁴⁺. U⁴⁺ will be present in the form of oxides deposited on TiO₂. This corresponds with the results obtained by Amadelli *et al.*¹⁸, namely that the photoreduced products of uranyl deposited on TiO₂ surfaces from solutions of uranium nitrate have a stoichiometry closely corresponding that of U₃O₈, and that they were reoxidized to U(VI) in air.

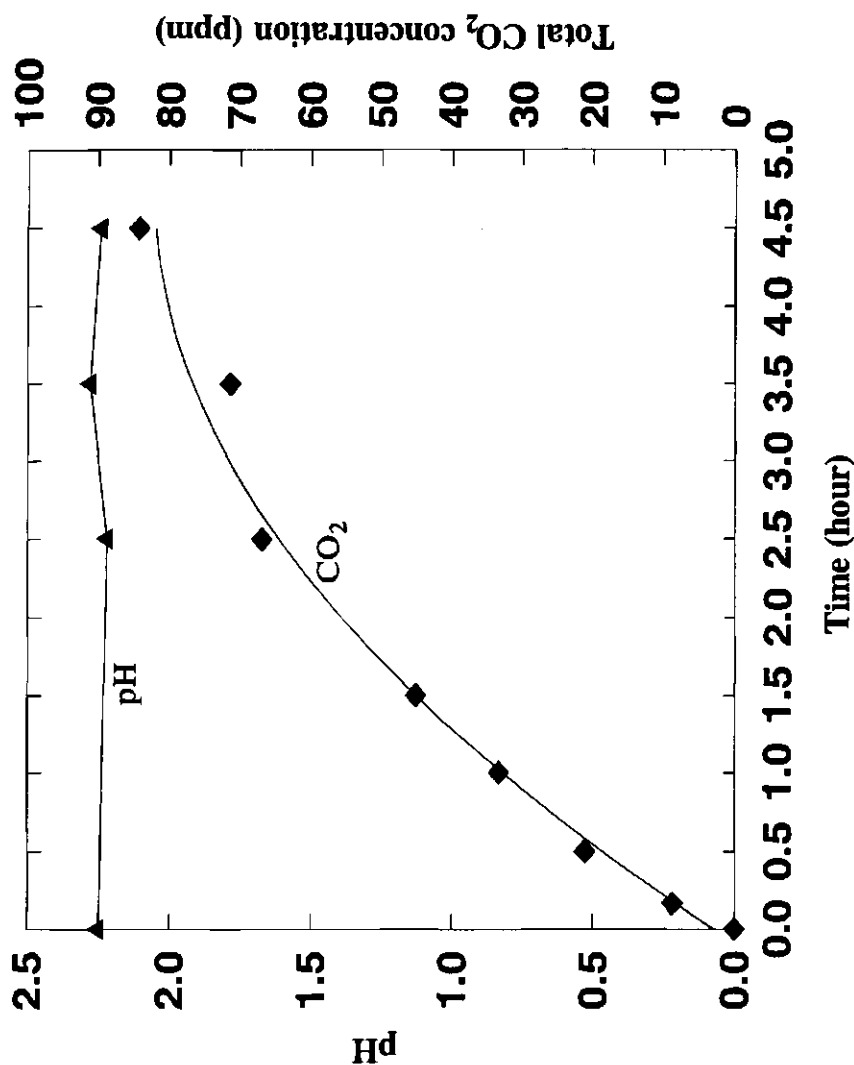
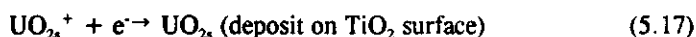


Fig. 5.8. The photocatalyzed oxidation of EDTA in an aqueous solution containing 620 ppm (initial concentration) of EDTA on 1%Pt/TiO₂ as a function of time. Deaerated, no uranyl added, solution volume: 600 ml, catalyst: 1 g/l.

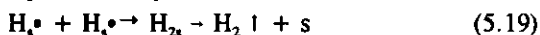
According to our experiments detailed and discussions given in Chapters 2 and 3 regarding a favorite surface-adsorption mechanism, a possible surface mechanism³⁸ for the reductive deposition of uranyl is given in the next section.

Reactions in the cathodic area of TiO_2

In deaerated system, the possible reductive reactions occurring in the cathodic area could be the reductive deposition of uranyl. The uranyl/EDTA chelate is also adsorbed in this area; uranyl accepts electrons and is reduced to a low valence uranium as follow:



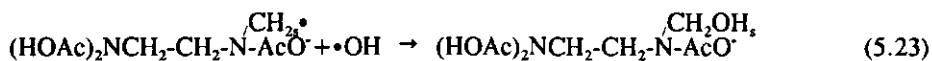
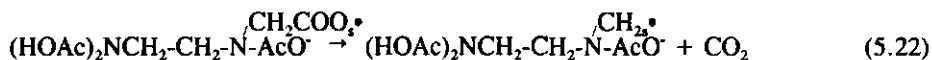
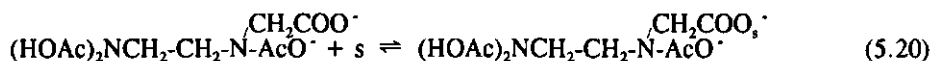
Because there is no oxygen in the system, a possible reductive reaction competitive and parallel with the reduction of uranyl in the cathodic area could be the reduction of protons in an aqueous solution resulting in either hydrogen atoms that are used during the oxidation of EDTA (see also Eq. 5.24), or hydrogen gas. The following reactions would occur:



Although we did not measure the produced hydrogen, it would have to exist in the system either as a result of a reduction reaction occurring in the cathodic area while EDTA was oxidized, or as a substrate (*e.g.*, hydrogen atoms) involved in EDTA oxidation in the anodic area as given below.

Reactions occurring in the anodic area of TiO_2

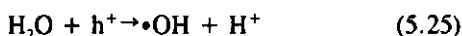
The oxidative reaction occurring in the anodic area may be EDTA oxidation. During our experiments, the release of carbon dioxide from EDTA was very probably caused by the decarboxylation of only one carboxyl group. It can be assumed that the oxidation process occurring in the anodic area of TiO_2 during the reduction of uranyl took place according to the following reaction scheme:



The single EDTA decarboxylation process may occur not only according to Eq.5.23 but also as follows:



Another possible oxidative reaction competitive or parallel with the oxidation of uranyl in the anodic area is the oxidation of water, resulting in hydroxyl radicals that could be used for EDTA oxidation (Eq.5.23):



5.4 CONCLUSIONS

1. Photocatalyzed deposition of uranyl complexed with EDTA on TiO_2 surfaces from an aqueous solution can occur in a deaerated system during UV illumination. The deposition efficiencies are 53% at $\text{pH} = 2.7$ on TiO_2 surfaces in six hours, and 62% at $\text{pH} = 2.8$ on Pt/TiO_2 surfaces in four hours.

2. Photocatalyzed reductive deposition of uranyl is largely reversible; it occurs when oxygen is added. The presence of dissolved oxygen in the aqueous solution or exposing the solution to air will prevent reductive deposition of uranyl and will result in rapid reoxidation of any deposited photoreduced uranyl. During our experiments, such reductive deposition followed by reoxidation can be repeated three times in one experiment.

3. Thus it appears possible to use this method for recovering uranium(VI) (uranyl) from aqueous solutions of dilute uranium(VI)-EDTA and concentrating it.

4. Platinization of TiO_2 has little effect on the reductive deposition of uranyl from solutions of U^{6+} -EDTA, although Pt has shown to accelerate the oxidative deposition of other metals on TiO_2 .
5. The amount of carbon dioxide released from EDTA during uranyl deposition corresponds with single decarboxylation of EDTA. The reason that only limited reductive deposition of uranyl occurs (around 50-60%) may be that single decarboxylation of EDTA results in tricarboxylic acid which cannot be easily oxidized further, and therefore rendering any further reductive process of uranyl on TiO_2 surfaces.

ACKNOWLEDGMENTS

Jian Chen wishes to express his gratitude for the financial support received from NCSU and the China Fujian Newland Development Company.

5.5 REFERENCES

1. *Threshold Limit Values - Discussion and Thirty-Five Year index with Recommendations*, Ed. Marshall L. Lanier, American Conference of Governmental Industrial Hygienists, 1984, Cincinnati Ohio, 2, pp. 354.
2. R.M. Orme, Proceedings of Workshop on Supercritical Fluid Processing of High Risk Waste, 1990, p. 5-7.
3. C.J. Wood, in *Radioactive Waste Technology*, Eds. A. Moghessi, H.W. Godbee, and S.A. Hobart, ASME, NY, NY, 1986 p. 551 et seq.
4. D.F. Ollis, E. Pelizzetti, N. Serpone, in *Photocatalysis Fundamentals and Applications*, N. Serpone, E. Pelizzetti, (Eds.) John Wiley & Sons Publication, 1989, pp. 603-637.
5. *Photocatalytic Purification and Treatment of Water and Air*, Eds. D.F. Ollis, H. Al-Ekabi, Elsevier Publication, Amsterdam, 1993.
6. N. Serpone, *Heterogeneous Photocatalysis at Work I. Selective Separations and Recovery of Metals from Industrial Waste Streams*, AIChE National Meeting, NYC, Nov. 1987.
7. E. Borgarello, N. Serpone, G. Emo, R. Harris, E. Pelizzetti and C. Minero, *Inorg. Chem.* **25**, 4499-4503, 1986.
8. K. Tanaka, K. Harada and S. Murata, *Solar Energy*, **36**(2), 159-161, 1986.
9. N. Serpone, Y.K. Ah-You, T.P. Tran, R. Harris, E. Pelizzetti, and H. Hidaka, *Solar Energy*, **39**, 491-498, 1987.
10. P. Pichat, in *Photocatalysis and Environment*, Ed. M. Schiavello, Kluwer Academic Publishers, 1988, P.399-424.

11. N. Serpone, E. Borgarello, and E. Pelizzetti, in *Photocatalysis and Environment*, M. Schiavello (Ed.), Kluwer Academic Publishers, 1988, P.527-565.
12. M.R. Prairie, B.M. Stange, and L.R. Evans, in *Photocatalytic Purification and Treatment of Water and Air*, D.F. Ollis, H. Al-Ekabi, (Eds.), Elsevier Publication, Amsterdam, 1993, P.353-363.
13. D. Lawless, A. Res, R. Harris, N. Serpone, C. Minero, E. Pelizzetti, H. Hidaka, *La Chimica & L'industria*, 72, 139-146, 1990.
14. *Radioactive Waste Technology*, A. Moghessi, H.W. Godbee, and S.A. Hobart (Eds.), ASME, NY, NY, 1986. pp. 551.
15. M.A. Sidhu, K.B. Kohli, P.V.K. Bhatia, S.S. Sandhu, *J. Radioanal. Nucl. Chem.* 187(5), 375-383, 1994.
16. (a). Yoon-Yul Park and Hiroshi Tomiyasu, *J. Photochem. Photobiol. A: Chem.* 74 11-14, 1993. (b). R. Billing, G.V. Zakharova, L.S. Atabekyan and H. Hennig, *J. Photochem. Photobiol. A: Chem.* 59 163-174, 1991.
17. Cleveland J. Dodge, and Arokiasamy J. Francis, *Environ. Sci. Technol.* 28(7), 1300-1306, 1994.
18. R. Amadelli, A. Maldotti, S. Sostero and V. Carassiti, *J. Chem. Soc. Faraday Trans.* 87(19), 3267-3273, 1991.
19. "Handbook of Chemistry & Physics" 70th edition, CRC PRESS Inc., Boca Raton, Florida, 1989-1990, p. D-151.
20. M.D. Ward and A.J. Bard, *J. Phys. Chem.* 86, 3599, 1982.
21. I. Izumi, W.W. Dinn, K.O. Wilbourn, Fu-Ren F. Fan, and A.J. Bard, *J. Phys. Chem.*, 84, 3207-3210, 1980.
22. T. Kobayashi, H. Yoneyama, and H. Tamura, *J. Electrochem. Soc.* 130, 1706-1711, 1983.
23. Gyoichi Nagomi, *J. Electrochem. Soc.* 139(12), 3415-3421, 1992.
24. S.S. Sandhu, R.J. Singh and S.K. Chawla, *J. Photochem. Photobiol. A: Chem.* 52 65-68, 1990.
25. K. R. Howes, A. Bakac, and J. H. Espenson, *Inorg. Chem.* 27, 791-794, 1988.
26. V. Natarajan, S.V. Godbole, A. Argekar, A.G. Page, M.D. Sastry, P.R. Natarajan, *J. Radioanal. Nucl. Chem., Letters*, 165(4) 255-261, 1992.
27. S.P.S. Badwal, M.J. Bannister, and M.J. Murray, *J. Electroanal.*, 168, 363, 1984
28. *Standard Methods for the Examination of Water and Wastewater*. Published by American Public Health Association, 16th Edition, 1985.
29. "Photometric Determination of Traces of Metals," Hiroshi Onishi, 4th edition, Wiley-Interscience Publication, Vol.3, Part IIB, P.608-668, 1989.
30. (a). K. Ohshita, H. Wada and G. Nakagawa, *Analytica Chimica Acta*, 149, 269-279, 1983.; (b). I. Brčić, E. Polla and M. Radošević, *Analyst*, 110, 1463-1465, Dec. 1985; (c). E.A. Jones, *Analytica Chimica Acta*, 169, 109-115, 1985; (d). I. Brčić, E. Polla and M. Radošević,

Mikrochimica Acta [Wien], **II**, 187-193, 1985.

31. S. Abe, M. Takahashi, *J. Radioanal. Nucl. Chem. Articles*, **90**(2), 247-254, 1985.

32. S. Abe, and K. Ojima, *Mikrochimica Acta [Wien]*, **III**, 309-319, 1986.

33. C.H. Ho and D.C. Doern, *Can. J. Chem.*, **63**, 1100, 1985.

34. *Complex Compounds of Uranium*, Editor I.I. Chernyaev, Israel Program for Scientific Translations, Jerusalem, 1966, p. 327.

35. B. Ohtani, Y. Oknagawa, S. Nishimoto and T. Kagiya, *J. Phys. Chem.* **91**, 3550, 1987.

36. J. Cunningham and S. Srijaranai, *J. Photochem. Photobiol. A*, **43**(3) 329-335, 1988.

37. H.D. Burrows and T.J. Kemp, *Chem. Soc. Rev.* **3**(2) 139-165, 1974.

38. B. Kraeutler and A.J. Bard, *J. Am. Chem. Soc.* **100**(19), 5985-5992, 1978.

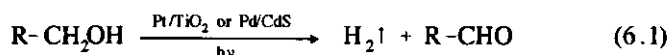
CHAPTER 6 PHOTOCATALYTIC DEHYDROGENATION OF ETHANOL ON M/CdS USING VISIBLE LIGHT, AND THE ROLES PLAYED BY PHOTOCATALYST PROMOTERS

This Chapter is based on:

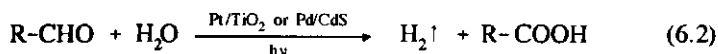
1. Photocatalytic Dehydrogenation of Aqueous Ethanol Solution Under Visible Light Irradiation, Qixing Zhuang, Jian Chen, Kangping Wang, *Journal of Xiamendaxie (Natural Science)*, 27(4), 414-420, 1988.
2. Effect of Promoters on the Photocatalytic Dehydrogenation Behavior of Aqueous Ethanol Solution, Qixing Zhuang, Jian Chen, Zenghua Wang, *Journal of Xiamendaxie (Natural Science)*, 27(5), 537-542, 1988.

6.1 INTRODUCTION

Photocatalytic dehydrogenation of alcohols under deaerated conditions using visible light and a catalyst such as Pt/TiO₂ or Pd/CdS has been studied extensively over the last 20 years^{1,2,3,4,5}. Under deaerated conditions, photocatalytic dehydrogenation of C₁ - C₄ alcohols in water yields hydrogen gas and aldehydes, and these aldehydes can be dehydrogenated further to form carboxylic acids. Such dehydrogenation comprises, in fact, oxidation reactions. For example:



Eq.6.1 is a self-redox reaction. Aldehydes can be dehydrogenated further according to:



In the case of C₁ - C₄ alcohols, Eq.6.1 and 6.2 have a reaction free energy of ΔG_{298}^0 in the order of 22 to 56 KJ/mol. Such reactions are storing energy reactions with a free energy of $\Delta G > 0$. Compared with other storing energy reactions, such as the decomposition of water ($\Delta G_{298}^0 = 237$ KJ/mol), their free energies are very low. The photocatalytic dehydrogenation of alcohols in deaerated systems is assumed to have a higher photo-utilization efficiency than the photocatalytic decomposition of water. The reactions given in Eq.6.1 and 6.2 can be used to treat wastewater containing alcohols and to simultaneously generate energy (in the form of hydrogen) by photo-utilization (visible light or sunlight). In addition, photocatalysis may be applied for chemical redox synthesis (for an example, see Eq.6.1).

A semiconductor such as Pt/TiO₂ or Pd/CdS can be used as a photocatalyst to promote the reactions given in Eq.6.1 and 6.2. The semiconductor CdS has a smaller band gap (2.42 eV) and a more negative flat band potential (~ -0.4 Volt) than TiO₂ (3.03 eV and ~ -0.05 Volt, respectively) (see Fig.1.7 in Chapter 1). Compared with TiO₂, CdS has a much higher photo-utilization efficiency in visible light and produces hydrogen gas at a higher rate. Metallization of TiO₂ with platinum or palladium, which increases the rate of photocatalytic alcohol oxidation in aerated systems, was presented in Chapters 2 and 3. Several authors^{6,7,8,9,10,11,12} observed that also in deaerated systems metallization of TiO₂ increases the rate of photocatalytic alcohol dehydrogenation. In heterogeneous catalysis, not only platinum and palladium but also transition metals such as rhodium, copper and silver have been applied as oxidation or dehydrogenation catalysts. Additionally, such substances have been used in photocatalysis¹³. The way in which metal(M)-modified CdS photocatalysts are prepared and

are pretreated at a high temperature greatly influences their photocatalytic dehydrogenation activity^{14,15,16}.

The aim of the research reported in this chapter is to further raise the photocatalytic activity of the photocatalyst CdS metallized with platinum or palladium, *e.g.*, Pt/CdS and Pd/CdS. In the case of Pt/CdS and Pd/CdS, such metals as rhodium, copper and silver and their compounds act either as a promoter or as a second metallic component (M_2) (*i.e.*, $M_2 + M_1/\text{CdS}$). X-ray Photoelectron Spectroscopy (XPS) and Transmission Electron Microscopy (TEM) are employed to investigate the surface state of catalysts, such as metal distribution, valence, energy states, and catalyst particle size. With respect to these photocatalysts, this chapter also discusses the effect of other reaction parameters on the rate of the photocatalytic dehydrogenation of ethanol, such as the amount of photocatalyst in solution, the ethanol concentration, and the reaction temperature.

6.2 EXPERIMENTAL

6.2.1 Reagents

The cadmium sulphide (CdS) used was spectrum-pure CdS from Shanghai First Reagent Company. Shanghai reagent companies also supplied the following analytically pure reagents: the ethanol used during the photocatalytic dehydrogenation experiments; palladium dichloride (PdCl_2), palladium nitrate ($\text{Pd}(\text{NO}_3)_2$), palladium black, chloroplatinic acid ($\text{H}_2\text{PtCl}_6 \cdot 6\text{H}_2\text{O}$) and platinum black, which were used to prepare the photocatalysts Pd/CdS and Pt/CdS; rhodium and dirhodium trioxide, which were used to prepare Rh/CdS and $\text{Rh}_2\text{O}_3/\text{CdS}$; (powder) silver and its compounds with nitrate (AgNO_3), acetate (AgAOc), carbonate (Ag_2CO_3) and oxide (Ag_2O); and (powder) copper and its compounds with acetate ($\text{Cu}(\text{AOc})_2$) and oxide (CuO and Cu_2O), which were used to prepare monometallized and bimetallized photocatalysts; glacial acetic acid and hydrazine hydrate ($\text{N}_2\text{H}_4 \cdot 2\text{H}_2\text{O}$), which were used to prepare photocatalysts. All these reagents were used without further purification.

6.2.2 Preparation of photocatalysts

6.2.2.1 Preparation of the photocatalyst Pd/CdS, and its pretreatment before use

The photocatalyst Pd/CdS used during XPS, TEM experiments and reaction parameter research was prepared by employing the chemical deposition method detailed below. Spectrum-pure (ultra analytical pure) CdS powder was dispersed in two PdCl_2 solutions of different temperature. The weight ratio between Pd and CdS was 5% (*i.e.*, a mole ratio of 6.67%). One solution was kept at 25°C, whereas the other was kept at 60°C, and both solutions were stirred

for two hours. Surplus hydrazine hydrate was added drop by drop to the solutions to ensure that all Pd^{2+} ions were reduced and deposited on CdS surfaces in the form of Pd^0 . The slurry was stirred for another 24 hours, and then centrifuged. The collected solid Pd/CdS was washed eight times with distilled water, dried at 100°C for two hours, and then ground to fine particles. The photocatalyst was pretreated before use by heating it in an N_2 flow for two hours at 673 K , and was then allowed to cool down at ambient temperature. The pretreated photocatalyst was stored in N_2 gas to preserve it before use.

6.2.2.2 The preparation of a monometallic-component photocatalyst (M/CdS), and its pretreatment before use

Monometallic-component photocatalysts (M/CdS , where M (metal) consisted of Pd, Pt, Cu, Ag or Rh), which were compared with double-metal-component photocatalysts, were prepared by employing four methods. Before preparation, plain CdS was pretreated in an N_2 flow for two hours at 360°C . The various proportions in which the various metals and CdS were combined are given in the discussion section.

Method 1. Physical mixing. CdS and metal powder were ground and then mixed carefully in a mortar.

Method 2. Chemical deposition. CdS powder was dispersed in a metal-ion solution, and then hydrazine hydrate was slowly added to the solution to reduce all metal ions and to deposit them on CdS surfaces. The catalyst was pretreated in an N_2 flow for two hours at 360°C .

Method 3. Heat decomposition. CdS powder and salt containing one of the metals were ground, mixed physically, and then left in an N_2 flow for two hours at 360°C to decompose the metal salt and deposit it on CdS surfaces.

Method 4. Photodecomposition. A physical mixture of CdS and Ag_2O ($\text{Ag}_2\text{O}/\text{CdS}$) was photodecomposed by illumination with a 250-W halogen lamp to produce Ag/CdS .

6.2.2.3 Preparation of bimetalized photocatalysts ($\text{M}_2+\text{M}_1/\text{CdS}$)

Bimetalized photocatalysts consisting of two metals on CdS ($\text{M}_2+\text{M}_1/\text{CdS}$) were prepared by employing five methods. Before preparation, plain CdS was pretreated in an N_2 flow for two hours at 360°C . The various proportions in which the various metals and CdS were combined are given in the discussion section.

Method 1. Physical mixture (Phys. mix.). CdS and metal powders M_1 and M_2 in certain proportions were ground and then thoroughly mixed in a mortar.

Method 2. Physical mixing and photodecomposition (photodecomp.). The main catalyst, M_1/CdS , was prepared by physical mixing and then pretreated by heating it in an N_2 flow for two hours at 360°C . Next, it was ground, mixed with an M_2 salt, and then photodecomposed by irradiation.

Method 3. Heat (Heat decomp.). CdS , M_1 and M_2 were mixed, ground, and then heated in an N_2 flow for two hours at 360°C . Before use it was ground again.

Method 4. Chemical deposition (Chem. depos.) and physical mixing. The main catalyst, M_1/CdS , was prepared by chemical deposition, pretreated and ground. Before use it was mixed with a metal powder (M_2) in a mortar.

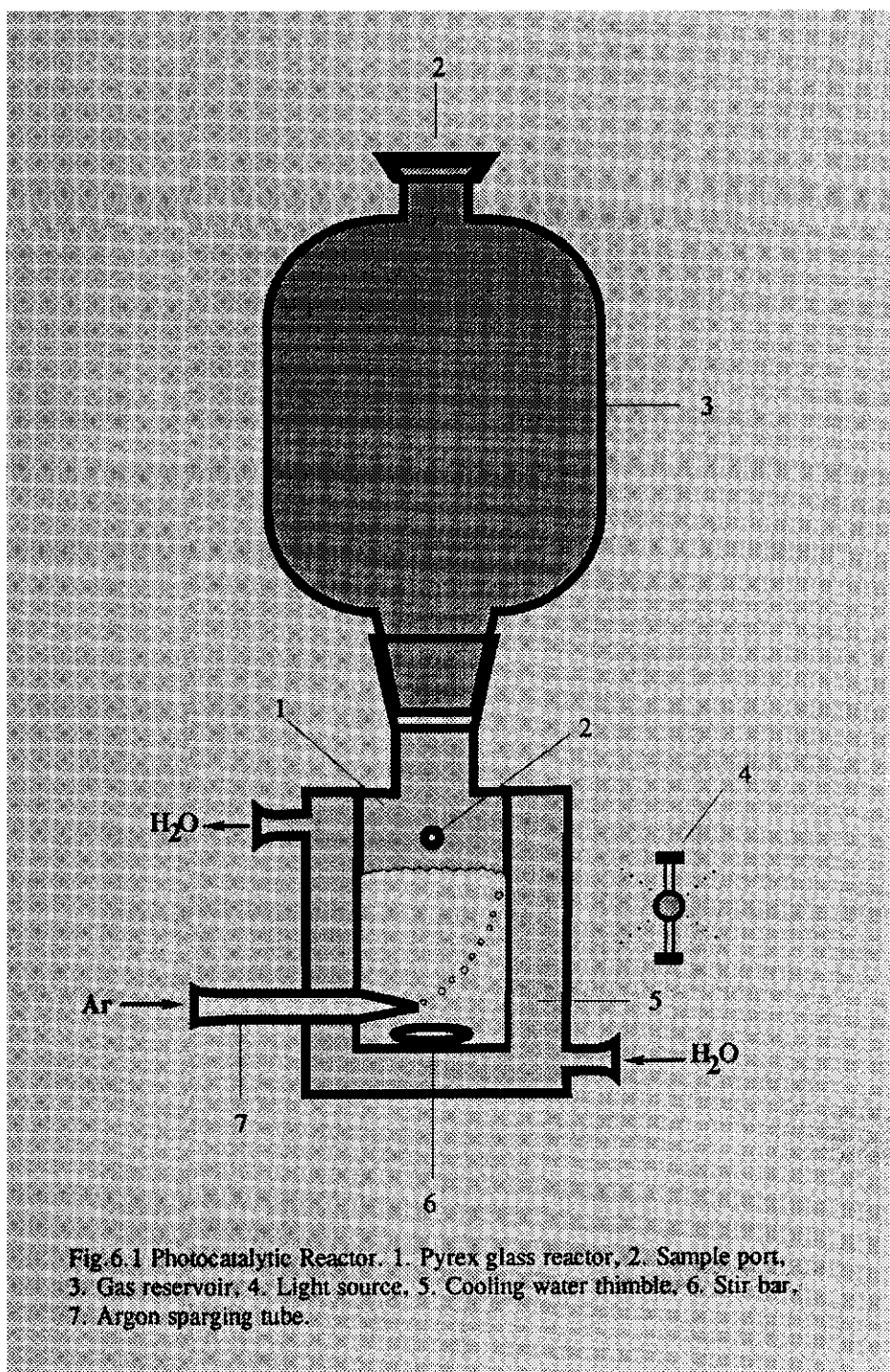
Method 5. Chemical deposition and heat decomposition. The main catalyst, M_1/CdS , was prepared by chemical deposition, ground, mixed with an M_2 salt, and then heated in an N_2 flow for two hours at 360°C . Before use it was ground again.

6.2.3 Reaction apparatus

All experiments were carried out under deaerated conditions in a sealable, 58-ml photoreactor made from Pyrex glass with a 165-ml gas reservoir at the top and a cooling water thimble (see Fig. 6.1).

6.2.4 Reaction procedure

All photocatalytic experiments were carried out according to the following procedure, except where indicated otherwise. 30 ml of 20% (by volume) ethanol in water was put into the photoreactor. Next, 0.1 g of photocatalyst was added. The solution was stirred magnetically, and argon gas was sparged through it for 20 minutes to expel all oxygen from the system. Then the reactor was sealed, and the reaction temperature was kept at 50°C using a water bath. A 250-W halogen lamp (only visible light) was used to illuminate the solution. The pH of the original solution was approximately 6.0 and was not adjusted before illumination. The experimental procedure followed during the control experiments to test the dark reaction (without illumination) and the photo reaction (without photocatalysts) was similar to the one followed during the photocatalytic experiments. Periodically, 100- μl gas samples and 1- μl liquid samples were taken from the reactor and directly injected into a gas chromatograph for analysis.



6.2.5 Analysis of products

Hydrogen gas was determined using a gas chromatograph (102G, Shanghai) fitted with a thermal conductor detector (TCD) and a 2-m column containing a 60 ~ 80 mesh 5A molecular sieve. Acetaldehyde and other dehydrogenated products were determined using a gas chromatograph (SP-2305, BEIJING) fitted with a flame ionization detector (FID) and a 2-m column containing 80 ~ 120 mesh microporous polymer beads (Chromosorb 102).

6.2.6 Surface-structure measurements

The specific surface area of all catalysts was measured by employing the dynamic BET method, using N_2 as an adsorbate. The size and number of CdS and Pd particles deposited on plain-CdS surfaces were measured based on pictures made with a Transmission Electron Microscope (TEM). The binding energies of catalyst components were determined by X-ray Photoelectron Spectroscopy (XPS).

6.3 RESULTS AND DISCUSSION

6.3.1 The effect of the amount of photocatalyst Pd/CdS suspended in solution on the photocatalytic dehydrogenation of ethanol

Because during photodegradation of ethanol in visible light under deaerated conditions hydrogen gas is the only photocatalytic reduction product, it is justified to use the production of hydrogen (H_2 ml/h) as a measure for the activity of the photocatalyst. During the control experiments carried out to test the dark reaction (without illumination) and the photo reaction (without photocatalyst), neither H_2 nor aldehyde products were detected in the gas and liquid phases, which means that in this deaerated system neither a heterogeneous catalytic reaction nor a photolytic reaction can occur. Plain CdS shows hardly any photocatalytic activity during ethanol dehydrogenation (about 0.03 ml of H_2 per hour of illumination). Therefore it can be concluded that reduction product hydrogen and main dehydrogenative product acetaldehyde result only from the photocatalytic reaction with ethanol occurring at Pd/CdS.

Fig.6.2 shows the relationship between hydrogen gas production and illumination time. From this figure it can be concluded that during a period of six hours the produced amount of hydrogen increased almost linearly with illumination time. When during our experiments the Pd/CdS photocatalyst was illuminated for twelve hours, its photoactivity did not significantly decrease. From literature¹⁷ it is known that, when illuminated to produce electron-hole pairs, some semiconductors (such as CdS) oxidize (or reduce) themselves instead of oxidizing or reducing substrates in solution. This process is called photocorrosion of semiconductors.

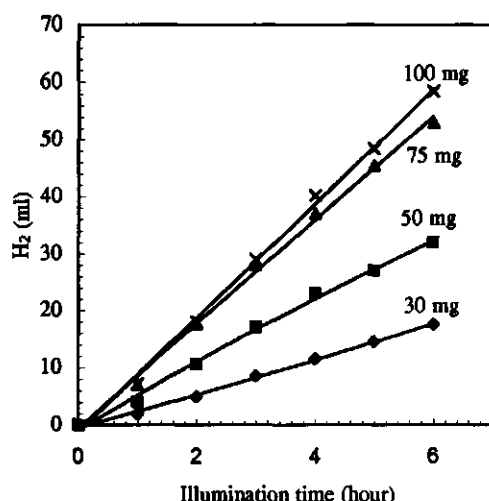


Fig. 6.2 The photocatalytic dehydrogenation of ethanol (H_2 production) vs. illumination time. Solution: 30 ml (20% volume ethanol). The amount of 5%Pd/CdS is shown in graph. Deaerated system, initial pH = 6.0, 50 °C, the other conditions are given in section 6.2.4.

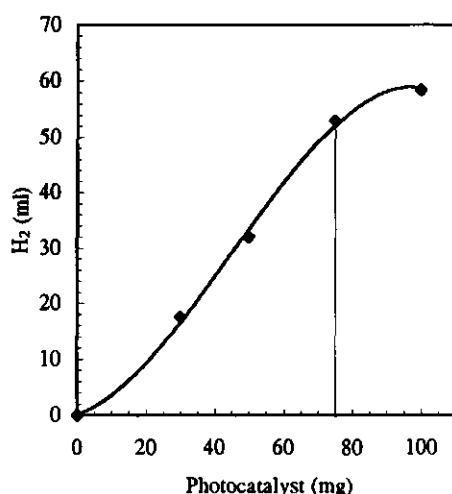


Fig.6.3 The relationship between the amount of 5%Pd/CdS and H_2 production. Illumination time: 6 hours. Solution: 30 ml (20% volume ethanol). Deaerated system, initial pH = 6.0, 50 °C, the other conditions are given in section 6.2.4.

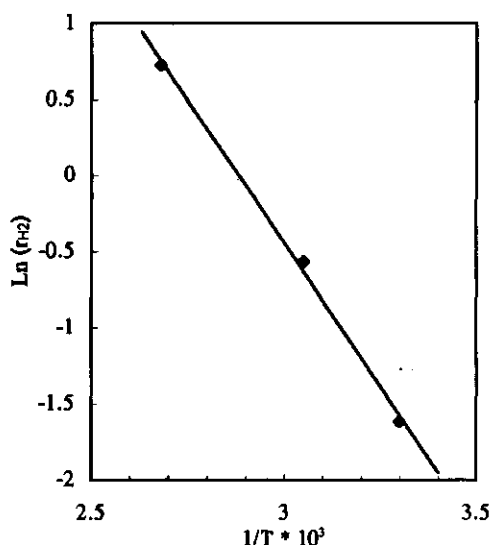


Fig.6.4 The Arrhenius relationship between reaction temperature (T) and the photocatalytic dehydrogenation rate (r_{12}) of ethanol.

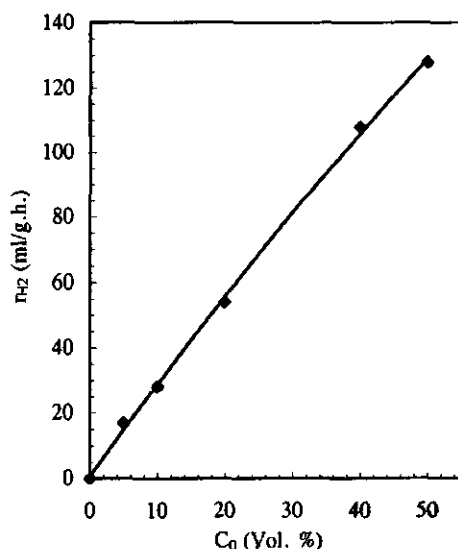


Fig. 6.5 The effect of initial ethanol concentration C_0 on the rate of hydrogen production. Solution: 30 ml. Catalyst: 0.1 g. 5%Pd/CdS, deaerated system, initial pH = 6.0, 50 °C, the other conditions are given in section 6.2.4.

Photocorrosion greatly decreases the photostability and photocatalytic activity of photocatalysts. This explains why no photocatalytic dehydrogenation was observed during the experiment represented in Table 6.1 during which plain CdS was used. However, Fig. 6.2 demonstrates that the photostability and photo life-span of CdS can be greatly improved by metallizing palladium on it. Fig. 6.3 shows the relationship between the amount of 5%Pd/CdS photocatalyst present and the amount of hydrogen gas produced. According to this figure, 75 mg of catalyst (which equals 2.5 mg/ml) is the optimum amount of catalyst in our reaction system, and the production of hydrogen reached a level of 300 ml per hour or 120 ml per hour per gram of catalyst. At catalyst concentrations in excess of 2.5 mg/ml, the hydrogen production hardly increased with an increase in the amount of catalyst. This may be due to the photo-screening effect that causes photons to penetrate less deeply at higher photocatalyst concentrations.

6.3.2 The effect of the particle size of deposited palladium on the photocatalytic activity of CdS

The photocatalytic activity of M/CdS is strongly affected by the average diameter (D) of metal particles, the average number (n) of deposited metal (M) particles per CdS particle, and the surface coverage (θ) of metal particles on CdS. Based on pictures made by TEM, the diameters of CdS and Pd particles were measured and the surfaces of plain CdS and two Pd/CdS photocatalysts were observed. All substances were pretreated at a high temperature. It was assumed that all CdS particles and all metal particles deposited on them were spherical. The diameter of photocatalyst particles can be calculated using Eq. 6.3, where D is the weight average diameter of particles, and N_i the number of particles with diameter D_i visible in a TEM picture. The number of metal particles deposited on a CdS particle can be calculated using Eq. 6.4, where n is the average ratio between the number of metal particles and the number of CdS particles, X the molar fraction of the metal present on the CdS particles, D_m the weight average diameter of metal particles, D_s the weight average diameter of CdS particles, d_m the metal density, and d_s the CdS density. The average surface coverage (θ) of metal deposited on CdS is expressed in Eq. 6.5.

$$D = \frac{\sum_i N_i D_i^3}{\sum_i N_i D_i^2} \quad (6.3)$$

$$n = \frac{X d_s D_s^3}{(1-X) d_m D_m^3} \quad (6.4)$$

$$\theta = \frac{X d_s D_s}{4(1-X) d_m D_m} \quad (6.5)$$

To evaluate photocatalyst quality, the production of hydrogen gas from various photocatalysts was measured. For the photocatalyst 5%Pd/CdS, Table 6.1 gives the diameter of cadmium-sulphide and palladium particles, the values for particle ratio and surface coverage calculated using Eq. 6.4 and 6.5, and their effect on the photocatalytic dehydrogenation of ethanol in the

form of H_2 production (ml/h.g.). The mean particle diameter D given in Table 6.1 was calculated by using Eq.6.3 and observing about 200 particles on TEM pictures.

Table 6.1 shows that, compared to Pd/CdS (2), the diameter of the palladium particles deposited on Pd/CdS (1) is smaller. Both Pd/CdS (1) and Pd/CdS (2) were pretreated at the same high temperature. The procedures followed for preparing Pd/CdS (1) and Pd/CdS (2) differed only in solution temperature. This difference in temperature resulted in a different size and distribution of the metal particles on the CdS surface. A low reduction temperature generates smaller deposition particles of metal than a high temperature. Therefore, the smaller diameter of the palladium particles in the catalyst Pd/CdS (1) compared to those in the catalyst Pd/CdS (2) is due to the lower reduction temperature at which Pd/CdS (1) was treated compared with Pd/CdS (2). According to Eq.6.5, a smaller diameter of palladium particles results in a higher surface coverage.

Table 6.1 Particle diameter (D), the particle ratio (n) between Pd and CdS, and the surface coverage Θ of the 5%wt. Pd on CdS, and the effect of these factors on the photocatalytic dehydrogenation of ethanol (hydrogen production).

	CdS	Pd in Pd/CdS (1)	Pd in Pd/CdS (2)
Diameter D (nm)	33.8	7.9	8.8
Coverage Θ (%)		3.2	2.9
Particle ratio		2.4	1.7
Rate of H_2 production (ml/h.g.)	0.01	120	60.6

Pd/CdS (1) was prepared by chemical reduction at 25°C , whereas Pd/CdS (2) was prepared by chemical reduction at 60°C . All catalysts listed in Table 6.1 were pretreated in an N_2 flow for two hours at 360°C . Hydrogen production is defined as the number of ml of hydrogen produced per hour per gram of catalyst (ml/h.g.).

Table 6.1 also shows that, although compared to Pd/CdS (2) the diameter of the palladium particles in Pd/CdS (1) was only about 10% smaller and their surface coverage only about 10% higher, the photocatalytic activity of Pd/CdS (1) was nearly twice as high as that of Pd/CdS (2). Although it does not seem logical that a 10% decrease in the size of palladium particles and a 10% increase in palladium coverage can raise the photocatalytic activity of Pd/CdS by nearly 100%, it can be explained by considering the effect of a decrease in particle diameter

on the number of particles. According to a calculation made, a 10% decrease in the diameter of palladium particles increases the number of palladium particles by 41% (see particle ratio in Table 6.1). Increasing the number of palladium particles means increasing the number of places where photocatalytic reduction can occur. A hydrogen molecule is 2.3 \AA (0.23 nm) in diameter and occupies only 0.1% of the surface of a palladium particle with the diameter of 80 \AA (8 nm). If the surface of such a palladium particle contains sufficient electrons, from a geometrical viewpoint it can simultaneously produce far more hydrogen molecules. Because smaller particles are more active, a 41% increase in the number of particles can raise the H_2 production (or photocatalytic activity) by 100%. Consequently, in the case of little metal coverage (*e.g.*, so little that it does not affect the absorption of light onto CdS), the following applies: the smaller the size of deposited metal particles, the higher the activity of the photocatalyst.

6.3.3 The effect of reaction temperature on the photocatalytic activity of Pd/CdS

The effect of reaction temperature on the rate of hydrogen production (γ) is represented in Fig. 6.4. The figure shows that, in the temperature range of $305 \sim 365 \text{ K}$, the reaction rate increases with temperature. Using the Arrhenius equation, the apparent activation energy (E_a) can be calculated from Fig. 6.4, resulting in a value of 37 KJ/mol . This is only an experimental value of the activation energy. The actual activation energy (E_a) of the dehydrogenation reaction can be calculated by adding at least the absorption heat of the alcohol present on catalyst surfaces applying to this temperature range. Therefore, the actual activation energy (E_a) is somewhat higher than 37 KJ/mol , but in general it is far lower than that of general non-catalytic reactions.

6.3.4 The effect of the concentration of ethanol on its photocatalytic dehydrogenation and on CdS corrosion

Fig. 6.5 shows the effect of the concentration of ethanol on hydrogen production. According to this figure, in the concentration range of $0 \sim 50\%$ the rate at which hydrogen is produced is proportional to the initial ethanol concentration. In this range, the photocatalytic dehydrogenation of ethanol in solution in deaerated systems may be considered a first-order reaction on Pd/CdS.

Ethanol is an electron acceptor. It acts not only as a reaction substrate but also as a scavenger of holes on photocatalyst surfaces. A high ethanol concentration will accelerate the scavenging of holes from catalyst surfaces. Therefore, it can suppress the photocorrosion (oxidation) of CdS itself. During our experiments, no oxidative photocorrosion of CdS ($\text{CdS} + 2 \text{ h}^+ \rightarrow \text{Cd}^{2+} + \text{S}$) was observed. Based on the redox potentials of the reactions $\text{EtOH} \rightarrow \text{EtO}^\cdot$ ($E^\circ = +0.19 \text{ V}$) and $\text{CdS} \rightarrow \text{Cd}^{2+} + \text{S}$ ($E^\circ = +0.32 \text{ V}$), it can be concluded that, from a thermodynamic

viewpoint, oxidative dehydrogenation of ethanol can occur much easier than oxidative photocorrosion of CdS.

6.3.5 The effect of pretreatment at a high temperature on the photocatalysts CdS and Pd/CdS

Experiments have demonstrated that plain CdS shows no photocatalytic activity after being pretreated at a high temperature. Table 6.2 shows the effects of pretreatment. Pretreatment of the catalyst Pd/CdS at a high temperature is essential for raising its photocatalytic activity, which may be raised as much as 10 times.

Table 6.2 Effect of pretreatment at a high temperature on the physicochemical surface properties of photocatalysts

	CdS ^b	CdS ^a	Pd/CdS ^b	Pd/CdS ^a
Specific surface area (m ² /g)	9.49	6.78	12.22	9.2
Diameter D (nm)		33.8	10.8 (Pd)	8.8 (Pd)
Coverage Θ (%)			2.4	2.9
Conc. of surface Pd* (%)			5.32	2.68
Rate of H ₂ production (ml/h.g.)	0.01	0.01	5.10	60.6

Pd/CdS was prepared by chemical reduction at 60 °C. a: after pretreatment. b: before pretreatment. *: the data were obtained by XPS and TEM.

According to Table 6.2, pretreatment at a high temperature results in a decrease in specific surface area, a decrease in the diameter of Pd particles on surfaces, and an increase in the surface coverage by palladium particles. As a result of pretreatment, the palladium particles on CdS surfaces become smaller and show a highly dispersed island distribution. Pretreatment at a high temperature may lead to the diffusion of palladium particles at surfaces into the interior of CdS particles. This may result in a significant decrease in palladium concentration at the surfaces (Table 6.2). This phenomenon was demonstrated by both XPS and TEM. Palladium particles diffused into CdS by entering either the pores by surface diffusion, where they formed a permanent dark reduction site⁸, or (partly) the bulk, thus promoting the transfer of electrons between CdS and Pd (see Fig.3.1 in Chapter 3).

Pretreatment at a high temperature promotes strong metal and semiconductor CdS interaction (SMSI)¹⁸. Such interaction increases the fluidity of the electrons flowing from semiconductor to metal and back (see Chapter 3, Section 3.1). To examine the direction of the electron flow, the electron-binding energies in certain atomic orbits of photocatalyst components were measured by XPS. Table 6.3 shows that pretreatment at a high temperature resulted in a displacement of binding energy (also called chemical displacement) by +1.4 and +1.5 eV in the 3d orbits of cadmium, a -0.9 eV displacement in the 3d orbits of palladium, and a -0.5 eV displacement in the 2p orbits of sulphur. If the displacement is positive, the oxidative number of the element will increase, otherwise will decrease. It means that, during pretreatment at a high temperature, electrons were transferred from Cd to Pd and from Cd to S, e.g., pretreatment at a high temperature raises the capability of Pd to remove free electrons from the surface of CdS, thus making Pd an area of high electron concentration and promoting catalytic reduction of H^+ to dihydrogen.

Table 6.3 The electron-binding energy of components of 5% wt.Pd/CdS, measured by XPS

Components of 5% Pd/CdS	Binding energy (eV) ^b	Binding energy (eV) ^a	Chemical displacement (eV)
Pd, 3d _{1/2}	337.5	336.6	- 0.9
Pd, 3d _{3/2}	342.7	341.8	- 0.9
Cd, 3d _{1/2}	404.7	406.1	+ 1.4
Cd, 3d _{3/2}	411.5	413.0	+ 1.5
S, 2P	162.5	162	- 0.5

a: after pretreatment at a high temperature, b: before pretreatment at a high temperature.

6.3.6 The selectivity of the photocatalytic dehydrogenation of ethanol on Pd/CdS surfaces

In addition to the reduction product H_2 , acetaldehyde is the dominant oxidation product of the photocatalytic dehydrogenation of ethanol in a deaerated system using visible light. If in solution only acetaldehyde is produced, the stoichiometric ratio between the produced molecular H_2 and acetaldehyde is 1:1. This means that the selectivity of acetaldehyde conversion can be calculated based on the deviation from this ratio. The amounts of hydrogen and acetaldehyde produced and the dependency of the stoichiometric ratio on the amount of photocatalyst present are listed in Table 6.4. The table shows an acetaldehyde selectivity of at

least 70% at the largest amount of catalyst (100 mg). The lower the photocatalyst concentration, the higher the acetaldehyde selectivity. The chance of electron transfer increases with the amount of catalyst added. Consequently, the amounts of oxidation products increase, and this leads to a decrease in selectivity. It was observed that the solution pH decreased somewhat during the photoreaction process. Analysis by GC revealed that traces of acetic acid were responsible for this decrease; no CO_2 was detected.

Table 6.4 The effect of the amount of photocatalyst on the ratio between the photocatalytic production of hydrogen and that of acetaldehyde in 30 ml of 20% vol. ethanol. Illumination time = 6 hours; pH = 6.0, temperature = 50°C.

5% Pd/CdS (mg)	CH_3CHO (mmol)	H_2 (mmol)	$\text{CH}_3\text{CHO} : \text{H}_2$ (average)
30	0.83	0.71	1.2
50	1.26	1.44	0.9
	1.35	1.31	1.0
75	1.72	2.31	0.8
	1.72	1.88	0.9
	1.72	2.26	0.8
100	1.68	2.41	0.7
	1.80	2.49	0.7

6.3.7 The dehydrogenation activity of M/CdS photocatalysts containing a monometallic component

Table 6.5 shows the photocatalytic activities observed during ethanol dehydrogenation using various monometallized CdS photocatalysts in a deaerated system. The activities demonstrated by these photocatalysts decreased in the following order: 5% wt. Pd/CdS (chem. depos., pretreatment) > 5% wt. Pt/CdS ((a) phys.mix., with or without pretreatment, (b) chem. depos., pretreatment) > 1% wt. $\text{Rh}_2\text{O}_3/\text{CdS}$ (phys. mix., no pretreatment) >> PdO, Rh, Ag, Cu, and CuO/CdS. Plain CdS showed practically no activity, whether or not it was pretreated. Pretreatment did not raise the activity of Pt/CdS prepared by physical mixing, but it raised 10 times the activities of Pt/CdS and Pd/CdS prepared by chemical deposition. The reason for this was discussed in § 6.3.5 and is also mentioned in literature¹⁰. Deposition of silver (oxide) or

copper (oxide) on CdS does not lead to any significant photocatalytic activity, as these substances cannot act as key components on CdS surfaces contrary to Pd and Pt.

Table 6.5 The photocatalytic dehydrogenation activity of monometallic components(M) on CdS

Photocatalyst	Preparation of photocatalyst	H ₂ production (ml/h.g.)
CdS	no pretreatment, or pretreatment*	~0
5%Pt/CdS	Phys.mix., no pretreatment	17.0
	Phys.mix., pretreatment	17.2
	Chem.depos., no pretreatment	2.0
	Chem.depos., pretreatment	18.1
5%Pd/CdS	Phys.mix., no pretreatment	4.8
	Chem.depos., no pretreatment	5.1
	Chem.depos., pretreatment	60.6
5%PdO/CdS	Heat decomp.* of nitrate	1.9
5%Rh/CdS	Phys.mix., no pretreatment	1.3
1%Rh ₂ O ₃ /CdS	Phys.mix., no pretreatment	11.1
5%Ag/CdS	Phys.mix., no pretreatment	2.0
	Heat decomp. from carbonate	3.4
3.2%Ag/CdS	Heat decomp. of acetate	2.0
4.6%Ag/CdS	Photo decomp. of oxide	2.0
5%Cu/CdS	Phys.mix., no pretreatment	1.5
5%CuO/CdS	Heat decomp. of acetate	0.8
5%CuO/CdS	Phys.mix., no pretreatment	1.3
5%Cu ₂ O/CdS	Phys.mix., no pretreatment	2.5

*: Pretreatment and heat decomposition occurred both under the following conditions: in an N₂ flow for two hours at 360°C.

6.3.8 The optimum amount of platinum deposited on Pt/CdS

Fig.6.6 and 6.7 show the dehydrogenation activities in a deaerated system of Pt/CdS containing various percentages of platinum. In Fig.6.7, the average rate of hydrogen production (\bar{r}_{H_2}) increases with platinum content in the range of 1-10%. The modified platinum on the semiconductor surface acts not only as a proton-bonding adsorption centre that catalytically reduces protons to hydrogen molecules, but also as an electron pump that draws free electrons from the CdS surface and thus reduces the recombination of photogenerated electron-hole pairs. The latter phenomenon appeared from our XPS data on Pd/CdS¹⁰, and was confirmed by Pichat's data on photoconductance¹⁹.

$\Delta \bar{r}_{H_2}$, the increase in average hydrogen production rate per increased percentage of Pt, shown in Fig.6.7, is defined as:

$$(\Delta \bar{r}_{H_2})_{Pt\%} = (\bar{r}_{H_2})_{Pt\%} - (\bar{r}_{H_2})_{Pt\% - 1\%} \quad (6.6)$$

In the platinum-content range of $\leq 5\%$, an increase in platinum content always results in an increase in $\Delta \bar{r}_{H_2}$. However, in the platinum-content range of $> 5\%$ an increase in platinum content results in a sharp decrease in $\Delta \bar{r}_{H_2}$. Taking the costs of platinum into account, it is best to modify about 5% of the platinum present on the CdS surface. The decrease in $\Delta \bar{r}_{H_2}$ resulting from platinum deposition by more than 5% may be due to: (1) The fact that the surface coverage by platinum on CdS increases with an increase in the amount of platinum. It results in a photoscreening effect that causes a decrease in photoabsorption on CdS surfaces and a decrease in the generation of electron-hole pairs. (2). The fact that an increase in platinum content shortens the distance between an active oxidation position on a CdS surface and an active reduction position on a platinum island. It may result in an increase in reverse reactions between oxidation and reduction products. (3). The fact that the metal platinum is a very effective heterogeneous catalyst for reductive hydrogenation of acetaldehyde to ethanol. This means that an increase in the amount of platinum results in an increase in the rate of a dark reverse reaction during which acetaldehyde is rehydrogenated back to ethanol.

6.3.9 The dehydrogenation activity of M_2+M_1/CdS (i.e., CdS photocatalysts containing bimetallic components)

To study how the photocatalytic activity of a M/CdS catalyst could be increased, we investigated the effect of adding a second metal, M_2 (Ag, Cu or their oxides), to some of the most active metallized semiconductor photocatalysts (M_1/CdS), such as 5%Pt/CdS prepared by phys. mix. with or without pretreatment, and 5%Pd/CdS prepared by chem. depos. with

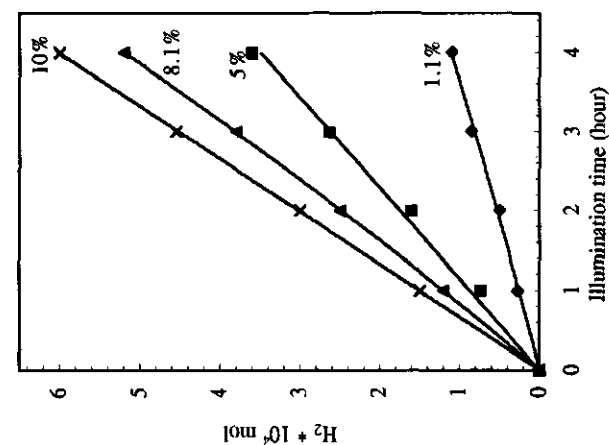


Fig. 6.6 The photocatalytic dehydrogenation of ethanol (H_2 production) vs. illumination time in the presence of Pt varying in weight% on CdS. Solution: 30 ml (20% volume ethanol). Degenerated system, initial pH = 6.0, catalyst: 0.1 g, the other conditions are given in section 6.2.4.

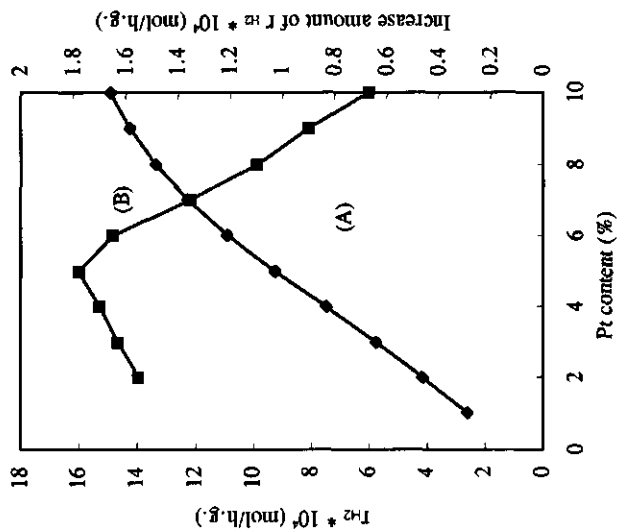


Fig. 6.7 The average H_2 production rate r_{H_2} (curve A) and the increased amount of r_{H_2} (curve B) vs. platinum content on CdS photocatalysts. Solution: 30 ml (20% volume ethanol). Initial pH = 6.0, catalyst: 0.1 g, the other reaction conditions are given in section 6.2.4.

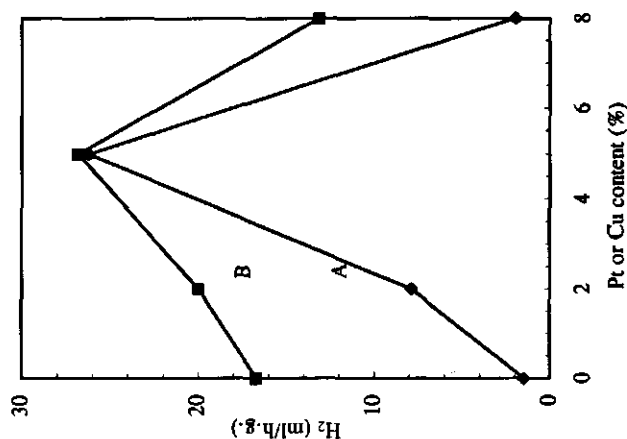


Fig. 6.8 Effects of Pt or Cu promoter content on the dehydrogenation activity of 5% Cu + Pt/CdS (Curve A) and Cu + 5% Pt/CdS (Curve B) photocatalysts. Solution: 30 ml (20% volume ethanol), catalyst: 0.1 g, the other reaction conditions are given in section 6.2.4.

pretreatment. Table 6.6 shows the initial results obtained with such bimetallic CdS photocatalysts.

Table 6.6 The photocatalytic dehydrogenation activity of bimetallic components ($M_2 + M_1$) on CdS

Photocatalyst M_1 /CdS (wt. %) ^{***}	Promoter M_2 (wt. %)	Preparation of M_1 and M_2 on CdS ^{**}	H ₂ production (ml/h.g.)	Increase in activity (%) [*]
5% Pt/CdS +	no	Phys. mix., no pretreatment	17.0	0
	5% Cu	Phys. mix., no pretreatment	25.8	52
	4% Cu ₂ O	Phys. mix., no pretreatment	16.1	-6
	5% CuO	Phys. mix., no pretreatment	10.9	-36
5% Pt/CdS +	no	Phys. mix., no pretreatment	22.0	0
	4.9% Ag	Phys. mix., no pretreatment	28.5	30
5% Pt/CdS +	no	Phys. mix., pretreatment	17.2	0
	3.2% Ag	Heat decomp. of acetate	34.2	98
	3.9% Ag	Heat decomp. of carbonate	23.7	37
	4.6% Ag	Photodecomp. of oxide	35.5	106
5% Pd/CdS +	no	Chem. depos., pretreatment	60.6	0
	5% Cu	Phys. mix., no pretreatment	80.5	33
5% Pd/CdS +	no	Chem. depos., pretreatment	42.5	0
	5% Ag	Heat decomp. of acetate	49.5	16

*: This increase is related to M_1 /CdS

** : Pretreatment and heat decomposition occurred under the following conditions: in an N₂ flow for two hours at 360°C.

***: This comparison applies only to the same M_1 /CdS in the same preparation batch.

Table 6.6 shows that metallic Cu and Ag create positive effects on the dehydrogenation activity of the photocatalysts Pt/CdS and Pd/CdS. However, Cu¹⁺ and Cu²⁺ do not create positive effects on the activity of these photocatalysts. Because no significant photocatalytic activity as a result of copper or silver deposited on CdS surfaces was observed (Table 6.5), the positive effect of the copper and silver components in the photocatalyst $M_2 + M_1$ /CdS should consist of affecting the main catalyst, Pt/CdS or Pd/CdS.

The photocatalytic activity of M/CdS or $M_2 + M_1$ /CdS depends on not only preparation method, particle size and the distribution and coverage of particles on CdS, but also the processes occurring during preparation and pretreatment. The speed at which the temperature is raised, the way in which the solution is stirred, the speed at which reductant is added, and the process and duration of physical mixing greatly influence the activity of catalysts. Although we prepared various photocatalysts with great care, we could not guarantee that different batches of catalysts prepared similarly showed the same activity. Therefore, the comparison made between photocatalytic activities as shown in Table 6.6 is most reliable for the photocatalysts prepared as part of the same batch.

In the case of a main photocatalyst (platinum or palladium) and a promoter (copper or silver) coexisting on a CdS surface, the role of the promoter may consist of promoting hydrogen gas desorption from the platinum or palladium surface according to the theory of heterogeneous catalysis. Because both copper and silver have a d^{10} electron structure while they coexist with platinum or palladium (especially when pretreated at a high temperature), the d electron of copper or silver will transfer to platinum or palladium, partly fill its d orbits, decrease its d hole density, and weaken its hydrogen adsorption. Consequently, the promoters Cu and Ag mainly affect the electron transfer in M/CdS and increase the electron density on Pt or Pd surfaces. They may be considered electron promoters.

6.3.10 Optimum proportion of promoter component M_2 on photocatalyst of M_1 /CdS

The amount of promoter M_2 in an M_1 /CdS photocatalyst is an important factor for the photocatalytic activity demonstrated. The amount of promoter may be so high that the photocatalytic activity and light absorption efficiency of CdS decreases. For Cu+Pt/CdS prepared by physical mixing without pretreatment, the effect of Cu and Pt content on the activity in a deaerated system was examined, as shown in Fig. 6.8. By fixing the Cu content at 5% and changing the Pt content (curve 1), and by fixing the Pt content at 5% and changing the Cu content (curve 2), two curves were obtained with a maximum at 5% Pt and 5% Cu (e.g., 5%Pt + 5%Cu/CdS). A photocatalytic dehydrogenation activity of 25.8 ml/h.g. was attained, which is 52% as high as that of 5%Pt/CdS and 16.4 times as high as that of 5%Cu/CdS.

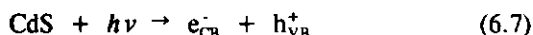
Copper and silver are heterogeneous catalysts used for ethanol oxidation, as well as valuable promoters of the dehydrogenation occurring during the photocatalytic oxidation of ethanol. This reveals the existence of an inherent link between heterogeneous catalysis and photocatalysis, although these processes differ in both theory and concept.

6.3.11 Possible reaction mechanisms for heterogenous photocatalysis

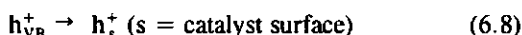
According to the results of the photocatalytic experiments and the theory of heterogenous catalysis for ethanol oxidation, two heterogenous catalysis mechanisms for the photocatalytic oxidative dehydrogenation of ethanol are proposed.

6.3.11.1 Surface reaction mechanism at the photocatalyst Pd/CdS

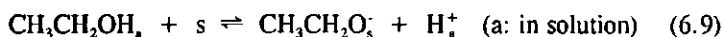
According to this mechanism, illumination results in the generation of electron-hole pairs on the n-type semiconductor CdS photocatalyst surface. The electrons have the potential of the conductor band (CB) of CdS, and the holes have the potential of the valence band (VB) of CdS:



The holes, which have the potential of the valence band, move to the photocatalyst surface:



Ethanol present in the solution dissociates and is adsorbed onto the catalyst surface:



Adsorbed ethanol reacts with one or two holes at the surface:



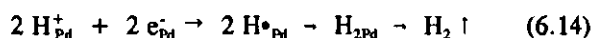
The e_{CB}^- electron generated at the CdS surface is concentrated at the Pd surface and still has the potential of the conductor band of CdS:



Hydrogen ions (protons) resulting from the dehydrogenation of ethanol (Eq.6.10) and the dissociation of water adsorb onto the Pd surface:



and are reduced at the Pd surface by extra electrons e_{Pd}^- to dihydrogen and then released:



6.3.11.2 Complexing catalysis mechanism involving Pd^{2+} and Pd^0

Fig.6.9 shows a possible complexing catalysis mechanism for the photocatalytic dehydrogenation of ethanol at Pd^{2+} . The conditions required for this mechanism are that the electrons can flow from Pd to CdS, and that Pd^0 can be oxidized to Pd^{2+} at the CdS surface. When palladium is deposited on CdS surfaces, the physical contact between Pd and CdS is a Schottky contact where electrons can flow only from CdS to Pd. If at the Pd-CdS junction a kind of chemical bond between Pd and Cd or between Pd and S is formed, the electrons can flow in two directions at the Pd-CdS junction. The following three reasons support this assumption. (1). If the deposited metal particles are so small that they provide insufficient capacity (atomic orbits) for maintaining their Fermi level when electrons flow from semiconductor to metal after their contacting, the height of Schottky barrier will decrease greatly (see Fig.1.9). It may result in electrons flowing from metal to semiconductor. (2). During pretreatment of the catalyst Pd/CdS at a high temperature, a strong metal and semiconductor interaction (SMSI) (e.g., a chemical bond between Pd and Cd or between Pd and S) may be created at the Pd-CdS junction. This SMSI may promote the flow of electrons from Pd to CdS. (3). According to the palladium standard redox potential shown as below:



where $E^\circ = +0.83 \text{ V}$, the hole h_{v}^+ at the CdS surface has sufficient potential to oxidize Pd^0 to Pd^{2+} . Therefore, if according to the complexing catalysis theory the following equilibrium



could exist at the CdS surface, photocatalytic oxidative dehydrogenation of ethanol could occur via an available recycling path for complexing catalysis. In Fig.6.9, photocatalytic oxidation of ethanol to acetaldehyde occurs via a transition state of the palladium(II)-ethanol complex. Consequently, the active positions for ethanol oxidation exist not only on the CdS surface where ethanol is activated by photogenerated holes, but also on $\text{Pd}^{2+}/\text{Pd}^0$ where ethanol is activated via the palladium(II)-ethanol complex. Only on Pd^0 exists an active position for proton reduction.

6.3.12 The rate-determining step of ethanol dehydrogenation

If the generation of hole-electron pairs (Eq.6.7) were a rate-determining step, the rate at which dihydrogen is produced would be independent of the ethanol concentration. However, this is contrary to the results of the experiments. It is not the rate-determining step, because Pd

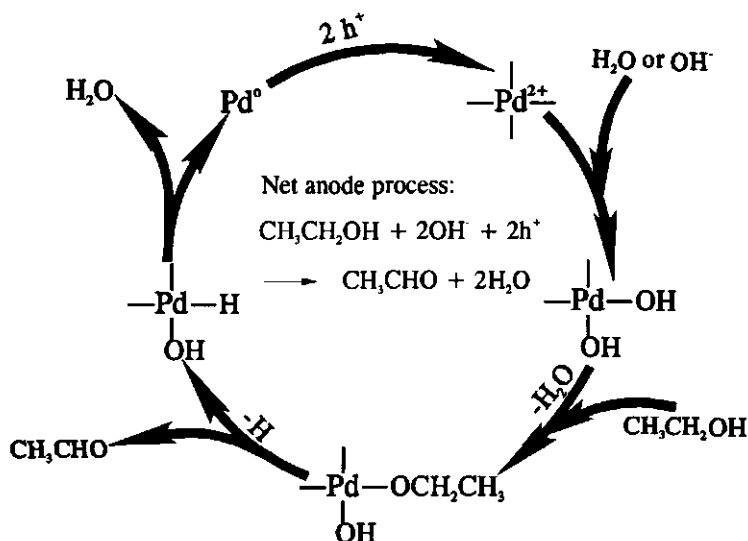


Fig. 6.9 The possible complexing catalysis mechanism of the photocatalytic dehydrogenation of ethanol on Pd(II).

collects an extra electron and the activation energy of the reductive reaction during which H^+ is converted to H_2 (Eq. 6.13 and 6.14) is not high. At a high reaction temperature (50°C), the desorption of hydrogen is not the rate-determining step either. Only the step of H dissociation occurring after the adsorption of ethanol onto the catalyst surface (Eq. 6.10), or the transfer of H occurring after the coordination and complexing of ethanol with Pd^{2+} at the CdS surface (Fig. 6.10) can be the rate-determining step. The rate of hydrogen production may depend mainly on the ethanol concentration, the reaction pH, and the concentration of extra electrons at Pd, in which the dependence of this rate on the ethanol concentration was observed during experiments.

6.4 CONCLUSIONS

1. 2.5 mg/ml 5%Pd/CdS was found to be the optimum catalyst amount for ethanol dehydrogenation under the conditions used during our experiments. The production of hydrogen reached a level of 300 ml per hour or 120 ml per hour per gram of photocatalyst.
2. Pretreatment of the photocatalyst Pd/CdS at a high temperature reduced the size of deposited palladium by 10% from 8.8 to 7.9 nm, and increased the number of palladium particles on CdS particles (with a diameter of 33.8 nm) by 41%. This resulted in a 100% increase in the photocatalytic activity of the photocatalyst Pd/CdS during ethanol dehydrogenation.

3. In the temperature range of 305 ~ 365 K, the rate of hydrogen production (γ) increases with temperature. Using the Arrhenius equation, the apparent activation energy (E_a) can be calculated, resulting in a value of $E_a = 37 \text{ KJ/mol}^{-1}$. This is only an experimental value of the activation energy. The actual activation energy (E_0) of the dehydrogenation reaction can be calculated by adding at least the absorption heat of the H_2 present on catalyst surfaces.

4. The rate of hydrogen production is proportional to the initial ethanol concentration in the concentration range of 0 ~ 50%. In this range, the photocatalytic deaerated dehydrogenation of an ethanol solution may be considered a first-order reaction on Pd/CdS.

5. Regarding the dehydrogenation of ethanol in deaerated systems, the observed photocatalytic activity of monometal M/CdS photocatalysts decreases in the following order: 5% wt. Pd/CdS (chem. depos., pretreatment) > 5% wt. Pt/CdS (phys. mix. with or without pretreatment, or chem. depos., without pretreatment) > 1% wt. $\text{Rh}_2\text{O}_3/\text{CdS}$ (phys. mix., without pretreatment) >> PdO, Rh, Ag, Cu, CuO/CdS. Plain CdS shows hardly any photocatalytic activity.

6. The Pt content is optimal around 5%. In bimetallic components/CdS, the second metallic component may serve as a promoter; the addition of Cu or Ag causes a considerable increase in photocatalytic activity in both Pt/CdS and Pd/CdS systems. The combination of 5% wt. Cu + 5% wt. Pt/CdS was found to be optimal under the conditions used during our experiments.

7. Pd loaded on the CdS surface acts as an electron pump that transfers photogenerated electrons (e_{CB}^-) from the CdS valence band to palladium (Eq.6.12). Pretreatment at a high temperature promotes the transfer of electrons and decreases the recombination of photogenerated hole-electron pairs. The fact that Pd has extra electrons is favorable for the catalytic reduction of hydrogen ions to dihydrogen (Eq.6.14).

8. The complexing catalysis process is probably one of the photocatalytic mechanisms according to which alcohol can be dehydrogenated, if electrons can flow from Pd to CdS and Pd^0 can be oxidized to Pd^{2+} on the CdS surface. When the photocatalyst Pd/CdS is pretreated at a high temperature, a strong metal and semiconductor interaction (SMSI) (*e.g.*, chemical bonds between Pd and Cd or between Pd and S) may be formed at the Pd-CdS junction. SMSI can promote the flowing of electrons from Pd to CdS. According to the palladium standard redox potential, the hole h_{VB}^+ at the CdS surface has sufficient potential to oxidize Pd^0 to Pd^{2+} .

ACKNOWLEDGMENTS

The authors wish to acknowledge the distinguished Chinese professor Qi-Rui CAI for his suggestion concerning the mechanism of complexing catalysis. The authors also wish to acknowledge Mrs. Jing-Shang YAO from the Analysis Center, Mr. Fa-Yan WANG from the Electron Microscope Group and Mr. Jing-Yin FU from the Catalysis Section for their great help in relation to XPS, TEM and experiments for the determination of specific surface areas.

6.5 REFERENCES

- 1.B. Ohtani, M. Kakimoto, S. Nishimoto, and T. Kagiya, *J. Photochem. Photobiol. A: Chem.*, **70**, 265-272, 1993.
- 2.J. Cunningham, and P. Sedláč, *J. Photochem. Photobiol. A: Chem.*, **77**, 255-263, 1994.
- 3.P. Pichat, Marie-Noelle Mozzanega and H. Courbon, *J. Chem. Soc., Faraday Trans. 1*, **83**, 697-704, 1987.
- 4.Y. C. Liu, G. L. Griffin, S. S. Chan, and I. E. Wachs, *Journal of Catalysis*, **94**, 108-119, 1985.
- 5.E. Borgarello, E. Pelizzetti, *La Chimica E L'Industria*, **65**(7-8), 474-478, 1983.
- 6.J. CHEN, Q.X. ZHUANG, Jiniang HE, Chen YU *Acta Energiæ Solaris Sinica*, **7**(4) 378-383, 1986.
- 7.J. CHEN, Qixing ZHUANG, *the Fifth International Conference on Photochemical Conversion and Storage of Solar Energy*, Book of Abstracts, 171-172, 1984.
- 8.J. CHEN, Qixing ZHUANG, *International Workshop on Electro-catalysis, Photo-electrocatalysis and enzyme Catalysis*, Extended Abstracts, B24, 1985.
- 9.Q.X. ZHUANG, J. CHEN, Kangping WANG, *Journal of Xiamendaxie (Natural Science)*, **27**(4), 414-420, 1988.
- 10.T. Sakata, T. Kawai, *Chem. Phys. Lett.*, **80**, 341-344, 1981.
- 11.T. Sakata, T. Kawai, *Chem. Phys. Lett.*, **88**, 50-54, 1982.
- 12.Y. Faniguchi, H. Yoneyama and H. Yamura, *chem. Lett.*, 269-272, 1983.
- 13.T. Sakata, T. Kawai, and K. Hashimoto, *J. Phys. Chem.*, **88**(11), 2344-2350, 1984.
- 14.F. H. Hussein, *et al.*, *Tetrahedron Lett.*, **25**, 3363-3364, 1984.
- 15.Q.L. LI, Z.S. JIN, *et al.*, *Sensitivity Science and Photochemistry*, **3**, 55-62, 1986.
- 16.Z.S. JIN, Q.L. LI, *J. of Molecular Catalysis*, **1**, 21-26, 1987.
- 17.J. Sabaté, M. A. Aguado, J. C. Escudero, J. Giménez, R. Simarro, and S. Cervera-March, *J. Of Colloid and Interface Science*, **140**(1), 35-40, 1990.
- 18.S. J. Tauster, S. C. Fung, and R. L. Garten, *J. Am. Chem. Soc.*, **100**, 170, 1978.
- 19.P. Pichat, *New Journal of Chemistry*, **2**(2), 135-140, 1987

CHAPTER 7 SUMMARY AND CONCLUSIONS

7.1. Summary and conclusions

The last two decennia have shown a growing interest in the photocatalytic treatment of wastewater, and more and more research has been carried out into the various aspects of photocatalysis, varying from highly fundamental aspects to practical application. However, despite all this research, there is still much to investigate. Suggested photocatalytic mechanisms, such as those for oxidation by hydroxyl radicals and for oxidation at the surface of photocatalysts, need to be verified experimentally for various types of pollutant under various reactive conditions. The kinetic processes occurring during photocatalytic reactions have still not been fully clarified. Efficient photocatalytic treatment of pollutants in wastewater has so far been achieved only by using the powdery photocatalyst TiO_2 in suspension. This method cannot be applied in practice unless there are means to keep or recycle the photocatalyst within the treatment unit. Optimization of the photocatalytic process requires modification of photocatalyst surfaces, the discovery of new efficient photocatalysts, and research into new combinations of photocatalysis with other methods. The present dissertation deals with photocatalytic processes and systems, their combination with photolysis and other advanced oxidation technologies, and their application for the treatment of environmental pollutants in wastewaters.

Chapter 1 introduces advanced oxidation technologies (AOTs), which consist mainly of the use of ozone, hydrogen peroxide, ultraviolet light (UV) and non-thermal plasmas; electrohydraulic cavitation and sonolysis; electron-beam and gamma irradiation; catalytic oxidation; wet air oxidation; supercritical water oxidation; electrochemical oxidation (electrolysis); and photocatalysis. The basic principles and applications of these technologies are discussed, focusing on photocatalysis for the treatment of wastewater, and more than two hundred references are given.

The general principle of the photocatalytic treatment of pollutants is as follows. When a semiconductor catalyst suspended in an aqueous solution is illuminated using light with an energy ($h\nu$) exceeding or equal to the band gap of the semiconductor ($h\nu \geq E_g$), electron-hole pairs (e^-h^+) with a certain electric potential are generated at the catalyst surface. For the semiconductor TiO_2 , which has a band gap of 3.05 eV, this light must be near-UV with a wavelength smaller than 410 nm. At catalyst surfaces, the generated holes with a positive charge move to the anodic area, whereas the generated electrons move to the cathodic area. At the anodic area of a catalyst, an oxidative half reaction will occur, such as the oxidation of organic pollutants in wastewater to CO_2 . At the cathodic area of a catalyst, a reductive half reaction will occur, such as the reduction of oxygen in wastewater to H_2O .

Chapter 2 discusses the photocatalytic oxidation of methanol, ethanol and chloroform, trichloroethylene (TCE), and dichloropropionic acid (DCP) in aerated aqueous slurries using

plain TiO_2 , Pd/TiO_2 or Pt/TiO_2 as a catalyst. Based on experimental data, various photocatalytic mechanisms are elaborated upon.

In TiO_2 suspensions, it was observed that during illumination with near-UV light ($320 \text{ nm} \leq \lambda \leq 410 \text{ nm}$) in the presence of oxygen the photocatalytic oxidation of methanol and ethanol was accelerated by modifying the catalyst with Pt or Pd. Pd present on TiO_2 created a less strong effect than Pt. During not any experiment involving methanol were intermediates of methanol oxidation (such as formaldehyde and formic acid) detected in the aqueous solution using a gas chromatograph. The only product detected was CO_2 . However, during the photocatalytic oxidation of ethanol, various types of intermediate (such as acetaldehyde and acetic acid) were detected in the aqueous solution. These intermediates varied in concentration depending on the type of catalyst. Under similar reaction conditions, the ratio between acetaldehyde and acetic acid was 30:1 with TiO_2 and 0.23:1 with Pt/TiO_2 , which means that with TiO_2 the acetaldehyde concentration was 130 times higher than with Pt/TiO_2 . Therefore, it can be concluded that further oxidation can be achieved easiest with Pt/TiO_2 . The rate at which alcohol was mineralized (*i.e.*, CO_2 was produced) was found to depend on the initial solution pH. At an acidic pH, CO_2 was produced immediately, whereas at an alkaline pH the mineralization process occurred much slower.

When plain TiO_2 was used as a photocatalyst, 98% of the TCE present in the water phase at an initial concentration of 25 ppm and 75% of the chloroform present in the water phase at an initial concentration of 120 ppm were oxidized after an illumination period of one hour and three hours, respectively. About 18% of DCP present at an initial concentration of 1,430 ppm was dechlorinated and 23% of this DCP was decarboxylated during an illumination period of three hours. Compared with the results obtained with plain TiO_2 , no effect of Pd metallized on TiO_2 was observed during the photocatalytic oxidation of either chloroform, TCE or DCP. The acceleration of DCP dechlorination affected by Pt/TiO_2 exceeded that affected by plain TiO_2 by 53%, but Pt/TiO_2 did not affect the rate at which DCP was decarboxylated.

Based on experimental data and an evaluation of possible reaction pathways, it was concluded that during aerated photo-oxidation of alcohols and organochlorides (*e.g.*, TCE, DCP) Pt accelerates the cathodic process of O_2 reduction occurring at catalyst surfaces. If a rate-controlling step is part of the anodic process occurring during a photocatalytic reaction (as is the case with the photocatalytic oxidation of organochlorides), modified Pt or Pd on TiO_2 cannot influence the rate of this reaction unless it can affect the reactants present at the anodic area. In general, the rate-controlling step of an anodic process can be attributed chiefly to the resistance to adsorption and electron transfer offered by reactants in relation to anodic surfaces. A pathway favourable for anodic processes occurring at catalyst surfaces is direct adsorption of reactants and direct electron transfer to holes with a positive charge (*i.e.*, a direct oxidation reaction occurring at surfaces).

Chapter 3 discusses the interaction occurring between Pt or Pd and TiO_2 . A porous micro-cell model for a system containing a powdery photocatalyst is presented. Furthermore, the kinetic

processes of the photocatalytic mineralization of alcohols occurring at the surface of metallized and native TiO_2 in aerated systems are detailed, the adsorption of alcohols present on TiO_2 surfaces is calculated, and the process during which oxygen is reduced at TiO_2 surfaces is discussed.

An X-ray diffraction experiment carried out to determine the crystal structures of catalyst components revealed a diffraction angle of $2\theta = 40^\circ$, which deviates from those shown by the crystal structure of the metal Pt, anatase and rutile present in a sample of Pt/TiO_2 pretreated at a high temperature. Based on the principle of strong metal-semiconductor interaction (SMSI) and diffraction data on Pt-Ti intermetallic compounds, it was supposed that it is the strongest diffraction angle of Pt-Ti intermetallic compounds.

Surface element analysis of the photocatalyst Pd/TiO_2 using an electron beam probe (X-ray exciting spectrum) reveals that not all Pd was deposited on the outside of the TiO_2 powder; therefore, part of it was probably deposited inside. Based on the results of this experiment and the experiment of XPS (X-ray Photoelectron Spectroscopy) in chapter 6, a new porous micro-cell model for a system containing a powdery photocatalyst was developed. In this model, the outer surface of a particle can be illuminated, but its pores form a dark, unilluminated area, which acts as a permanent cathode.

The overall photocatalytic reaction occurs at two areas of photocatalyst surfaces. Ethanol is oxidized at the anodic area, whereas oxygen is reduced at the cathodic area. Experiments revealed that the photocatalytic degradation of alcohols occurring at the anodic area is a first-order reaction. This can be easily explained by assuming the existence of a Langmuir adsorption isotherm, *i.e.*, alcohols are first adsorbed onto the catalyst surface and then oxidized photocatalytically. This surface mechanism can be described by the Langmuir adsorption constant (K) and the real reaction rate constant (k) applying to this reaction. Therefore, it can be assumed that, at least in a dilute aqueous solution, one of kinetic mechanisms of photocatalysis occurring during the oxidation of some organic compounds is similar to a gas-phase reaction occurring at the solid surface of a heterogeneous catalyst, which can be described by the Langmuir equation. Consequently, the fact that no intermediates were detected in solution during the photocatalytic oxidation of methanol must be due to the fact that the intermediates formaldehyde and formic acid remained at the photocatalyst surface and were not desorbed into solution before being further oxidized to the final product, CO_2 .

According to a calculation of the surface coverage by alcohols on photocatalyst particles, at similar molar concentrations the coverage of ethanol was twice as high as that of methanol. The maximum rate and efficiency of the photocatalytic oxidation of methanol and ethanol at catalyst surfaces can be estimated based on the results obtained. To explain the surface mechanisms taking place during the photocatalytic oxidation of alcohols, it is suggested that at catalyst surfaces end-group adsorption of methanol and ethanol occurs.

Chapter 4 details lab-scale experiments during which various photochemical methods for the elimination of pollutants from wastewater were employed in combination under aerated

conditions. These pollutants included pure phenol in aqueous solutions (initial concentration = 25 ppm), and substituted phenols and COD (Chemical Oxygen Demand) in industrial wastewaters, such as those from the production of phenolic resins, oil refinement, the dry distillation of shale oil, and the production of naphthenic acid. The combinations applied included illumination with UV light (using a 200-W high-pressure mercury lamp, wavelength $313 \leq \lambda \leq 456$ nm), the use of magnetite or aluminum oxide as a photocatalyst, H_2O_2 , and iron compounds (FeCl_3 and $\text{Fe}(\text{NH}_4)_2(\text{SO}_4)_2$ as Fenton reagents). Using magnetite simultaneously as a photocatalyst and a solidified Fenton reagent proved to be a sophisticated method for combining photocatalysis with the photo Fenton reaction.

The experimental results presented in this chapter show clearly the separate and combined effects of UV light, a photocatalyst, ferric compounds, and H_2O_2 . For example, magnetite or aluminum oxide combined with UV light decreased the COD of certain toxic industrial wastewaters by around 60-70% in 1-4 hours. The separate use of UV light and magnetite had little effect on the degradation of COD and phenol.

The rate of phenol photolysis during illumination with UV light was found to depend on the solution pH and was highest at an initial pH of 3.5. Hydrogen peroxide or ferric ions ($\text{Fe}^{3+}/\text{Fe}^{2+}$) in an aqueous solution of phenol greatly increased the rate of phenol elimination, when only UV photolysis was applied and no catalyst was present. The photo Fenton reaction system of $\text{UV}/\text{H}_2\text{O}_2/\text{Fe}$ -compounds showed the highest rate of photochemical elimination of phenol and other organic compounds in the above-mentioned combinations.

An improved photochemical method, using a calcium compound as a chemical promoter, clearly made a ferric and an aluminium photocatalyst more effective in the treatment of toxic compounds (particularly phenols in various wastewaters). According to the experimental results, the combined photochemical method employing UV light, hydrogen peroxide and a photocatalyst (used simultaneously as a solidified Fenton-reagent) is a very promising method of photochemical wastewater treatment.

Chapter 5 discusses the photocatalyzed deposition and concentration of uranium(VI) (uranyl) in wastewaters, using suspended TiO_2 or Pt/TiO_2 as a catalyst. As a result of pretreatment, uranium-containing wastewaters usually contain several types of chelating reagent, such as EDTA (ethylenediaminetetraacetic acid). In deaerated $\text{U(VI)}/\text{EDTA}$ solutions, reductive deposition of uranium and release of CO_2 from EDTA occurred as a result of photocatalysis at TiO_2 or Pt/TiO_2 surfaces during illumination with near-UV light. In the experimental set-up chosen, at most 50-60% of the uranium(VI) present in the solution was deposited. Pt promoted this reductive deposition of uranium(VI) on TiO_2 only to a slight degree, although it accelerated the oxidative deposition of other metals on TiO_2 during other experiments. The ultimate amount of CO_2 released during experiments was equivalent to a single decarboxylation of EDTA and was independent of illumination time. This explains the limited reductive deposition of uranyl (around 50-60%). Furthermore, it means that the tricarboxylic acid resulting from

EDTA oxidation cannot be easily oxidized further, and then it renders any further reductive process of uranyl on TiO_2 surfaces.

In aerated solutions, no uranium was deposited but a lot of CO_2 was released, probably as a result of EDTA mineralization on photocatalyst surfaces. Nearly 100% of the deposited, reduced product of uranium(VI) present at TiO_2 or Pt/TiO_2 surfaces was reoxidized reversibly and desorbed into solution to form dissolved uranium(VI), simply by exposing the solution to air after illumination. During one experiment, the reductive deposition process, during which around 55% of the uranium(VI) in solution could be deposited, was repeated three times. This is therefore a promising photocatalytic method for the recovery and concentration of uranium(VI) in uranium-containing wastewaters.

Chapter 6 deals with the photocatalytic dehydrogenation of ethanol in the presence of metallized CdS (*i.e.*, M/CdS with one or two metals) in a deaerated system using visible light for illumination. The effect of various M/CdS photocatalysts, present in solution in an optimal amount, on the dehydrogenation of ethanol was investigated. This process results in the release of H_2 and the production of acetaldehyde. A study was also conducted of the effect of pretreating M/CdS at a high temperature on the distribution of Pd on CdS surfaces, the role of Pd or Pt present on CdS, and the role of a photocatalytic promoter, *i.e.*, a second metal component (*e.g.*, Cu, Ag, Rh), present on CdS. In addition, a complex catalysis mechanism for the photocatalytic dehydrogenation of alcohols was suggested.

The optimum amount of photocatalyst was found to be 2.5 g/l, which was accompanied by a hydrogen production of 300 ml/h.l. Pretreatment at a high temperature reduced the size of deposited Pd particles by 10% from 8.8 nm to 7.9 nm, and increased the number of Pd particles present on CdS particles (with a diameter of 33.8 nm) by 41%. This resulted in a 100% increase in photocatalytic activity of the photocatalyst Pd/CdS during ethanol dehydrogenation. The deaerated dehydrogenation of ethanol was found to be a first-order reaction at an ethanol concentration below 50%. The reaction activity of the photocatalysts tested decreased in the following order: 5% wt. Pd/CdS (prepared by chemical deposition, pretreated at a high temperature) > 5% wt. Pt/CdS (physical mixing or chemical deposition with or without pretreatment) > 1% wt. $\text{Rh}_2\text{O}_3/\text{CdS}$ (physical mixing, no pretreatment) > > PdO, Rh, Ag, Cu, CuO/CdS . Plain CdS showed a negligible photocatalytic activity during ethanol dehydrogenation. The optimal Pt content in a Pt/CdS system was found to be around 5%. From the experimental results, it was concluded that the second metallic component on CdS possibly acts as a promoter during dehydrogenation. 5% wt. Pt + 5% wt. Cu/CdS was found to be the optimum combination in a system containing these two metallic components under the conditions used during our experiments. Pd or Pt loaded on a CdS surface acts as an electron pump that transfers photogenerated electrons e_{cb}^- from the valence band of CdS to Pd. Pd acts as a proton-bonding adsorption centre.

If at Pd/CdS surfaces electrons can flow from Pd to CdS and Pd^0 can be oxidized to Pd^{2+} during illumination, the photocatalytic oxidation of alcohols at such surfaces may also occur according to a heterogeneous catalytic mechanism called a complexing catalysis mechanism, because after a Pd/CdS catalyst has been pretreated at a high temperature, a strong metal and semiconductor interaction (SMSI) (*e.g.*, chemical bonds between either Pd and Cd or Pd and S) can occur at the Pd-CdS junction. This interaction can increase the flow of electrons from Pd to CdS. In view of the palladium standard redox potential, the holes ($h_{\nu_B}^+$) with a positive charge at CdS surfaces have sufficient electric potential to oxidize Pd^0 to Pd^{2+} .

From the investigations into photocatalysis applied to wastewater treatment detailed in this dissertation, the following general conclusions can be drawn.

- Experiments carried out to study the photocatalytic oxidation of methanol and ethanol have resulted in an increased insight into and better understanding of the mechanisms occurring during the photocatalytic treatment of wastewaters.
- During this study, more insight has been gained into the practical application of photocatalysis and the problems that still need to be solved regarding the treatment of certain industrial wastewaters.
- Organochlorides can also be easily degraded using a photocatalyst; this process may be a promising application.
- Combined photochemical methods that include the use of a photocatalyst may be attractive for the treatment of phenol-containing industrial wastewaters.
- Experimental results of the photocatalytic deposition and concentration of soluble uranium show that photocatalytic treatment is an interesting method for the recovery of radioactive heavy metals.
- Metallization is a popular method for raising the activity of photocatalysts consisting of a semiconductor. The functions of metallization were revealed as a result of experiments involving the use of metallized TiO_2 and CdS.

7.2 Samenvatting

De afgelopen twintig jaar is er een groeiende belangstelling ontstaan naar de fotokatalytische behandeling van afvalwater. Deze belangstelling blijkt duidelijk uit het onderzoek dat is verricht naar de verschillende aspecten van het fotokatalytische zuiveringsproces. Dit onderzoek heeft betrekking op zowel de meer fundamentele als op de praktische aspecten en heeft geleid tot een vergroting van het inzicht in de werking en de toepassingsmogelijkheden van het fotokatalytische zuiveringsproces. Echter veel aspecten, zoals bijvoorbeeld de veronderstelde reactiemechanismen die optreden bij de oxidatie van verontreinigingen in oplossing door hydroxyl-radicalen en van verontreinigingen aan het oppervlak van een fotokatalysator, zullen nog nader experimenteel moeten worden geverifieerd voor een groot aantal typen verontreinigingen en procescondities. Ook de kinetiek van de omzettingsprocessen tijdens fotokatalytische reacties is nog niet volledig opgehelderd. Een efficiënte fotokatalytische behandeling van verontreinigingen in afvalwater is tot dusver op praktijkschaal alleen succesvol gebleken met behulp van de in suspensie gebrachte poedervormige fotokatalysator TiO_2 . De praktische toepassing van deze methode voor afvalwaterzuivering vereist echter dat de gesuspenderde fotokatalysator niet met het behandelde afvalwater wordt afgevoerd maar volledig wordt teruggewonnen voor hergebruik. Een verdere optimalisatie van het fotokatalytische proces vereist een verbetering van het fotokatalytische oppervlak van bestaande fotokatalysatoren en de ontwikkeling van nieuwe, meer efficiënte fotokatalysatoren. Ook de combinatie van een fotokatalytische behandeling met andere zuiveringsmethoden voor afvalwater kan mogelijk leiden tot meer efficiënte processen. Het in dit proefschrift beschreven onderzoek heeft ten doel: a. een aantal fotokatalytische processen en systemen voor de reiniging van afvalwaterstromen nader te bestuderen, b. de combinatie van fotokatalyse met fotolyse en andere geavanceerde oxidatietechnieken te onderzoeken en c. de praktische toepasbaarheid van dergelijke systemen nader aan te geven.

In hoofdstuk 1 wordt een kort overzicht gegeven van de verschillende typen geavanceerde oxidatietechnologieën (AOTs). Als belangrijkste kunnen daarbij genoemd worden het gebruik van ozon, waterstofperoxide en ultraviolet licht (UV) alsmede van niet thermische plasma's, elektrohydraulische cavitatie en sonolyse, katalytische oxidatie, natte lucht oxidatie, superkritische water oxidatie, elektrochemische oxidatie (elektrolyse) en fotokatalyse. Van elk van deze technieken wordt het basisprincipe en de praktische toepassing aangegeven. Daarbij wordt vooral ingegaan op de reiniging van afvalwater door middel van fotokatalyse. Het algemene principe van de fotokatalytische behandeling van afvalwater is als volgt. Wanneer een halfgeleider (katalysatordeeltje) wordt gesuspenderd in een waterige oplossing en deze oplossing wordt bestraald met licht met een energie ($h\nu$) die groter of gelijk is aan de *bandgap* E_g van de halfgeleider, worden er elektron-*hole*-paren, aangeduid met $(e^- - h^+)$, met een bepaalde elektrische potentiaal gegenereerd aan het oppervlak van de katalysator. Voor de halfgeleider TiO_2 is deze *bandgap* 3,05 eV. Licht uit het nabije UV met een golflengte kleiner

dan 410 nm is hiervoor geschikt. Als gevolg van de bestraling ontstaat er op de belichte zijde van het katalysatordeeltje een accumulatie van positief geladen *holes* wat resulteert in een anode gebied. Evenzo leidt een accumulatie van elektronen op de schaduwzijde tot een kathode gebied. In het anode gebied van de katalysator zal een oxidatieve half reactie kunnen plaatsvinden, zoals de oxidatie van een organische verontreiniging tot CO_2 . In het kathode gebied van de katalysator zal een reductieve halfreactie kunnen plaatsvinden zoals de reductie van zuurstof tot H_2O .

In hoofdstuk 2 wordt de fotokatalytische oxidatie van methanol, ethanol, chloroform, trichloorethyleen (TCE) en dichloorpropionzuur (DCP) in beluchte waterige slurries van fotokatalysatoren bestaande uit zuiver TiO_2 , Pd/TiO_2 , and Pt/TiO_2 bestudeerd. Op basis van experimentele resultaten kunnen daarbij verschillende typen fotokatalytische reacties worden afgeleid.

Voor beluchte TiO_2 suspensies werd, voor water waaraan geringe hoeveelheden methanol of ethanol waren toegevoegd, waargenomen dat bij bestraling met licht uit het nabije UV ($320 \text{ nm} \leq \lambda \leq 410 \text{ nm}$) (λ is golflengte van het licht) de fotokatalytische oxidatie van methanol en ethanol werd versneld door de katalysator te modificeren met Pt of Pd, waarbij het grootste effect werd verkregen met Pt. Bij geen van de fotokatalytische experimenten met waterige oplossingen van methanol werden opgeloste intermediären zoals formaldehyde en mierenzuur aangetroffen. Alleen CO_2 werd aangetoond. Dit in tegenstelling tot de fotokatalytische oxidatie van een waterige oplossing van ethanol waarbij wel intermediären (zoals acetaldehyde en azijnzuur) in de oplossing werden gevonden. De concentratie van deze intermediären varieerde afhankelijk van het type katalysator. Bij dezelfde reactiecondities bedroeg de verhouding van acetaldehyde en azijnzuur 30 voor het geval dat zuiver TiO_2 als fotokatalysator werd toegepast en 0,23 bij gebruik van Pt/TiO_2 . Geconcludeerd kan dus worden dat een vergaande oxidatie het gemakkelijkst verkregen kan worden met Pt/TiO_2 . De snelheid waarmee alcohol werd gemineraliseerd, af te leiden uit de productie van CO_2 , bleek sterk afhankelijk te zijn van de begin-pH van de oplossing. In het zure pH-gebied kwam de productie van CO_2 onmiddellijk op gang, terwijl in het basische pH-gebied het mineralisatieproces veel langzamer plaats vond.

Bij gebruik van zuiver TiO_2 als fotokatalysator bleek 98% van trichloorethyleen (TCE) aanwezig in een waterige oplossing (beginconcentratie 25 ppm) te worden geoxideerd na bestraling gedurende een periode van één uur. Voor een oplossing van chloroform in een waterfase (beginconcentratie 120 ppm) werd een omzetting verkregen van 75% na bestraling gedurende een periode van drie uur en gebruik van zuiver TiO_2 als katalysator. Voor een oplossing dichloorpropionzuur (DCP) met een beginconcentratie van 1430 ppm werd een omzetting van 18% verkregen indien deze oplossing gedurende drie uur werd bestraald en zuiver TiO_2 werd gebruikt als fotokatalysator. Bij dit experiment bleek dat 23% van het DCP werd gedecarboxyleerd. Metallisering van het TiO_2 met Pd had geen effect op de oxidatie van

chloroform, TCE en DCP. De snelheid van de dechlorering van DCP die werd verkregen bij gebruik van Pt/TiO₂ was 53% hoger dan de snelheid die werd waargenomen bij gebruik van zuiver TiO₂. De decarboxylerings-snelheid van DCP was bij gebruik van zuiver TiO₂ nagenoeg identiek aan die welke werd waargenomen bij gebruik van Pt/TiO₂.

Op basis van de experimentele gegevens en een evaluatie van mogelijk reactieroutes kan worden geconcludeerd dat tijdens de foto-oxidatie van alcoholen en organo-chloorverbindingen (zoals TCE, en DCP) Pt het proces van O₂ reductie aan het kathode oppervlak van de katalysator versnelt. Als een snelheidsbepalende stap deel uit maakt van een fotokatalytische reactie aan de anode (zoals het geval is met de fotokatalytische omzetting van organochloorverbindingen), dan kan een modificatie van de TiO₂ katalysator met Pt of Pd de snelheid van de reactie niet beïnvloeden, tenzij er een directe beïnvloeding is van de reactanten aanwezig aan de anode. In het algemeen geldt dat de snelheidsbepalende stap van een reactie aan de anode hoofdzakelijk wordt bepaald door de weerstand tegen adsorptie en elektronentransport van de reactanten aan het anodeoppervlak. Een gunstige route voor omzettingsprocessen die in het anodegebied van de fotokatalysator plaatsvinden is directe adsorptie van reactanten en directe elektronenoverdracht naar positief geladen *holes* (bijvoorbeeld een directe oxidatie die aan het oppervlak plaatsvindt).

Hoofdstuk 3 gaat nader in op de interactie tussen Pt of Pd en TiO₂. Uitgaande van een systeem van poedervormige fotokatalysatordeeltjes in een waterige suspensie wordt voor deze interactie een micro-cel-poeder-model gegeven. Daarnaast wordt het kinetische proces van de mineralisatie van alcoholen zoals dat plaats vindt aan het oppervlak van zuiver of gemetalliseerd TiO₂ in detail weergegeven. Ook wordt de adsorptie van alcoholen aan TiO₂ oppervlakken berekend en wordt het reductieproces van zuurstof aan TiO₂ bediscussieerd.

Uit een röntgendiffractie experiment, uitgevoerd om de structuur van de katalysator op te helderen, bleek diffractie op te treden bij een hoek $2\theta = 40^\circ$ welke niet gevonden wordt bij het metaal Pt en bij anatase en rutiel TiO₂, die aanwezig zijn in een monster Pt/TiO₂ dat is behandeld bij hoge temperatuur. Op basis van de aanname van een sterke metaal-semiconductor interactie (SMSI) en informatie over de diffractiegegevens van het intermetallische systeem Pt-Ti, kan worden aangenomen dat de gevonden diffractiehoek correspondeert met een sterke binding tussen Pt en Ti.

Oppervlakte elementen analyse van de fotokatalysator Pd/TiO₂ door middel van elektronenbestraling (röntgen emissiespectrum) toonde aan dat niet alle Pd zich tijdens het bereidingsproces van de katalysator had afgezet op het buitenoppervlak van katalysatordeeltjes maar dat een deel ook was afgezet in de inwendige poriën binnen het deeltje. Op basis van de resultaten van deze experimenten en de röntgen foto-elektrische spectroscopie experimenten beschreven in hoofdstuk 6, werd een nieuw micro-cel model voor een poreus poedervormig fotokatalysator deeltje ontwikkeld. In dit model wordt er van uitgegaan dat alleen het

buitenoppervlak van een deeltje kan worden aangestraald, maar dat inwendige poriën in feite een permanent kathode gebied vormen.

Zoals ook reeds in het voorafgaande is gesteld vindt de overall fotokatalytische reactie plaats in zowel het kathode gebied als het anode gebied. Ethanol wordt geoxideerd aan de anode onder gelijktijdige reductie van zuurstof in het kathode gebied. Uit experimenten is verder gebleken dat de fotokatalytische afbraak van alcoholen die plaats vindt in het anode gebied een eerste orde reactie is. Dit kan eenvoudig worden verklaard door uit te gaan van een Langmuir adsorptie gedrag van de alcoholen. De alcoholen worden eerst geadsorbeerd aan het katalysator oppervlak en dan fotokatalytisch geoxideerd. Dit oppervlakmechanisme kan mathematisch worden beschreven door middel van een Langmuir adsorptieconstante K en de werkelijke reactiesnelheidsconstante k van de reactie. Er kan daarom worden aangenomen, in ieder geval voor verdunde waterige oplossingen, dat de kinetiek en het mechanisme van de fotokatalytische reactie tijdens de oxidatie van organische verbindingen vergelijkbaar is met een gasfase reactie die plaats vindt op het vaste oppervlak van een heterogene katalysator, een reactie die ook kan worden beschreven met de Langmuir vergelijking. Het verschijnsel dat geen intermediären werden gemeten gedurende de oxidatie van methanol betekent derhalve dat de intermediären formaldehyde en mierenzuur aan het oppervlak geadsorbeerd blijven en daar ook worden geoxideerd tot het eindproduct CO_2 .

Op basis van berekeningen van de oppervlakte bedekking van de fotokatalysatordeeltjes door alcoholen, kon worden vastgesteld dat bij een gelijke molaire concentratie van de alcoholen in de omringende vloeistoffase de bedekking van het oppervlak door ethanol twee maal zo hoog was als die door methanol. Aan de hand van de verkregen resultaten kan de maximale omzettingssnelheid en efficiëntie van de fotokatalytische oxidatie van methanol en ethanol worden ingeschat. Het verschil tussen de fotokatalytische oxidatie van ethanol en methanol is mogelijk te verklaren door uit te gaan van adsorptie van de beide typen alcoholen aan het oppervlak van de katalysator op basis van dezelfde eindgroepen.

Hoofdstuk 4 beschrijft laboratoriumexperimenten met verschillende typen afvalwater waarbij verschillende typen fotokatalytische methoden al of niet in combinatie met elkaar werden toegepast. De typen verontreinigingen die werden onderzocht waren zuivere fenol (in waterige oplossing), beginconcentratie ongeveer 25 ppm, CZV (chemische zuurstofverbruik) en gesubstitueerde fenolen zoals die worden aangetroffen in afvalwater afkomstig van de productie van fenolische harsen, olieraffinage, droge destillatie van oliehoudend gesteente en de productie van naftazuren. Als gecombineerde behandelingstechnieken voor deze afvalwaterstromen werden de navolgende processen toegepast: UV (gebruik makend van een 200 W hoge druk kwik lamp, golflengte λ van de uitgezonden straling tussen 313 en 456 nm), gebruik van magnetiet of aluminiumoxide als fotokatalysator, H_2O_2 en gebruik van ijzerverbindingen (FeCl_3 en $\text{Fe}(\text{NH}_4)_2(\text{SO}_4)_2$) als Fenton reagens. De gelijktijdige toepassing

van magnetiet als fotokatalysator en een vast Fenton reagens bleek een zeer geavanceerde behandelingscombinatie te zijn.

De experimenteel verkregen resultaten die in dit hoofdstuk worden beschreven, laten duidelijk het separate en gecombineerde effect van UV, fotokatalysator, ijzerverbindingen en H_2O_2 zien. Toepassing van bijvoorbeeld magnetiet of aluminiumoxide, gecombineerd met UV licht, verlaagt de CZV concentratie van enkele onderzochte toxische industriële afvalwaterstromen met 60-70% gedurende een behandelingstijd die varieert tussen 1 en 4 uur. De separate toepassing van UV en magnetiet had nauwelijks enige afbraak van CZV tot gevolg. Vergelijkbare resultaten zijn gevonden voor fenol.

De snelheid van fenol fotolyse tijdens bestraling met UV bleek sterk afhankelijk te zijn van de pH en was het hoogst bij een begin pH van 3,5. Waterstofperoxide of ijzerionen ($\text{Fe}^{3+}/\text{Fe}^{2+}$) in een waterige oplossing van fenol verhoogde in sterke mate de snelheid van fenolafbraak voor de situatie dat alleen UV fotolyse werd toegepast en geen katalysator aanwezig was. Het foto Fenton reactiesysteem bestaande uit $\text{UV}/\text{H}_2\text{O}_2/\text{Fe}$ -componenten vertoonde de hoogste fotochemische afbraak van fenol en andere organische componenten.

Indien een calciumverbinding als z.g.n. chemische promotor werd toegevoegd aan het afvalwater, dat fotochemisch werd behandeld met ijzeroxide of aluminiumoxide als katalysator, bleek dat een duidelijke verbetering van de omzetting van met name fenolachtige verbindingen werd verkregen. De experimentele resultaten lieten duidelijk zien dat de fotochemische methode waarbij gecombineerd een fotokatalysator (eventueel een fotokatalysator die ook als een vast Fentonreagens werkt), UV straling en waterstofperoxide werd gebruikt, zeer veelbelovend is voor de behandeling van afvalwater.

In hoofdstuk 5 wordt de fotokatalytische concentrering van uranium(VI) verbindingen (uranylverbindingen) uit waterige oplossing, waarbij gebruik gemaakt wordt van gesuspenderde TiO_2 of Pt/TiO_2 katalysatordeeltjes, behandeld. In de praktijk bevat dergelijke uraniumionenhoudend afvalwater gewoonlijk ook verschillende typen complexvormers zoals EDTA (ethyleendiaminetetra-azijnzuur). In een zuurstofvrije uranium(VI)/EDTA oplossing vindt de reductieve depositie van uranium(VI) op het oppervlak van de fotokatalysator en het gelijktijdig vrijkomen van CO_2 uit het aanwezige EDTA plaats als gevolg van de fotokatalytische reactie op het oppervlak van de fotokatalysator bij belichting met UV-A-licht. Middels de gekozen experimentele werkwijze bleek tenminste 50 tot 60% van het aanwezige uranium(VI) neer te slaan. Het blijkt dat Pt deze reductieve neerslagvorming van uranium(VI) op het oppervlak van de TiO_2 deeltjes slechts in zeer geringe mate bevordert, dit in tegenstelling tot verschillende andere typen metalen, waarbij Pt wel een duidelijke verbetering laat zien. De uiteindelijke hoeveelheid CO_2 die vrij kwam bij de experimenten kwam overeen met een enkelvoudige decarboxylatie van EDTA en was onafhankelijk van de belichtingstijd. Dit verklaart waarschijnlijk de relatief geringe reductieve depositie van uranium (VI), ongeveer 50 à 60 %. Bovendien betekent dit dat het tricarbonzuur dat bij de oxidatie van EDTA wordt

verkregen niet gemakkelijk verder kan worden geoxideerd en dan ook de verdere reductieve depositie van uranium (VI) op TiO_2 deeltjes limiteert.

In beluchte oplossing werd geen depositie van uranium waargenomen. Alleen grote hoeveelheden CO_2 kwamen daarbij vrij, waarschijnlijk het gevolg van de mineralisatie van EDTA aan het oppervlak van de fotokatalysator. Bij beluchting van systemen, waarin depositie van uranium(VI) op TiO_2 of Pt/TiO_2 had plaats gevonden, werd nagenoeg weer een volledige oxidatie en het weer in oplossing gaan van het neergeslagen uranium verkregen. Tijdens een experiment werd het proces van depositie en weer in oplossing gaan van de uranium component een drietal malen achter elkaar herhaald, nagenoeg met steeds hetzelfde resultaat. De conclusie is dan ook dat dit proces een veelbelovende techniek is om uranium(VI) uit afvalwaterstromen te verwijderen en te concentreren.

Hoofdstuk 6 beschrijft de fotokatalytische dehydrogenering van ethanol in de aanwezigheid van gemetalliseerd CdS (M/CdS met een of twee metalen) in zuurstofvrije systemen waarbij gebruik werd gemaakt van zichtbaar licht. Daarbij werd met name gekeken naar het effect van de verschillende typen metalen. Het hier onderzochte proces resulteert in het algemeen in het vrijkomen van H_2 en de productie van acetaldehyde. Ook werd onderzocht wat het effect is van een voorbehandeling van de M/CdS fotokatalysator bij hoge temperatuur, hoe de distributie van Pd over het CdS oppervlak is, alsmede de rol van Pd en Pt in het katalytische proces en de rol van een fotokatalytische promotor, in het algemeen een tweede metaal (zoals Cu, Ag, Rh) op het oppervlak van de CdS fotokatalysator. Op basis van de experimentele resultaten kon een complex mechanisme voor de fotokatalytische dehydrogenering van alcoholen worden voorgesteld.

In de gekozen experimentele opzet bleek de optimale hoeveelheid fotokatalysator circa 25 g/l te bedragen. De hoeveelheid H_2 die hierbij tijdens de experimenten werd gevormd bedroeg 300 ml/h.l. Voor fotokatalysatoren waarbij Pd deeltjes waren afgezet op het katalysatoroppervlak bleek dat een hoge temperatuur voorbehandeling de grootte van deze Pd deeltjes reduceerde met circa 10%, overeenkomend met een verkleining in diameter van circa 8,8 nm naar 7,9 nm. Gelijktijdig werd daarbij het aantal Pd deeltjes op het oppervlak van de CdS katalysator met circa 41% vergroot. Voor de dehydrogenering van ethanol resulteerde dit in een toename van de fotokatalytische activiteit met 100 %. De dehydrogenering van ethanol bleek een eerste orde reactie te zijn, althans voor ethanol concentraties lager dan 50%. De activiteit van de onderzochte fotokatalysatoren nam af in de volgorde: 5% (gewicht) Pt/CdS (verkregen via chemische depositie en voorbehandeld bij hoge temperatuur) > 5% (gewicht) Pt/CdS (verkregen door fysische menging of chemische depositie al of niet gecombineerd met een voorbehandeling) > 1% (gewicht) $\text{Rh}_2\text{O}_3/\text{CdS}$ (fysische menging, geen voorbehandeling) > PdO, Rh, Ag, Cu, CuO/CdS. Zuivere Cds vertoonde een verwaarloosbare activiteit met betrekking tot de dehydrogenering van ethanol. De optimale hoeveelheid Pt in het systeem Pt/CdS bleek ongeveer 5% (gewicht) te bedragen. Aan de hand van de experimenteel

verkregen resultaten kon worden geconcludeerd dat een tweede metaal component op het oppervlak van de CdS fotokatalysator werkt als een promotor tijdens de dehydrogenering. 5 gewichtsprocent Pt + 5 gewichtsprocent Cu ten opzichte van de hoeveelheid CdS bleek voor het onderzochte systeem, en de toegepaste procescondities de meest optimale combinatie te zijn. Depositie van Pt en Pd op het oppervlak van een CdS fotokatalysator resulteert in een elektronenpomp die zorg draagt voor het transport van fotogegenereerde vrije elektronen van de valentieband van CdS naar Pd. Pd zelf fungeert daarbij als een protonen bindende adsorptiekern. Indien aan het Pd/CdS oppervlak elektronen kunnen stromen van Pd naar CdS en Pd^0 kan worden geoxideerd tot Pd^{2+} onder invloed van licht, kan de fotokatalytische oxidatie van alcoholen aan dergelijke oppervlakken ook plaatsvinden overeenkomstig een heterogeen katalytisch mechanisme, aangeduid als een complexvormend katalytisch mechanisme. Dit wordt veroorzaakt door het feit dat na een voorbehandeling van de Pd/CdS katalysator bij hoge temperatuur, een sterke interactie tussen metaal en halfgeleider (aangeduid met SMSI) wordt verkregen (chemische bindingen tussen of Pd en Cd of tussen Pd en S) aan de Pd-CdS junctie. Deze interactie kan een toename van de elektronenstroom veroorzaken van Pd naar CdS. Op basis van de palladium standaard redoxpotentiaal, hebben de *holes* aan het CdS oppervlak met een positieve lading voldoende elektrische potentiaal om Pd^0 te oxideren tot Pd^{2+} .

Uit het onderzoek naar de toepassing van fotokatalyse voor de behandeling van afvalwaterstromen, zoals dit in dit proefschrift is weergegeven, kunnen de volgende algemene conclusies worden getrokken:

- Experimenten naar de fotokatalytische oxidatie van methanol en ethanol hebben geresulteerd in een uitgebreider en meer diepgaand inzicht in de mechanismen die plaats vinden bij de fotochemische behandeling van afvalwaterstromen.
- Het onderzoek heeft ook meer inzicht opgeleverd in de praktische toepassing van fotokatalyse en de problemen die daarbij voor verschillende typen industriële afvalwaterstromen nog moeten worden opgelost.
- Organochloorverbindingen kunnen gemakkelijk worden gedegradeerd door middel van fotokatalyse. Dit proces biedt veelbelovende perspectieven voor de praktische toepassing.
- Gecombineerde (foto)chemische methoden en fotokatalytische methoden kunnen attractief zijn voor de behandeling van fenolhoudende industriële afvalwaterstromen.
- Experimentele resultaten op het gebied van de fotokatalytische depositie en concentrering van oplosbare uraniumverbindingen laten zien dat deze route interessant kan zijn voor de terugwinning c.q. verwijdering van radioactieve componenten.
- Het onderzoek heeft een bijdrage geleverd in het inzicht in de werking en betekenis van metallisering van de fotokatalysator, een gebruikelijke methode om de activiteit van de halfgeleider-fotokatalysator te vergroten.

**APPENDIX I : REFERENCES ON PHOTOCATALYTIC
DEGRADATION OF ORGANIC COMPOUNDS (IN TABLE 1.4)**

References concerning the photocatalytic oxidation of various organic compounds are presented in this appendix in the ascendent order of the name of organic compounds. A short sentence rather than the title is given to show the research subject of a reference.

Acetic acid, BIDEAU M., B. Claudel, L. Faure, and H. Kazouan, *J. Photochem. Photobiol. A: Chem.*, **61**, 269-280, 1991. "Photooxidation of acetic acid by oxygen O₂ on TiO₂, and dissolved Copper ions, mechanism."

KAISE M., H. Kondoh, C. Nishihara, H. Nozoye, H. Shindo, S. Nimura, and O. KIKUCHI, *J. Chem. Soc., Chem. Commun.*, 395-396, 1993. "ESR, acetic acid, platinum, Pt/TiO₂, radical, surface mechanism."

KRAEUTLER B., and A. J. Bard, *J. Am. Chem. Soc.* **100**(19), 5985-5992, 1978. Heterogeneous photocatalytic decomposition of saturated carboxylic acids (acetic acid) on TiO₂ powder. Decarboxylative route to alkanes. Without or with oxygen."

SATO Shinri, *J. Phys. Chem.*, **87**(18), 3531-3537, 1983. "Photo-Kolbe reaction at gas-solid interfaces, the oxidation of acetic acid, the formation of methane and ethane, on TiO₂ and Pt/TiO₂, H₂ evolution, mechanism."

YONEYAMA H., Y. Takao, H. Tamura, and A.J. Bard, *J. Phys. Chem.*, **87**(8), 417-1422, 1983. "Factors influencing product distribution in photocatalytic decomposition of aqueous acetic acid on platinized TiO₂. Pt/TiO₂, H₂ evolution, methane, ethane formation, mechanism."

Acetylene, LIN Lufei, and Robert R. Kuntz, *Langmuir*, **8**(3), 870-875, 1992. "Photoreduction hydrogenation of acetylene on molybdenum-sulfur complexes (MoS₂) supported on TiO₂, mechanism, pH, catalyst loading, light intensity, density."

Alcohols, CUNNINGHAM Joseph, Benjamin K. Hodnett, Mohammad Ilyas, Edward M. Leahy, and John P. Tobin, *J. Chem. Soc., Faraday Trans. 1*, **78**, 3297-3306, 1982. "Electron transfer at semiconductor surfaces: nature and origins of photoactivity on oxides of 3d transition metals for elimination (oxidation) reactions of secondary alcohols, photocatalysis principle and properties of semiconductor surface."

OHTANI B., M. Kakimoto, S. Nishimoto, and T. Kagiya, *J. Photochem. Photobiol. A: Chem.*, **70**, 265-272, 1993. "Neat alcohols, 2-propanol, organics, Pt/TiO₂, Argon, Hydrogen (H₂), intermediates."

PICHAT P., Marie-Noelle Mozzanega and H. Courbon, *J. Chem. Soc., Faraday Trans. 1*, **83**, 697-704, 1987. "Photocatalytic oxidation of organic alcohol on Pt/TiO₂, using poisons and labelled ethanol, mechanism, isotope, hydrogen released."

Aldehydes, YANAGIDA Shozo, Roshiteru Ishmaru, Yoshio Miyake, Tsutomu Shiragami, Chyongjin Pac, Kazuhito Hashimoto, and tadayoshi Sakata, *J. Phys. Chem.*, **93**(6), 2576-2582, 1989. "Photocatalytic reduction and oxidation of organic aldehydes and its

derivatives using catalyst ZnS, Pt/TiO₂ without O₂, (Ar). H₂, thanol, acetic acid, biacetyl, and acetoin as oxidation products."

Aliphatic alcohols, BORGARELLO E., E. Pelizzetti, *La Chimica E L'Industria*, **65**(7-8), 474-478, 1983. "Photocatalytic oxidation of aliphatic alcohols on semiconductors of TiO₂, ZnO, SnO₂, metallized, Pt/TiO₂, RuO₂/TiO₂, H₂ evolution, UV, sunlight."

JIN Zhensheng, FENG Liangbo, LI Qinglin, WANG Chuanping and SHI Mengyang, *J. of Molecular Catalysis*, **70**, 351-361, 1991. "Photocatalytic oxidation of aliphatic alcohols on air-treated Pt/CdS, H₂ release, evolution, ESR."

Alkanes, DIEGHRI N., M. Formenti, F. Juillet, and S. J. Teichner, *Faraday Discuss. Chem. Soc.*, **58**, 185-193, 1975. "Photointeraction on the surface of titanium dioxide between oxygen and alkanes. Photocatalytic oxidation of organic alkanes with oxygen (gas phase research)."

Alkylbenzaldehydes, MOZZANEGA Marie-Noëlle, Jean Marie Herrmann, and Pierre Pichat, *Tetrahedron Letters*, **34**, 2965-2966, 1977. "Photocatalytic oxidation of organic aromatic d'alkyltoluenes and alkylbenzaldehydes on TiO₂."

Anthraquinone-2-sulfonic sodium salt (ASS), KRWI John, *Environmental toxicology and Chemistry*, **13**(10), 1569-1575, 1994. "TiO₂, air, CO, anthraquinone-2-sulfonic sodium salt (ASS) oxidation, O₂ promotor, temperature, adding H₂O₂ and its decomposition, O₂ and dye adsorption."

Aromatics, MALDOTTI A., R. Amadelli, c. Bartocci, and V. Carassiti, *J. photochem. Photobiol. A: Chem.*, **53**, 263-271, 1990. "Photosynthesis: photo-cyanation (oxidation?) of aromatics on platinized WO₃ and TiO₂. mechanism, intermediates, spin trapping technique, free radical first finding."

Atrazine, BELTRAN F. J., Juan F. Garcia-Araya, and Benito Acedo, *Wat. Res.* **28**(10), 2153-2164, 1994. "Ozone, ozonation, atrazine oxidation, kinetics. partial pressure, pH, temperature, and hydroxyl radical scavengers."

BELTRÁN F. J., G. Ovejero, and B. Acedo, *Wat. Res.* **27**(6), 1013-1021, 1993. "Atrazine photolysis adding hydrogen peroxide, and the additives of bicarbonate or carbonate ions."

BELTRÁN F. J., J. F. García-Araya, and Benito Acedo, *Wat. Res.* **28**(10), 2165-2174, 1994. "Ozone, ultraviolet, atrazine oxidation, photolysis, ozonation, hydroxyl radical. Chlorophenols."

PELIZZETTI E., C. Minero, E. Borgarello, L. Tinucci, N. Serpone, *Langmuir* **9**, 2995-3001, 1993. "Different TiO₂ catalysts, preparation, including sol-gel TiO₂, different effect on phenol and atrazine photooxidation."

PELIZZETTI Ezio, Valter Maurino, Claudio Minero, Vilma Carlin, Edmondo Pramauro, and Orfeo Zerbinati, Maria L. Tosato, *Environ. Sci. Technol.*, **24**(10), 1559-1565, 1990. "Photocatalytic oxidation of organic atrazine and other s-triazine herbicides on TiO₂, O₂. intermediate and mechanism."

- Bentazon**, PELIZZETTI E., V. Maurino, C. Minero, O. Zerbinati, *Chemosphere*, **18**(7-8), 1437-1445, 1989. "Photocatalytic oxidation of organic bentazon, sunlight, herbicide, pH, complete mineralization, very low concentration."
- Benzene**, TURCHI Craig S., and David F. Ollis, *J. Catalysis*, **119**, 483-496, 1989. "The photocatalytic oxidation of organic benzene and perchloroethylene (PCE), kinetic equation, mechanism, intermediates."
- Benzoic acid**, IZUMI Ikuichiro, Fu-Ren F. Fan, and Allen J. Bard, *J. Phys. Chem.* **85**(3), 218-223, 1981. "Photocatalytic oxidation of benzoic acid and adipic acid on Pt/TiO₂, the photo-kolbe decarboxylative route to the breakdown of the benzene ring and to the production of butane. Mechanism, intermediate."
- Butanol**, BLACK N. R., and G. L. Griffin, *J. Phys. Chem.*, **92**(20), 5697-5701, 1988. "Photocatalytic selective oxidation of butanol on TiO₂, mechanism, temperature, first-order."
- BLAKEN. R., and G. L. Griffin, *Submitted to Annual Meeting of the AIChE, November, 1987*. "Photo-assisted vs. Thermal selective oxidation of organic 1-butanol on TiO₂, temperature, intermediates with light and without light, mechanism, reaction order."
- Chlorinated dioxins**, BARBENI Massimo, Edmondo Pramauro, and Ezio Pelizzetti, Enrico Borgarello, Nick Serpone, and Mary A. Jamieson, *Chemosphere*, **15**(9), 1913-1916, 1986. "Photocatalytic oxidation of chlorinated dioxins, biphenyls, phenols and benzene on semiconductor dispersion. Properties of catalyst, mineralization of halophenols."
- Chlorinated phenols**, AL-EKABI Hassain, and Nick Serpone, *J. Phys. Chem.*, **92**, 5726-5731, 1988. "Kinetic, mechanism studies in heterogeneous photocatalysis: Photocatalytic oxidation of chlorinated phenols in aerated aqueous solutions over TiO₂ supported on a glass matrix."
- Chloro-3-(phenyldideuteriomethyl)diazirine**, LIU M. T. H., R. Bonneau, S. Wierlacher and W. Sander, *J. Photochem. Photobiol. A: Chem.*, **84**, 133-137, 1994. "Laser flash photolysis of 3-chloro-3-benzylidiazirine and 3-chloro-3-(phenyldideuteriomethyl)diazirine, temperature, Arrhenius plots, solvent, kinetics."
- Chloro-4-hydroxybenzoic acid (CHBzA)**, CUNNINGHAM Joseph, and Petr Sedláč, *J. Photochem. Photobiol. A: Chem.*, **77**, 255-263, 1994. "Monochlorophenols (Cp), 3-chloro-4-hydroxybenzoic acid (CHBzA), isopropanol, or furfuryl alcohol, oxidation, TiO₂, dark adsorption, initial rates, kinetic equation, zero-order, high flux light, low apparent efficiency, low flux light, high apparent efficiency, added metal Ag⁺, greatly increased the initial rates and the apparent efficiency."
- Chlorofluorocarbons**, RAVISHANKARA A. R., and Edward R. Lovejoy, *J. Chem. Soc. Faraday Trans. 90*(15), 2159-2169, 1994. "Atmospheric lifetime, atmospheric chemistry, and determining their kinetic parameters of chlorofluorocarbons (CFCs) and substitutes; hydrochlorofluorocarbons (HCFCs) and hydrofluorocarbons (HFCs) and questions."

- Chlorofluoromethanes**, FILBY W. G., M. Mintas, and H. Güsten, *Ber. Bunsenges. Phys. Chem.* **85**, 189-192, 1981. "Heterogeneous catalytic degradation (photocatalytic oxidation) of chlorofluoromethanes on ZnO surfaces."
- Chloroform**, HOWARD Tom, and David F. Ollis, presented at *Chicago Ill. AIChE meeting*, Nov. 1985. "Effect of (platinum) metallization on photoassisted organic chloroform decomposition. Oxidation of chloroform on Pt/TiO₂."
- KESSELMAN Janet M., Gary A. Shreve, Michael R. Hoffmann, and Nathan S. Lewis, *J. Phys. Chem.* **98**, 13385-13395, 1994. "Electrode research, mechanism of O₂ reduction rate-limiting stage. CHCl₃ oxidation on TiO₂ electrodes, the role of platinum on Pt/TiO₂."
- KORMANN C., D. W. Bahnemann, and M. R. Hoffmann, *Environ. Sci. Technol.*, **25**(3), 494-500, 1991. "Chloroform photooxidation on TiO₂, mechanism of •OH and the adsorption of organics on TiO₂."
- Chloromethane**, JO Sam K., and J. M. White, *Surface Science*, **255**, 321-326, 1991. "Photolysis mechanism of CH₃Cl through D₂O spacer layers."
- Chloronitrobenzenes**, HUSTERT K., D. Kotzias, and F. Korte, *Chemosphere*, **16**(4), 809-812, 1987. "Photocatalytic oxidation of organic chloronitrobenzenes on TiO₂, intermediate."
- Chloroorganics**, HISANAGA Teruaki, Kenji Harada, and Keiichi Tanaka, *J. Photochem. Photobiol. A: Chem.*, **54**, 113-118, 1990. "Twelve organic chlorides were photooxidized on TiO₂, Pt/TiO₂ (platinized), and with H₂O₂, mechanism."
- Chlorophenol**, BARBENI Massimo, Edmondo Pramauro, Ezio Pelizzetti, Enrico Borgarello, Michael Grätzel, and Nick Serpone, *Nouveau Journal de Chimie*, **8**(8-9), 547-550, 1984. "Photocatalytic oxidation of chlorophenol on TiO₂, intermediate, mechanism, sunlight."
- KLAUSNER J.F., A. R. Martin, D. Y. Goswami, K. S. Schanze, *J. of Solar Energy Engineering*, **116**, 19-24, 1994. "TiO₂, air, Determination, measurement of reaction rate constants and kinetics, batch-type reactor, 4-chlorophenol (4CP), first order."
- MARTIN Scot. T., Colin L. Morrison, and Michael R. Hoffmann, *J. Phys. Chem.* **98**, 13695-13704, 1994. "Vanadium doped in TiO₂, air, CO₂, negative effect on 4-chlorophenol oxidation."
- MILLS Andrew, Richard Davies, *J. Photochem. Photobiol. A: Chemistry* **85**, 173-178, 1995. "TiO₂, air, CO₂, 4-chlorophenol oxidation, activation energy, a model of Arrhenius-type functions using in general rate equation to calculate the activation energy."
- VINODGOPAL K., Surat Hotchandani, and Prashant V. Kamat, *J. Phys. Chem.* **97**(35) 9040-9044, 1993. "TiO₂ supported on conducting glass plates, electrode, organic 4-chlorophenol oxidation greatly increases if maintained at an external anodic bias, during the UV light."
- WYNESS P., J. F. Klausner, D. Y. Goswami, K. S. Schanze, *J. of Solar Energy Engineering*, **116**, 8-13, 1994. "Different big scale batch-type reactors, solar light,

TiO₂ slurry or adhered on fiberglass. 4-chlorophenol (4CP) oxidation, first order rate constant increase with decreasing initial concentration."

Chlorophenols, DAVIS A. P., and C. P. Huang, *Wat. Sci. Tech.*, **21**, 455-464, 1989.

"Photocatalytic oxidation of chlorophenols on CdS, pH, concentration, temperature, oxygen, light intensity."

LI X., P. Fitzgerald and L. Bowen, *Wat. Sci. Tech.* **26**(1-2), 367-376, 1992, "Real industry wastewater containing various chlorophenols, photooxidation on dye-sensitized photolysis using visible light."

MYLONAS A., E. Papaconstantinou, *J. of Molecular Catalysis*, **92**, 261-267, 1994.

"Homogeneous photocatalysis of $W_{10}O_{32}^{4-}$, $PW_{12}Q_0^{3-}$, $SiW_{12}Q_0^{4-}$ on chlorophenols, CO₂, comparing with TiO₂."

SEHILI Tahar, Pierre Boule, and Jacques Lemaire, *J. Photochem. Photobio. A: Chem.*, **50**, 117-127, 1989. "Photo oxidation of organic chloroaromatic derivatives (chlorophenols) on ZnO, mechanism, adsorption and desorption, OH radicals, intermediates, self-inhibition, the formation of H₂O₂."

Chlorosalicylic acid, SABATE J., M. A. Anderson, H. Kikkawa, M. Edwards, and C. G. Hill, Jr., *J. of Catalysis*, **127**, 167-177, 1991. "A kinetic study of the photocatalytic degradation of chlorosalicylic acid on TiO₂ membranes supported on glass. mechanism, photoreactor."

SABATE J., M. A. Anderson, H. Kikkawa, Q. Xu, S. Cervera-March, C. G. Hill, Jr., *J. of Catalysis*, **134**, 36-46, 1992. "Plain, pure and Nb-doped TiO₂ ceramic membranes supported on glass, properties, photooxidation of 3-chlorosalicylic acid, light absorption."

Cyclic ethers and cyclohexane, KISCH H., *J. Inf. Rec. Mater*, **17**(5/6), 363-372, 1989. "Photo oxidation of organic cyclic ethers and cyclohexane by catalysts of ZnS, Pt/CdS, isotope H₂, evolution, released, mechanism."

Dibromo 3-chloro propane, MILANO J. C., C. Bernat-Escallon, and J. L. Vernet, *Wat. Res.* **24**(5), 557-564, 1990. "Photolysis of organic 1,2-Dibromo 3-chloro propane, trace, H₂O₂, kinetics, mechanism, intermediates."

Dibromoethane, NGUYEN T. and D. F. Ollis, *J. Phys. Chem.*, **88**(16), 3386-3388, 1984. "Photocatalytic oxidation of organic dibromoethane to CO₂ and HBr. Mechanisms."

OLIVER Barry G., Ernest G. Cosgrove, and John H. Carey, *Environ. Sci. Technol.*, **13**(9), 1075-1077, 1979. "Effect of suspended sediments on the photolysis of organics in water. Photocatalytic oxidation of organic alcohol and dichlorobenzene on TiO₂, OH mechanism, introduction."

Dichlorobenzenes, SEHILI Tahar, Pierre Boule, and Jacques Lemaire, *J. Photochem. Photobio. A: Chem.*, **50**, 103-116, 1989. "Photo oxidation of organic chloroaromatic derivatives (dichlorobenzenes) on ZnO, mechanism, adsorption and desorption, OH radicals, intermediates, self-inhibition, the formation of H₂O₂."

- Dichlorobiphenyl, TUNESI Simonetta, and Marc A. Anderson, *Chemosphere*, **16**(7), 1447-1456, 1987. "Photocatalysis of organic 3,4-DCB (dichlorobiphenyl) in TiO_2 aqueous suspensions; effects of temperature and light intensity; CIR-FTIR interfacial analysis. Spectrum."
- Dichloroethane, CHEN H. Y., O. Zahraa, M. Bouchy, F. Thomas, J. Y. Bottero, *J. Photochem. Photobiol. A: Chemistry* **85**, 179-186, 1995. " TiO_2 , air, CO_2 , adsorption equilibrium and kinetic equation, 1,2-dichloroethane (DCE) oxidation, mass transfer."
- Dichloromethane, HSIAO Chen-Yung, Chung-Li Lee, and David F. Ollis, *J. Catalysis*, **82**, 418-423, 1983. "Photocatalytic oxidation of organic dichloromethane, chloroform, and carbon tetrachloride on TiO_2 , kinetic equation, mechanism."
- TANGUAY James F., Robert W. Coughlin, and Steven L. Suib, *Emerging Technologies in Hazardous waste Management*, ACS Symp. Ser. 1990, pp. 114-118. "Photooxidation of organic dichloromethane to CO_2 and HCl with O_2 and different TiO_2 fixed on supporters."
- Dimedthoxybenzenes, AMALRIC Laurence, Chantal Guillard, Nick Serpone, Pierre Pichat, *J. Environ. Sci. Health*, **A28**(6), 1393-1408, 1993. "Three organics of dimedthoxybenzenes (DMBs) were photooxidized on TiO_2 -UV, different wavelenth have defferent intermediates."
- Dimethyl-2-butene, YOKOTA Toshiyuki, Yasuyuki Takahata, Jun Hosoya, Keiichi Suzuki, and Kon Takahashi, *J. Of Chemical Engineering of Japan*, **22**(5), 543-548, 1989. "Photolysis oxydation, oxygenation, of organic 2,3-dimethyl-2-butene using dye sensitizer supported on solid particles. light absorption rate, photosensitizer, heterogeneous photolysis."
- Dodecane, PELIZZETTI Ezio, Claudio Minero, Valter Maurino, Hisao Hidaka, Nick Serpone, Rita Terzian, *Annali di Chimica*, **80**, 81-87, 1990. "Photooxidation of organic dodecane and of some dodecyl derivatives. mechanism and kinetics."
- Dyes, NEEVEL J. G., H. C. A. van Beek, H. H. I. den Ouden, and B. van de Graaf, *JSDC*, **106**, May/June 1990. "Photolysis oxidation of dyes with O_2 to phenolic and qinonoids, fading of dyes. the Netherlands."
- Ethanoic acid, MARCHESE L., S. Coluccia, E. Borello, L. Palmisano, A. Sclafani, and M. Schiavello, *Structure and Reactivity of Surfaces*, (eds.) C. Morterra, A. Zecchina, and G. Costa, Amsterdam, Elsevier Science Publishers B.V., 1989, 643-652. "Photoassisted mechanisms in heterogeneous catalysis: the Role of surface OH in the oxidation decomposition of organic ethanoic acid on semiconductor magnesium oxide."
- Ethanol, SAKATA T., T. Kawai, *Chem. Phys. Lett.*, **80**(2), 341-344, 1981. "Heterogeneous photocatalytic production of hydrogen (H_2), and methane from ethanol and water. Pt/ TiO_2 , and other metals deposited on TiO_2 ."
- YASUMORI A., K. Yamazaki, S. Shibata, and M. Yamane, *J. of the Ceramic Soc. of Japan*, **102**(8), 702-707, 1994. " TiO_2 adhered or fixed on silica gel, preperation of Pt/ TiO_2 , H_2 , ethanol, pre-treatment."

- Ethoxyethanol**, YAMAGATA Sadamu, Ryo baba, and Akira Fujishima, *Bull. Chem. Soc. Jpn.*, **62**(4), 1004-1010, 1989. "Photocatalytic oxidation of organic 2-ethoxyethanol on TiO_2 , spectrums, GC-MS, IR, ESR, with spin trapping technique, intermediates, Pt/TiO_2 , mechanism."
- Ethylene glycol**, BAMWENDA G. R., S. Tsubota, T. Kobayashi and M. Haruta, *J. Photochem. Photobiol. A: Chem.*, **77**, 59-67, 1994. "Ethylene glycol oxidation, H_2 evolution, gold, Au/TiO_2 , calcination temperature, duration of irradiation, gold loading, initial concentration, pH, temperature and activation energy."
- Formic Acid**, KIM Dong Hyun, and Marc A. Anderson, *Environ. Sci. Technol.* **28**(3), 479-483, 1994. "Formic Acid (HOOH) oxydation, photocatalytic and photoelectrocatalytic, TiO_2 film thickness, biasing potential, presence of oxygen."
- Furandimethanol**, RICHARD C., A. M. Martre, and P. Boule, *J. Photochem. Photobiol. A: Chem.* **66** 225-234, 1992. "Photocatalytic oxidation (synthesis) of 2,5-furandimethanol organics on ZnO to form other organics with O_2 , mechanism of hydroxyl and surface mechanism."
- Halobenzenes**, KOCHANY Jan, and James R. Bolton, *Environ. Sci. Technol.* **26**(2)262-265, "EPR, measuring the primary rate constants of $\bullet\text{OH}$ with benzene and some halobenzenes in the photolysis of H_2O_2 ."
- Haloorganics**, PELIZZETTI Ezio, Edmondo Pramauro, C. Minero, and Nick Serpone, *Waste Management*, **10**, 65-71, 1990. "Sunlight photooxidation of organic pollutants of haloorganics, surfactants, pesticides, on TiO_2 , CO_2 , visible light, O_2 , intermediates, and mechanism."
- Halothane**, BAHNEMANN D. W., J. Monig, and R. Chapman, *J. Phys. Chem.*, **91**(14), 3782-3788, 1987. "Photocatalytic reduction of organic halothane on platinized Pt/TiO_2 , mechanism."
- Hydrocarbons**, HASHIMOTO Kazuhito, Tomoji Kawai, Tadayoshi Sakata, *J. Phys. Chem.*, **88**(18), 4083-4088, 1984. "Photocatalytic reactions of organic hydrocarbons and fossil fuels with water. Hydrogen evolution and oxidation, mechanism.
IZUMI I., W. W. Dunn, K. O. Willbourn, Fu-Ren F. Fan, and A. J. Bard, *J. Phys. Chem.* **84**, 3207-3210, 1980. "Photocatalytic oxidation of organic hydrocarbons on Pt/TiO_2 , mechanism, intermediates."
- Hydroxybenzoic acid**, HUSTERT K., D. Kotzias, and F. Korte, *Chemosphere*, **12**(1), 55-58, 1983. "Photocatalytic oxidation of organic compounds: hydroxybenzoessäure, dichlorthiamid, trichlorphenol, atazin, diethylphthalat, the possibility of these compounds being oxidized by TiO_2 ."
- DDT**, BORELLO Roberta, Claudio Menero, Edmondo Pramauro, Ezio Pelizzetti, Nick Serpone, Hisao Hidaka, *Environmental Toxicology and Chemistry*, **8**, 997-1002, 1989. "Photocatalytic oxidation of organic insecticide of DDT on catalyst surfaces of Pt/TiO_2 , TiO_2 , ZnO , CdS , WO_3 , $\alpha\text{-Fe}_2\text{O}_3$, and under the illumination of simulated sunlight."

- Isobutane, COURBON Henri, Marc Formenti, and Pierre Pichat, *The Journal of Physical Chemistry*, **81**(6), 1977. "Study of oxygen isotope exchange over UV irradiated anatase samples and comparison with the photooxidation of isobutane into acetone. Photocatalytic oxidation of organic isobutane only to acetone."
- HERRMANN J. M., J. Disdier, M.-N. Mozzanega, and P. Pichat, *J. Catalysis*, **60**, 369-377, 1979. "Heterogeneous photocatalysis: *In Situ* photoconductivity study of TiO_2 during photocatalytic oxidation of organic isobutane into acetone. Gas reaction, oxygen mechanism, kinetic equation."
- Isopropanol, BICKLEY R. I., and R. K. M. Jayanty, *Faraday discuss. Chem. Soc.* **58**, 194-204, 1975. "Photo-adsorption and photo-catalysis on titanium dioxide surface. Photo-adsorption of oxygen and the photocatalyzed oxidation of organic isopropanol, mechanism, intermediates."
- BICKLEY R. I., G. Munuera, and F. S. Stone, *J. Catalysis*, **31**, 398-407, 1973. "Photoadsorption and photocatalysis at Rutile surfaces. II. Photocatalytic oxidation of isopropanol. (Gas phase), mechanism."
- KOBAYAKAWA Koichi, Yochitake Nakazawa, Masato Ikeda, Yuichi Sato, and Akira Tujishima, *Ber. Bunsenges. Phys. Chem.*, **94**, 1439-1443, 1990. "Influence of density of surface hydroxyl groups on TiO_2 photocatalytic activities. mechanism. reduction of inorganic silver ions and the oxidation of organic isopropanol."
- Methanol, MICIC O. I., Y. Zhang, K. R. Cromack, A. D. Trifunac, and M. C. Thurnauer, *J. Phys. Chem.* **97**(50), 13284-13288, 1993. "EPR, methanol, radical, TiO_2 surface mechanism."
- Methyl orange, ZANG Ling, Chun-Yan Liu, Xin-Min Ren, *J. Photochem. Photobiol. A: Chemistry* **85**, 239-245, 1995. "ZnS sols, methyl orange reduction, without air, steady state equation, reaction kinetics, surface charge change on adsorption of cation or anion."
- Methyl viologen, LIU Xinsheng, Kai-Kong Lu and J. Kerry Thomas, *J. Chem. Soc. Faraday Trans.* **89**(11), 1861-1865, 1993. " TiO_2 , support on zeolite, photoreduction of methyl viologen to methyl viologen radical cation."
- Methylbutane, DJEGHRI N., and S. J. Teichner, *J. Catalysis*, **62**, 99-106, 1980. "Photocatalytic oxidation of 2-methylbutane, pathway, mechanism."
- Methylbutanols, WALKER A., M. Formenti, P. Meriaudeau, and S. J. Teichner, *J. Catalysis*, **50**, 237-243, 1977. "Heterogeneous photocatalysis: photo-oxidation of organic methylbutanols."
- Methylene blue, MATTHEWS Ralph W., *J. Chem. Soc., Faraday Trans. I*, **85**(6), 1291-1302, 1989. "Photocatalytic oxidation of organic methylene blue, sunlight, mechanism, TiO_2 supported thin films."
- Naphthalene (NPH), GUILLARD Chantal, Herve Delprat, Can Hoang-van and Pierre Pichat, *J. Atmospheric Chemistry* **16**, 47-59, 1993. "Laboratory study of the rates and products

of the phototransformations of naphthalene adsorbed on samples of titanium dioxide, ferric oxide, muscovite, and fly ash,"

Nitrogen-organics, PELIZZETTI E., C. Minero, P. Piccinini and M. Vincenti, *Coordination Chemistry Reviews*, **125**, 183-194, 1993. "Nitrogen-organics, nitrobenzene, atrazine, photooxidation, intermediate, TiO_2 , ZnO ."

Nitroguanidine, BURROWS W. Dickinson, and Charles I. Noss, *Hazard. Ind. Waste*, **21st.**, 269-281, 1989. "Photolysis oxidation of organic nitroguanidine production industrial wastewater by UV and sunlight."

Nitrophenol, AUGUGLIARO V., M. J. López-Muñoz, L. Palmisano, J. Soria, *Applied Catalysis A: General* **101**, 7-13, 1993. "2-, 3-, and 4-nitrophenol, TiO_2 , organics, pH, initial concentration, adsorption mechanism."

PALMISANO L., V. Augugliaro, M. Schiavello, and A. Sclafani, *J. Molecular Catalysis*, **56**, 284-295, 1989. "pH influence, a lot of semiconductors as catalysts, ZnO , WO_3 , Cr_2O_3 , Fe_2O_3 , MgO , $\gamma\text{-Al}_2\text{O}_3$, SiO_2 , TiO_2 for the photocatalytic oxidation of acetic acid, phenol, and nitrophenol isomers in gas phase and liquid phase. with and without oxygen."

Odor compounds, SUZUKI Ken-ichirou, Shigeyuki Satoh, and Takashi Yoshida, *DENKI KAGAKU*, **59(6)**, 521-523, 1991. "Photocatalytic deodorization (oxidation of organics) on TiO_2 coated, supported on honeycomb ceramics."

Oligocarboxylic acids, Marta I. Litter, José A. Navío, *J. Photochem. Photobiol. A: Chem.* **84**, 183-193, 1994. "Comparison of the photocatalytic efficiency of TiO_2 , iron oxides and mixed Ti(IV)-Fe(III) oxides: photodegradation of oligocarboxylic acids. Photocatalytic oxidation of organics, different influence factors on photocatalytic activity, comparison on catalysts, surface complexes, intermediates, preparation of the catalysts."

Organic acid, Kraeutler B., and A. J. Bard, *J. Am. Chem. Soc.* **100(7)**, 2239-2240, 1978.

"Heterogeneous photocatalytic synthesis of methane from acetic acid-New kolbe reaction pathway, photocatalytic oxidation of organic acid, intermediate, mechanism."

CHEMSEDDINE A., and H. P. Boehm, *J. of Molecular Catalysis*, **60**, 295-311, 1990.

"Photocatalytic oxidation of four organic acids under oxygen (O_2), nitrogen (N_2), and N_2O , mechanism, intermediates, free radicals, and spin-trap experiments."

SAKATA Tadayoshi, Tomoji Kawai, and Kazuhito Hashimoto, *J. Phys. Chem.*, **88(11)**, 2344-2350, 1984. "Heterogeneous photocatalytic reaction of organic acids and water. New reaction paths, mechanism, besides the photo-kolbe reaction, oxidation of acetic, propionic, and butyric acids on catalysts of semiconductors, the influence of Ag^+ , pH, hydrogen evolution."

Organic carbon, ABDULLAH Mohammad, Gary K.-C. Low, and Ralph W. Matthews, *J. Phys. Chem.*, **94(17)**, 6820-6825, 1990. "The influence of inorganic anions, pH on the photocatalytic oxidation of organic carbon over TiO_2 supported on glass, CO_2 , evolution."

- Organic solutes, MATTHEWS Ralph W., *J. Catalysis*, **111**, 264-272, 1988. "Kinetics of photocatalytic oxidation of organic solutes on TiO_2 , concentration, pH, mechanism, 88-89."
- Organics, HERRMANN J.-M., C. Guillard, and P. Pichat, "Heterogeneous photocatalysis," *Catalysis Today*, **17**, 7-20, 1993. "Introduction, review, history, heterogeneous photocatalysis, organics oxidation."
- LICHTIN Norman N., Junchang Dong, and K. M. Vijayakumar, *Water Poll. Res. J. Canada*, **27**(1), 203-210, 1992. "Sixteen organics photooxidation in water or in gas vapor on TiO_2 and H_2O_2 , kinetics, and influence of the H_2O_2 on these compounds."
- LINK Hal, and Craig S. Turchi, "Cost and Performance Projections for Solar Water Detoxification Systems", presented at: ASME International Solar Energy Meeting, Reno, Nevada, USA. March 17-22, 1991. "Solar light, small-scale experiments of photooxidation of organics, cost of commercial system."
- MATTHEWS R. W. and Stephen R. McEvoy, *J. Photochem. Photobiol. A. Chem.* **64**, 231-246, 1992. "Organics of phenol photooxidation on TiO_2 , and TiO_2 supported on Sand, with near UV and visible sun light, kinetics, adsorption equilibrium constant."
- MATTHEWS Ralph W., *Wat. Res.* **24**(5), 653-660, 1990. "A lot of organics were photooxidized on TiO_2 , air, CO_2 , mechanism."
- MATTHEWS Ralph W., *J. Phys. Chem.*, **91**(12), 3328-3333, 1987. "Photocatalytic oxidation of organics on TiO_2 supported on thin films. Mechanism, activation energy."
- MATTHEWS Ralph W., *Wat. Res.* **20**(5) 569-578, 1986. "Photo oxidation of organic compounds on TiO_2 , solar light and UV light, CO_2 released, pH."
- MATTHEWS Ralph W., *Journal of Catalysis*, **97**, 565-568, 1986. "Photocatalytic oxidation of organic on TiO_2 , CO_2 release."
- PACHECO James, and John T. Holmes, *Emerging Technologies in Hazardous waste Management*, ACS Symp. Ser. 1990, pp. 40-51. "Two bench scale solar photocatalytic reactors for organics oxidation, and kinetics."
- PELIZZETTI Ezio, Claudio Minero, and Valter Maurino, *Advances in Colloid and Interface Science*, **32**, 271-316, 1990. "Principle, overview, history of photocatalysis, organics, inorganics elimination, photooxidation, kinetics, reactor design."
- Organo-nitrates, LIPCZYNSKA-KOCHANY Ewa, *Water Poll. Res. J. Canada*, **27**(1), 97-122, 1992. "Photolysis of 4 organo-nitrates (nitro-benzene, -phenols), with Fenton reagent ($\text{FeCl}_2/\text{H}_2\text{O}_2$)."
- Organochlorine, HIDAKA Hisao, Kayo Nohara and Jincai Zhao, Nick Serpone, Ezio Pelizzetti *J. Photochem. Photobiol. A. Chem.* **64** 247-254, 1992. "Organochlorine, pesticide, e.g. permethrin photooxidation on TiO_2 , and modified TiO_2 by photosensitizer, visible sun light, first order kinetics."
- Organophosphate, HUNG Sze To, and Mark K. S. Mak, *Environmental Technology*, **14**, 265-269, 1993. " TiO_2 , organophosphate photooxidation, (fulvic acid), pesticide."

- Organophosphorous**, HARADA Kenji, Teruaki Hisanaga, and Keiichi Tanaka, *Wat. Res.* **24**(11), 1415-1417, 1990. "Photocatalytic oxidation of organophosphorous insecticides on TiO_2 , Pt/TiO_2 , WO_3 , Fe_2O_3 , O_2 ."
- GRÄTZEL C. K., M. Jirousek and M. Grätzel, *J. Mol. Cat.* **39** 347-353, 1987. "Photocatalytic oxidation of organic phosphates on TiO_2 , Nb-dope TiO_2 , intermediate, mechanism."
- GRÄTZEL Carole K., Marie Jirousek, and Michael Grätzel, *J. of Molecular Catalysis*, **60**, 375-387, 1990. "Photooxidation of organophosphorus on TiO_2 powder, mechanism."
- HARADA K., T. Hisanaga, and K. Tanaka, *New Journal of Chemistry*, **11**(8-9), 597-600, 1987. "Photocatalytic oxidation of organophosphorus on TiO_2 , intermediates."
- LU Ming-Chun, Gwo-Dong Roam, Jong-Nan Chen, and C. P. Huang, *J. Photochem. Photobiol. A: Chem.*, **76**, 103-110, 1993. "Photooxidation of organophosphorus insecticide: dichlorvos on glass-supported TiO_2 , initial concentration, oxygen, electrolytes, flow rate and temperature."
- PCB's**, CAREY John H., John Lawrence, and Helle M. Tosine, *Bulletin of Environmental Contamination & Toxicology*, **16**(6), 697-701, 1976, "Photodechlorination of PCB's in the presence of titanium dioxide in aqueous suspensions. Photocatalytic oxidation of organic PCB's on TiO_2 ."
- Pentachlorophenol**, BARBENI Massimo, Edmondo Pramauro, and Ezio Pelizzetti, Enrico Borgarello, and Nick Serpone, *Chemosphere*, **14**(2), 195-208, 1985. "Photocatalytic oxidation of organic pentachlorophenol (PCP, found in the pulp, paper industries wastewater) on semiconductor catalysts: TiO_2 , ZnO , CdS , WQ , and SnO with sun light."
- Perchloroethylene**, OLLIS D. F., Chen-Yung Hsiao, L. Budiman, and Chung-Li Lee, *J. Catalysis*, **88**, 89-96, 1984. "Photocatalytic oxidation of organic perchloroethylene, dichloroethane, chloroacetic acids, and chlorobenzenes, mechanism, intermediates."
- Pesticides**, KLÖPFER Walter *The Science of the Total Environment* **123/124**, 145-159, 1992. "Photochemical degradation of pesticides and other chemicals in the environment: a critical assessment of the state of the art. Introduction, review of photochemical oxidation of organic pesticides."
- Ph_3CCOOH** , LAI Cuiwei, Yeong Il Kim, Chong Mou Wang, and Thomas E. Mallouk, *J. Org. Chem.* **58**(6), 1393-1399, 1993. "Radical, photo-Kolbe reaction, mechanism, Ph_3CCOOH , and Ph_2CCOOH photooxidize to $\text{Ph}_3\text{C}^\bullet$."
- Phenol**, AUGUGLIARO V., L. Palmisano, and A. Sclafani, C. Minero, and E. Pelizzetti, *Toxicological and Environmental Chemistry*, **16**, 89-109, 1988. "Photocatalytic oxidation of organic phenol on TiO_2 , pH, concentration, oxygen pressure, intermediate, mechanism, kinetic models."
- KAWAGUCHI H., *Environmental Technology Letters*, **5**, 471-474, 1984. "Photocatalytic oxidation of organic phenol on TiO_2 , mechanism, intermediates."

OKAMOTO Ken-ichi, Yasunori Yamamoto, Hiroki Tanaka, Masashi Tanaka, and Akira Itaya, *Bull. Chem. Soc. Jpn.*, **58**(7), 2015-2022, 1985. "Heterogeneous photocatalytic decomposition of phenol over TiO_2 powder, oxidation of organic phenol, mechanism, intermediates."

PERAL José, Juan Casado, and Javier Doménech, *J. Photochem. Photobiol. A: Chem.*, **44**(2), 209-217, 1988. "Photocatalytic oxidation of organic phenol on ZnO , concentration, pH, oxygen, hydrogen peroxide, mechanism."

SCLAFANI A., L. Palmisano, and M. Schiavello, *J. Phys. Chem.*, **94**(2), 829-832, 1990. "Properties of TiO_2 from different preparation methods, and the photocatalytic oxidation of phenol."

SCLAFANI Antonino, Leonardo Palmisano and Eugenio Davì, *New J. Chem.* **14**(4), 265-268, 1990. "Photooxidation of phenol on TiO_2 (anatase and rutile), the influence of pH, O_2 , Ag^+ , and H_2O_2 , kinetics and mechanism."

TSENG Jesseming, and c. P. Huang, *Emerging Technologies in Hazardous Waste Management*, ACS symp. Ser. 1990, pp. 12-39. "Mechanism of photocatalytic oxidation of phenol, the influence of catalyst properties, O_2 , (oxygen), temperature, pH, concentration, chloride, intermediates, and free radicals."

WEI Tsong-Yang, Yung-Yun Wang, and Chi-Chao Wan, *J. Photochem. Photobiol. A: chem.*, **55**, 115-126, 1990. "Photocatalytic oxidation of organic phenol with H_2O_2 and TiO_2 , effect of hydrogen peroxide and Fe^{2+} , and Cu^{2+} ."

Phenols, CASTRANTAS Harry M., and Robert D. Gibilisco, *Emerging Technologies in Hazardous waste Management*, ACS Symp. Ser. 1991, pp. 77-99. "Photolysis of organic phenols and substituted phenols by $\text{UV-H}_2\text{O}_2$, concentration, pH, Fenton's reagent."

DAVIS Allen P., and C. P. Huang, *Wat. Res.* **24**(5), 543-540, 1990. "The photocatalytic oxidation of organic substituted phenols on cadmium sulfide (CdS), mechanism, pH, adsorption."

Polychlorinated dioxins, PELIZZETTI Ezio, Marco Borgarello, Claudio Minero, Edmondo Pramauro, Enrico Borgarello, and Nick Serpone, *Chemosphere*, **17**(3), 499-510, 1988. "Photocatalytic oxidation of organic polychlorinated dioxins and polychlorinated biphenyls in aqueous suspensions of different semiconductors catalyst irradiated with simulated solar light, TiO_2 , ZnO , CdS , Pt/TiO_2 , Fe_2O_3 , mechanism, intermediates."

Polynuclear aromatic hydrocarbons, DAS S., M. Muneer, and K. R. Gopidas, *J. Photochem. Photobiol. A: Chem.*, **77**, 83-88, 1994. "Photooxidation of polynuclear aromatic hydrocarbons, e.g. acenaphthene, anthracene, fluorene and naphthalene on TiO_2 , O_2 , light and sunlight, intermediates, hydroxyl and superoxide radicals mechanism."

Polysyclic aromatic hydrocarbons (PAHs), LIU Yuan S., Paul de Mayo, and William R. Ware, *J. Phys. Chem.* **97**(22), 5987-5994, 1993. "Photophysics, photolysis of Polysyclic aromatic hydrocarbons (PAHs), adsorption on silica gel surfaces, fluorescence quantum yields."

LIU Yuan S., Paul de Mayo, and William R. Ware, *J. Phys. Chem.* **97**(22), 5995-6001, 1993. "Photophysics, photolysis of Polysyclic aromatic hydrocarbons (PAHs), adsorption on silica gel surfaces, fluorescence quantum yields."

Propan-2-ol photooxidize, GREEN K. J., and Robert Rudham, *J. Chem. Soc. Faraday Trans.*, **89**(11), 1867-1870, 1993. "Liquid organic of propan-2-ol photooxidize to propanone using CdS or TiO₂ in Y zeolite supporter, O₂, H₂O, activation energies."

Propene, PICHAT Pierre, Jean-Marie Herrmann, Jean Disdier, and Marie-Noëlle Mozzanega, *The Journal of Physical Chemistry*, **83**(24), 1979. "Photocatalytic oxidation of organic propene over various semiconductor oxides catalysts at 320 K. Selectivity oxidation."

Propionic acid, BIDEAU M., B. Claudel, L. Faure and H. Kazouan, *J. Photochem. Photobiol. A: Chem.* **67**, 337-348, 1992. "Photooxidation of propionic acid on TiO₂ and dissolved or adsorbed copper, mechanism, intermediate."

Pyridine, MAILLARD-DUPUY Catherine, Chantal Guillard, Henri Courbon, and Pierre Pichat, *Environ. Sci. Technol.* **28**, 2176-2183, 1994. "TiO₂, air, CO₂, pyridine (Pyr) oxidation, intermediates identified, GC/MS, organic nitrogen oxidize to NH₄⁺, and very slow to nitrate."

SAMPATH Srinivasan, Hiroyuki Uchida, and Hiroshi Yoneyama, *J. of Catalysis*, **149**, 189-194, 1994. "TiO₂ on Zeolite supported (mordenite), gas phase pyridine oxidation."

Salicylic acid, DAGAN Geula, and Micha Tomkiewicz, *J. Phys. Chem.* **97**(49), 12651-12655, 1993. "Preparation of aerogel TiO₂ (e.g. gel TiO₂), catalyst, higher activity than P-25, for the oxidation of salicylic acid."

PAPPJ., H.-S. Shen, R. Kershaw, K. Dwight, and A. Wold, *chem. Mater.* **5**, 284-288, 1993. "Pd/TiO₂, salicylic acid oxidation, powder, film, different preparation."

Sulfonated aromatics, SANGCHAKR Benchang, Teruaki Hisanaga, Keiichi Tanaka, *J. Photochem. Photobiol. A: Chemistry* **85**, 187-190, 1995. "TiO₂, air, CQ, sulfonated aromatics oxidation, concentration, temperature, substituent group, activation energy, Hammett's constant, electrophilic nature."

Surfactants, HIDAKA Hisao, Shinya Yamada, Shinichi Suenaga, Jincai Zhao, *J. of Molecular Catalysis*, **59**, 279-290, 1990. "Photooxidation of surfactants on TiO₂, (anionic, cationic, and nonionic surfactants). CO₂."

HIDAKA Hisao, Jincai Zhao, Shinichi Suenaga, Nick Serpone, and Ezio Pelizzetti, *J. Jpn. Oil Chem. Soc. (Yukagaku)*, **39**(11), 45-48, 1990. "Photooxidation of non-ionic surfactants on TiO₂, intermediates, pH."

PELIZZETTI Ezio, Claudio Minero, Valter Maurino, Antonono Sciafani, Hisao Hidaka, and Nick Serpone, *Environ. Sci. Technol.* **23**(11), 1380-1385, 1989. "Photo oxidation of organic Nonylphenol Ethoxylated Surfactants, mechanism, kinetic equations."

- Tetrachloroethene, MERTENS Ralf, Clemens von Sonntag, *J. Photochem. Photobiol. A: Chemistry* **85**, 1-9, 1995. "Photolysis, tetrachloroethene oxidation, CO₂, add scavenging alcohols with and without O₂, quantum yield, rate constants."
- Tetrachloromethane, CHOI Wonyong, Andreas Termin, and Michael R. Hoffmann, *J. Phys. Chem.* **98**, 13669-13679, 1994. "Doped Fe³⁺, Mo⁵⁺, Ru³⁺, Os³⁺, Re³⁺, V⁴⁺, and Rh³⁺ in TiO₂, enhance photoreactivities of CCl₄ reduction, or CHCl₃ oxidation."
- Thioethers, CHAMBERS R. Carlisle, and Craig L. Hill, *J. Am. Chem. Soc.*, **112**(23), 8427-8433, 1990. "Photooxidation of thioethers by heterogeneous photocatalysis of polyoxotungstates (W₁₀O₃₂⁴⁻)."
- Toluene, BUTLER Elizabeth C., and Allen P. Davis, *J. Photochem. Photobiol. A: Chem.*, **70**, 273-283, 1993. "Transition metals, Cu, Fe, and Mn, TiO₂, Toluene, organics, mechanism, photooxidation."
- IBUSUKI Takashi, and Kon Takeuchi, *Atmospheric Environment*, **20**(9), 1711-1715, 1986. "Photocatalytic oxidation of organic toluene on TiO₂ with and without O₂, NO or H₂O at ambient temperature, mechanism, intermediate."
- Trichloroethane (TCA), SKOCYPEC R. D., R. E. Hogan, Jr., *J. of Solar Energy Engineering*. **116**, 14-18, February, 1994. "Direct catalytic absorption reactors (DCARs) use a porous solid matrix, catalyst: rhodium coated porous alumina absorber, solar energy, a numerical mode for solar volumetric air-heating receivers and methane-reforming is used, 1,1,1-trichloroethane (TCA) oxidation, solar furnace."
- Trichloroethylene (TCE), DIBBLE Lynette A., and Gregory B. Raupp, *Catalysis Letters*, **4**, 345-354, 1990. "Photooxidation of TCE on gas/solid phases, TiO₂, mechanism, O₂, concentration, water vapor."
- CABRERA Maria L., Orlando M. Alfano, and Alberto E. Cassano, *Ind. Eng. Chem. Res.* **33**, 3031-3042, 1994. "New reactor, new evaluation, determination of the absorbed radiant energy, radiation distribution model, trichloroethylene oxidation, TiO₂ suspension."
- PACHECO James, Mike Prairie, Lindsay Evans, and Larry Yellowhorse, *Proc. Intersoc. Energy Conver. Eng. Conf.* 1990, 25th, **5**, 141-145. "Engineering-industrial-scale reactor of solar photocatalytic oxidation of organic trichloroethylene, TiO₂ suspension or fixed."
- PRUDEN Ann L., and David F. Ollis, *J. Catalysis*, **82**, 404-417, 1983. "Photocatalytic oxidation of organic trichloroethylene on TiO₂, mechanism, intermediate, 83-7."
- TANAKA K., T. Hisanaga, and K. Harada, *New J. Chem.*, **13**, 5-7, 1989. "Photo oxidation of organohalide (trichloroethylene) compounds on TiO₂, with added hydrogen peroxide (H₂O₂/Fe²⁺), acetic acid was as an intermediate."
- Trichlorophenols, D'OLIVEIRA Jean-Christophe, Chaudio MINERO, Ezio PELIZZETTI, and Pierre PICHAT, *J. Photochem. Photobiol.* **72**, 261-267, 1993. "Organics, six

dichlorophenols (DCPs), three trichlorophenols (TCPs), photooxidation, TiO_2 , intermediate, kinetics, mechanism."

Trichlorophenoxy-acetic acid BARBENI M., M. Morello, E. Pramauro, E. Pelizzetti, M. Vincenti, E. Borgarello, and N. Serpone, *Chemosphere*, **16**(6), 1165-1179, 1987. "Sunlight photodegradation (oxidation) of organic 2,4,5-trichlorophenoxy-acetic acid and 2,4,5-trichlorophenol on TiO_2 . Identification of intermediates and degradation pathway, mechanism."

Triethylamine (TEA), SHIRAGAMI Tsutomu, Shinako Fukami, Yuji Wada, and Shozo Yanagida, *J. Phys. Chem.* **97**(49), 12882-12887, 1993. "Light intensity, density on product distribution, mechanism, small nanoscale CdS, triethylamine (TEA) as donor, aromatic ketones, electron-deficient alkenes, or 1-benzylnicotinamide (BNA^+) as substrates."

INDEX

activation energy	177	DDVP	32
activity of photocatalysts	180	deaerated systems	168
Advanced Oxidation Processes	2	dehydrogenation	168
Advanced Oxidation Technologies	2	DEP	32
air pollutant treatment	8, 10	doping	16
alcohol oxidation	88	dyes	12
aluminum oxide	126	E_{cb}	14
AOPs	2	E_F	17
AOTs	2	E_g	14
aromatic hydrocarbons	5	electrochemical method	11
Arrhenius equation	177	electrohydraulic cavitation	9
automotive emission control	10	electrolysis	11
band gap	14	electron equilibrium	17
band edge	14	electron affinity	25
band bending	18	electron beams	9
benzene	9	Electron Beam Probe	101
biopharmaceutical wastes	11	electron-hole pairs	18
bromodichloromethane	5	Eley-Rideal process	94
cadmium	11	energy gap	14
catalytic oxidation	10	energy band	14
CB	14	E_{vb}	14
CdS	168	Fenton reaction	7
chapter		Fenton reaction	129
outline	35	chemical limitations	129
chemical limitations	7	Fermi level	17
chemical warfare agents	11	ferric oxide	126
chromium	12	flat band	21
cobalt	11	gamma-rays	9
COD	11	gas emissions	10
complexing catalysis	187	gold	12
conclusions		halo-organic compounds	10
thesis	192	halogenated hydrocarbons	28
conduction band	14	halogenated organics	11
conductors	14	halogenated alkenes	5
copper	11	heavy metal	12
coverage	90, 95, 108	herbicides	32
cyanide	12	hole	17
DDT	32	hydrogen peroxide	5

hydrogen sulfide	9	particle size	175
hydroxyl radicals	2	PCBs	9, 11
industrial wastewater	118, 119, 126, 128	PCB's	11
insecticides	32	PCE	9
insulators	14	phenol	11
junction	17	phosphorus	32
Metal-semiconductor	25	photo Fenton reaction	7, 129, 133
semiconductor-liquid	17	photocatalysis	12
kinetic equations	91, 109	advantages	34
Eley-Rideal	94	assortment	12
Langmuir-Hinshelwood	94	definitions	13
parameters	108	heterogeneous	12
single gas molecule	91	history	27
two gas molecules	92	homogeneous	12
kinetic process	86	problems	35
alcohol oxidation	87	photocatalyst	12
Langmuir adsorption isotherm	90	photocatalyst property	
Langmuir-Hinshelwood process	94	selectivity	179
lead	11	bimetallic components	182
$M_2 + M_1/\text{CdS}$	182	diameter	176
mechanism		optimum amount	182
methanol	94	photocatalytic mechanism	187
mercury	11	complexing catalysis	187
metal ions	11	dehydrogenation	186
metal particle distribution on catalyst	175	photocatalytic elimination	28
military life support systems	10	inorganic compounds	28
n-type semiconductors	17	organic compounds	28
nitrogen oxide	8	photochemical methods	118
non-thermal plasmas (NTP)	8	photolysis	130
$\text{O}(^1\text{D})$	8	photoreactor	100
$\text{O}(^3\text{P})$	8	plasma	8, 9
$\text{O}_3/\text{H}_2\text{O}_2$	2	polychlorinated biphenyls	9
Ohmic contact	27	powder micro-cell model	96, 104
organics		preparation of photocatalysts	169, 178
references	205	Pd/TiO ₂	98
outline of the dissertation	35	Pt/TiO ₂	99
overpotential	21	TiO ₂	97
oxidation		M/CdS	170
COD	118, 126, 128	$M_2 + M_1/\text{CdS}$	169
phenol	118, 120, 126, 128, 130, 131	Pd/CdS	169
ozonation	3	CdS	170
ozone	3, 5	Pd/CdS	170
p-type semiconductors	17	promoter of photocatalyst	185

-
- | | | | |
|--|---------|--|----------|
| radicals | 3 | surfactants | 34 |
| rate-determining step | 187 | TCE | 9 |
| dehydrogenation | 187 | tetrachloroethylene | 9 |
| reduction | | tetrachloromethane | 9 |
| metals | 86 | Transmission Electron Microscopy (TEM) | |
| oxygen | 96, 109 | | 169, 175 |
| rocket propellant | 11 | triazine | 32 |
| Schottky contact | 25 | trichloroethylene | 9 |
| SCWO | 11 | trihalomethanes | 2 |
| semiconductor photocatalysis | 14 | UV/hydrogen peroxide | 131 |
| semiconductors | 14 | UV/ferric oxide | 133 |
| optical property | 23 | UV/H ₂ O ₂ | 2 |
| redox potentials | 21 | application | 7 |
| sewage sludge | 11 | UV/photocatalyst | 126 |
| silver | 12 | UV/ozone | 5 |
| sintering | 104 | UV/O ₃ | 2 |
| sludges | 11 | applications | 5 |
| SMSI | 104 | UV/hydrogen peroxide | 5 |
| sonolysis | 9 | valence band | 14 |
| space depletion region | 18 | VB | 14 |
| space charge layer | 18 | volatile organic compounds | 10 |
| sulfur dioxide | 8 | WAO | 10 |
| summary | | wet air oxidation | 10 |
| thesis | 192 | work function | 25 |
| supercritical water oxidation | 11 | X-ray Photoelectron Spectroscopy | |
| surface analysis | | (XPS) | 169 |
| Electron Beam Probe | 101 | X-ray powder crystal diffraction | 100, 102 |
| X-ray powder crystal diffraction | 100 | zinc | 11 |
| surface coverage | 175 | | |

CURRICULUM VITAE

Jian Chen, the author of this dissertation, was born in Shanghai, China, on 20 July 1957. After having graduated from secondary school in 1974, he worked as a farmer in the countryside for three years. During this period, he gained experience in hydraulic engineering for two and a half years as a supervisor of tunnel construction. In 1980, he graduated at the Department of Chemistry of Xiamen University, and at the same department he continued working as a teacher and researcher. He attended the MSc Class of this department in 1985 and graduated in 1987. The subjects he dealt with while teaching and doing research were catalysis, photocatalysis, chemical analysis and electrochemistry, and he applied these subjects to the fields of chemical synthesis, application of solar energy, and wastewater treatment. From 1985 to 1991, he was a lecturer in chemistry at Xiamen University. In 1991, he became a sandwich PhD student at the Department of Environmental Technology of Wageningen Agricultural University, the Netherlands. From 1992 to 1995, he was a visiting scholar and research associate at the Department of Chemical Engineering of North Carolina State University, USA, and worked on photocatalysis for wastewater treatment. Since 1995, he has been working at the Department of Environmental Technology of Wageningen Agricultural University in order to finish his PhD study.